The effects of ocean acidification on the establishment and maintenance of a model cnidarian-dinoflagellate symbiosis

Jacquie Bown

A thesis submitted to the Victoria University of Wellington
in partial fulfilment of the requirements for the degree of

Master of Science

in Marine Biology

Victoria University of Wellington, New Zealand

2022

VICTORIA UNIVERSITY OF WELLINGTON
TE HERENGA WAKA

Front cover: Photo courtesy of Matthew Nitschke

Abstract

Coral reefs are increasingly under threat from the effects of anthropogenic climate change, including rising sea surface temperatures and more acidified waters. At the foundation of these diverse and valuable ecosystems is the symbiotic relationship between calcifying corals and their endosymbiotic dinoflagellate algae, Symbiodiniaceae – one that is particularly sensitive to environmental stressors. Ocean acidification (OA) results in the lowering of pH and changes to carbonate chemistry and the inorganic carbon species available to marine organisms. Cnidarians such as reef-building corals may be particularly at risk from OA, as changes in pH and carbon availability can alter central physiological processes, including calcification, photosynthesis, acid-base regulation, metabolism and cell-cycle regulation. Yet, while responses to OA have been well researched at the physiological level, results have often been contradictory, and a clear understanding of the nature and extent of impacts on the cnidarian-dinoflagellate symbiosis remains equivocal. This thesis therefore aimed to provide further insights into the effects of OA on the establishment and maintenance of the cnidarian-dinoflagellate symbiosis. My research utilised the well-established model system for this symbiosis: the sea anemone *Exaiptasia diaphana* ('Aiptasia') and its native symbiont *Breviolum minutum*.

In Chapter 2, I sought to determine the impact of decreased pH (7.68) on the ongoing health and maintenance of the cnidarian-dinoflagellate symbiosis. I coupled proteomics with a range of physiological measures to examine the responses of both Aiptasia and *B. minutum*. I found that, while decreased pH had little effect on physiological parameters, changes in the proteome expression of both partners indicated a cellular-level response to OA. In the dinoflagellate symbiont, the proteomic response to low pH was characterised by the relative over-abundance of photosynthesis-related proteins. These included six chlorophyll *a*-chlorophyll *c*2-peridinin-proteins, and Photosystem I and II reaction centre proteins active in chlorophyll binding and electron transfer in the light harvesting complexes, as well as the upregulation of heat shock proteins (HSPs), catalase and superoxide dismutase, with roles in reactive oxygen species (ROS) management. This photosynthetic activity was associated with an upregulation of central metabolic and biosynthetic processes, and the translocase H^+-exporting diphosphatase, suggesting an increase in photosynthate transfer to the host anemone. Increased abundance of carbonic anhydrase 2 was observed in the host, implying an intensification of carbon concentrating mechanisms, which would support increased photosynthetic activity.

In the anemone host, the proteomic data indicated an overall increase in cellular respiration and ATP synthesis at low pH, together with enhanced fatty acid synthesis, indicating a stimulatory effect of photosynthetically-derived nutrition. Over time, however, this benefit may also incur costs, as indicated by an apparent triggering of the host's innate immune response – potentially driven by photosynthetically-derived ROS. Immune-response activation was signalled by increased abundance of alkaline phosphatases, an interferon-induced protein, collagen alpha chain, and a Golgi-associated plant pathogenesis-related protein, while HSPs, catalase and enolase indicated the upregulation of ROS management pathways. Interestingly, melanotransferrin, which is involved in cellular iron homeostasis, was downregulated in symbiotic host tissues over time. Iron is a key nutrient required for photosynthesis, and may imply that the anemones were restricting iron supply to their symbionts as a means of controlling population densities. Collectively, these findings suggest that, through the coordination of cellular processes, this model cnidarian-dinoflagellate symbiosis can likely acclimate to moderate OA exposure.

In Chapter 3, I examined whether decreased pH (7.68 and 7.85) impacts the capacity of Aiptasia to acquire and establish a symbiosis with *B. minutum*. I found that low pH did not reduce symbiont uptake, colonisation rate, photosynthetic performance or final symbiont density during symbiosis establishment over four weeks, except where the symbiont was pre-exposed to reduced pH. In this case, there was an initial and short-term decrease in colonisation rate, followed by recovery. The implications for the health and availability of free-living Symbiodiniaceae populations, and any such delayed uptake in the early stages of colonisation are unknown and warrant further research. However, these data indicate that Aiptasia remains able to establish a functional symbiosis with *B. minutum* at low pH.

This thesis indicates that soft-bodied cnidarians will be relatively resilient to future OA scenarios, and provides valuable insights to inform further work in reef-building corals. The findings presented here provide baselines from which to explore two under-researched aspects of OA impacts on the cnidarian-dinoflagellate symbiosis: responses at the cellular-level, and symbiont uptake and colonisation. To address the growing threat of climate change, further work is needed to understand cellular responses to OA, particularly during key life-stage events such as the establishment of symbiosis.

For Sarah

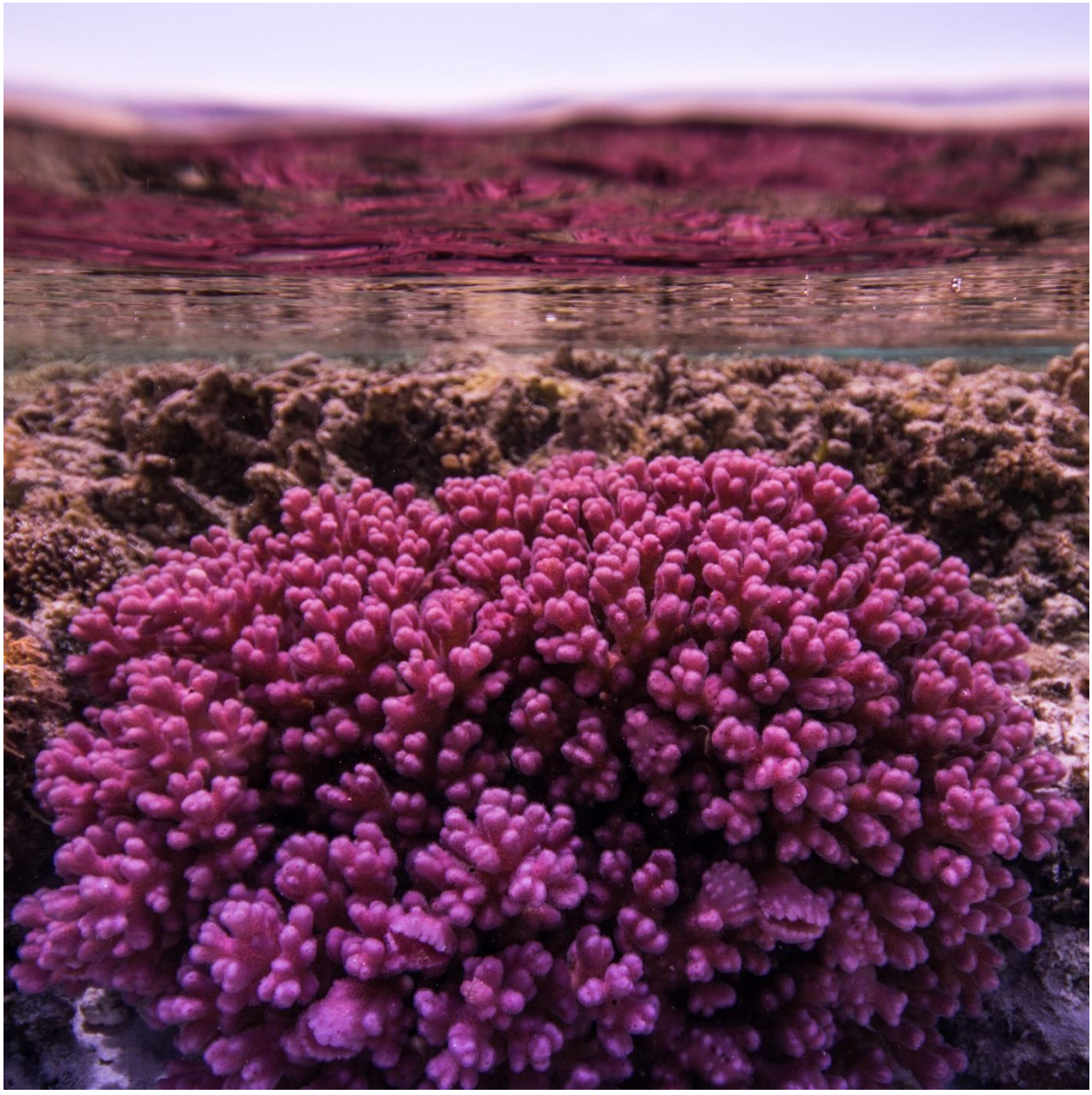

Photo courtesy of Matthew Nitschke

Acknowledgements

This project has taught me much about science, about my subject and about myself. I am grateful to the Wellington Masters by Thesis scholarship for supporting my second year of study, and the many people who have supported me through this journey. Firstly, huge thanks go to my primary supervisor Prof. Simon Davy. Thank you for believing in me, for your patience, wisdom, positive support and kindness. I have learned an incredible amount in the last few years; much of that is because of the learning environment you create, and the encouragement you give us to realise our potential. Many thanks also to my secondary supervisor Dr Christopher Cornwall for your unerring guidance, expertise and patience in answering my questions, and for your good humour along the way.

Special thanks go to Dr Clint Oakley. Your guidance on proteomics in particular has been invaluable, and I have learned so much from you over the course of this thesis. You always make time for us even when you have none, and you have a knack for explaining things – both the how and the why – in ways that just make sense. Thank you for your guidance and patience throughout, and for the painfully accurate science memes. Thanks also to Dr Matthew Nitschke and Dr Nina Rosset, for believing in me, especially in the early days, and to Matt for permission to use your stunning photos – you have an incredible eye for detail.

To Davy lab members past and present – Agustina Giovagnoli, Amirhossein Mashini, Andrea Gamba, Bobby Lust, Evan Heit, Evan Raymond, Immy Ashley, Lauren Fracasso, Lucy Gorman, Maggie Wuerz, Marina Botana and Rob Lewis. What an amazing group of supportive, inspiring, encouraging and incredibly fun people to have the privilege to work alongside. You all rock and I'm looking forward to hanging out some more from now on! Special thanks to Immy, Rob, and Supplementary Evan for lending a hand when I most needed it – it's times like those that make it such a great team.

Thanks also to members of the Cornwall lab, in particular Erik Krieger and Aleluia Taise for your guidance in the early days of building and getting to know my experimental system, and to Yann Tassin for the total alkalinity R code. Technician Paul Roulston provided expertise and assistance in building my experimental system – I couldn't have done it without you, and the political debates were an added bonus.

To Trina and Sam – my NZ whānau. It would have been so much harder without you both to support me not just through this thesis but in all aspects of my life. Thank you for everything you do and for being there through all the challenges and the joy.

To Sarah for always looking at the world with curiosity, kindness and calm. You still inspire me to do the same every day. I hope you would be proud.

And to Mum and Dad – for everything. In every sense, I wouldn't be here without you.

Table of Contents

List of Figures

List of Tables

List of Abbreviations

AIC	Akaike's information criteria
ASW	artificial seawater
A_T	total alkalinity
ATP	adenosine 5'-triphosphate
BME	B-mercaptoethanol
CA	carbonic anhydrase
Ca^{2+}	calcium
$CaCO_3$	calcium carbonate
CCA	crustose coralline algae
CCM	carbon concentrating mechanism
CE	calicoblastic epithelium
C_i	inorganic carbon
chl	chlorophyll
CO_2	carbon dioxide
CO_3^{-2}	carbonate
cyt *c*	cytochrome *c*
DAP	differentially abundant proteins
DIC	dissolved inorganic carbon
DIC_T	total dissolved inorganic carbon
DIN	dissolved inorganic nitrogen
DIP	dissolved inorganic phosphorus
ECM	extracellular calcifying medium
ER	endoplasmic reticulum
ETC	electron transport chain
FDR	false discovery rate
F_v/F_m	maximum quantum yield of PSII
GDH	glutamate dehydrogenase
GHG	greenhouse gas
GO	gene ontology
GS	glutamine synthetase
H^+	hydrogen ions H_2CO_3 carbonic acid
H_2O_2	hydrogen peroxide
HCl	hydrochloric acid
HCO_3^-	bicarbonate
HPLC	high-performance liquid chromatography
HSP	heat shock protein
HTCM	high throughput confocal microscopy
HvCN	voltage-gated proton channel
IPCC	International Panel on Climate Change
K^+	potassium
LC MS-MS	liquid chromatography-tandem mass spectrometry
LHC	light harvesting complex
MAMPs	microbe-associated-molecular patterns
$_m$ETC	mitochondrial electron transport chain
N	nitrogen
Na^+	sodium
NADPH	nicotinamide adenine dinucleotide phosphate
$NaHCO_3$	sodium bicarbonate
NFκB	nuclear factor kappa B
NO	nitric oxide
NPQ	non-photochemical quenching
$O_2\cdot^-$	superoxide

OA	ocean acidification
OW	ocean warming
P	phosphorous
PAM	pulse amplitude modulated
PAR	photosynthetically active radiation
PCA	principal component analysis
PCD	programmed cell death
pCO_2	partial pressure of carbon dioxide
P_g	gross photosynthesis
pH_e	extracellular pH
pH_{ECM}	extracellular calcifying medium pH
pH_i	intracellular pH
pH_T	pH (total scale)
PRRs	pattern recognition receptors
PSI	Photosystem I
PSII	Photosystem II
R	cellular respiration
ROS	reactive oxygen species
sAC	soluble adenylyl cyclase
SDC	sodium deoxycholate
SSPs	Shared Socioeconomic Pathways
SST	sea surface temperatures
TCA cycle	tricarboxylic acid cycle
TGFβ	transforming growth factor beta
TLR	toll-like receptor
TSR	thrombospondin type 1 repeat
UPR	unfolded protein response
Φ^{PSII}	effective quantum yield of PSII
Ω_{arag}	aragonite saturation state

Photo courtesy of Matthew Nitschke

Chapter 1: General Introduction

1.1. Coral reefs and symbiosis

1.1.1 Symbiosis

Symbiosis was originally defined by de Bary in 1989 as "the living together of two unlike organisms" (Apprill 2020) and is now typically defined as intimate, enduring associations between individuals of different species (Goff 1982). Symbioses may be obligate, where at least one partner requires the other to survive, or facultative, where one or both partners can exist outside of the symbiosis but remain with their partner organism for conferred benefits, such as nutrients, protection and transport (Nguyen and van Baalen 2020). Obligate symbioses cover a continuum of intra-specific interactions ranging from mutualism, "reciprocal exploitations that nonetheless provide benefit to both partners" (Herre et al. 1999), to parasitism, where one partner benefits at some cost to the other (Douglas 2008). The nature of symbiosis between two partners may change over time in response to environmental conditions such as resource availability (Herre et al. 1999; Wooldridge 2009; 2010; Lesser et al. 2013). Physical characteristics also differ. Ectosymbiosis describes a relationship where one partner (the symbiont) resides externally to the other (the host), whereas endosymbiosis refers to symbionts residing within the body of the host for example, intracellularly (Apprill 2020). Symbiosis is increasingly recognized as a selective force behind evolution, and in obligate symbioses both partners adapt to one another in a state of coevolution reinforcing the intricacy of their relationship (Apprill 2020). There are wide-ranging benefits to this arrangement. However, it represents a highly committed strategy where host adaptations to symbiosis may also present vulnerabilities. Such examples include increased metabolic costs, immune-system modifications, and evolution of specialised mechanisms and tissues for supporting symbionts (Bennett and Moran 2015). These are discussed further below.

Symbioses have long been a focus of ecological and biological interest. Some of the more well-known and ancient partnerships including those between terrestrial plants and the mycorrhizal fungi which live among their root systems, supporting an estimated 75% and 80% of their host's phosphorus and nitrogen uptake, respectively (van der Heijden et al. 1998; Wardle et al. 2004). Other examples

include the endosymbiotic bacteria *Wolbachia* which synthesize necessary amino acids for their aphid hosts, and the presence of multiple bacterial strains in a diverse range of animal intestines, which can support digestion and immune system health (Bennett and Moran 2015; Mazmanian et al. 2005; Kostic et al. 2013). Marine examples also abound, and of these the most well-studied are the relationships between photosynthetic dinoflagellates of the family Symbiodiniaceae and a range of marine organisms including sponges, giant clams, flatworms and the cnidarians: coral, jellyfish and sea anemones.

1.1.2 Evolution of the cnidarian-dinoflagellate symbiosis

The Symbiodiniaceae are unicellular dinoflagellate photoautotrophs of around 5-15 µm diameter, appearing yellow-brown in colour due to their photosynthetic pigments. Originally thought to be a single species, *Symbiodinium microadriaticum*, (Freudenthal 1962; Taylor 1974), from early work identifying the existence of four distinct species of *Symbiodinium* (Blank and Trench 1985) these dinoflagellates are now recognised as highly genetically diverse. Fifteen distinct clades (A-I) and a multitude of sub-clades or 'types' were previously identified, including both symbiotic and free-living types (e.g., Blank and Trench 1985; Rowan and Knowlton 1995; Pochon and Gates 2010; Jeong et al. 2014), prior to a major reclassification of clades into the family Symbiodiniaceae (LaJeunesse et al. 2018). While the 15 clades or sub-clades previously identified are all candidates to be recognised as Symbiodiniaceae genera, presently only ten are formally described (LaJeunesse et al. 2018; Nitschke et al. 2020; Pochon and LaJeunesse 2021). Within this context, there are many candidate niches yet to explore and further novel species to be classified (e.g., Lewis et al. 2019; Lee et al. 2020; Nitschke et al. 2020), and it is evident that much remains to be discovered about this diverse family. The Symbiodiniaceae are known to form symbioses across phyla including the Porifera (sponges), Platyhelminthes (flatworms), certain species of Mollusca (gastropods and bivalves e.g., giant clams) and Cnidaria (coral, jellyfish and sea anemones) (Venn et al. 2008). Of these, the relationship with the stony corals (Order Scleractinia) is by far the most iconic and well researched, and is typical of the Symbiodiniaceae genera *Symbiodinium, Breviolum, Cladocopium* and *Durusdinium* (formerly clades A-D; Baker 2003; Pochon and Gates 2010; LaJeunesse et al. 2018). This association is thought to have originated 146-200 million years ago and coincided with the adaptive radiation of stony corals and reef formation in the Jurassic period (LaJeunesse et al. 2018). The evolutionary and ecological

success of scleractinian corals and coral reefs since this time has been attributed to this mutualistic symbiosis (Lesser et al. 2013).

Cnidarian-dinoflagellate associations vary in their degree of partner specificity (Gabay et al. 2019). Most coral species associate with one dominant symbiont type or species, and this selective specificity appears to be stable at the onset of symbiosis and remain so over time (Weis et al. 2001; Sampayo et al. 2008; Stat et al. 2009; Thornhill et al. 2014; 2017). It is thought that specialist symbionts have evolved to out-compete more generalist types within a given host species (Thornhill et al. 2014). However, some coral species may host multiple symbiont types as codominant or rare populations (Kemp et al. 2015; Boulotte et al. 2016). The host coral does not comprise a uniform environment, and while the morphologically-simple body plan of cnidarians provides a large surface area to volume relationship that is well suited to light capture, and therefore to photosynthetic symbionts, degrees of light exposure may vary (e.g., apex *vs*. base) (Venn et al. 2008). The host therefore represents a landscape of more and less suitable conditions, and different symbiont types within a coral colony appear to exhibit niche partitioning, for example through photoacclimation to different light levels (Herre et al. 1999; Boulotte et al. 2016). As such, while a dominant symbiont type often prevails, low-density populations of background or 'cryptic' types can coexist within the same coral colony (LaJeunesse et al. 2009; Silverstein et al. 2012; Cunning et al. 2015). Symbiodiniaceae vary in their functional characteristics, for example in terms of their photophysiology, degree of thermotolerance, or susceptibility to disease (Rowan 2004; Loram et al. 2007; Sampayo et al. 2008; Stat et al. 2009; Cunning et al. 2015; Hoadley et al. 2019). These differences can affect their functionality in symbiosis, for example with respect to the quantity of nutrients provided to the host or the resistance of the partnership to bleaching under elevated temperature (Starzak et al. 2014; Matthews et al. 2017). This suggests that certain symbiont types are more advantageous than others under given conditions (Loram et al. 2007; Stat et al. 2009; Cunning et al. 2015). However, given the generally high degree of inter-partner specificity, the extent to which symbiont community composition within a given host can shift to provide adaptive capacity is likely limited (Stat et al. 2009; Cunning et al. 2015; Hoadley et al. 2016a; 2019; Gabay et al. 2019).

1.1.3 Nutritional exchange and biomass regulation

The cnidarian-dinoflagellate symbiosis is based on dynamic nutrient exchange and the coordinated growth of both partners (**Figure 1.1**; Muscatine et al. 1981; 1984; Yellowlees et al. 2008; Weis 2019). The dinoflagellate symbionts translocate photosynthetically fixed carbon to their host in the form of glucose, lipids, amino acids and fatty acids, providing ~95% of the energy needed to support key processes including respiration, growth, calcification and reproduction (Muscatine et al. 1984; Whitehead and Douglas 2003; Yellowlees et al. 2008; Burriesci et al. 2012; Hillyer et al. 2017). In exchange, in addition to protection and a high light environment, the symbionts receive inorganic carbon, nitrogen, phosphorus and other compounds such as iron to support photosynthesis, growth and nitrogen assimilation (Muller-Parker and D'Elia 1997; Venn et al. 2008; Reich et al. 2020; Pupier et al. 2021). This tight recycling of nutrients provides an ecological advantage in typically oligotrophic tropical waters (Muscatine et al. 1984; Radecker et al. 2015; Pupier et al. 2021). For stony corals this is an obligate symbiosis; given the proportion of energy provided by their symbionts, without them they are at increased risk of starvation, disease and reproductive failure (Glynn 1993; Brown 1997; Baker et al. 2008; Hoegh-Guldberg et al. 2017). In comparison, while Symbiodiniaceae can exist in a free-living state and may therefore be facultative, when *in hospite* (i.e., within their host), they are reliant on their host to provide the requisite nutrients for survival (Lesser et al. 2013; Baker et al. 2018).

Inorganic carbon (C_i) may originate from the surrounding seawater, largely as bicarbonate (HCO_3), or alternately as CO_2 from host and symbiont respiration or as a by-product of calcification (**Figure 1.1**) (Allemand et al. 1998; Furla et al. 2000; Venn et al. 2011; Tansik et al. 2017). Symbiodiniaceae are thought to be carbon limited at current ocean pH levels and rely on their host to supply ~85% of the dissolved inorganic carbon (DIC) needed for photosynthesis (Allemand et al. 1998; Davy and Cook 2001; Tansik 2017). For eventual use in photosynthesis by Rubisco, C_i must be in the form of CO_2, where it is fixed through the Calvin-Benson cycle (Venn et al. 2008; Roth 2014). As part of their photosynthetic machinery, Symbiodiniaceae possess Type II Rubisco, which has a lower affinity for CO_2 than the more common Type I Rubisco (Whitney et al. 1995; Brading et al. 2013). In response, symbiotic cnidarians have evolved carbon-concentrating mechanisms (CCMs) to supply DIC in the form of CO_2 to their endosymbionts to fuel photosynthesis (Weis et al. 1989; Leggat et al. 1999). DIC uptake by the cnidarian host involves the secretion of H^+ by H^+-ATPase, which results in

the protonation of HCO_3^- to H_2CO_3 (Furla et al. 2000). Carbonic anhydrase (CA) then catalyses the conversion of H_2CO_3 to CO_2, which, unlike H_2CO_3, can diffuse across cell membranes (Furla et al. 2000). Uptake of DIC by Symbiodiniaceae is mediated by H_2CO_3 transporters, H^+-ATPase and CA (Bertucci et al. 2013).

Photosynthate, the metabolic product of photosynthesis, is translocated back to the host to complete the nutritional exchange. The major component of the photosynthate released in the cnidarian-dinoflagellate symbiosis is believed to be glucose, with other carbon compounds released including glycerol, amino acids and lipids (Burriesci et al. 2012; Hillyer et al. 2016; 2017; Matthews et al. 2018; Starzak et al. 2020). Moreover, Symbiodiniaceae also allow their host to access pools of dissolved inorganic nitrogen (DIN) and phosphorus (DIP) (Dagenais-Bellefeuille and Morse 2013; Rosset et al. 2017). In particular, the symbiont can assimilate DIN as nitrate and ammonium from seawater or ammonium as waste from host catabolic processes into glutamate *via* the glutamine synthetase/glutamine 2-oxoglutarate amido transferase (GS/GOGAT) pathway (Roberts et al. 2011; Pernice et al. 2012). Glutamate acts as a precursor for essential amino acids, which are then released to the host, efficiently recycling and retaining nitrogen within the symbiosis (Wang and Douglas 1998; Venn et al. 2008; Radecker et al. 2015; Pupier et al. 2021). Ammonium may also be assimilated by the host *via* glutamine synthase (GS) and glutamate dehydrogenase (GDH) pathways (Miller and Yellowlees 1989; Wang and Douglas 1998 Dagenais-Bellefeuille and Morse 2013). Less is known about the assimilation and metabolism of phosphorus within the symbiosis, however ATPase activity implies the use of pumps or ionic exchange transporters to actively transport phosphate from external sources across cell membranes (Rands et al. 1993; Gerencser et al. 2002; Godinot et al. 2011; Ferrier-Pagès et al. 2016). Godinot et al. (2011) also suggested the presence of an active sodium/phosphate symporter, after observing inhibited phosphate uptake in the absence of sodium. Interestingly, *in hospite* symbionts appear to be severely phosphorus-deficient relative to their surrounding host tissue (Krueger et al. 2020).

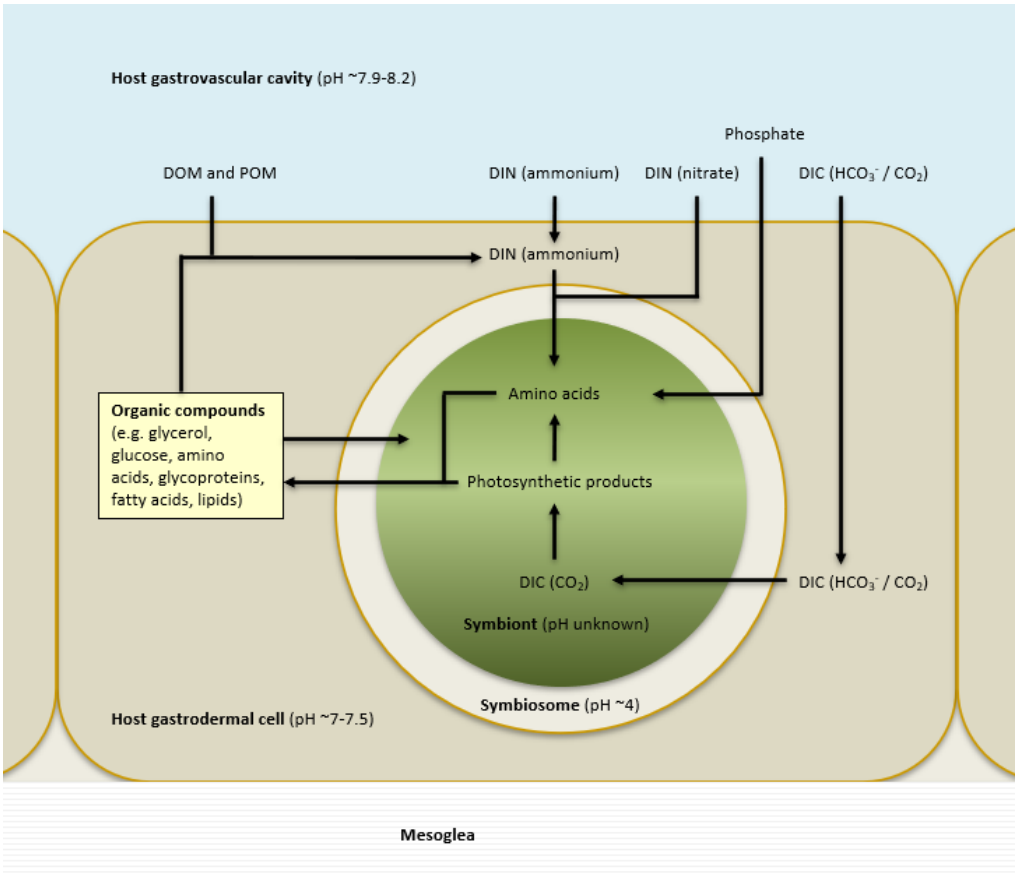

Figure 1.1: Schematic overview of nutritional exchange in the cnidarian-dinoflagellate symbiosis. DIN = Dissolved Organic Nitrogen; DIP = Dissolved Organic Phosphate; DIC = Dissolved Organic Carbon (after Davy et al. 2012).

The host is thought to tightly control nutrient supply to its intracellular symbionts as a means of controlling their population density, thereby ensuring an excess of photosynthetic carbon for release back to the host (Jokiel et al. 1994; Tivey et al. 2020, Xiang et al. 2020). Symbionts are nitrogen-limited *in hospite*, and carbon, nitrogen and phosphorus are used in mitosis (Fagoonee et al. 1999). Therefore, in controlling supply, nutrient competition acts as a means of population control (Krueger et al. 2020). However, nutrient limitation can also lead to increases in symbiont starch and lipid storage, suggestive of symbionts 'hoarding' nutrients from the host (Wooldridge 2009; 2010; Baker et al. 2018; Tivey et al. 2020). Additionally, the identity and specificity of both partners can greatly influence the success of the symbiosis. Suboptimal partners can incur increased metabolic costs, and effective nutritional exchange will depend on the compatibility between the symbiont and host (Loram et al. 2007; Starzak et al. 2014; Matthews et al. 2017; 2018). Variable rates of carbon uptake and translocation have been observed, and heterologous (i.e., non-native) symbionts may provide

reduced glucose and fatty acid pools, leading to host lipogenesis and slower growth rates (Davy and Cook 2001; Gabay et al. 2018; Matthews et al. 2018). Heterologous symbionts may also sustain themselves by manipulating host nitrogen cycling, overcoming this regulator of cell cycling (Matthews et al. 2018). Given the tightly-coupled nature of the cnidarian-dinoflagellate relationship, work is still required to understand the regulation of nutrients – including the degree to which each partner can exert control and the precise mechanisms involved (Davy et al. 2012; Krueger et al. 2020).

1.1.4 Symbiosis establishment

The establishment of the cnidarian-dinoflagellate symbiosis has been the focus of much research and is explored more fully in **Chapter 3**. Around 85% of corals acquire Symbiodiniaceae from the environment with each new generation – known as horizontal transmission – with the remaining ~15% inheriting their symbionts maternally through the reproductive cycle – known as vertical transmission (Baird et al. 2009; Fransolet et al. 2012). Horizontal transmission typically occurs at the larval stage, though it can also occur at other life stages – for example post-bleaching (Baker 2003; Lewis 2004; Kishimoto et al. 2020). Symbionts are ingested *via* phagocytosis by the host's gastrodermal layer and become enveloped within a vacuole derived from the phagosome membrane called the 'symbiosome' (**Figure 1.2a,b**) (Hohman et al. 1982; Wakefield and Kempf 2001; Mohamed et al. 2016). This process involves an arrested immune response, whereby phagocytosis is an initial pathogenic response to microbial invasion. This is followed by a complex array of inter-partner signalling events involving Rab family proteins, the TGFβ signalling pathway and TSR proteins, whereby lysosomal degradation is inhibited resulting in the retention of compatible symbionts and removal of incompatible species (**Figure 1.2a**) (Chen 2003; 2005; Weis et al. 2008; 2019; Peng et al. 2010; Detournay et al. 2012; Neubauer et al. 2017). The maintenance of symbiosis then involves ongoing regulation of the host's immune response and nutritional exchange (Davy et al. 2012; Weis 2019). Endosymbiosis occurs only in specific gastrodermal cells in the host, where the symbiosome separates symbionts from the host cytoplasm and provides ongoing protection from lysosomal degradation (Fitt and Trench 1983; Rodriguez-Lanetty et al. 2006; Peng et al. 2010; Bucher et al. 2016). The symbiosome membrane is the interface for host-symbiont interactions and is thought to play key functional roles in inter-partner recognition, nutrient and molecular transport, cellular homeostasis and cell-cycle regulation (Peng et al. 2010; Mohamed et al. 2016; Yuyama et al. 2018).

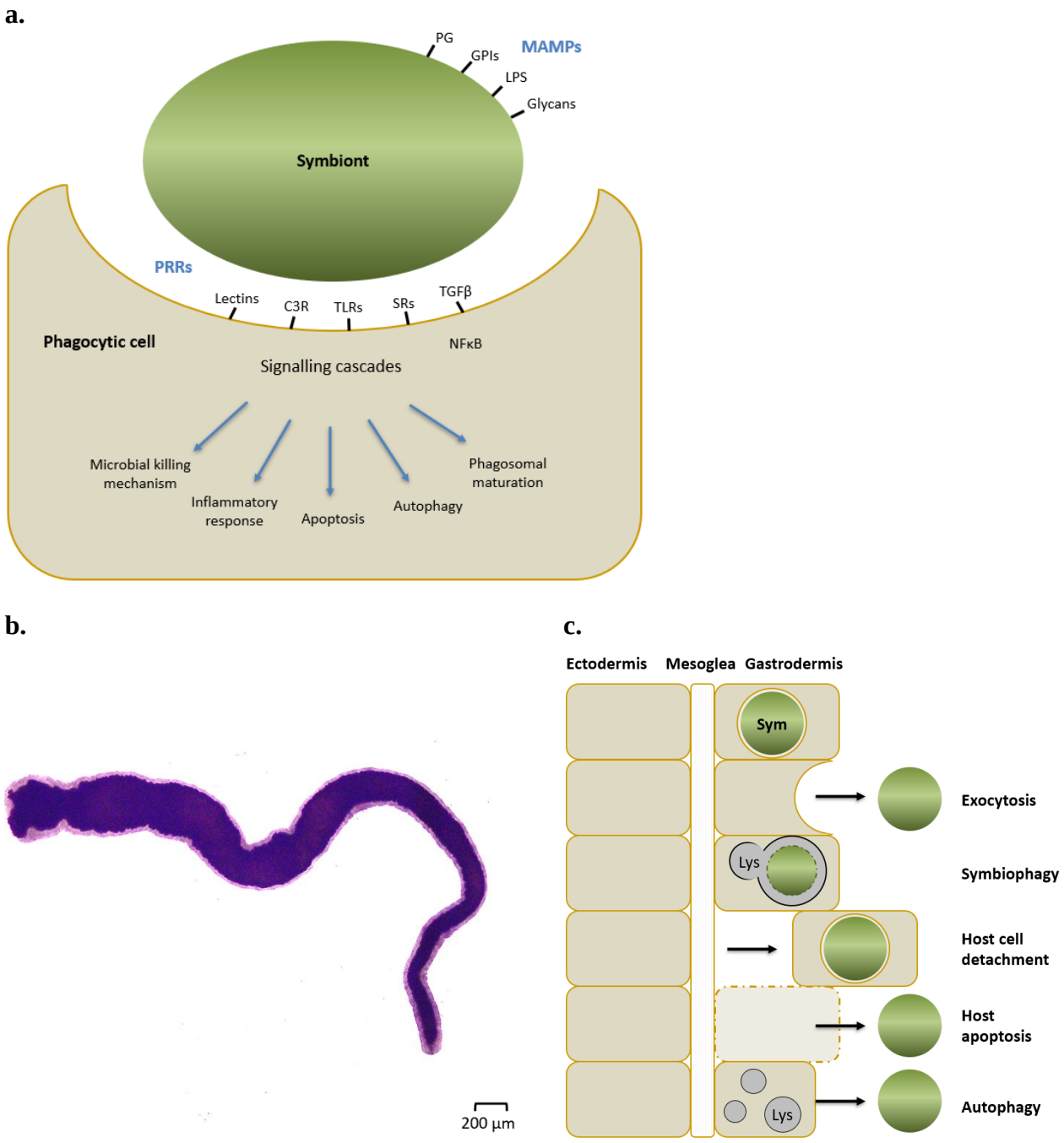

Figure 1.2: Processes of symbiont uptake and expulsion. a. Schematic of immune processes involved in the establishment of the cnidarian-dinoflagellate symbiosis. Symbiodiniaceae cell surfaces are covered with microbe-associated-molecular patterns (MAMPs) that can be detected by pattern recognition receptors (PRRs) on the host's cell surfaces. Recognition activates the host's innate immune pathways which either tolerate the symbiont's presence or activate defence mechanisms as shown. If tolerated, the phagosome becomes the symbiosome. PG = peptidoglycan; GPI = glycosylphosphatidylinositol; LPS = lipopolysaccharide; C3R = complement 3 receptor; TLR = toll-like receptor; SR = scavenger receptors; TGFβ = transforming growth factor β. NFκB = nuclear factor κB. Adapted from Davy et al. (2012) and Weis (2019). **b.** Excised tentacle of the sea anemone *Exaiptasia diaphana* showing the dense symbiont distribution within the gastrodermis, and absence of symbionts from the ectodermis. Photo: J Bown. **c.** Mechanisms of symbiont loss from cnidarian host cells. Sym = Symbiodiniaceae cell. Lys = host lysosome. After Weis (2008), Bieri et al. (2016), and Oakley and Davy (2018).

1.1.5 Threats to coral reefs

Coral reefs are among the most biologically diverse and socioeconomically important ecosystems on Earth. They support up to one third of all marine species and provide wide-ranging ecosystem services to millions of people worldwide, such as supporting fisheries and tourism and providing coastal protection (Hoegh-Guldberg et al. 2007; Hughes et al. 2017). The underpinning symbiotic relationship between reef-building corals and Symbiodiniaceae tolerates a narrow range of environmental conditions and is becoming increasingly threatened by climate change stressors (Kleypas et al. 1999; Hoegh-Guldberg et al. 2007; Heron et al. 2016; IPCC 2019).

Climate change stressors

Two of the major effects of climate change on marine environments are ocean warming (OW) and ocean acidification (OA). Warming of the Earth's climate is unequivocal, with unprecedented changes since the 1950s (Hoegh-Guldberg et al. 2017; IPCC 2019). OW accounts for more than 90% of this increase in stored energy, with only about 1% stored in the atmosphere (IPCC 2021). OW is greatest in the surface waters occupied by symbiotic cnidarians, and sea surface temperatures (SST) are predicted to continue to rise with mean global sea surface warming of 1-3°C+ by 2100, depending on emissions of greenhouse gases (GHG) such as CO_2 (Reid 2016). Over 30% of anthropogenic CO_2 is taken up by the ocean, which in addition to OW leads to OA, a process which lowers seawater pH, changes ocean carbonate chemistry and alters the availability of dissolved inorganic carbon (DIC) species available to marine organisms (**Figure 1.3a**) (Kleypas 1999; Sabine et al. 2004; Doney et al. 2009; 2020; Gruber et al. 2019). Global mean open ocean pH is estimated to have decreased by 0.018 *per* decade during 1991-2011 (Lauvset et al. 2015). However, such changes can be exacerbated on coral-dominated reefs which can also exhibit high diel pH variability, due to respiration and often low levels of mixing with open ocean waters (Hofmann et al. 2011; Cornwall et al. 2013; 2018; Rivest et al. 2017; Torres et al. 2021).

The International Panel on Climate Change (IPCC) has made predictions according to five Shared Socioeconomic Pathways (SSPs), which cover a range of future climate change scenarios based on projected socioeconomic global trends up to the year 2100, from which it is possible to model the likely severity of climate change impacts (IPCC 2021). These data place current mean global ocean

surface pH at 8.05, with 2100 levels reaching pH 7.68 under the very high GHG emissions scenario SSP5-8.5 (**Figure 1.3b**) (IPCC 2021). Increasing, it is widely agreed that OA will have negative consequences for many marine organisms, including reef-building corals and coralline algae, molluscs, crustaceans and other sessile fauna (e.g., Doney et al. 2009; 2020; Veron et al. 2009; Kroeker et al. 2013; Bindoff et al. 2019; Canadell et al. 2021; Cornwall et al. 2021) (see **Section 1.2**).

a.

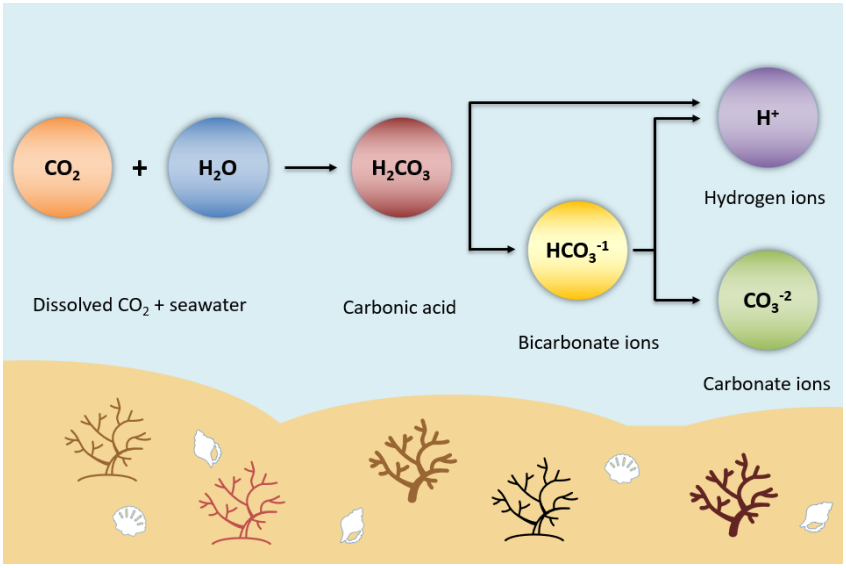

b.

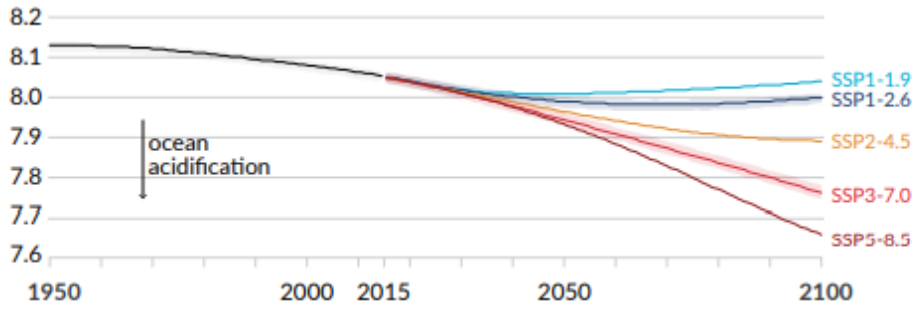

Figure 1.3: Processes and impacts of ocean acidification. a. The process of ocean acidification. As carbon dioxide (CO_2) is absorbed by the ocean, it reacts with water to form carbonic acid (H_2CO_3), lowering pH levels. Hydrogen ions released by H_2CO_3 bind to carbonate ions to form bicarbonate (HCO_3^-), reducing the concentration of carbonate ions in the water column, and so their availability to calcifying organisms to form calcium carbonate ($CaCO_3$) structures **b.** IPCC predictions of global average surface ocean pH to 2100 based on five Shared Socioeconomic Pathways (SSPs). Starting in 2015, they include the following scenarios: SSP5-8.5 – very high GHG emissions with CO_2 emissions doubling from current levels by 2050; SSP3-7.0 – high GHG emissions with CO_2 emissions doubling from current levels by 2100; SSP2-4.5 – intermediate GHG emissions and CO_2 emissions remaining around current levels until mid-century; SSP1-2.6 – low, and SSP1-1.9 – very low, GHG emissions and CO_2 emissions declining to net zero around or after 2050 followed by varying levels of net negative CO_2 emissions. Shading around SSP1-2.6 and SSP5-7.0 indicate 95% confidence ranges. Reproduced from IPCC (2021).

Coral bleaching

The phenomenon of coral bleaching has been recognised for decades and is now posited as an ecological crisis (Glynn 1983; 1991; Gates 1990; Lesser 1996; 1997; Hughes et al. 2017; Suggett et al. 2017). Bleaching is highly correlated with periods of both increased SST and irradiance (Hoegh-Guldberg et al. 2007; Hughes et al. 2017) and is caused by a breakdown of symbiosis (dysbiosis) leading to the elimination of symbiont cells, resulting in reduced host fitness and, if sustained, mortality (Brown 1997; Weis 2019). Under currently accepted theory, coral bleaching results from the generation of reactive oxygen species (ROS) in response to light and/or thermal stress (Weis 2008; 2019; Blackstone and Golladay 2018; Oakley and Davy 2018). In the symbiont, ROS are produced under normal photosynthetic and respiratory functioning and are managed through antioxidant enzymes and other defensive mechanism in both partners (Kregel 2002; Richier et al. 2005; Lesser 2006). However, light and thermal stress drive overexcitation of the photosynthetic apparatus, increasing ROS production to the point of overwhelming these mechanisms and triggering a cascade of detrimental cellular processes (Weis 2008; Lesser 2011; Oakley and Davy 2018). These processes are still being elucidated (Weis 2008; 2019; Oakley and Davy 2018), however it is known that, at excess levels, ROS cause significant cellular damage, including to DNA, lipids, chlorophyll pigments, protein function and membrane integrity, and induce photooxidative damage of the photosynthetic apparatus (Venn et al. 2008; Weis 2008; Lesser 2011; Rehman et al. 2016).

In Symbiodiniaceae, ROS defence mechanisms include photorespiration and non-photochemical quenching (NPQ). Photorespiration provides an alternate electron pathway to divert overexcitation energy that may otherwise produce ROS (Crawley et al. 2010; Roth 2014). In NPQ, excess excitation energy is dissipated as heat or autofluorescence, reducing excess electron flow through the photosystems (Venn et al. 2008; Roth 2014). When these photoprotective mechanisms fail, inhibition of the photosynthetic machinery occurs through disruption at several key sites including the D1 protein (Ohad et al. 1994; Warner et al. 1999; Takahashi et al. 2009; Hill et al. 2011), Calvin-Benson cycle (Lesser 1996; Venn et al. 2008; Lilley et al. 2010; Rehman et al. 2016), thylakoid membrane integrity of chloroplasts (Tchernov et al. 2004; Weis 2008), and chlorophyll and accessory pigments in the thylakoids (Venn et al. 2008; Lesser 2011).

Multiple stress responses have also been identified within the host, the primary source of ROS being the mitochondria (Dunn et al. 2012; Tolleter et al. 2013; Gardner et al. 2017). Mitochondria are central regulators of cellular stress and have dedicated recovery pathways, including the unfolded protein response (UPR) which promotes the detoxification of ROS (Haynes and Ron 2010; Dimos et al. 2019). Thermal stress can overwhelm these defences, causing loss of mitochondrial integrity and disruption of proteins associated with electron transport and ATP production (Dunn et al. 2012; Dimos et al. 2019). The mitochondria are closely linked with the endoplasmic reticulum (ER), which has a key role in cell signalling pathways alongside its primary role is in protein synthesis, folding, and export (Hetz 2012; Rainbolt et al. 2014). Protein folding is temperature-sensitive and, as such, is directly impacted by thermal stress (Orrenius et al. 2003; Rainbolt et al. 2014). These changes can disrupt host cell homeostasis and trigger host cell apoptosis (Dunn et al. 2012; see below). Nitric oxide (NO), which is a ubiquitous signalling molecule and cytotoxin, has also been implicated in coral bleaching and is produced by both host and symbiont (Weis 2008; Hawkins et al. 2012; 2013; 2014). In the host, superoxide ($O_2 \cdot^-$) is generated following mitochondrial membrane damage, which in turn triggers the production of NO (Weis 2008). NO is also produced directly by the symbiont at a rate that increases under photoinhibition and diffuses into the host (Weis 2008; Hawkins et al. 2014; Berthelier et al. 2017). NO is involved in parasitic signalling, suggesting that its production could be a host response to a shift towards parasitism by its symbionts (Perez and Weis 2006).

The ultimate outcome of these cellular processes is symbiont loss, which can occur *via* multiple mechanisms as outlined in **Figure 1.2c**. The relative contributions of these pathways to bleaching are unclear, and they may act alone or in combination dependent on the duration and intensity of the thermal stress (Gates et al. 1992; Dunn et al. 2004; 2007; Bieri et al. 2016). Apoptosis is a form of programmed cell death (PCD) and may be triggered by at least two pathways (Dunn et al. 2007; Paxton et al. 2013). In the first, ER stress can disrupt Ca^{2+} regulation and cause release of Ca^{2+} into the cytochrome where it is taken up by the mitochondria (Orrenius et al. 2003; Ron and Walter 2007). In the second, NO or ROS can disrupt the regulation of cytochrome *c* (cyt *c)*, an anti-apoptotic protein (Kvitt et al. 2011; Hawkins et al. 2013). Both pathways promote the release of cyt *c*, initiating caspase activity and leading to host cell apoptosis by widespread protein degradation (Kvitt et al. 2016; Man and Kanneganti 2016; Ricaurte et al. 2016). Alternately, host cell detachment occurs where entire host cells containing symbionts are released from temperature-stressed cnidarians (Gates et al. 1992;

Bieri et al. 2016). This mechanism lacks strong evidence, however, and may be the downstream result of the PCD pathways (Weis 2008; Bieri et al. 2016; Oakley and Davy 2018).

Autophagy is the controlled destruction of obsolete cellular structures and begins with the identification of target structures, which are enveloped in phagocytic vacuoles generated by the ER or Golgi (Dunn et al. 2007) to become an autophagosome, which then fuses with a lysosome containing digestive enzymes (Dunn et al. 2007; Hanes and Kempf 2013). In some cases, autophagic digestion results in the death of entire host cells (Dunn et al. 2007; Paxton et al. 2013). Symbiophagy is the degradation or consumption of symbionts within the host cells *via* autophagic pathways (Downs et al. 2009). As noted in **Section 1.1.4**, the symbiosome is an arrested phagosome, and symbiophagy may involve the reactivation of the phagocytic pathway e.g., *via* Rab marker signalling to the symbiosome membrane (Chen et al. 2003; 2005; Downs et al. 2009; Mohamed et al. 2016). Finally, exocytosis occurs where whole symbiont cells are expelled from the host cells into the gastrovascular cavity and out of the mouth, and occurs normally as a mechanism to control symbiont populations in many cnidarians (Baghdasarian and Muscatine 2000; Weis 2008; Starcevic et al. 2010). The relative contributions of these different mechanisms to the bleaching process are debated, however exocytosis, apoptosis and symbiophagy likely play significant roles (Dunn et al. 2007; Starcevic et al. 2010; Hanes and Kempf 2013; Bieri et al. 2016; Dani et al. 2016; Roberty and Plumier 2022).

1.2 Effects of ocean acidification

1.2.1 Effects on marine organisms

The potential effects of OA on reef-building organisms were raised over 20 years ago (Kleypas et al. 1999) and have generated an expansive and rapidly growing body of literature (e.g., Sabine et al. 2004; Raven et al. 2005; Fabry et al. 2008; Doney et al. 2009; Veron et al. 2009; Hofmann et al. 2010; Boyd et al. 2016; Browman 2016; Cornwall et al. 2019; 2021). OA is suggested to be detrimental for calcifying larvae due to their small and fragile skeletons (Kurihara 2008). Mollusc larvae may be particularly at threat given their exposed external shells, although again, some species show little to no effect (Kroeker et al. 2013; Chan et al. 2016; Kelly et al. 2016; Aranda and Manzano 2017). Crustose coralline algae (CCA) are a critical contributor to reef accretion and binding, and there is strong evidence of susceptibility to a reduced pH (Diaz-Pulido et al. 2012; Cornwall et al. 2018;

2019), although responses may be species-specific and tolerance to low pH over generations has been observed (Comeau et al. 2018; Cornwall et al. 2020). CCA provide preferred substrate for coral settlement, and OA-driven declines may have a depleting effect on coral recruitment, both by limiting substrate availability and reducing settlement cues (Fabricius et al. 2017; Cornwall et al. 2018; 2019). Larval settlement and metamorphosis may be reduced by up to 50% when exposed to photodamaged *vs.* healthy CCA, following the loss of both chemical and colour settlement cues (Webster et al. 2013; Fabricus et al. 2017). Further, reduced growth rates in coral recruits may result in them being outcompeted for space by larger benthic organisms, including algae, sponges and ascidians (Richmond et al. 2019).

1.2.2 Impacts on the cnidarian-dinoflagellate symbiosis

pH affects many inorganic compounds and, as such, OA-driven changes in pCO_2 can alter central physiological processes in the cnidarian-dinoflagellate symbiosis dependent on inorganic carbon species, including calcification and photosynthesis (Kleypas 1999; Hoegh-Guldberg 2007). As pH also plays a key role in cellular processes, OA has the potential to alter a wide array of physiological processes, including acid-base regulation, metabolism, cell-cycle regulation and apoptosis (Albright 2018). Effects on calcification are the most well-researched OA responses in symbiotic cnidarians, and reef-building corals in particular (Kornder et al. 2018). Scleractinian corals secrete their aragonite skeletons by elevating pH in the extracellular calcifying medium (ECM; pH_{ECM}) relative to adjacent seawater (Venn et al. 2013). This shifts carbonate chemistry in the ECM from HCO_3^- to CO_3^{-2}, increasing the aragonite saturation state (Ω_{arag}) and enhancing aragonite precipitation (Cohen and Holcomb 2009; McCulloch et al. 2012; Zoccola et al. 2015). The ECM underlies the calicoblastic epithelium (CE), which drives this pH_{ECM} increase *via* the removal of protons by Ca^{2+}ATPase (Allemand et al. 2011; Venn et al. 2011). Corals are able to calcify under moderately elevated pCO_2 by upregulating calcifying fluid pH, Ω_{arag} and Ca^{2+} concentration at the tissue-skeleton interface, through upregulated expression of genes involved in ion transport (Kaniewska et al. 2012; Vidal-Dupiol et al. 2013; Venn et al. 2013; Davies et al. 2016; DeCarlo et al. 2018). For example, at moderate pH decreases (to pH 7.8 or 7.4), Ca^{2+} and HCO_3^- transport to the ECM were reported to increase through upregulation of Ca^{2+} and HCO_3^- transporters in the corals *Pocillopora damicornis* and *Acropora millepora* (Kaniewska et al. 2012; Vidal-Dupiol et al. 2013). CA catalyses the

interconversion between HCO_3^- and CO_2, so is central to carbon supply for calcification, and was also reported to be upregulated under a moderate pH decrease (Leggat et al. 1999; Vidal-Dupiol et al. 2013). However, these results reversed at pH 7.2, likely identifying a tipping point beyond which corals could no longer compensate (Vidal-Dupiol et al. 2013). Calcification is an energetically costly process, consuming up to 30% of a coral's daily energy budget, with the energy required to maintain pH_{ECM} homeostasis under OA thought to increase this expenditure (Krief et al. 2010; Allemand et al. 2011; McCulloch et al. 2012; Venn et al. 2013). Upregulation of lipolysis and β-oxidation metabolic pathways has been observed under low pH conditions, indicating that corals may use fatty acid reserves to meet this demand (Vidal-Dupiol et al. 2013; Jiang et al. 2019). Further, a meta-analysis by Kornder et al. (2018) found that particulate food supply can ameliorate decreased calcification under elevated pH conditions, supporting this hypothesis (e.g., Edmunds 2011). It is possible that increased symbiont photosynthetic performance and translocation of photosynthetic products (see below) could offset these increased energetic costs under moderate pH decreases (Castillo et al. 2014; Tresguerres et al. 2017).

Photosynthesis is a fundamental aspect of cnidarian-dinoflagellate symbioses, however the effects of OA on photophysiology remain equivocal, with many remaining knowledge gaps (Hoadley et al. 2015; Comeau et al. 2016; Albright 2018; Jiang and Lu 2019; Herrera et al. 2021). Enhanced primary productivity – the balance between gross photosynthesis (P_g) and cellular respiration (R) – has been reported in several cnidarian-dinoflagellate symbioses exposed to increasing levels of pCO_2. In soft-bodied cnidarians, P_g, and to a lesser extent R, of the sea anemone *Anemonia viridis* significantly increased along a natural CO_2 gradient (Suggett et al. 2012), with similar results seen in the sea anemones *Anthopleura elegantissima* (Towanda and Thuesen 2012) and *Exaiptasia diaphana* (formerly *Exaiptasia pallida*; Gibbin and Davy 2014) in laboratory experiments. In corals, high pCO_2 increased P_g in *Stylophora pistillata* (Reynaud et al. 2003), *Porites* sp., *A. millepora*, and *P. damicornis* (Strahl et al. 2015), and 11 out of 12 species (Biscere et al. 2019), where again increases in P_g outweighed those of R. These reports of enhanced endosymbiont productivity under elevated pCO_2 suggest that increased DIC availability has a 'fertilisation effect', alleviating carbon limitation at the Calvin-Benson cycle and facilitating increased photosynthetic rates (Suggett et al. 2012; Towanda and Thuesen 2012; Jarrold et al. 2013). However, such effects may be timescale dependent. A meta-analysis of 11 studies found that the effect of CO_2 on coral photosynthesis was non-significant

(Kroeker et al. 2013), with some studies over short time periods (<14 days) reporting nil effects on P_g and R in coral species (Schneider and Erez 2006; Crawley et al. 2010; Comeau et al. 2016) and *A. viridis* (Jarrold et al. 2013). Conversely, longer term exposure and higher levels of pCO_2 (>1000 µatm) have resulted in significant declines in photosynthetic rates and efficiency, with either no effect (Reynaud et al. 2003; Anthony et al. 2008) or a decrease (Kaniewska et al. 2012) in R. These results suggest a threshold and/or duration of elevated pCO_2 beyond which physiological performance cannot be supported, and/or varying capacity between species to regulate their physiology under OA (McCulloch et al. 2012; Comeau et al. 2016). An initial increase in R may be due to higher energetic costs of functioning under OA conditions, for example active cross-membrane transport or increasing costs of calcification (McCulloch et al. 2012; Tresguerres 2017). Equally, the decrease in R seen at higher pCO_2 levels may indicate that thresholds have been reached and signal the onset of metabolic depression (Pörtner et al. 2004), as discussed further below.

A shift in available carbon species towards more easily diffusible CO_2 has been suggested to reduce the need for host CCMs, reducing associated energetic costs (Krief et al. 2010; Hoadley et al. 2015). Downregulation of CA activity has been reported in the anemone *A. viridis* at high pCO_2 sites (30% decrease *vs.* control sites; Ventura et al. 2016), in the coral *A. millepora* (decreases of 27% at 750 µatm and 53% at 1000 µatm; Moya et al. 2012), and in Symbiodiniaceae-zoanthid associations under high pCO_2 (~584 µatm and ~1003 µatm; Graham et al. 2015). Given the key role of CAs in pH homeostasis (see below), this reduction could provide an adaptive mechanism to mitigate low pH (Ventura et al. 2016). However, multiple CAs exist with different functional roles which are still being elucidated (Hopkinson et al. 2015; Zoccola et al. 2016; Herrera et al. 2021). Downregulation of DIC uptake-related genes in Symbiodiniaceae has also been observed in response to elevated pCO_2, which supports the theory that endosymbionts rely on passive diffusion of CO_2 across the symbiosome membrane (Ventura et al. 2016; Lin et al. 2018). Variable effects on photosynthetic parameters are reported in *ex hospite* Symbiodiniaceae, however elevated pools of amino acids, fatty acids and carbohydrates suggest compensatory upregulation of metabolic and homeostatic processes (Hill et al. 2019; Jiang and Lu 2019). These results suggest that physiological performance may be maintained under moderate OA conditions, due to high physiological plasticity in both partners, but that this is likely an acclimation response rather than a beneficial effect of OA (Jarrold et al. 2013; Jiang and Lu 2019; Herrera et al. 2021).

Photosynthetic performance may also be altered by changes in symbiont density and chlorophyll *a* (chl *a*) content under OA conditions. Several studies have reported a reduction in Symbiodiniaceae density in conjunction with an increase in chl *a* content *per* symbiont cell, resulting in overall maintenance of P_g rates and suggesting higher productivity at lower pH levels (Anthony et al. 2008; Krief et al. 2010; Jarrold et al. 2013; Tremblay et al. 2013; Ventura et al. 2016; Mason 2018; Ge et al. 2021). Additionally, Crawley et al. (2010) reported increases in chl *a* under acidified conditions without a change in symbiont cell density, suggesting that this is due to release from carbon limitation (Wooldridge 2009). It is suggested that, as symbiont density is controlled by the host, such increased productivity under elevated pCO_2 may lead to symbiont expulsion to prevent damage and maintain 'steady state' levels (Baghdasarian and Muscatine 2000; Towanda and Thuesen 2012; Jarrold et al. 2013). Decreasing symbiont density under OA is not universal among symbiotic cnidarians however (Mason 2018). *E. diaphana* exposed to intermediate (~690 μatm) and high (~1460 μatm) levels of CO_2 exhibited 32% and 81% increases respectively after two months of incubation *vs.* ambient pCO_2 (Gibbin and Davy 2014), with similar results reported for *A. viridis*, with a four-fold increase in cell density at CO_2 vents (~1430 μatm) *vs.* control sites (~300 μatm) (Suggett et al. 2012). Similarly, Symbiodiniaceae cell density in polyps of the jellyfish *Cassiopea* sp. was 39% higher at low pH than in ambient conditions, with a corresponding increase in chl *a per* symbiont cell (Klein et al. 2017). It may be that increased CO_2 availability as a substrate for photosynthesis can increase symbiont cell populations in host tissues (Wooldridge 2009). However, the expulsion of proliferating symbionts observed in some cases and not others suggests species-specific responses of one or both partners (Brading et al. 2011; Gibbin and Davy 2014; Tansik et al. 2017; Herrera et al 2021).

Combined, such shifts in photophysiology may mean that, for species able to exhibit physiological plasticity, maintenance or increase of photosynthetic performance results in increased translocation of photosynthate to help mitigate the increased metabolic costs of OA (Brownlee 2009; McCulloch et al. 2012; Venn et al. 2013; Gibbin and Davy 2014). While this supports the carbon budget of the host, there is some evidence that this comes at the expense of symbionts acquiring carbon for their own needs (Tremblay et al. 2013). Where decreasing P_g *per* symbiont cell does occur, this may lead to a reduction in photosynthate translocated to the host (Kaniewska et al. 2012). Hoadley et al. (2015) tested this effect in three symbiont strains in the sea anemone *E. diaphana* and found increased translocation rates for two, with a loss in cell density for the third strain that counteracted any potential

gain in photosynthate *per* symbiont cell contributed to the host. If sustained, such suboptimal nutritional exchange may ultimately lead to dysbiosis (Wooldridge 2009; Davy et al. 2012; Matthews et al. 2017).

Photosynthetic performance is closely linked with the ability of host cells to maintain intracellular pH (pH_i) under elevated pCO_2 (Gibbin et al. 2014; Ventura et al. 2016). pH_i regulation is critical for most aspects of cell metabolism, including membrane functioning, ion transport, enzyme regulation and intracellular signalling, as well as DNA, RNA and protein synthesis (Madshus 1988; Venn et al. 2009). Additionally, optimal pH_i levels are specific to given metabolic pathways, requiring tight control to balance these differing functional needs (Casey 2010; Tresguerres et al. 2017). This is particularly the case for calcifying corals, as while photosynthesis requires an acidic pH to ensure the speciation of DIC into CO_2 – which consumes H^+ – calcification requires an alkaline pH for CO_3^{2-} formation, which generates H^+ (Venn et al. 2009; Tresguerres et al. 2017). Cnidarians experience significant daily fluctuations in external pH from the metabolism of reef-associated organisms, tides and upwellings, as well as metabolic activity of both host and symbiont (Doney 2009; Gibbin and Davy 2013; Barott et al. 2017; Cornwall et al. 2018). Photosynthesis, and respiration of both partners, can drive wide variations in cnidarian extracellular pH (pH_e), which can range from pH 8.9 during the day to pH 7.4 at night (Laurent et al. 2013; 2014). pH_i regulation is also important for calcifying corals to achieve aragonite precipitation, a process becoming increasingly costly under OA conditions (Jokiel 2011; Venn et al. 2013).

Deviations from optimal pH_i, known as cellular acidosis, can lead to dysfunction of these processes with serious physiological implications (Pörtner et al. 2004; Fabry et al. 2008; Kaniewska et al. 2012). Even small decreases in pH_i (0.1–0.2 units) can lead to metabolic depression, and while many cnidarians can endure short-term acidosis, ongoing suppression can result in decreased fitness (Pörtner et al. 2004; Fabry et al. 2008; Kaniewska et al. 2012; Moya et al. 2012; Glazier et al. 2020). Accordingly, pH_i regulation is tightly controlled, with acute, localised pH_i fluctuations managed through passive intracellular buffering by proteins, phosphates and CO_2/HCO_3^-, while active transmembrane ion transport mitigates longer-term deviations (Boron 2004; Casey 2010; Laurent et al. 2014). Changes in cnidarian pH_i are sensed by soluble adenylyl cyclase (sAC), an evolutionarily conserved HCO_3^--sensitive enzyme that produces the secondary messenger molecule cyclic AMP

(cAMP) (Buck et al. 1999; Chen et al. 2000). sAC can sense HCO_3^-, pH and pCO_2, so is a key component of the cnidarian response to acid-base stress and OA, with the potential to mediate multiple homeostatic mechanisms in response to pH disturbances (Barott et al. 2017). The specific proteins that sAC controls to regulate pH_i are unknown, however likely candidates include Na^+/H^+-exchangers, V-H^+-ATPases, Na^+/K^+-ATPases and voltage-gated proton channel (HvCN) families (Barott et al. 2017; Capasso et al. 2021). Elevated pH_e resulting from OA can create H^+ gradients, leading to passive CO_2 diffusion into the cell and/or limits on R-generated CO_2 diffusing out of the cell. The resultant conversion of CO_2 into HCO_3^- and H^+ can drive acidosis (Laurent et al. 2014; Tresguerres et al. 2017). Na^+/H^+-exchangers and V-H^+-ATPases have been identified as membrane transporters capable of transporting H^+ against a concentration gradient (Laurent et al. 2014; Barott et al. 2015; Capasso et al. 2021).

Upregulation of H^+ transport pathways and ATP synthesis-coupled H^+ transport genes have been reported in corals maintained at low pH, suggesting that upregulation of H^+ transport is a key component of the cnidarian response to OA (Kaniewska et al. 2012; Davies et al. 2016). OA-driven changes in H^+ gradients may result in increased energetic costs given a greater reliance on active H^+ transport out of the cell (Laurent et al. 2014). In CO_2 addition experiments, Gibbin et al. (2014) observed that, while pH_i of symbiotic host cells showed a full recovery to control levels within 105 min of CO_2-addition, pH_i of aposymbiotic host cells did not make the same recovery. Further, symbiotic host cell recovery was negated with the addition of the photosynthesis-inhibitor DCMU, confirming the key influence of symbionts on both the pH_i and intracellular buffering capacity of host cells in response to CO_2-induced pH changes (Gibbin and Davy 2013; Gibbin et al. 2014). Symbiont photosynthesis results in alkalinisation of the host cell through uptake of excess CO_2 and H^+, which may benefit the host through reduced exposure to acidosis and/or enhanced translocation of photosynthate to meet the increased energetic costs of pH_i regulation (Venn et al. 2009; Gibbin et al. 2014).

The upregulation of mitochondrial ATPase transcripts has been reported for the coral *A. millepora* under OA stress (Kaniewska et al. 2012). Cellular apoptosis is often preceded by an increase in mitochondrial ATPase activity, resulting in potassium influx, caspase activation and ultimately cell death (Kaniewska et al. 2012). Tellingly, anti-apoptotic responses have been reported under decreased

pH. Bcl-2 proteins and HSPs, which regulate apoptosis, were upregulated in juvenile *A. millepora* (Moya et al. 2015) and *A. viridis* (Urbarova et al. 2019), suggesting that anti-apoptotic molecules may play an important role in mitigating OA-driven cell loss (Kvitt et al. 2011). However, the opposite response was reported by Kaniewska et al. (2012) for adult *A. millepora*, suggesting species- and/or life stage-specific responses, or that longer term exposure to decreased pH may overwhelm these anti-apoptotic mechanisms, possibly due to host mitochondrial impairment (Kaniewska et al. 2012; Rocker et al. 2015; Urbarova et al. 2019).

1.2.3 Interactive effects of climate change

Investigation into the combined effects of climate change stressors is a growing area of research. The effects of OA on OW-driven declines in symbiont density have yet to be resolved (Mason 2018). Responses have been variable, including no effect (Crawley et al. 2010; Baghdasarian et al. 2017) or additive reductions (Anthony et al. 2008; Kaniewska et al. 2015; Hoadley et al. 2016b). Increases in photosynthetic performance and chl *a* content have been recorded under moderate increases in temperature and pCO_2, but are lost under highly elevated pCO_2 (Crawley et al. 2010; Kaniewska et al. 2015; Hoadley et al. 2016; Baghdasarian et al. 2017), including in the thermally tolerant symbiont *Durusdinium trenchii* (Hoadley et al. 2016b). This initial increase may be due to enhanced CCMs and capacity of Symbiodiniaceae to take up DIC under moderate temperature increases (Oakley et al. 2014). These findings give a mixed picture under moderate OA/OW but suggest that any ameliorative effects will be lost under conditions predicted for 2100 (Kornder et al. 2018).

OA has been shown to increase ROS generation and induce oxidative stress in cnidarians (Luz et al. 2018; Urbarova et al. 2019). Stress responses may include upregulation of HSPs, molecular chaperones, and glucose-regulated proteins involved in ER stress, UPR and suppression of caspase activation (Kaniewska et al. 2012; 2015; Moya et al. 2015; Urbarova et al. 2019). These point to upregulation of host innate immune responses and apoptotic processes under combined OA/OW stress (Kaniewska et al. 2015; Urbarova et al. 2019). Further, expression of phosphoglycolate phosphatase (PGPase), the enzyme that removes phosphoglycolate from symbiont chloroplasts during photorespiration, may be reduced at elevated pCO_2 (1160–1500 µatm; Crawley et al. 2010). The resulting build-up of phosphoglycolate inhibits both carbon fixation at the Calvin-Benson cycle and photorespiration (Crawley et al. 2010; Iguchi et al. 2012). As such, a decrease of PGPase may

result in increased ROS production, subsequent oxidative stress and symbiont loss (Crawley et al. 2010; Iguchi et al. 2012).

Thermal stress and resulting photosynthetic dysfunction may induce cellular acidosis under OA conditions and can impair the host's ability to recover from low pH_i, so prolonging the physiological impacts of acidosis (Gibbin et al. 2014; 2015; Davies et al. 2016; Innis et al. 2021). Similar responses across various species – *E. diaphana* (Gibbin and Davy 2014), *P. damicornis*, *Montipora capitata* (Gibbin et al. 2015) and *Siderastrea siderea* (Davies et al. 2016) – suggest a universal response to OA/OW stress. Genes associated with the transport and exchange of Ca^{2+} and other ions are tightly regulated under pH fluctuation and may be involved in acid-base regulation (Lin et al. 2018). Downregulation of Ca^{2+}-binding proteins and protein-folding transcripts has also been observed at low pH, indicating that OA contributes to mitochondrial dysfunction and UPR, which are already elevated under temperature stress (Dunn et al. 2012; Kaniewska et al. 2012; Dimons et al. 2019).

Several studies have reported gene regulation consistent with increased energetic costs under OA/OW stress. Increased expression of genes encoding for cellular respiration, ion-transport and energy-production proteins at low pH suggest increased metabolic demands under OA stress (Vidal-Dupiol et al. 2013; Davies et al. 2016). Likewise, thermal stress leads to upregulation of wide-ranging cellular processes, leading to a shift in metabolic activity and increased ATP demand to deploy and maintain stress responses (Gibbin et al. 2015; Lin et al. 2018). In addition to photosynthate transfer, host fitness, lipid and protein content, tissue biomass and changes in fatty acid metabolism may promote resistance to environmental stress (Gibbin et al. 2015; Strahl et al. 2015; Camp et al. 2018; Anderson et al. 2019). Increased catabolism of host lipid and starch stores has been widely reported during the onset of dysbiosis (Grottoli et al. 2004; Davies et al. 2016; Hillyer et al. 2017; Anderson et al. 2019). Genes involved in lipolysis and β-oxidation pathways have been reported to be upregulated in response to OA, also suggesting tissue reorganisation and the catabolism of fatty acid reserves (Kaniewska et al. 2012; Wall et al. 2017). As energetic costs increase, this may lead to trade-offs between energy-demanding processes, including pH homeostasis, UPR, antioxidant production and ROS scavenging (Kaniewska et al. 2015; Jiang et al. 2019). In stony corals, energy may be preferentially diverted towards calcification (Wall et al 2017; Jiang et al. 2019). At low pH this leads to reduced oxidative metabolism and capacity to generate ATP and NADPH, inducing metabolic

depression (Kaniewska et al. 2015; Moya et al. 2012). Coupled with decreased biomass, this may have wide-reaching effects on coral performance, including the ability to survive or recover from bleaching events (Kaniewska et al. 2015; Wall et al. 2017).

The mechanisms discussed above indicate the potential range of physiological responses among cnidarian-dinoflagellate symbioses to climate change stressors. These variable and often contradictory results indicate that responses may vary according to species, genotype and the adaptive capacity of both partners, as well as life-stage, exposure duration and history (Weis 2010; Kornder et al. 2018; Albright 2018; McLachlan et al. 2020). The cellular mechanisms underpinning these responses are only beginning to be unpicked and will provide a more detailed understanding of likely adaptations or dysbiosis resulting from climate change (Weis 2008; Oakley and Davy 2018; Apprill 2020).

1.3 Research tools

1.3.1 The Aiptasia model system

The sea anemone *Exaiptasia diaphana* (formerly *Exaiptasia pallida;* commonly referred to as 'Aiptasia'; **Figure 1.4a**) is an ideal model system to study the cnidarian-dinoflagellate symbiosis due to its tractability, rapid growth and ability to live in an aposymbiotic (i.e., symbiont-free) state (**Figure 1.4c,d**) (Weis et al. 2008; Baumgarten et al. 2015). Due to these characteristics, Aiptasia is becoming increasingly well established as a model organism and allows the study of the likely effects of future climate change scenarios over much shorter timescales than would be possible with coral species, due to the difficulty in maintaining corals in laboratory settings and their slow growth rates (Lehnert et al. 2012; Weis 2019). This allows proof-of-concept, where research findings can then inform further work, for example in classic coral study organisms such as *Acropora* species (Pernice et al. 2011; Shinzato, 2011; Hawkins et al. 2014).

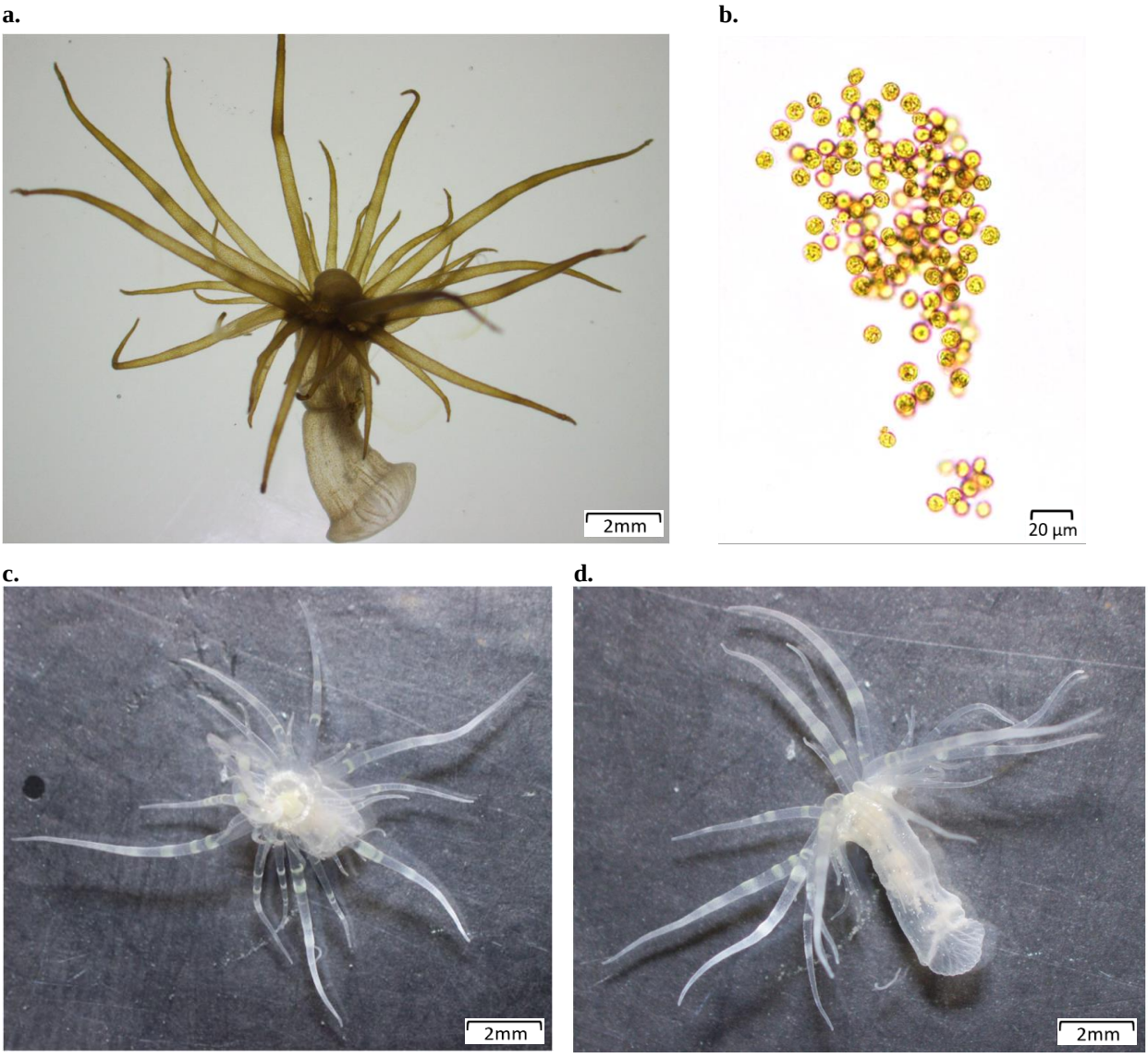

Figure 1.4: The Aiptasia model system. a. Aiptasia in symbiosis with its native symbiont *Breviolum minutum*, illustrating the patchy distribution of symbiont cells around the gastrovascular cavity and more dense distribution throughout the tentacles. **b.** *B. minutum* cells freshly isolated from the host; Aposymbiotic Aiptasia, **c.** dorsal and **d.** lateral views. Photos: J. Bown.

As Aiptasia can live in an aposymbiotic state, it allows researchers to isolate the effects of symbiosis in comparison to symbiont-free (i.e., aposymbiotic) specimens. This feature has been invaluable in elucidating the cellular mechanisms underlying processes of coral bleaching and partner specificity, as well as symbiosis establishment and host-symbiont regulation (Starzak et al. 2014; Bucher et al. 2016; Gabay et al. 2019; Kishimoto et al. 2020). Further, Aiptasia associates with *Breviolum minutum* (**Figure 1.4b**) as its native symbiont across its Indo-Pacific range, yet also harbours other symbiont

genera (Thornhill et al. 2013). As such, this anemone is able to take up multiple symbiont types under laboratory conditions, though this occurs at lower densities and with apparent fitness costs to the host due to suboptimal nutrient exchange (Matthews et al. 2017; Gabay et al. 2019; Tortorelli et al. 2020). While Aiptasia shares many characteristics with coral species, as a soft-bodied cnidarian it is a non-calcifying organism. This is an advantage as it allows the examination of the impacts of reduced pH on physiological processes without the potential influence of calcification regulation as discussed in **Section 1.2.2** (Suggett et al. 2012; Towanda and Thuesen et al. 2012; Gibbin and Davy 2014), and greatly facilities the discrete examination of non-calcification processes at the cellular level (Lehnert et al. 2012). There is now an extensive range of omics resources available for Aiptasia, including at the level of the genome (Baumgarten et al. 2015), transcriptome (Sunagawa et al. 2009; Lehnert et al. 2012) and increasingly, proteome (e.g., Oakley et al. 2016; 2017; Sproles et al. 2019) and metabolome (e.g., Hillyer et al. 2016; Matthews et al. 2017), allowing the linking of phenotype expression to genetic traits.

1.3.2 The power of proteomics

As noted above, there are still many unanswered questions regarding the cnidarian-dinoflagellate symbiosis. However, a focus on molecular and cell biology over the last decade is helping to elucidate some of the key underpinning processes of symbiosis and dysbiosis (Weis et al. 2008; Davy et al. 2012; Oakley and Davy 2018; Weis 2019; Rosset et al. 2021). The increasing availability of genetic resources is allowing researchers to take a systems biology approach to understanding cellular processes and the networks they may be involved in (Lehnert et al. 2012; Meyer and Weis 2012; Cooper 2019). A rapidly evolving body of genomic and transcriptomic resources are now available for cnidarians (Sunagawa et al. 2009; Shinzato et al. 2011; Lehnert et al. 2012; 2014; Baumgarten et al. 2013; 2015; Vidal-Dupiol et al. 2013; Mohamed et al. 2016; González-Pech et al. 2017; Li et al. 2018; Vargas et al. 2021), and increasingly for Symbiodiniaceae (Sunagawa et al. 2009; Bayer et al. 2012; Shoguchi et al. 2013; Lin et al. 2015; 2018; Aranda et al. 2016). Invaluable in their own right to understand the structure, function, evolution and expression of genomes, they also increase the ability of other "omics" approaches to provide a functional understanding of cnidarian-dinoflagellate symbioses at the molecular level and so unpick changes at the phenotype level, for example in response to environmental stressors (Weis et al. 2008; Chaston and Douglas 2012; Meyer and Weis 2012; Oakley and Davy 2018). Transcriptomic work has helped to elucidate changes in gene

expression of the coral *Acropora digitifera* early in the establishment of symbiosis, providing further support for symbiosis as an arrested immune response (Mohamed et al. 2016). Several studies (discussed in **Section 1.2.2**) have explored the transcriptomic response of cnidarians and cnidarian-algal interactions to altered pH levels (Kaniewska et al. 2012; Vidal-Dupiol et al. 2013; González-Pech et al. 2017; Li et al. 2018; Vargas et al. 2021). Metabolomic studies, involving the large-scale study of metabolites, have identified changes to central metabolism, oxidative state, cell structure, biosynthesis and signalling in both partners in response to thermal stress (Hillyer et al. 2016; 2017). Metabolomics also revealed underlying impacts of OA conditions on B. minutum – despite limited effect on photosynthetic parameters (see **Section 1.2.2**), acidification affected biosynthesis of amino acids and proteins and thereby inhibited growth rate (Jiang and Lu 2019).

While genomes and transcriptomes provide a high-level understanding of cell dynamics, it is proteins that carry out cellular activities. Proteomics involves the large-scale study of the structure and function of proteins, including identifying and quantifying what proteins are actually expressed, whereabouts in the cell they are located and clues as to the network of interactions that they are involved in (Wilkins et al. 1996; Cooper 2019). This allows a detailed understanding of biological systems at a given time-point to answer specific biological questions (Aebersold and Mann 2003; Vaudel et al. 2014). Although limited by the availability of gene and protein information currently available, existing work has provided insight into the proteins involved in the cnidarian-dinoflagellate symbiosis. These include the regulation of host proteins involved in nutrient exchange, metabolic processes, ROS mediation, cell recognition, cell cycling, and immune responses dependent on symbiotic state and partner suitability (Peng et al. 2010; Oakley et al. 2016; Sproles et al. 2019), and the profiling of the skeletal organic matrix proteins involved in calcification (Ramos-Silva et al. 2013). Exploratory work of key elements of symbiont proteomes is also underway; for example the characterisation of cell wall proteins in *B. minutum* and *Cladocopium goreaui* (Tortorelli et al. 2021). Armed with such information, researchers are investigating potential climate change responses. For example, a comparative study of bleached *vs.* unbleached *Acropora palmata* following a mass bleaching event identified significant upregulation of proteins involved in heat- and UV-stress responses and apoptosis, and downregulation of proteins involved in immunity, biomineralization, cytoskeletal organisation, and endo-exophagocytosis (Ricaurte et al. 2016). Thermal shock was also found to result in proteome disruption in Aiptasia, including proteins involved in central metabolism,

protein folding and synthesis, and redox homeostasis (Oakley et al. 2017). These studies illustrate the power of proteomics to reveal the detailed cellular mechanisms underlying responses to climate stressors.

1.4 Aims and objectives

The effects of OA on the cnidarian-dinoflagellate symbiosis remain equivocal (Browman 2016; Kornder et al. 2018). Moreover, very few studies have explored the effects of OA on the establishment phase of the cnidarian-dinoflagellate symbiosis, and these provide a mixed picture. For example, some report no discernible effect of OA (Sun et al. 2020; Jiang et al. 2021), while others report delayed colonisation (Suwa et al. 2010) or reduced symbiosis establishment success (Noonan et al. 2013). More is known about the effects of OA on maintenance of the symbiosis, including changes in photosynthesis and respiration (Suggett et al. 2012; Towanda and Thuesen 2012; Gibbin and Davy 2014; Strahl et al. 2016; Biscere et al. 2019), symbiont density (Anthony et al. 2008; Krief et al. 2010; Jarrold et al. 2013; Tremblay et al. 2013; Ventura et al. 2016; Klein et al. 2017; Mason 2018) and cellular homeostasis (Kaniewska et al. 2012; Gibbin et al. 2014); however reports are often contradictory across species. Unpicking the cellular mechanisms underpinning these observed phenotypic changes is key to improving our understanding of, and ability to predict responses to, stressors such as OA (Weis et al. 2008; Oakley and Davy 2018). Developing this understanding is increasingly critical as the rate of climate change increases (IPCC 2021), which in addition to the absolute degree of change, is critical to whether the delicate cnidarian-dinoflagellate symbiosis will be able to adapt or will break down under acidification stress.

This thesis therefore aimed to further understand the impact of OA on the establishment and maintenance of the cnidarian-dinoflagellate symbiosis.

Specific Objective 1 was to determine the impact of decreased pH on the ongoing health and maintenance of the cnidarian-dinoflagellate symbiosis. This research aimed to provide an understanding of the cellular mechanisms underlying any changes in host and/or symbiont physiology at the phenotype level, by measuring protein expression under decreased pH. As noted above, previous studies have suggested benefits conferred from symbiont to host under reduced pH (e.g.,

increased translocation of photosynthetic products), potentially providing some mitigation against acidification stress (McCulloch et al. 2012; Suggett et al. 2012; Towanda and Thuesen 2012; Venn et al. 2013; Gibbin and Davy 2014). Effects in symbiotic Aiptasia were therefore compared with observations in aposymbiotic Aiptasia, to distinguish the response of the host *vs.* the intact symbiosis. Responses in the dinoflagellate symbiont *B. minutum* were also assessed. I hypothesised that: 1) symbiont density and photosynthetic performance would increase as pH levels decreased; 2) proteomes would be differentially expressed under decreased pH, including the downregulation of proteins associated with CCMs and upregulation of proteins involved in metabolism, cellular homeostasis and transmembrane transport, and stress responses; and 3) stress-related proteins would be more abundant in aposymbiotic *vs.* symbiotic anemones, as photosynthetic products are not available to mediate the effects of exposure to low pH.

Specific Objective 2 was to establish whether decreased pH impacts the capacity of Aiptasia to acquire and establish a symbiosis with its native symbiont, *B. minutum*. Based on indications from the limited studies to date (Suwa et al. 2010; Noonan et al. 2013; but see Sun et al. 2020; Jiang et al. 2021), my hypotheses for this chapter were that: 1) exposure to decreased pH would reduce symbiont uptake and colonisation rate; and 2) there would be greater impact of low pH in the first few days of symbiosis than at later time points.

Disclaimer

The first study objective will be addressed in Chapter 2, while the second will be addressed in Chapter 3. These two chapters are structured as independent manuscripts, and as such there may be some repetition between chapters, especially in their introductions. Chapter 4 integrates the results of these two research chapters and positions the findings in context of the wider implications for corals and coral reefs.

Photo courtesy of Matthew Nitschke

Chapter 2: Effects of Ocean Acidification on the Cnidarian-Dinoflagellate Symbiosis: A Proteomics Approach

2.1 Introduction

Coral reefs are biologically diverse ecosystems and provide wide-ranging socioeconomic benefits to millions of people worldwide (Hoegh-Guldberg et al. 2007; Hughes et al. 2017). The foundation of these ecosystems is the symbiotic relationship between reef-building corals and their endosymbiotic dinoflagellate algae (Family: Symbiodiniaceae), which is based on nutritional exchange and the coordinated growth of both partners (Muscatine et al. 1981; 1984; Wooldridge 2009; Davy et al. 2012). The dinoflagellate symbionts translocate photosynthetically fixed carbon to their coral host, for example in the form of glucose, lipids and fatty acids, providing ~95% of the energy required to support host metabolism (Muscatine et al. 1984; Whitehead and Douglas 2003; Yellowlees et al. 2008; Burriesci et al. 2012). In exchange, the symbionts receive inorganic nitrogen, phosphorus and carbon, protection from herbivory and a high light environment (Venn et al. 2008; Davy et al. 2012). This delicate symbiosis tolerates a narrow range of environmental conditions and is becoming increasingly threatened by the effects of climate change, including ocean warming, ocean acidification (OA) and sea level rise (Doney et al. 2009; Hughes et al. 2017; Cornwall et al. 2019; 2021).

The world's oceans have absorbed around one third of anthropogenic CO_2 since pre-industrial times, causing warmer and more acidic waters and altering seawater carbonate chemistry (IPCC 2019; Sabine et al. 2004; Doney et al. 2009; 2020). Further declines in surface water pH levels of up to 0.4 pH units are predicted by 2100 (IPCC 2019). These shifts have wide ranging effects on marine organisms and are of particular concern for corals due to their ecological importance (Fabry 2008; Doney et al. 2020). Stony corals are calcifying reef builders, laying down calcium carbonate ($CaCO_3$) skeletons reliant on internal carbonate ion availability, which is compromised by OA due to reduced seawater pH (Kleypas 1999; Feely 2004). Many studies have reported detrimental impacts of OA on the coral holobiont (i.e., the intact symbiosis), including to calcification, growth and metabolism, as well as cellular acidosis due to decreased pH and changes in available carbon species (e.g., McCulloch et al. 2012; Kaniewska et al. 2012; Venn et al. 2013; Vidal-Dupiol et al. 2013). However, variable

responses have been reported across different cnidarian-dinoflagellate associations, providing a complex and incomplete picture of OA impacts (Anthony et al. 2008; Suggett et al. 2012; Gibbin and Davy 2014; Klein et al. 2017; Mason 2018; Biscere et al. 2019; Doney et al. 2020). As such, a clear understanding of how OA affects the cnidarian-dinoflagellate symbiosis remains elusive (Tresguerres et al. 2017; Herrera et al. 2021; Lin et al. 2022).

Increasingly, molecular techniques have been used to further understand this complex issue. 'Omics' technologies offer insights into organism responses at the cellular level and have the potential to address wide ranging biological questions (Aebersold and Mann 2003; Vaudel et al. 2014; Oakley and Davy 2018; Weis 2019). Such investigations into OA effects lag far behind those into the impacts of thermal stress, and to date most have been transcriptomic analyses (e.g., Kaniewska et al. 2012; 2015; Vidal-Dupiol et al. 2013; Moya et al. 2015; Davies et al. 2016; González-Pech et al. 2017; Kenkel et al. 2017; Rivest et al. 2018; Urbarova et al. 2019; Herrera et al. 2021; Vargas 2021). These studies have reported differential expression of genes relating to biomineralization, acid-base regulation, cytoskeletal remodelling, respiration, symbiont interactions, immunity, and tolerance of stressors. Some have reported effects on gene expression prior to observable effects on physiological processes (e.g., calcification; Kaniewska et al. 2012). However, results obtained *via* transcript-based gene expression methods may not reflect actual protein abundance or post-translational modifications and so may not be an accurate representation of organism responses to OA (Zoccola et al. 2016; Kenkel et al. 2017; Wang et al. 2017; Cziesielski et al. 2018). This may particularly be the case for dinoflagellates, where responses have been observed to be more subtle, and to exhibit less congruency between mRNA expression and protein abundance (Feussner and Polle 2015; Morse et al. 2018). Further, most of these studies have focused on the cnidarian host, with a relative dearth of studies investigating the dinoflagellate symbionts (González-Pech et al. 2017; Kenkel et al. 2018; Rivest et al. 2018; Jiang and Lu 2019; Herrera et al. 2021).

Proteomics, the large-scale study of the structure and function of proteins, can provide data on what proteins are present and in what quantities, and clues as to the network of interactions that they are involved in (Wilkins et al. 1996; Cziesielski et al. 2018; Cooper 2019). To date, only one other proteomics study has explored the effects of OA on the cnidarian-dinoflagellate symbiosis. Lin et al. (2022) examined the acute response of the *Galaxea fascicularis* coral holobiont over 10 days'

exposure to low pH. They found differential abundance of proteins involved in key processes within the cnidarian-dinoflagellate symbiosis, including metabolic homeostasis, nutrient cycling and carbon budgets, signalling activity and host immune defences. Their analysis focused strongly on the observed metabolic interactions and suggested that maintaining and enhancing metabolic compatibility were key mechanisms operating as part of an early OA stress response (Lin et al. 2022). Notably, the indicative stress responses and upregulation of proteins involved in core biological pathways reported in this study, including metabolism, energy homeostasis, signalling activity and immune responses, share some commonalities with reported proteomic responses to thermal stress. Heat stress responses also include proteostasis disruption, potential protein synthesis inhibition and the triggering of antioxidant mechanisms (Ricaurte et al. 2016; Oakley et al. 2017; Cziesielski et al. 2018). Furthermore, proteomic studies of a wider range of marine animal and algal taxa indicate that these pathways may also form part of a more universal stress response to OA. For example, differential abundance of proteins involved in metabolism, immune, cellular stress and antioxidant responses, cytoskeletal processes, protein sorting and turnover, and signal transduction have been reported in abalone (Carroll and Coyne 2021), sea urchins (Migliaccio et al. 2019), shrimp (Chang et al. 2016) and oysters (Tomanek, et al. 2011; Timmins-Schiffman et al. 2014; Dineshram et al. 2015; Thompson et al. 2016). Similarly, under OA, photosynthesis of diatoms has been observed to decrease, alongside downregulation of proteins associated with energy production and homeostasis (Zhang et al. 2021; Jin et al. 2022).

To further understand the impacts of future OA conditions on the cnidarian–dinoflagellate symbiosis, this research characterised the physiological and proteomic responses of the sea anemone *Exaiptasia diaphana* (commonly referred to as ‘Aiptasia’) and its freshly isolated symbiont *Breviolum minutum* over 26 days’ exposure to either ambient (pH 7.95) or decreased pH (pH 7.68). Given the variable physiological responses observed to date, combining proteomic and physiological data enables multi-scale analysis of OA responses, and may provide biomarkers for future studies (Sogin et al. 2016). Aiptasia is a widely used model system for the cnidarian-dinoflagellate symbiosis (Weis et al. 2008; Lehnert et al. 2012; Thornhill et al. 2013; Baumgarten et al. 2015) that can be rendered and maintained symbiont-free (i.e., aposymbiotic) in the lab, so facilitating the study of the host and symbiont in isolation, as well as together in symbiosis. For OA research, this model system has the further advantage of allowing discrete examination of non-calcification effects (Lehnert et al. 2012; Suggett

et al. 2012; Towanda and Thuesen et al. 2012; Gibbin and Davy 2014). These can be challenging to unpick given their close inter-relationship with other fundamental elements of coral-dinoflagellate symbiosis physiology (Bertucci et al. 2011; Lehnert et al. 2012). Here, I measured the effects of OA on the proteome of the host, in both the symbiotic and aposymbiotic states, and, for the first time, the symbiont when in symbiosis. I hypothesised that: 1) symbiont density and photosynthetic performance in symbiotic anemones would increase as pH decreased as a result of greater CO_2 availability for photosynthesis; 2) the proteome of symbiotic anemones would be differentially expressed under decreased pH, with downregulation of proteins associated with carbon concentrating mechanisms (CCMs), again due to increased CO_2 availability, but the upregulation of proteins involved in metabolism and stress responses; and 3) stress-related proteins would be less abundant in symbiotic *vs.* aposymbiotic anemones, due to the ameliorating effects of photosynthetic CO_2 utilisation and the supply of photosynthetic products.

2.2 Methods

2.2.1 Experimental organisms

These experiments used a clonal stock of the symbiotic sea anemone Aiptasia (culture ID: NZ1), obtained from the Indo-Pacific region. Responses of Aiptasia and its native dinoflagellate symbiont *Breviolum minutum* (**Figure 1.4a,b)** were compared when in symbiosis with the response of aposymbiotic (i.e., symbiont-free) Aiptasia (**Figure 1.4c,d**). Anemones were rendered aposymbiotic *via* menthol bleaching, with the addition to anemone stock tanks of menthol in ethanol to a final concentration of 0.27 mM (Matthews et al. 2016). Aposymbiotic anemones were kept in the dark at 24 °C (± 0.5 °C) for 12 months prior to the experiment start date. Aposymbiotic status was confirmed in a 20% subsample *via* lack of chlorophyll autofluorescence under fluorescence microscopy (IX53, Olympus, Japan with X-Cite 120Q, Excelitas Technologies, USA; settings: FITC, magnification x10 and x20, ISO200). Symbiotic anemones were maintained under ~40 µmol photons m^{-2} s^{-1} photosynthetically active radiation (PAR) on a 12:12 h light:dark cycle (using 4 x 54W Master TLS HO bulbs, Philips, Holland) at 24 °C (± 0.5 °C) for three months prior to the experiment start date.

2.2.2 Experimental set-up

A custom built closed-loop CO_2 system was developed to run this experiment based on best practice guidance for OA experiments (Riebesell et al. 2010; Cornwall and Hurd 2016), as outlined in **Figure 2.1**. pH levels within this 100-L closed-loop system were controlled through the automated release of CO_2 gas, which acts to reduce seawater pH levels. Each header tank contained a Double Junction Lab Grade pH Probe connected to a control unit (1 x Apex EL Controller System and 5 x "extensions" i.e., PM1 pH/ORP Probe Modules) programmed within pH tolerance ranges *via* Apex Fusion software (all control system hardware and software Neptune Systems, USA). The Apex system controlled on/off solenoid valves (Autoline Industrial, New Zealand) which released food-grade CO_2 gas, with flow rate controlled *via* a regulator and flow meter (BOC, Australia). 10-L plastic header tanks contained water pumps to assist mixing and pH stability. In header tanks supplying seawater to experimental tanks in the ambient condition, air pumps passed through soda lime containers (Sofnolime™ 8-12 Mesh NI (Grade 797), Molecular Products Ltd, UK) to channel in CO_2-free air to increase pH levels.

Experimental tanks (*n* = 15 *per* treatment) consisted of food-grade plastic holding ~300 mL ASW (Sea Salt, Aquaforest, Poland), with three header tanks *per* pH level. Water flow from the header tanks was passive, with valves to control flow rate and passive outflow of water into the drainage tank. Water from the drainage tank was pumped back to the header tanks *via* a UV water steriliser (Vecton 600 V2, TMC, UK) to remove any expelled Symbiodiniaceae cells and minimise build-up of other organic matter, e.g., algae and bacteria. Experimental tanks were sealed to avoid cross-contamination of aposymbiotic Aiptasia by expelled symbionts from symbiotic Aiptasia. The set-up was situated in a temperature-controlled room maintained at 24 °C (± 0.5 °C). Lighting was on a 12:12 h light/dark cycle at 40 ± 5 µmol photons m^{-2} s^{-1} (PAR) (4 x 54 W Master TLS HO bulbs, Philips, Holland). Artificial seawater (ASW) was used in the experimental system to minimise build-up of organic material. ASW (Sea Salt, Aquaforest, Poland) was made up with ddH_2O to salinity 35 ppt and pH 8.28 at 24 °C.

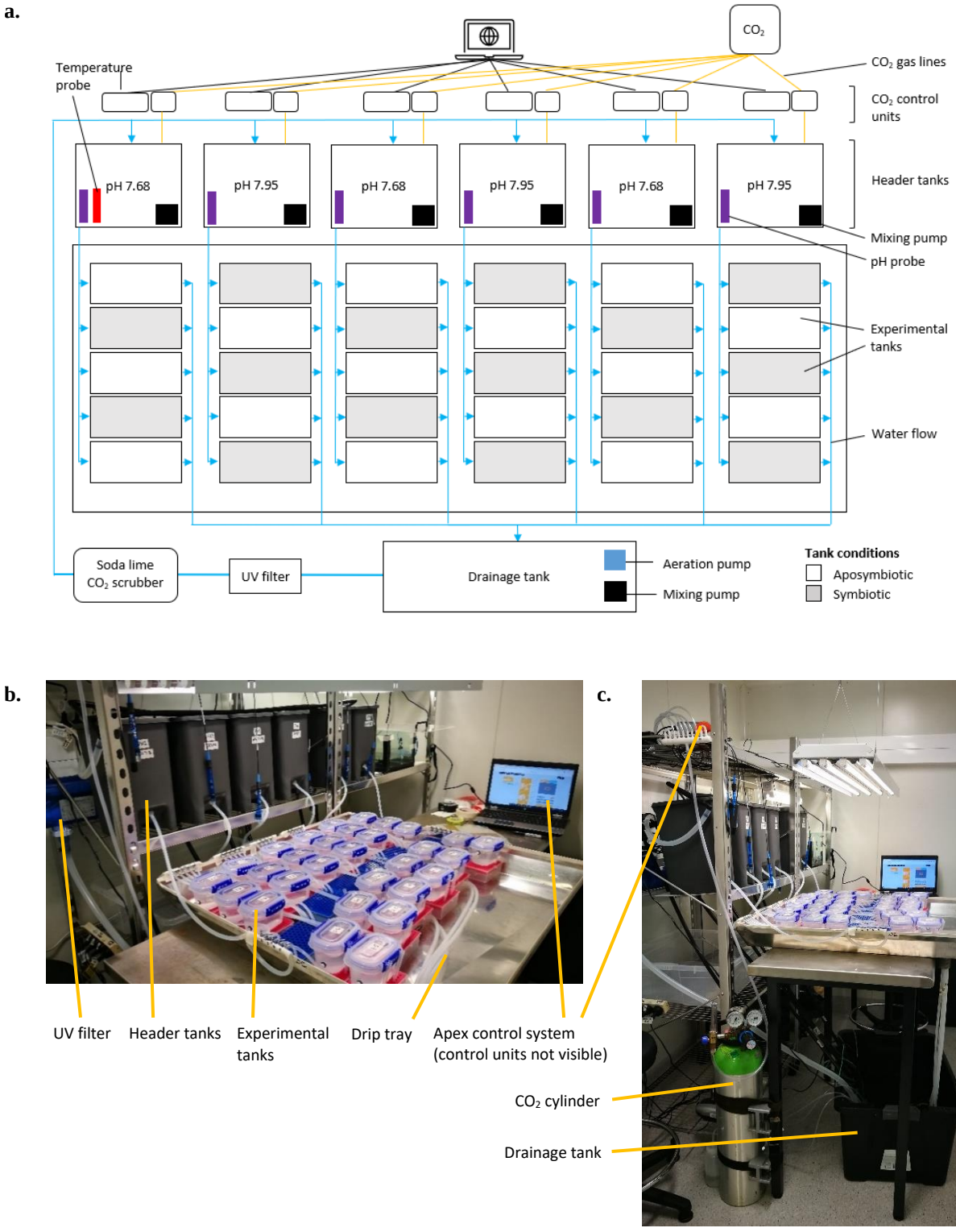

Figure 2.1: Experimental set-up schematic. a. Schematic showing distribution of OA treatments. Yellow lines indicate gas flow; blue lines indicate water flow. For details see **Section 2.2.2**; **b.** and **c.** Photos of the experimental set-up.

This experimental set-up had several features designed to minimise non-treatment effects and interdependence within treatments. To minimise non-treatment effects being confused with treatment effects, all experimental units of all treatments were housed in the same room in a single drip-tray, outflowing into a single drainage tank. ASW was added to the drainage tank from where it was pumped to the header tanks, providing a single water source prior to CO_2 manipulation. To reduce tank effects and interdependence within treatments, each header tank fed $n = 5$ experimental tanks in a systematically dispersed distribution of treatments (i.e., a mixture of tanks containing aposymbiotic and symbiotic anemones – see tank distribution, **Figure 2.1a**) (Hurlbert 1984; Cornwall and Hurd 2016). Variation in all other parameters was minimised as far as was practicable.

pH manipulation

Importantly, any changes in a single component of the seawater carbonate chemistry system will result in changes to several, if not all, other components (Gattuso et al. 2010; **Figure 1.3a**). To ensure relevance to the research question, pH manipulation therefore altered seawater chemistry in a way that simulates future OA, i.e., increasing total dissolved inorganic carbon (DIC_T) and keeping total alkalinity (A_T) constant (Gattuso et al. 2010; Cornwall and Hurd 2016). While the design was largely effective in providing the desired experimental conditions, the small scale of the system (total volume 100 L) led to difficulties in achieving optimum separation between pH levels due to a build-up of CO_2 within the experimental system and/or room. To counter this, the following measures were taken: 1) Regulation of CO_2 gas volumes released, using both a CO_2 regulator and flow meter. 2) Use of soda lime pumps in the ambient treatment header tanks, where air was pumped through soda lime (Sofnolime™ 8-12 Mesh NI (Grade 797), Molecular Products Ltd, UK) containers to channel in CO_2-free air to increase pH levels. 3) Regular topping up with ddH_2O to maintain salinity levels, with a small effect in increasing system pH (~0.01-0.02 pH units). 4) Addition of a protein skimmer in the drainage tank to aerate the water, raising system pH by ~0.02 pH units.

Experimental conditions

Two pH treatments, pH 8.05 and pH 7.68, were selected based on IPCC (2019) scenarios for 2100, where pH 8.05 corresponds to SSP1-1.9 (sustainability; most comparable to present day) and pH 7.68 corresponds to SSP5-8.5 (fossil-fuelled development; worst-case predicted scenario). Due its small scale, the system was unable to operate at the target levels of pH 8.05 (ambient) and pH 7.68 (low)

concurrently (see **Section 1.1.5**). Achieving a steady value of pH 7.68 in the "low" treatment resulted in an "ambient" treatment of pH 7.95, which is not uncommon in present day coral reef systems (**Section 1.1.5**; Cornwall et al. 2018; Sutton et al. 2019; Torres et al. 2021; Manzello et al. 2021). As such, this was considered a realistic control condition. Accordingly, for these experiments, the distribution of experimental tanks was: 1) for pH 7.95: n = 15 tanks and 2) for pH 7.68: n = 15 tanks, each containing 14 anemones (**Figure 2.1a**). To avoid pseudoreplication, experimental tanks were treated as the evaluation unit, with individual anemones classed as technical replicates (Hurlbert 1984; Cornwall and Hurd 2016). The initial experiment (Experiment 1) was designed to test the response of both symbiotic states (i.e., symbiotic and aposymbiotic) to the two pH levels simultaneously. However, due to cross-infection of aposymbiotic anemones during this first experiment, the aposymbiotic condition was excluded and later rerun as a second experiment (Experiment 2) with aposymbiotic anemones only.

2.2.3 Sampling and preparation of experimental organisms

Experimental organisms were acclimated to the target pH levels to mitigate any potential effects of pH shock (Kamenos et al. 2013; Munday et al. 2013; Munguia and Alenius 2013). Symbiotic and aposymbiotic anemones (n = 210 for both) were haphazardly distributed among pH treatments and introduced to the experimental system, before being allowed to settle for 48 h prior to pH ramping. For this, the pH of the tanks was reduced by 0.05 pH units *per* day to the target pH levels, followed by a two-week acclimation period. During the experiments, organisms were maintained at 24 °C (± 0.5 °C) under a standard light regime of 40 ±5 µmol photons m^{-2} s^{-1} PAR on a 12:12 h light:dark cycle (4 x 54W Master TLS HO bulbs, Philips, Holland). Anemones were fed once *per* week with freshly hatched *Artemia* sp. nauplii at around 17:00 h, with experimental tanks cleaned and a 50 L (i.e., 50%) ASW change the following morning.

System measures

During the acclimation period and duration of the experiment, measures of pH_T (hereafter, pH unless otherwise stated), A_T, salinity and temperature were taken every 2-3 days. In addition, at the beginning and end of each experiment, system measurements (temperature, salinity, pH and A_T) were taken every ~4 h over a 20 h period to assess any variances over the diel cycle. System measurements

during the two experiments are outlined in **Table 2.1** and **Figure 2.2a**, and pH values during the 20 h measurement cycles are outlined in **Figure 2.2b.** Tris buffers were made up to the standard recipe given in the *Guide to Best Practices for Ocean CO_2 Measurements* – SOP 6a (Dickson et al. 2007). Twice weekly during the experiment, mV was measured at ~2 °C intervals between 19-27 °C to obtain a standard reference curve, using a pH meter (Lab 850, Schott® Instruments, Germany). These seawater environmental parameters were measured through manual sampling of header tanks and experimental tanks three times *per* week, with three sets of measurements taken over the diel cycle to capture any variability due to photosynthesis and respiration (Hurd et al. 2009; McGraw et al. 2010). To confirm equivalence and stability of pH between header tanks and experimental tanks as water flowed through the system, measurements were taken from each header tank before and after measurements of its associated experimental tanks McGraw et al. 2010). In both experiments, mean pH was consistent across header and experimental tanks. All pH measurements were calculated from mV, temperature and salinity calibrated to bi-weekly Tris measurements, using the R package seacarb v3.3.0 (Gattuso et al. 2021).

Table 2.1: Experimental system parameters. Mean values and standard deviations (where applicable) of system parameters during the two experiments. pH_T and A_T are measured values, DIC_T and pCO_2 are calculated values. A_T, C_T = µmol kg^{-1}, pCO_2 = µatm.

Experiment 1 – symbiotic anemones

Treatment	Temperature	Salinity	pH_T	A_T	DIC_T	pCO_2
pH 7.95	24 ± 0.5 °C	35 ppt	7.95 ± 0.02	2243 ± 13	2009	505
pH 7.68	24 ± 0.5 °C	35 ppt	7.68 ± 0.03	2243 ± 13	2127	1031

Experiment 2 – aposymbiotic anemones

Treatment	Temperature	Salinity	pH_T	A_T	DIC_T	pCO_2
pH 7.95	24 ± 0.5 °C	35 ppt	7.95 ± 0.02	2243 ± 12	2009	505
pH 7.68	24 ± 0.5 °C	35 ppt	7.68 ± 0.02	2243 ± 12	2127	1031

a.

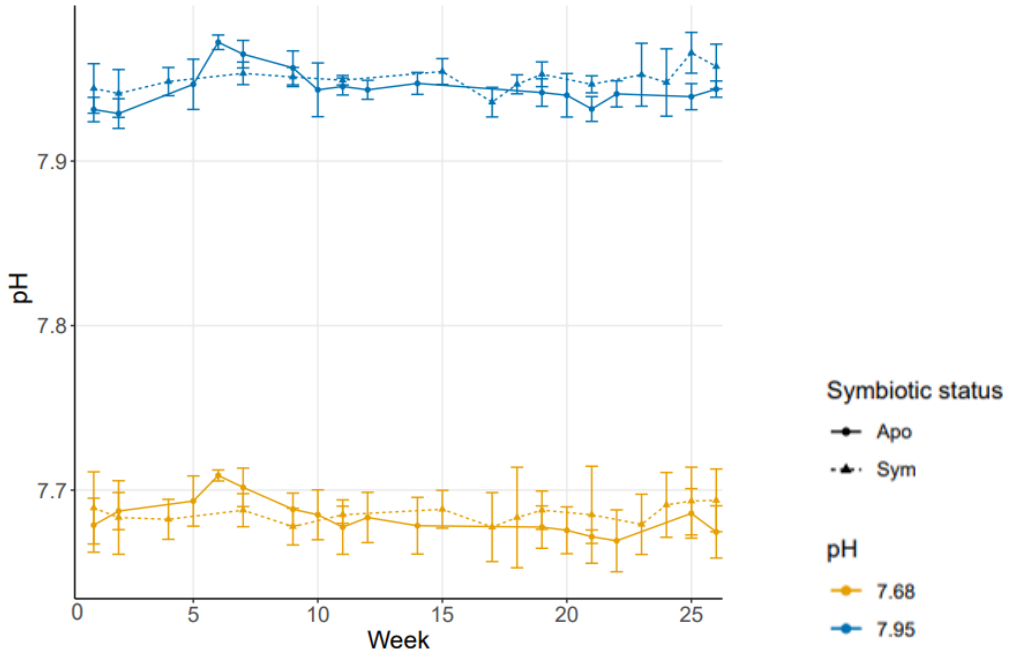

b.

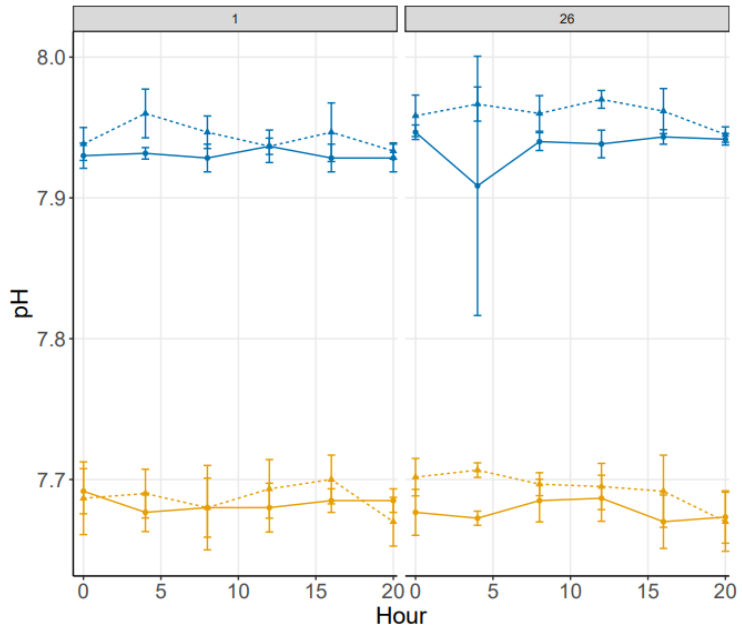

Figure 2.2: pH values for each treatment. a) pH values over the duration of the experiments. **b)** pH values over two 20-h cycles at the beginning and end of each experiment (Days 1 and 26). Values are mean ± standard deviation. For each treatment, *n* = 12 *per* timepoint.

A_T was measured following the procedures outlined in the *Guide to Best Practices for Ocean CO_2 Measurements* – SOP 3b (Dickson et al. 2007), by Gran titration (Gran 1952). This followed the open cell method using a semi-automatic titration system (AS-ALK2, Apollo Scitech, USA), consisting of two syringe pumps (Kloehn™ #50300, USA; 1 mL and 25 mL), and a combination pH glass electrode (Orion™ ROSS Ultra™ Glass Triode™ pH/ATC Combination Electrodes, Thermo Scientific, USA), and the R package seacarb v3.3.0 (Gattuso et al. 2021) calibrated against certified reference materials (CRM batch 176) every ~2 days. A_T samples were taken weekly across a rotating selection of experimental tanks (n = 3 *per* treatment), as well as the corresponding header tanks so that any header tank effects could be detected. Samples were collected by placing the tank outflow tube into a 250 mL screw-top container which was filled, sealed with Parafilm and secured with masking tape to avoid any air space and prevent off-gassing. Samples were stored at 4 °C and 0.22 µm-filtered prior to measurement and were processed within seven days of collection. The mass of each sample to be titrated was recorded to 0.001 g, and the temperature of the HCl and sample was kept constant by using a circulating water bath set to 25 °C and enclosing the sample in a water jacket during titration (Fangue et al. 2010). Duplicate measurements were taken for each sample, with a third taken if there was ≥10 µmol kg^{-1} difference between measurements. A_T was calculated using custom-built R code largely utilising seacarb but creating a user-friendly interface custom-made for the Apollo titrator output (Y. Tassin, unpublished).

Physiological measurements

A range of physiological measures were taken to aid the interpretation of proteomic data. Baseline samples of symbiotic and aposymbiotic anemones were collected prior to their introduction to the experimental system, and at 3, 14 and 28 days (all n = 7 *per* treatment/time-point). Based on pre-experiment trials, two anemones were used *per* n to provide sufficient biomass for analysis. Anemones were haphazardly selected, and then carefully removed from experimental tanks and placed into 0.5 mL Protein Lobind tubes (Eppendorf, Germany) and residual ASW removed. Lobind tubes were immediately placed into an aluminium block chilled to -80 °C and samples were stored at -80 °C until processing.

Symbiont cell counts, host protein quantification and estimation of symbiont cell density

All samples were rinsed twice in 500 µL high-performance liquid chromatography (HPLC)- grade H_2O to remove any remaining ASW and Symbiodiniaceae cells external to the anemones. Samples were mechanically homogenised (Ultra-Turrax T10 basic, IKA, Germany) in 500 µL HPLC-grade H_2O using 2 mL Protein Lobind tubes (Eppendorf, Germany) and centrifuged for 3 min at 200 x g to separate the host (supernatant) and algal (pellet) fractions. Algal pellets were resuspended in 500 µL ASW, mixed thoroughly by pipette and aliquoted for cell density quantification (20 µL), chlorophyll *a* extraction (80 µL) and proteomic analysis (400 µL). Cell counts were performed immediately, while the host fraction and remaining algal fractions were stored at -80 °C until processing. Algal fractions were stored as dry pellets. Cell count aliquots were fixed with 37% formalin to a 4% final volume (0.8 µL) to avoid cell degradation, and then diluted 1:20 in 380 µL ASW, vortexed and passed through a 23-gauge syringe needle 5-10 times to disperse any clumps of cells and remove excess host material. Samples were then pipetted into a 384-well plate (Perkin Elmer Ultra, USA) to be read by HTCM (n = 10 wells *per* sample, 20 µL *per* well; IN Cell Analyzer 6500 HS, GE Healthcare, USA; settings: magnification x10, excitation 642, emission Far Red 488, exposure 40 ms). Images were analysed using IN Carta Image Analysis Software (GE Healthcare, USA; settings 72% sensitivity, 10 µm minimum diameter) and validated using ImageJ (Abramoff et al. 2004; all images). In ImageJ, images were processed as batches, using a macro with the following settings: 'threshold' was set to 'moments dark no-reset'; black background was enabled; and particle analysis was set as size 10 µm to infinity. There was < 2% variation between IN Carta and ImageJ results, with any differences and a minimum 15% subsample *per* batch validated manually. Aliquots (10 µL) of host samples were diluted 10:90 with ddH_2O (90 µL) for Qubit™ protein assays (Invitrogen, USA), which were run following the manufacturer's standard protocol using 10 µL diluted sample:190 µL Qubit working solution and read using a Qubit™ 2.0 fluorometer (Invitrogen, USA). Cell counts were then normalised to host protein content to calculate symbiont density. Host protein content was also used to estimate anemone growth rate, and pedal disc diameter of all anemones was recorded to the nearest 1 mm weekly during the experiment.

Photosynthetic health

Pulse amplitude modulated (PAM) fluorometry was used to measure chlorophyll fluorescence of Symbiodiniaceae cells *in hospite* (i.e., inside the anemones) weekly (n = 7 *per* treatment/time-point),

as an indicator of photosynthetic health. A Diving PAM (Walz, Germany; settings: measuring light = 7, saturation intensity = 7, saturation width = 0.8 s, gain = 5 and damping = 2) was used to measure light-adapted minimum (F_t) and maximum fluorescence (F_m') at 11:30 h after 2 h light exposure. Dark-adapted minimum (F_o) and maximum fluorescence (F_m) were then measured after ~20 min dark adaptation. These measurements were used to calculate the effective quantum yield of PSII ($\Phi_{PSII} = F_m' – F_t/F_m'$; Genty et al. 1989) and maximum quantum yield of PSII ($F_v/F_m = F_m - F_0/F_m$; Kitajima and Butler 1975). To estimate chlorophyll *a* content, 100% ethanol (160 µL) was added to the 80 µL algal pellet, vortexed and stored at -20 °C in the dark for 18 h to extract chlorophyll (Ritchie 2006). The samples were then vortexed, centrifuged for 2 min at 15,000 x g and the supernatant pipetted into a 96-well plate (CELLSTAR®, Greiner, Austria). Absorbance was read at 629 nm and 665 nm (Ritchie 2006) by spectrophotometer (EnSpire 2300 Multilabel Reader, Perkin Elmer, USA) and results normalised to cell density.

Proteome expression

Sample processing for proteomic analysis followed the methods of Oakley et al. (2016) (modified from Wiśniewski et al. 2009), as *per* the workflow in **Figure 2.3**. Following fractionation (as described above), algal fractions were washed by resuspension in 500 µL 1% sodium deoxycholate (SDC) in HPLC grade H_2O, mixed by pipettte and passed through a 23-gauge syringe needle 5-10 times to disperse any clumps of cells and remove excess host material, then re-pelleted and supernatant removed (Mashini 2022). Algal pellets were then resuspended in 500 µL 5% SDC in HPLC-grade H_2O, with the SDC acting as a detergent. Host fractions were homogenised in 500 µL HPLC-grade H_2O, so 25 mg SDC powder were added to achieve the same effect. All the following steps apply to both host and algal fractions.

To extract proteins, samples were ultrasonicated to lyse cells (Vibracell, Sonics, USA; settings: 20% output, 2 s between pulses, 2 s pulse duration, 20 pulses = 1 min 20 s total duration), with samples kept on ice throughout to slow protein degradation. B-mercaptoethanol (BME; 5 uL) was then added to reduce and denature proteins, *via* incubation at 85 °C for 30 min. Pigments were removed by adding 1 mL ethyl acetate, vortexing for 1 min to mix, and then centrifuging for 1 min at 10,000 x g to isolate the pigment-containing ethyl acetate, which was removed by pipette. This step was repeated before final removal of ethyl acetate and the samples transferred to 0.5 mL centrifugal filters (Amicron®

Ultra; Millipore®, Ireland). Samples were centrifuged through centrifugal filters for 15 min at 14,000 x g to remove dilutants (particularly SDC), leaving 20 µL in the filter, which was then washed twice with 380 µL 50 mM Tris and centrifuged for 15 min at 14,000 x g, with a final aliquot of 380 µL 50 mM Tris added to the remaining 20 µL sample.

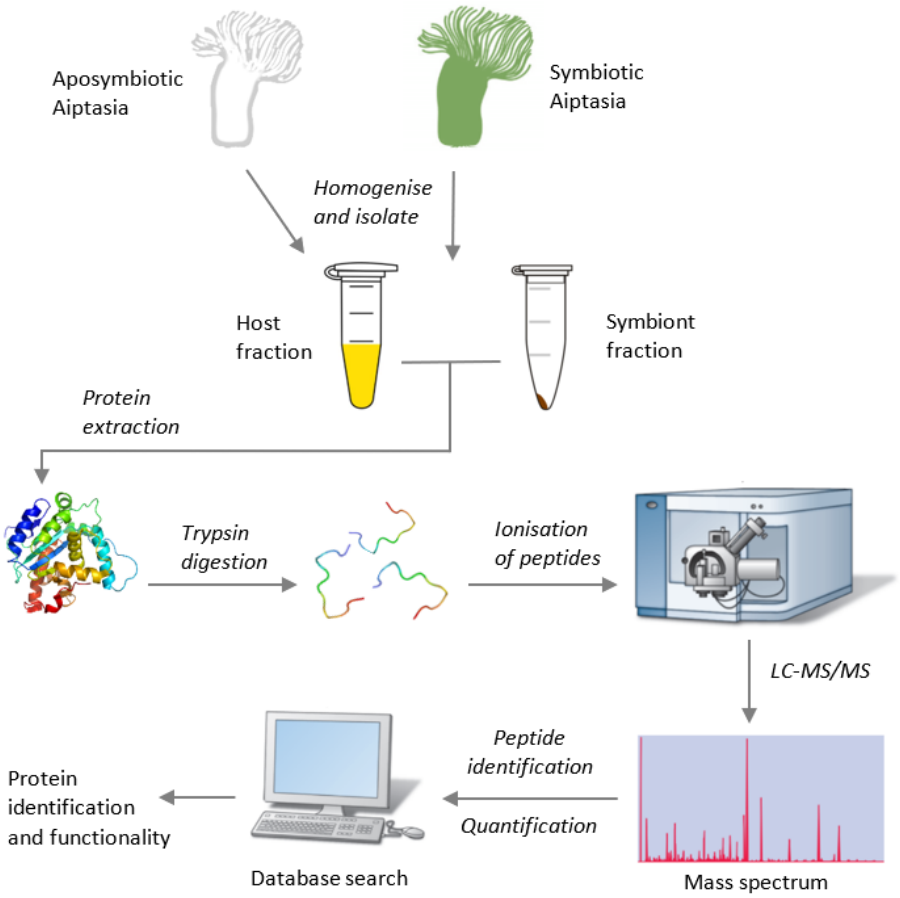

Figure 2.3: Workflow for proteomic analysis.

Samples were desalted using ZipTips (Omix 96 C18 100 µL, Agilent Technologies, USA). ZipTips were pre-wet with 100% acetonitrile by aspirating and discarding three times, then similarly rinsed with 0.1% formic acid in HPLC-grade H_2O. Samples were passed through the ZipTip column 25 times to bind peptides, rinsed again with 0.1% formic acid (x 3) and eluted into 20 µL 0.1% formic

acid in 50% acetonitrile by aspirating 15 times, and the full contents expelled. To expand the range of proteins extracted, this process was repeated using 20 µL 0.1% formic acid in 30% acetonitrile. The two eluates were then combined and dried down by vacuum centrifugation at 45 °C and stored at -80 °C until analysis by liquid chromatography-tandem mass spectrometry (LC MS-MS). On the day of analysis, samples were brought up to 50 µL with 0.1% formic acid in HPLC-grade H_2O, incubated at 37 °C for 30 min to redissolve peptides and vortexed briefly. Final peptide content was quantified by Qubit (5 µL undiluted sample:195 µL Qubit working solution) and samples centrifuged (5 min at 23,000 x g) to pellet any potential particulates, before being transferred to glass vials (Short Thread, 11.6mm, Thermo Scientific, USA) for reading *via* LC MS-MS.

LC MS-MS analysis used 200 ng of peptides *per* sample, separating peptides by liquid chromatography (Ultimate 3000, Dionex, USA) on an Acclaim PepMap C18 column (3 µm particles, 0.1 nm ID, 50 cm length; Thermo Scientific, USA) using a 75 min linear gradient from 5%:95% to 35%:65% of buffer A (0.1% formic acid) to buffer B (80% acetonitrile, 0.1% formic acid), with a flow rate of 300 nL min^{-1}. Peptides were ionised by electrospray at 1.8 kV and analysed by mass spectrometer (Orbitrap Fusion Lumos Tribrid, Thermo Scientific, USA). Precursor mass spectra were acquired at the following Orbitrap settings: resolution 120,000; singly-charged ions rejected; quadrupole isolation enabled; automatic gain target 7.0e5 and maximum injection time 50 ms. Sequencing was performed on the 20 most intense precursor spectra, which were fragmented by higher-energy collision dissociation and analysed in the ion trap (automatic gain target 5.0e3; maximum injection time 300 ms). Dynamic exclusion was enabled with a duration of 60 s. Instruments were controlled using Xcalibur v4.3 software (Thermo Scientific, USA).

Due to some variability in quality during the processing of samples for proteomic analysis, additional samples were occasionally processed. Following quality assurance, all samples were found to be of high or adequate quality and as such were included in further analyses to avoid discarding useful data. As such, for proteomic analysis and physiological measurements requiring invasive sampling (symbiont cell counts, host protein quantification and estimation of symbiont cell density, and chl *a* measurements), sample numbers vary slightly between treatments. Full details are given in the supplementary material (**S1.1**).

2.2.4 Data analysis

Statistical analysis

All statistical analyses of physiological data were performed in R v4.1.1 (R Core Team 2021). Linear mixed effects models were constructed to test the effects of the explanatory variables of pH and time, and their interaction terms. Models were constructed for each response variable: estimated symbiont cell density; dark- and light-adapted chlorophyll fluorescence; symbiont chl *a* concentrations; anemone protein content; and anemone pedal disc size. 'Header tank' was included as a random effect to identify the influence of any unintended tank effects in the data (Cornwall and Hurd 2016). Model assumptions were assessed using residual plots (residuals *vs.* fitted, normal Q-Q and scale-location), and outlying data points identified using residuals *vs.* leverage plots based on an assessment of Cook's distance with a threshold of 1. No data points exceeded this threshold. Q-Q plots were validated using the Shapiro-Wilk test to ensure normal distribution of data. In multiple linear regressions, best fit models were selected based on lowest Akaike's information criteria (AIC) values, while always retaining 'header tank' as a random effect. Where relevant, the Tukey's honest significant differences (HSD) test was used for *post hoc* analysis ($\alpha = 0.05$). Details of linear models and statistical tests are available in the supplementary material (**S1.2**).

Proteomic data analysis

Proteins were identified from MS-MS raw spectrum files using the Andromeda search algorithm in MaxQuant v1.6.10.43 (Cox et al. 2014). Aiptasia spectra were searched against protein models from the *Exaiptasia diaphana* CC7 genome (v1.1, reefgenomics.org) (Baumgarten et al. 2015). *B. minutum* spectra were searched against a custom database developed from the *B. minutum* genome (Parkinson et al. 2016). A built-in contaminants database from MaxQuant was included in the search. For both searches, the specified digest enzyme was trypsin with a maximum of two missed cleavages allowed. Oxidation of methionine and acetylation of the protein n-terminus were specified as variable modifications and cysteine carbamidomethylation as a fixed modification. The mass tolerance for precursor ions was 20 ppm in the first search and 4.5 ppm in the main search, with a mass tolerance of 0.5 Da for fragment ions in the MS-MS ion trap search. Label-free quantification was enabled, with a minimum of two unique plus razor peptides for quantification, and match between runs

enabled. The peptide spectrum match and protein false discovery rate (FDR) were each set to 1%, with a minimum of two peptides required for verification.

The resulting datasets were analysed to identify differentially abundant proteins (DAPs) using PolySTest (Veit Schwämmle et al. 2020). The FDR was 0.05, with lower and upper log-ratio thresholds of -0.25 and 0.25 respectively. Comparisons were conducted by symbiotic state, pH level and time-point, and all nested analyses within these treatments (e.g., pH 7.68 *vs*. pH 7.95 at T1, T2 and T3). Fold changes were derived by performing a $\log_2$ transformation of protein abundance ratios. Lists were filtered to remove any DAPs with <1.25-fold changes to ensure that only meaningful changes were included in further analyses. Initial analyses of DAPs by pH at each time point indicated temporal trends which approached significance, but which in individual time-point analyses did not meet the 0.05 FDR threshold. To enhance statistical power in order to understand whether these apparent trends were material, data for T2 and T3 were then grouped for analysis *vs.* T1, resulting in higher numbers of DAPs by pH over time. Proteins were annotated with gene ontology (GO) terms using PANNZER (Koskinen et al. 2015; Toronen and Holm 2022). In the few cases where no PANNZER annotation was available, proteins were manually annotated from the UniprotKB database by homology. Full lists of DAPs, annotated GO terms and annotation sources are available in the supplementary material (*B. minutum* (**S1.2**); aposymbiotic Aiptasia (**S1.3**); symbiotic Aiptasia (**S1.4**)). Proteins were then categorised into functional groups based on using parent GO terms as annotated in QuickGO (Binns et al. 2009; Huntley et al. 2015). Venn diagrams were produced using jvenn from lists of DAPs in each treatment (Bardou et al. 2014). Principal component analysis (PCA) and heatmap plots were generated using ClustVis (Metsalu and Vilo, 2015), using ln(x) transformed protein abundance values. Unit variance scaling was applied, and singular value decomposition with imputation was used to calculate principal components. Heatmaps used Pearson's correlations for row and column clustering, and average distances for row and column linkage.

2.3 Results

All results presented below are based on general linear models unless otherwise specified, with full model details and sample numbers for each treatment provided in the supplementary material (**S1.1**).

2.3.1 Physiological measurements

Symbiont cell density and host growth rate

Overall, pH had minimal effect on the physiological variables measured, with most analyses resulting in no significant differences. There were, however, some differences over time. Cell densities of *B. minutum (*cells *per* µg of host protein) did not change significantly in response to pH ($R^2 < 0.001$, $F_{1, 29} = 0.02$, $p = 0.88$) (**Figure 2.4a**). However, changes in cell density over the course of the experiment approached significance ($R^2 = 0.12$, $F_{1, 29} = 3.87$, $p = 0.059$), suggesting that symbiont population density increased over time at both pH levels. Host growth rate, as measured by protein content, did not change in response to pH (aposymbiotic Aiptasia: $R^2 < 0.001$, $F_{1, 36} = 0.02$, $p = 0.88$; symbiotic Aiptasia: $R^2 = 0.05$, $F_{1, 32} = 1.85$, $p = 1.84$), or time (aposymbiotic Aiptasia: $R^2 = 0.06$, $F_{1, 36} = 2.14$, $p = 0.15$; symbiotic Aiptasia: $R^2 = 0.04$, $F_{1, 32} = 1.42$, $p = 0.24$) (**Figure 2.4b**). Growth was, however, evident based on pedal disc diameter (**Figure 2.4c**). For symbiotic Aiptasia, there was a small but significant effect of low pH, with pedal disc diameter of anemones at pH 7.68 increasing 8.6% more than those at pH 7.95. Time explained a further 25% increase in pedal disc diameter over the course of the experiment (β = 5.60 mm + 0.48 mm (pH 7.68) + 1.40 mm (time), $R^2 = 0.12$, $F_{2, 580} = 41.23$, $p < 0.001$). The interaction between pH and time was not significant ($p = 0.66$). A pH effect was not observed for aposymbiotic Aiptasia, where there was no difference between treatments ($R^2 < 0.001$, $F_{1, 654} = 0.47$, $p = 0.49$). However, pedal disc diameter of aposymbiotic anemones did grow 59.5% over the course of the experiment (β = 2.69 mm + 1.60 mm; $R^2 = 0.21$, $F_{1, 654} = 185.1$, $p < 0.001$).

Photosynthetic health

Decreased pH had little effect on the photosynthetic performance of *in hospite B. minutum.* Light-adapted chlorophyll fluorescence (Φ_{PSII}) measurements showed no significant differences either with pH treatment ($R^2 = 0.04$, $F_{1, 52} = 2.01$, $p = 0.16$) or over time ($R^2 = 0.05$, $F_{1, 52} = 2.51$, $p = 0.12$) (**Figure 2.5a**). At Week 1, dark-adapted chlorophyll fluorescence (F_v/F_m) values were 0.10 (15.6%) lower at pH 7.68 than at pH 7.95 ($R^2 = 0.3476$, $F_{3, 48} = 8.524$, $p < 0.001$) (**Figure 2.5b**). No significant differences in chl *a* concentration were observed either due to decreased pH ($R^2 < 0.001$, $F_{1, 31} < 0.001$, $p = 0.98$) or over time ($R^2 = 10.03$, $F_{1, 31} = 0.90$, $p = 0.35$) (**Figure 2.5c**).

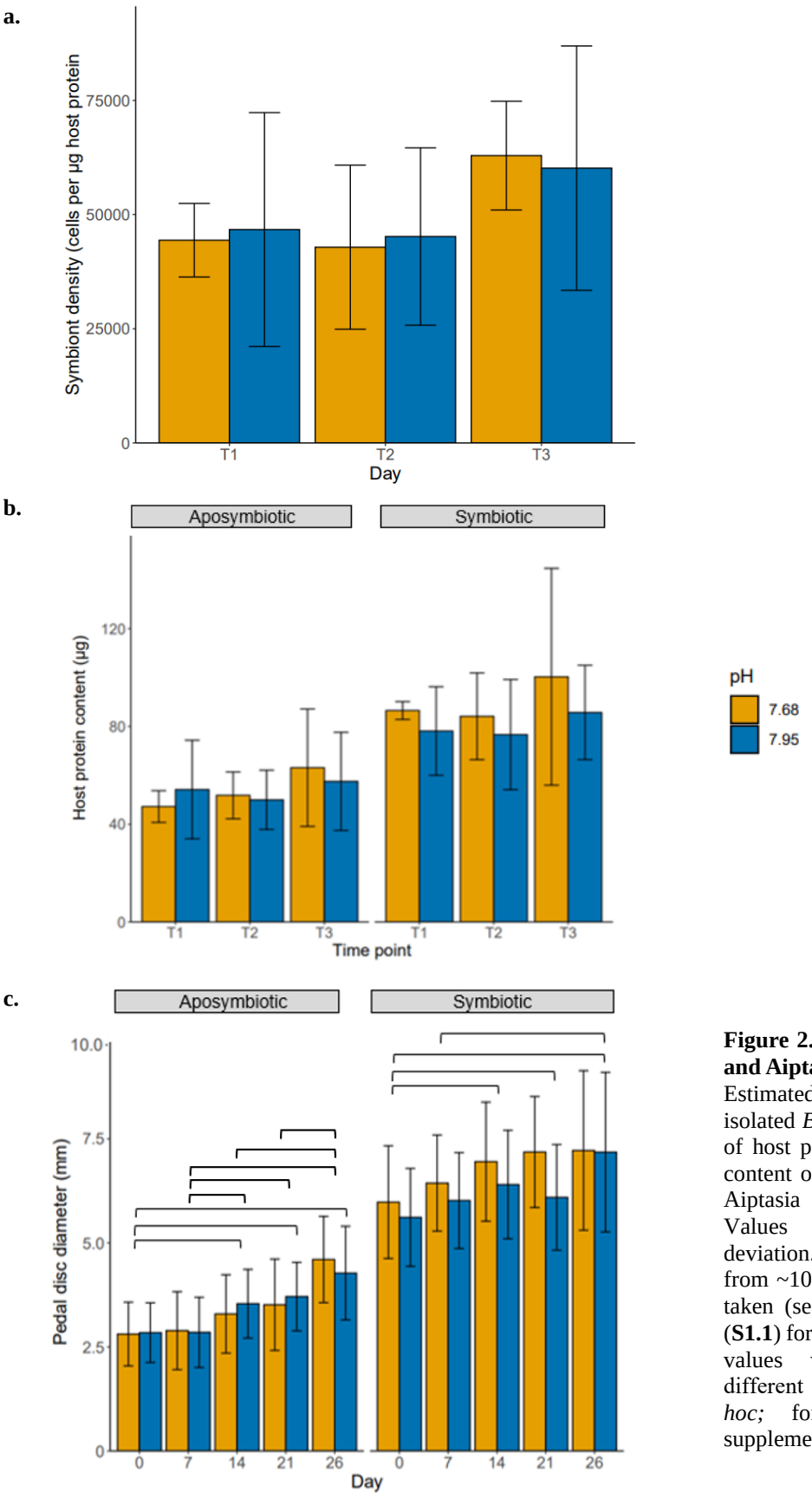

Figure 2.4: Symbiont cell density and Aiptasia biomass over time. a. Estimated cell densities of freshly isolated *Breviolum minutum per* µg of host protein (n = 7); **b.** Protein content of Aiptasia (n = 7); and **c.** Aiptasia pedal disc diameter. Values are mean ± standard deviation. n decreased over time from ~100 to ~40 as samples were taken (see supplementary material (**S1.1**) for details). Brackets indicate values which are statistically different over time (Tukey's *post hoc;* for statistical tests see supplementary material (**S1.1**)).

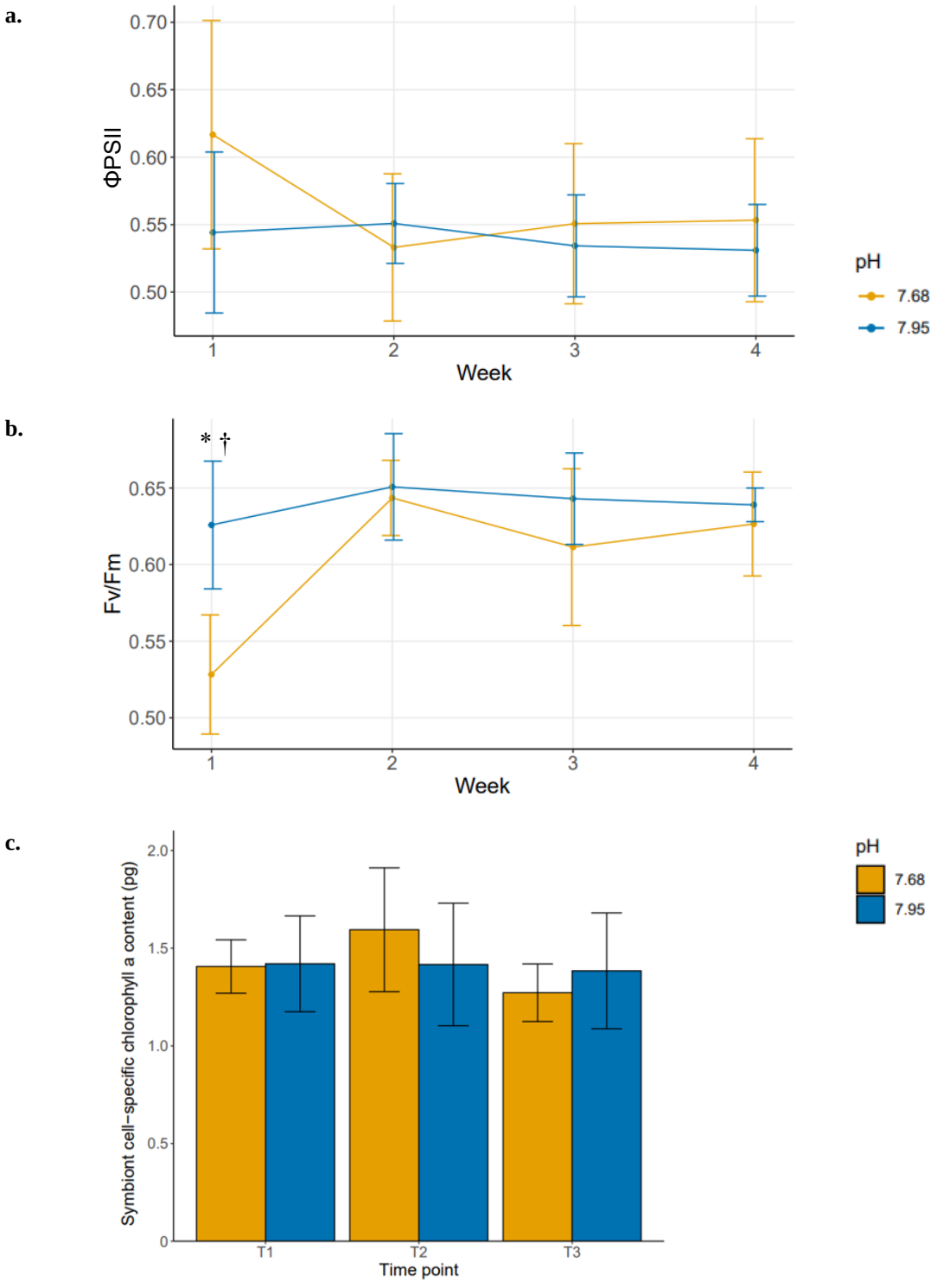

Figure 2.5: **Measures of photosynthetic health of *in hospite Breviolum minutum*. a.** Light-adapted chlorophyll fluorescence measurements (ΦPSII) (*n* = 7); **b.** Dark-adapted chlorophyll fluorescence measurements (F_v/F_m) (*n* = 7); **c.** Concentration of chlorophyll *a per B. minutum* cell (for *n* see supplementary material (**S1.1**)). Values represent mean ± standard deviation. * indicates values which are statistically different between pH treatments; † indicates values which are statistically different over time (Tukey's *post hoc*; for statistical tests see supplementary material (**S1.1**)).

2.3.2 Proteome expression

A total of 2095 unique *Breviolum minutum* and 4631 unique Aiptasia proteins were identified across all treatments. Among these totals, the data confirmed 977 hypothetical (i.e., predicted from genomic data but unconfirmed, and as such, unnamed) proteins identified for *B. minutum*, while 494 hypothetical proteins were confirmed for Aiptasia. Full lists of the proteins identified are available in the supplementary material as follows: *B. minutum* full list (**S1.5**) and detected "hypothetical" proteins (**S1.7**), and Aiptasia full list (**S1.6**) and detected "hypothetical" proteins (**S1.8**). In Aiptasia, symbiotic state drove the largest observed differences, with 1162 significantly differentially abundant proteins (DAPs) between aposymbiotic and symbiotic anemones ($q < 0.05$), representing 25.1% of all identified proteins. These DAPs also exhibited the greatest fold changes; at the extremes a 30.42-fold increase and 13.72-fold decrease in symbiotic *vs.* aposymbiotic Aiptasia. The mean fold-change was 1.93. A full list of DAPs by symbiotic state is available in the supplementary material (**S1.9**).

Overall, the data indicated only a minimal effect of pH treatment on both the host and symbiont, with no DAPs between the *B. minutum* datasets when comparing all pH 7.68 *vs.* all pH 7.95 samples. A greater, but still small, impact of pH was seen in aposymbiotic than symbiotic anemones (10 *vs.* 3 DAPs). However, there were significant differences in the profiles of protein abundance over time in the different pH treatments. Comparing between anemones in the two pH treatments at each timepoint illustrated trends in the up- and downregulation of DAPs, with these largely becoming significant at T3 (Day 26) (aposymbiotic Aiptasia = 9 DAPs; symbiotic Aiptasia = 15 DAPs). To explore these changes over time more fully, data for the later timepoints were subsequently grouped for analysis of DAPs at T1 (Day 1) *vs.* the later timepoints T2 and T3 (Days 12 and 26, respectively). This enhanced statistical power elucidated the temporal shifts more strongly, with 53 DAPs between the two pH levels in *B. minutum* (**Figure 2.6a**; **Table 2.2**) (2.5% of all identified proteins), 114 (2.5%) in aposymbiotic Aiptasia (**Figure 2.6b**; **Table 2.3**), and 89 (1.9%) in symbiotic Aiptasia (**Figure 2.6**; **Table 2.3**). Principal component analyses (PCAs) (**Figure 2.7**) and heatmaps of DAPs (**Figure 2.8**) further illustrated the differential impact on the organisms in symbiotic *vs.* aposymbiotic anemones, with a clear distinction between pH treatments for aposymbiotic Aiptasia, but less defined differences by pH for both *B. minutum* and symbiotic Aiptasia. Full lists of DAPs and GO terms are available in the supplementary material (*B. minutum* (**S1.2**); Aiptasia: aposymbiotic (**S1.3**); and symbiotic (**S1.4**)).

GO term annotations indicated a broad range of biological processes represented by the DAPs in each sample group. These GO terms were assigned into functional categories as described in **Section 2.2.4** (**Figure 2.9**), and full lists of GO terms by functional category are available in the supplementary material (*B. minutum* (**S1.10**); aposymbiotic Aiptasia (**S1.11**); symbiotic Aiptasia (**S1.12**)). The results indicate that, under decreased pH, there were significant differences in metabolic and cytoskeletal processes and cell signalling, activation of the cell stress response, changes in cellular homeostasis and regulation of cell proliferation, increased photosynthetic activity in *B. minutum*, and immune responses in Aiptasia. Details of the number of proteins in each category and associated mean fold-changes are given in **Table 2.2** for *B. minutum* and **Table 2.3** for Aiptasia. Results outlined below refer to DAPs at T1 *vs.* grouped data for T2 and T3, unless otherwise stated. Details of the selected proteins discussed, along with their abbreviations, are given in **Tables 2.4**, **2.5** and **2.6** for *B. minutum*, and aposymbiotic and symbiotic Aiptasia, respectively.

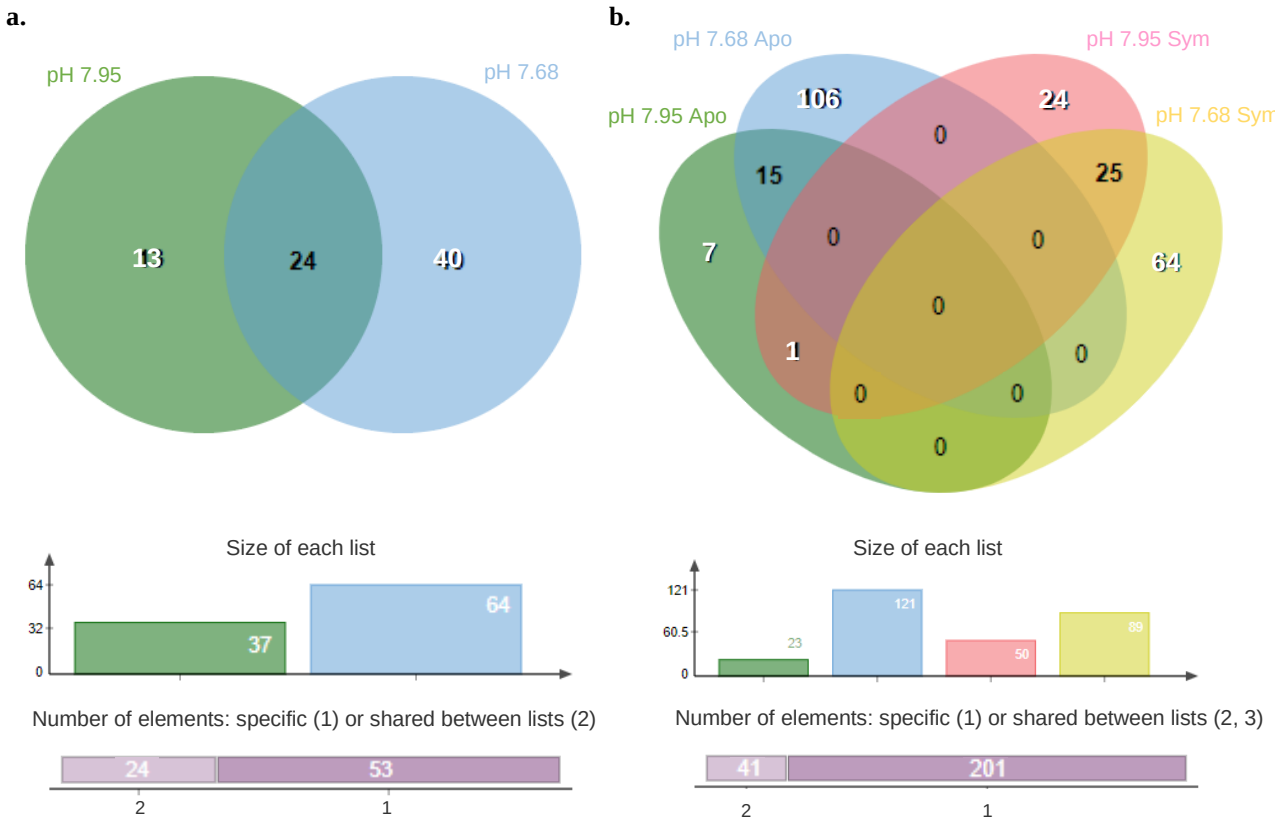

Figure 2.6: Venn diagrams of differentially abundant proteins (DAPs, $q < 0.05$) in **a.** *Breviolum minutum*; **b.** Aiptasia. Apo = aposymbiotic, Sym = symbiotic. Analysed lists are of DAPs at T1(Day 1) *vs.* T2 and T3 (Days 12 and 26, respectively), at each pH level (7.95 or 7.68). DAPs between pH 7.95 and 7.68 for *B. minutum* = 53, for aposymbiotic Aiptasia = 114, and for symbiotic Aiptasia = 89; highlighted in white text.

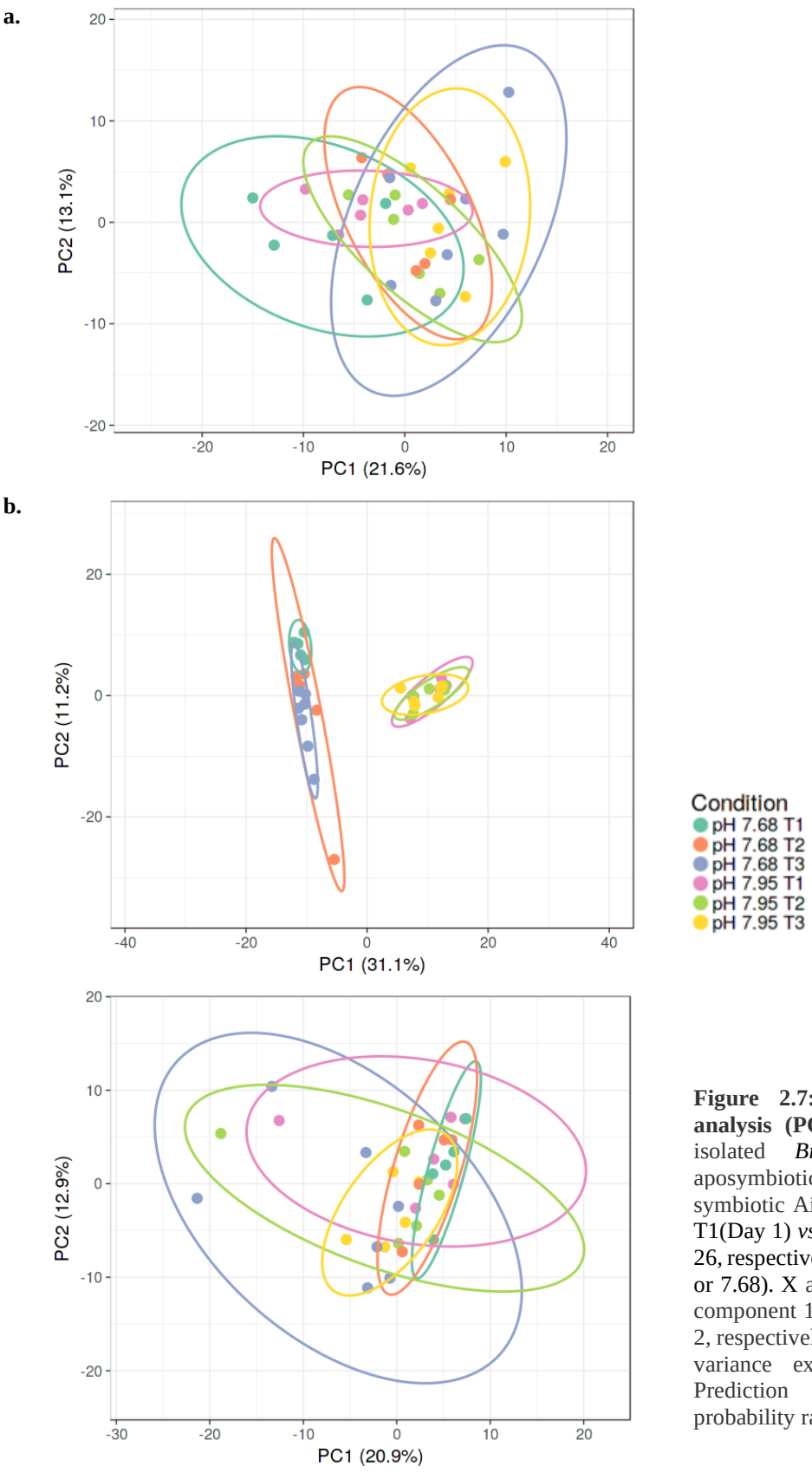

Figure 2.7: Principal component analysis (PCA) plots for **a.** freshly isolated *Breviolum minutum*; **b.** aposymbiotic Aiptasia; and **c.** symbiotic Aiptasia, based on DAPs at T1(Day 1) *vs.* T2 and T3 (Days 12 and 26, respectively), at each pH level (7.95 or 7.68). X and Y axes show principal component 1 and principal component 2, respectively, with percentage of total variance explained in parentheses. Prediction ellipses indicate 95% probability ranges.

a. Heatmap for *Breviolum minutum*. Colour distribution in red box shows mixed distribution between pH treatments and over time.

b. Heatmap for aposymbiotic Aiptasia. Colour distribution in red box shows clear distinction between pH 7.95 (left) and pH 7.68 (right). At pH 7.95 (control) the time points are interspersed, however at pH 7.68 there is separation between T1 (turquoise, far right) and T2/T3 (orange/blue).

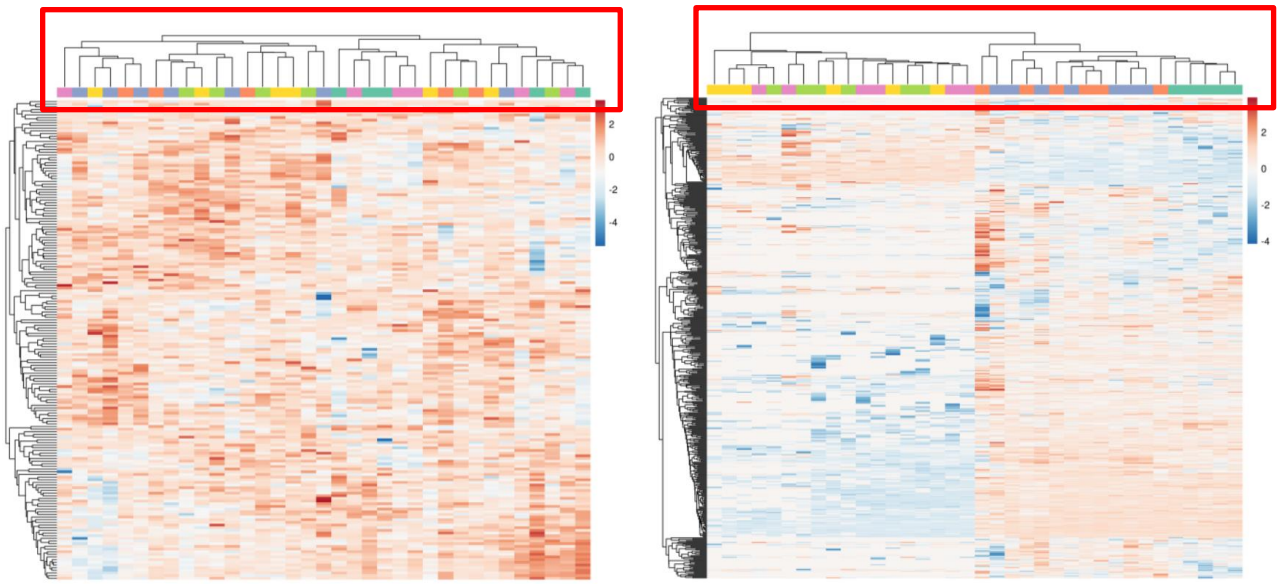

c. Heatmap for symbiotic Aiptasia. Colour distribution in red box shows a more mixed distribution between pH treatments relative to aposymbiotic Aiptasia. At pH 7.68, there is distinction between T1 (turquoise) and T3 (blue).

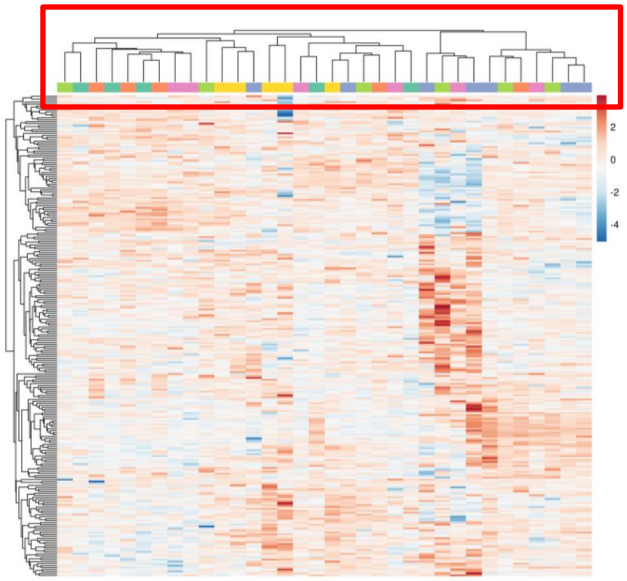

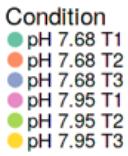

Figure 2.8: Heatmaps for **a.** freshly isolated *Breviolum minutum*; **b.** aposymbiotic Aiptasia; **c.** symbiotic Aiptasia, based on differentially abundant proteins (DAPs) between T1 (Day 1) *vs.* grouped data for T2 and T3 (Days 12 and 26, respectively) at each pH level (7.95 or 7.68). Each row represents one DAP, and each column represents one biological replicate. Proteins and biological replicates are clustered using average linkage and Pearson correlation distance. Red and blue shading indicate proteins that were upregulated and downregulated respectively under pH 7.68 *vs.* pH 7.95.

Table 2.2: Differentially abundant proteins (DAPs) in *Breviolum minutum* between T1 *vs.* grouped data for T2 and T3. Red and blue shading indicate proteins that were upregulated and downregulated respectively under pH 7.68 *vs.* pH 7.95. Standard error: [1] = 0.02; [2] = 0.05. Functional categories based on gene ontology (GO) term assignment – see text for details.

Functional category	**# DAPs**	# ↑	Mean fold change	# ↓	Mean fold change
Total DAPs*	**53**	42	1.38[1]	11	-1.48[2]
Catabolism	**23**	21	1.75	2	-1.57
Anabolism	**12**	12	1.69	0	n/a
Photosynthesis	**12**	9	1.40	3	-1.41
Cytoskeletal	**21**	17	1.37	4	-1.55
Signalling	**1**	1	1.36	0	n/a
Cellular homeostasis	**4**	4	1.38	0	n/a
Cell stress response	**8**	6	1.38	2	-1.46
Cell regulation	**1**	1	1.37	0	n/a
Unknown	**16**	11	1.39	5	-1.42

Table 2.3: Differentially abundant proteins (DAPs) in Aiptasia between T1 *vs.* grouped data for T2 and T3. Red and blue shading indicate proteins that were upregulated and downregulated respectively under pH 7.68 *vs.* pH 7.95. Standard error: [1] = 0.04; [2] = 0.07; [3] = 0.03; [4] = 0.01. Functional categories are based on gene ontology (GO) term assignment – see text for details.

	Aposymbiotic					**Symbiotic**				
Functional category	**# DAPs**	# ↑	Mean fold change	# ↓	Mean fold change	**# DAPs**	# ↑	Mean fold change	# ↓	Mean fold change
Total DAPs*	**114**	72	1.58[1]	42	-1.69[2]	**89**	79	1.50[3]	10	-1.44[4]
Catabolism	**64**	40	1.50	24	-1.67	**48**	44	1.48	4	-1.42
Anabolism	**30**	21	1.49	9	-1.74	**36**	33	1.46	3	-1.38
Cytoskeletal	**57**	36	1.56	21	-1.71	**53**	48	1.49	5	-1.42
Signalling	**14**	8	1.75	6	-1.49	**13**	11	1.43	2	-1.36
Cellular homeostasis	**14**	12	1.53	2	-1.47	**18**	16	1.51	2	-1.46
Cell stress response	**10**	5	2.04	5	-1.52	**4**	3	1.31	1	-1.38
Cell regulation	**12**	9	1.71	3	-2.00	**13**	12	1.42	1	-1.36
Immune response	**10**	3	1.60	7	-1.55	**14**	13	1.51	1	-1.38
Unknown	**16**	8	1.58	8	-1.81	**11**	8	1.51	3	-1.49

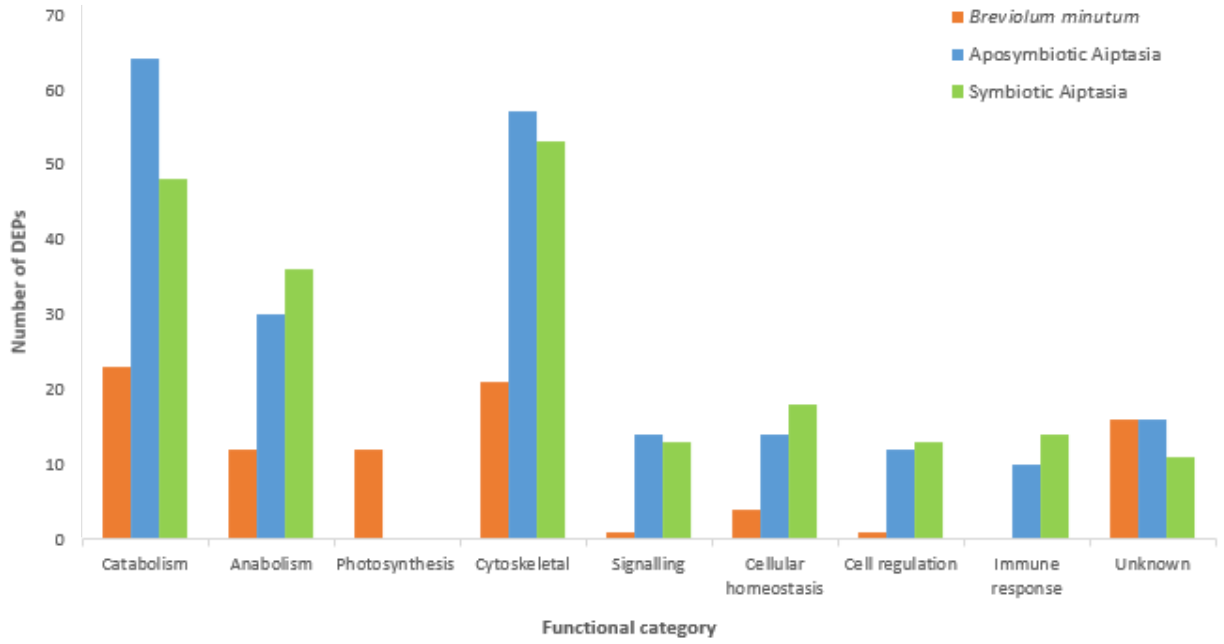

Figure 2.9: Differentially abundant proteins (DAPs) by functional category at pH 7.68 *vs.* pH 7.95, at T1 (Day 1) *vs.* grouped data for T2 and T3 (Days 12 and 26, respectively). Functional categories based on gene ontology (GO) term assignment – see text for details.

Metabolism and photosynthetic activity

Proteins involved in metabolic processes were the most abundant among DAPs at pH 7.68 *vs.* pH 7.95 across all three sample groups. In *B. minutum*, of 53 total DAPs, 28 (52.8%) were involved in either catabolism (16), anabolism (5) or both (7). These included the upregulation of GAPDH+, GMPS, enolase, two FBPases, and GAD (see **Table 2.4** for protein abbreviations), which are all active in glutamate and glutamine metabolic processes – key components of metabolite synthesis. Eleven of 53 DAPs (22.6%) in *B. minutum* were related to photosynthesis, exhibiting the greatest fold-changes among this sample group (at the extremes, ↑1.75-fold and ↓1.56-fold). This included six fucoxanthin-chlorophyll binding proteins (FCPs) and PSII CP47, which constitute major elements of the PSII-associated light harvesting complex (LHC), with roles in chlorophyll binding and electron transfer. At PSI, PsaA and FNR were both upregulated.

In aposymbiotic Aiptasia, 74 of 114 (64.9%) DAPs were involved in either catabolism (44), anabolism (10) or both (20)**.** This included the upregulation of proteins involved in lipid metabolism including TECR, and GDH which is essential for N assimilation (see **Table 2.5** for protein abbreviations). Also upregulated were MS and NDUFS2, which both have roles in cellular respiration. Symbiotic Aiptasia exhibited the highest proportion of DAPs involved in metabolism, at 66 of 89 DAPs (74.1%). This sample group also had the highest proportion of anabolism-annotated DAPs (18), with 30 involved in catabolism and 18 in both. Notable DAPs included a relative increase in ACC (see **Table 2.6** for protein abbreviations), which is active in fatty acid synthesis, and upregulation of several proteins involved in transcription and translation, including histones and ribosomal proteins. Further differences in metabolic processes were observed in the upregulation of CYTBC1 and CYTC6, which are active in the mitochondrial electron transport chain ($_{m}$ETC) as well as in transmembrane transport (discussed further below). Increased tricarboxylic acid (TCA) cycle activity was also signalled by the differential regulation of ACC, ACL, MS and MDH. Interestingly, there were also changes in protein abundance relating to heterotrophy under low pH. In aposymbiotic Aiptasia, this involved AMCase, CTRB and CTRC, which are involved in the breakdown of chitin such as that found in the anemone's food *Artemia* sp., while in symbiotic Aiptasia this was reflected in the upregulation of CHB.

Cytoskeleton and cell signalling

Proteins involved in cytoskeletal and cell signalling processes were the second most abundant functional group among DAPs. These comprised 21 (39.6%) and 1 (1.9%) DAPs in *B. minutum* respectively, with most DAPs annotated with cytoskeletal GO terms involved in the photosynthetic machinery. In aposymbiotic Aiptasia, 58 of 114 (50.9%) DAPs were involved in either cytoskeletal (44) or cell signalling (1) processes, or both (13). This included the prominent upregulation (1.75-2.58-fold) of multiple proteins active in cell adhesion, which plays an integral role not only in cell structure and tissue development but also in cell communication and regulation. The abundance of several actin-related proteins also significantly differed, with wide-ranging roles including in cell structure and organisation, and regulation of DNA transcription, recombination and repair. These included both upregulated (e.g., ACTL6A) and downregulated (e.g., MTPN) proteins, further illustrating the ubiquitous nature of this protein family. Differential signalling activity was observed in the upregulation of NRX, involved in the Wnt signalling pathway, and the widespread signal transductor and regulator, GPCR. TNFAIP3, with roles in multiple immune response signalling

pathways (discussed further below), including NF-kβ signalling, myD88-dependent toll-like receptor signalling and ERK cascade, was strongly downregulated.

A similar response was observed in symbiotic Aiptasia, with 55 DAPs (61.8%) active in cytoskeletal (42) and cell signalling (2) processes, and 11 involved in both. Here, numerous proteins involved in actin binding, actin filament generation and microtubule activity were upregulated, potentially related to cytoskeletal reorganisation and/or growth, as well as proteins involved in extra cellular matrix and cell-matrix adhesion activity. Differential signalling activity included the upregulation of R-Ras2, involved in cell-surface recognition, and of COLA, active in the immune response and the TGFβ signalling pathway, which is involved in multiple cellular functions including cell growth, cell differentiation, cell migration, apoptosis and cellular homeostasis.

Cellular homeostasis and transmembrane transport

Across sample groups there were small but pertinent differences seen in proteins involved in cellular homeostasis and transport. In *B. minutum* there was limited differential abundance (4 DAPs; 7.5%). However, this included the upregulation of both H^+-PPase, which participates in active transmembrane transport, and HSP905, which has been implicated in N transport. A similar response was observed in anemones in both symbiotic states, with 14 (6.6%) and 18 (8.5%) DAPs in aposymbiotic and symbiotic Aiptasia, respectively, which were largely upregulated. In aposymbiotic Aiptasia these DAPs included NDUFS2 and ABO8, and proteins active in the transport and regulation of specific nutrients, including sodium (CDCP1), potassium (CTRB) and calcium (CTRC and NRX). APL, which is involved in lipid transport, was downregulated. In symbiotic Aiptasia, the upregulation of active transport was more pronounced, including CYTBC1 and CYTC6, as well as the ADP/ATP carrier protein AAC1, and the 2.34-fold upregulation of SMCT1. Notably, there was differential abundance of several proteins with active roles in pH homeostasis. CAII is a key regulator of intracellular pH (↑1.70-fold), while two voltage-dependent calcium channel proteins (VGCC and CSC1) also showed significant differences. PEPCK was upregulated 2.09-fold at T3, a protein with roles in response to potassium ion starvation and glucose influx, as well as the regulation of transcription under acidic pH. Of note, MTf was downregulated in symbiotic Aiptasia. This protein is involved in cellular iron homeostasis, with iron being a key nutrient required for photosynthesis.

Oxidative stress responses and regulation of cell proliferation

Observations of proteins involved in oxidative stress responses were universal across sample groups at pH 7.68 and indicated responses to reactive oxygen species (ROS). In *B. minutum*, eight DAPs (15.1%) related to the cell stress response, while one (1.9%) related to cell regulation. These included two HSPs, plus CAT and SOD, all of which work to reduce ROS, and two BIP5s, which are active during the UPR. Similar responses were seen in anemones, with subtle but notable differences. In aposymbiotic Aiptasia, the numbers of DAPs relating to oxidative stress and regulation of cell proliferation were 10 (8.8%) and 12 (10.5%), respectively, while in symbiotic anemones there were four (4.5%) and 13 (14.6%), respectively. While relatively few in number, these proteins exhibited some of the largest fold-changes among all DAPs. For example, TXNDC12 was upregulated 3.25-fold in aposymbiotic Aiptasia and PPIase was upregulated 2.5-fold in symbiotic Aiptasia at T3. Across both symbiotic states at reduced pH, anemone DAPs were putatively linked to the ROS response (e.g., CAT, HSPs, NDUFS2, TXNDC12), endoplasmic reticulum (ER) stress and the unfolded protein response (UPR) (e.g., ATP5mg, Efl2, ENO1, PDI), and the initiation of apoptotic and autophagic pathways (e.g., LAMP1, NSFL1C, PD6, RAB14).

Under oxidative stress theories, cell regulation is characterised as part of an adaptive immune response in the cnidarian-dinoflagellate symbiosis. In symbiotic Aiptasia, evidence of a strongly upregulated immune response was observed, along with several proteins involved in the modulation of processes of another organism, (e.g., the symbiont *B. minutum*), with this category comprising 14 DAPs (15.7%). These included the greatest fold-change in symbiotic Aiptasia, IFI44 (↑2.78-fold), GBP6 and GAPR-1 (immune response), as well as two ALPs and TYR3 (modulation of another organism). In aposymbiotic Aiptasia, the reverse effect was observed, with immune response-annotated proteins largely downregulated, including ADAMTS, IFI44, MMR, RAB14 and TNFAIP3. DAPs in this category totalled 10 (8.8%) in aposymbiotic samples.

Table 2.4: Selected differentially abundant proteins (DAPs) in *Breviolum minutum*. Fold changes in red and blue indicate proteins upregulated and downregulated respectively under pH 7.68 *vs.* pH 7.95. Proteins are listed alphabetically by their abbreviation for ease of reference. Columns to the right shaded grey indicate functional categories based on gene ontology (GO) term assignment. FC = fold change; Cat. = catabolism; Ana. = anabolism; Pht. = photosynthesis; Cyt. = cytoskeletal; Sig. = signalling; CelH = cellular homeostasis; ROS = oxidative stress response. Proteins listed are those discussed in the text.

Protein ID	Protein name	Abbrev.	FC	Cat.	Ana.	Pht.	Cyt.	Sig.	CelH	ROS
43672_seq1.61079	Luminal-binding protein 5	BIP5	1.36							
43935_seq3.62095	Luminal-binding protein 5	BIP5	-1.56							
30121_seq1.30621	Catalase decomposes hydrogen peroxide to molecular oxygen and water	CAT	1.25							
39062_seq4.48579	Phosphopyruvate hydratase (Fragment)	Enolase	1.36							
15857_seq1.12741	Fructose-bisphosphatase	FBPase	1.37							
26595_seq1.25045	Fructose-bisphosphate aldolase	FBPase	1.28							
33071_seq1.36005	FCPE protein (Fragment)	FCP	1.27							
34512_seq1.38849	FCPF protein (Fragment)	FCP	1.31							
43451_seq4.60327	FCPF protein (Fragment)	FCP	-1.33							
19397_seq2.16785	Fucoxanthin-chlorophyll a-c binding protein A, chloroplastic (Fragment)	FCP	-1.33							
42410_seq2.57236	Fucoxanthin-chlorophyll a-c binding protein F, chloroplastic	FCP	1.75							
19571_seq1.16979	Light-harvesting chlorophyll a-c binding protein (Fragment)	FCP	1.29							
45175_seq1.63986	Ferredoxin—$NADP^+$ reductase (Fragment)	FNR	1.34							
46757_seq1.65019	Glutamate decarboxylase	GAD	1.25							
43936_seq2.62096	Glyceraldehyde-3-phosphate dehydrogenase	GAPDH	1.69							
36609_seq1.43074	GMP synthase [glutamine-hydrolyzing]	GMPS	1.61							
44591_seq1.63626	H^+-exporting diphosphatase	H^+-PPase	1.33							
44999_seq1.63899	Heat shock protein DnaJ, putative	HSP DnaJ	1.42							
40576_seq1.52322	Heat shock protein 90-5, chloroplastic	HSP905	1.37							
39329_seq1.49220	Photosystem I P700 chlorophyll a apoprotein A1	PsaA	1.56							
42802_seq12.58290	Photosystem II CP47 reaction centre protein	PSII CP47	1.32							
41349_seq2.54304	Superoxide dismutase	SOD	-1.36							

Table 2.5: Selected differentially abundant proteins (DAPs) in aposymbiotic Aiptasia. Fold changes in red and blue indicate proteins upregulated and downregulated respectively under pH 7.68 *vs.* pH 7.95. Proteins are listed alphabetically by their abbreviation for ease of reference. Columns to the right shaded grey indicate functional categories based on gene ontology (GO) term assignment. FC = fold change; Cat. = catabolism; Ana. = anabolism; Cyt. = cytoskeletal; Sig. = signalling; CelH = cellular homeostasis; ROS = oxidative stress response; CelR – cell proliferation regulation; ImR = immune response. Proteins listed are those discussed in the text.

Protein ID	Protein name	Abbrev.	FC	Cat.	Ana.	Cyt.	Sig.	CelH	ROS	CelR	ImR
KXJ25031.1	Actin-like protein 6A	ACTL6A	-2.14								
KXJ25146.1	A disintegrin and metalloproteinase with thrombospondin motifs 17	ADAMTS	-1.54								
KXJ13879.1	Acidic mammalian chitinase	AMCase	1.58								
KXJ28841.1	Anoctamin-8	ANO8	1.62								
KXJ12820.1	Apolipophorin	APL	1.40								
KXJ30135.1	CUB and peptidase domain-containing protein 1	CDCP1	1.96								
KXJ10614.1	Chymotrypsinogen B	CTRB	1.52								
KXJ30165.1	Chymotrypsin-C	CTRC	1.49								
KXJ19990.1	Cytochrome P450 20A1	CYP20A1	1.36								
KXJ13944.1	Cytochrome P450 3A4	CYP3A4	2.82								
KXJ12522.1	Protein lethal(2)essential for life	Efl2	-1.57								
KXJ12532.1	Protein lethal(2)essential for life	Efl2	-1.65								
KXJ20472.1	Glutamate dehydrogenase	GDH	1.92								
KXJ28654.1	G protein-coupled receptor kinase 5	GPCR	-1.39								
KXJ29225.1	Glutathione S-transferase U25	GST	-1.38								
KXJ22133.1	Interferon-induced protein 44-like	IFI44	-1.63								
KXJ26269.1	Macrophage mannose receptor 1	MMR	-1.35								
KXJ11283.1	Malate synthase	MS	1.40								
KXJ28313.1	Myotrophin	MTPN	-2.38								
KXJ29678.1	NADH dehydrogenase [ubiquinone] iron-sulfur protein 2, mitochondrial	NDUFS2	1.46								
KXJ29402.1	Nucleoredoxin	NRX	-1.25								
KXJ20961.1	NSFL1 cofactor p47	NSFL1C	-2.95								
KXJ16424.1	Programmed cell death protein 6	PD6	1.31								
KXJ26778.1	Protein disulfide-isomerase	PDI	1.60								
KXJ29597.1	Ras-related protein Rab-14	RAB14	1.45								
KXJ20404.1 KXJ15080.1	Soluble scavenger receptor cysteine-rich domain-containing protein SSC5D	SSC5D	-1.65								
KXJ12595.1 KXJ24044.1	putative very-long-chain enoyl-CoA reductase art-1	TECR	1.50								
KXJ27728.1	TNFAIP3-interacting protein 1	TNFAIP3	-1.72								
KXJ15023.1	Thioredoxin domain-containing protein 12	TXNDC12	3.25								

Table 2.6: Selected differentially abundant proteins (DAPs) in symbiotic Aiptasia. Fold changes in red and blue indicate proteins upregulated and downregulated respectively under pH 7.68 *vs.* pH 7.95. Proteins are listed alphabetically by their abbreviation for ease of reference. Columns to the right shaded grey indicate functional categories based on gene ontology (GO) term assignment. FC = fold change; Cat. = catabolism; Ana. = anabolism; Cyt. = cytoskeletal; Sig. = signalling; CelH = cellular homeostasis; ROS = oxidative stress response; CelR – cell proliferation regulation; ImR = immune response. Proteins listed are those discussed in the text.

Protein ID	Protein name	Abbrev.	FC	Cat.	Ana.	Cyt.	Sig.	CelH	ROS	CelR	ImR
KXJ09412.1	ADP,ATP carrier protein	AAC1	1.35								
KXJ26351.1	Acetyl-CoA carboxylase	ACC	1.74								
KXJ23302.1	ATP-citrate synthase	ACL	1.29								
KXJ22643.1	Alkaline phosphatase, tissue-nonspecific isozyme	ALP	1.25								
KXJ24357.1	Intestinal-type alkaline phosphatase 1	ALP	1.85								
KXJ15067.1	ATP synthase subunit g, mitochondrial	ATP5mg	1.56								
KXJ08873.1	Carbonic anhydrase 2	CAII	1.70								
KXJ18065.1	Catalase	CAT	1.25								
KXJ23456.1	Chitobiase	CHB	1.79								
KXJ21174.1	Collagen alpha chain	COLA	1.46								
KXJ26461.1	CSC1-like protein	CSC1	-1.44								
KXJ14074.1	Cytochrome b-c1 complex subunit 7	CYTBC1	1.52								
KXJ21558.1	Cytochrome c oxidase subunit 6A1, mitochondrial	CYTC6	1.48								
KXJ09141.1	Alpha-enolase	ENO1	1.35								
KXJ05943.1 KXJ05531.1	Golgi-associated plant pathogenesis-related protein 1	GAPR-1	1.82								
KXJ07707.1	Guanylate-binding protein 6	GBP6	1.52								
KXJ08512.1	putative glutathione S-transferase 6	GST	-1.38								
KXJ23319.1	Histone H3	H3	2.06								
KXJ23319.1	Histone H3	H3	4.61								
KXJ16950.1	Heat shock 70 kDa protein	HSP70	1.34								
KXJ22112.1	Interferon-induced protein 44-like	IFI44	2.78								
KXJ16580.1	Lysosome-associated membrane glycoprotein 1	LAMP1	1.44								
KXJ15998.1	Malate dehydrogenase, mitochondrial	MDH	1.29								
KXJ11283.1	Malate synthase	MS	-1.36								
KXJ10685.1	Melanotransferrin	MTf	1.48								
KXJ20768.1	Programmed cell death 6-interacting protein	PD6	1.39								
KXJ27376.1	Phosphoenolpyruvate carboxykinase [GTP], mitochondrial	PEPCK	2.09								
KXJ12328.1	60S ribosomal protein L15	RPL15	1.65								
KXJ10179.1 KXJ07551.1	60S ribosomal protein L17	RPL17	1.37								
KXJ15968.1	40S ribosomal protein S7	RPS7	1.69								
KXJ09448.1	Ras-like protein RAS2	R-Ras2	1.32								
KXJ27016.1	Sodium-coupled monocarboxylate transporter 1	SMCT1	2.34								
KXJ22105.1	putative tyrosinase-like protein tyr-3	TYR3	-1.42								
KXJ24157.1	Voltage-dependent calcium channel subunit alpha-2/delta-3	VGCC	1.66								

2.4 Discussion

2.4.1 Overview

A clear understanding of how OA affects the cnidarian-dinoflagellate symbiosis at the cellular level remains elusive (Tresguerres et al. 2017; Herrera et al. 2021; Lin et al. 2022). To further explore this issue, this research characterised the physiological responses and proteome of both partners in a model cnidarian–dinoflagellate symbiosis, over 26 days' exposure to either ambient (pH 7.95) or decreased pH (pH 7.68). Consistent with my hypotheses, I observed that proteins involved in metabolism and stress responses were upregulated in both host and symbiont, and that an indicative stress response was more pronounced in aposymbiotic Aiptasia than in symbiotic anemones. However, contrary to my hypotheses, photosynthetic performance was largely unaffected by low pH, while proteins associated with carbon concentrating mechanisms (CCMs) were upregulated rather than downregulated in symbiotic Aiptasia.

Impacts of OA on photophysiology and host-symbiont biomass

I hypothesised that photosynthetic performance would improve as pH levels decreased, due to release from carbon limitation, however this was not observed. Indeed, decreased pH had little effect on the photosynthetic parameters measured here. No significant differences were seen in light-adapted measures of chlorophyll fluorescence (Φ_{PSII}) or in concentrations of chlorophyll *a per* symbiont cell. However, there was a significant effect on the maximum quantum yield of PSII (F_v/F_m) at T1 (though not at the later timepoints), with a lower yield observed at pH 7.68 than pH 7.95. With respect to growth, pH regime did not significantly impact symbiont cell density or host biomass as assessed by protein content. However, there were signs that symbiont density was increasing by the final timepoint (consistent with my hypothesis), while host size as measured by pedal disc diameter did increase more at the lower pH in symbiotic Aiptasia.

Reports of photophysiological measures have been highly variable under low pH, however soft-bodied cnidarians have typically fared more favourably than have calcifying corals (e.g., Reynaud et al. 2003; Anthony et al. 2008; Kaniewska et al. 2012; Herrera et al. 2021; but see Comeau et al. 2017). Consistent with my observations, previous studies with soft-bodied symbiotic cnidarians, including

Aiptasia, have reported no change (Jarrold et al. 2013; Ventura et al. 2016; Jiang and Lu 2019) or an increase in F_v/F_m (Suggett et al. 2012; Towanda and Thuesen 2012; Gibbin and Davy 2013; Hoadley et al. 2015), typically coupled with a stable or increased symbiont population density. In contrast, Jiang and Lu (2019) reported a decrease in cell density of *B. minutum* in culture when exposed to low pH, suggesting that the host may buffer its symbionts to some degree from external stressors (Muller-Parker and D'Elia 1997; Venn et al. 2008; Davy et al. 2012).

In the intact symbiosis, improved photosynthetic performance combined with a stable or increased symbiont density would be predicted to enhance host growth, given the nutritional importance of symbiont-derived photosynthate to host metabolism (Muscatine et al. 1981; 1984; Yellowlees et al. 2008; Lehnert et al. 2014). While an increase (non-significant) in symbiont density was only seen at the final timepoint in the current study, the increased pedal disc diameter over time is consistent with an enhanced supply of photosynthate from the symbiont population. The reason why this same trend was not apparent in the protein content data is unknown, though the proteomics dataset (see below) once again suggests a positive effect of elevated CO_2/reduced pH on the provision of photosynthate to the host.

The duration and rate of change of exposure are also important considerations, with short timescales (hour to days) having been reported to induce signs of pH stress (Moya et al. 2012; Laurent et al. 2014; Lin et al. 2018), whereas some longer timescales (weeks to months) have revealed a less marked response (Takahashi et al. 2013; Wall et al. 2014; Zhou et al. 2016; Comeau et al. 2017). These observations are consistent with the initial dip in F_v/F_m followed by recovery seen in the current study, and suggest some capacity to acclimate to a new, moderate pH regime in the medium- to long-term. It would be interesting to run a longer-term experiment in the future, to assess what the impacts of protracted pH change are on symbiosis physiology and biomass. Nonetheless, when taken together, the relatively stable photophysiology seen here, combined with enhanced symbiotic host growth and the absence of any obvious negative impacts of reduced pH on the aposymbiotic anemone, suggest that future OA conditions are unlikely to have negative effects on the Aiptasia-*B. minutum* symbiosis.

Impacts of OA on the host and symbiont proteome

The number and breadth of proteins identified in this study provided a robust dataset for analysis and confirmed large numbers of proteins predicted from genomic data that were previously hypothetical, i.e., lacking strong sequence similarity to previously described proteins (977 for *B. minutum*, and 494 for Aiptasia). These previously unconfirmed proteins represented 47% and 11% of the proteins identified for *B. minutum* and Aiptasia, respectively, illustrating differences in the extent of existing genome mapping for each species. Despite its significance to understanding the complexities of this intricate symbiosis, the dinoflagellate genome remains poorly characterised (Sunagawa et al. 2009; Wang et al. 2014; Aranda et al. 2016). The available protein annotations are even more limited, hindering the identification of both proteins and their functionality (Wang et al. 2014; Supasri et al. 2021; Lin et al. 2022). However, the data provided by this study, along with the growing body of 'omics' research into the cnidarian-dinoflagellate symbiosis, provide further clues to assist in closing this knowledge gap. The protein abbreviations used in the following discussion are provided in **Tables 2.4**, **2.5** and **2.6** for *B. minutum*, and aposymbiotic and symbiotic Aiptasia, respectively.

In this study, symbiotic state was by far the biggest driver of observed differences in the cnidarian host, both in terms of the number of DAPs and their relative levels of abundance. In symbiosis, Aiptasia showed significantly higher abundance of proteins annotated for lipid metabolism and transport, carbohydrate metabolism, nitrogen assimilation and amino acid transport. Also differentially regulated were several CAs, which act as inorganic carbon transporters, and two Na^+/H^+ antiporters. Notably, the most extreme change was a 30-fold increase in a mothers-against-decapentaplegic-like protein associated with the innate immune response and TGFβ signalling pathways. Significantly upregulated in aposymbiotic Aiptasia were proteins annotated for cytoskeletal organisation, including multiple COL proteins. Markers of ROS responses, including SOD, CAT, ENO1, a TXNDC protein and an apoptosis-inducing factor were all highly abundant in aposymbiotic animals. Increased heterotrophy was also marked by the upregulation of AMCase, CTRB and CTRC. These findings confirm previous work identifying significant differences in the proteomes of symbiotic *vs.* aposymbiotic Aiptasia (Lehnert et al. 2014; Oakley et al. 2016; Sproles et al. 2019). Results here indicate a similar magnitude of difference, and show close alignment with both the functional groups and specific proteins identified in these previous analyses.

Overall, my data indicated only a minimal effect of pH treatment on both the host and symbiont, both in terms of DAP numbers and the relatively modest size of fold-changes. However, there were significant differences in the profiles of protein abundance over time under the different pH levels. In both symbiont and host, these differences occurred with respect to metabolic processes and activation of the cell stress response. In *B. minutum*, this appeared to be driven by increased photosynthetic activity, while in Aiptasia, differences also included cellular homeostasis, regulation of cell proliferation and the innate immune response. A proposed model summarising these changes is outlined in **Figure 2.10**. The discussion below refers to DAPs between the first (T1) and two later timepoints (T2 and T3) under pH 7.68 *vs.* pH 7.95, unless otherwise stated.

2.4.2 Response of the dinoflagellate symbiont

Photosynthesis

Photosynthesis-annotated proteins comprised nearly one quarter of DAPs in *B. minutum* and exhibited the largest fold-differences between the two pH levels, consistent with an upregulation in photosynthetic activity at the lower pH. This is despite only limited differences being seen in the photophysiology data over the course of the experiment. Indeed, while a suppression of dark-adapted chlorophyll fluorescence (F_v/F_m) occurred under decreased pH during the first week, other photophysiological effects were not subsequently apparent. It is also notable that protein regulation occurred beyond the earliest timepoints (i.e., changes between T1 and T2, and between T2 and T3), suggesting that the observed proteomic changes may have been uncoupled from photosynthetic performance (Dubinsky and Berman-Frank 2001; Herrera et al. 2021).

Seven of the 12 photosynthesis-annotated DAPs (six FCPs, and PSII CP47) were associated with the LHC at PSII. FCPs non-covalently bind the components of the LHC: fucoxanthin and chlorophylls *a* and *c* (Büchel 2020; Pajot et al. 2022). While annotated as FCPs in publicly-available databases, some if not all of these proteins are likely chlorophyll *a*-chlorophyll *c*2-peridinin-protein (apcPC; Jiang et al. 2014). LHCs capture and deliver excitation energy to their associated photosystems, with energy being transferred from peridinin and chl *c* to chl *a* and the photosynthetic reaction centre (at PSII, P680), where it is used to synthesise ATP and reducing power (Büchel 2020). At PSI, PsaA and FNR were both upregulated. PsaA binds the photosynthetic reaction centre (at PSI, P700), while FNR

catalyses the final step of electron transfer from PSI to the reducing equivalent NADPH (Michelet et al. 2013; Warner and Suggett 2016). These changes at both photosystems therefore suggest an upregulation of chlorophyll binding and electron transfer activity through the electron transfer chain (ETC), increasing ATP and NADPH synthesis. ATP and NADPH ultimately provide fuel for the second and third stages of the Calvin-Benson cycle (reduction and regeneration) (Roth 2014; Warner and Suggett 2016). Notably, GAPDH, a key enzyme in the Calvin-Benson cycle, was also upregulated. GAPDH catalyses reduction and regeneration, and its activation is dependent on photosynthetic electron transport (Michelet et al. 2013). Interestingly, there was no differential abundance of Rubisco, which catalyses the first, CO_2 fixation stage. This differs from the results of Lin et al. (2022) – one of the few other proteomics studies to examine the cnidarian-dinoflagellate symbiosis under OA. They found that Rubisco synthesis decreased linearly with decreasing pH in the symbiosis between the scleractinian coral *Galaxea fascicularis* and *Cladocopium* sp. Further study is merited to understand the origins of these differing findings.

Overall, the proteome expression here aligns with Scucchia et al. (2021), who found an overall upregulation of genes related to photosynthetic carbon fixation in *Symbiodinium microadriaticum* in symbiosis with the coral *Stylophora pistillata* under low pH. The upregulation of several proteins involved in symbiont ROS management pathways (discussed further below) also suggests an increase in photosynthetic activity over time at the lower pH (Richier et al. 2005; Lesser 2006). Further, these increases in photosynthetic activity are aligned to the upregulation of CAII in symbiotic Aiptasia, which likely plays a key role in host CCMs (Furla et al. 2000; Bertucci et al. 2011; Zoccola et al. 2015) – discussed further below. No differential regulation of symbiont CCMs in response to reduced pH was observed in the current study. This result was contrary to my hypothesis, as well as to the findings of Lin et al. (2018) who observed an overall downregulation of DIC-uptake related genes in *Cladocopium* sp., including three symbiont-derived CAs.

Metabolism

Aligned to the increase in photosynthetic activity hypothesised from these data, proteins involved in central metabolic pathways and biosynthesis were also differentially abundant. GAPDH catalyses the conversion of 3-phosphoglyceric acid (3-PGA) to glyceraldehyde-3-phosphate (G3P) during the reduction stage of the Calvin-Benson cycle (Austin et al. 1992; Streamer et al. 1993). This 3-carbon

sugar is used in the synthesis of fructose bisphosphate, which is then used to make other carbohydrates such as glucose, sucrose, and starch, as catalysed by FBPase (Bassham 1971; Miyagawa et al. 2001; Michelet et al. 2013). The upregulation of both GAPDH and FBPase observed here points towards increased gluconeogenesis in the symbiont under decreased pH, driven by the likely increase in photosynthetic activity described above (Lesser, 1997; Venn et al. 2008). Resulting carbohydrate products could then follow several different pathways. Firstly, they may be metabolised *via* the TCA cycle for ATP production (Fernie et al. 2004; Pernice et al. 2012). While there was no differential regulation of TCA-annotated proteins in this study, there was upregulation of enzymes active in the glycolytic pathway (FBPase, GAPDH and ENO1). Glycolysis transforms glucose into pyruvate, which feeds into the TCA cycle (Fernie et al. 2004). This agrees with Scucchia et al. (2021), who found an upregulation of genes involved in cellular respiration at pH 7.6 *vs.* pH 7.8 and pH 8.2. Conversely, both transcriptomic (Kaniewska et al. 2012; Moya et al. 2014) and metabolomic (Jiang and Lu 2019) studies have reported a downregulation of TCA cycle and/or glycolytic activity. Measurements of cellular respiration were not taken during this study and would be a useful addition to couple with proteomic data in future OA research to further unpick this pathway.

In a second pathway, glutamates may be metabolised *via* the purine pathway for nitrogen storage as derived compounds (Wang and Douglas 1999; Pernice et al. 2012). The upregulation of GMPS provides some support for this, as this enzyme is active in GMP biosynthesis, a subpathway of purine metabolism (Xiang et al. 2020). GMPS assimilates ammonia to reclaim nitrogen, which promotes algal cell division, potentially supporting the increase in symbiont density tentatively identified at the final timepoint in the current study (Dagenais-Bellefeuille and Morse 2013; Bayram et al. 2020). Thirdly, carbohydrate products could be translocated directly to the host, as glucose is likely to be the main metabolite transferred from symbiont to host in the cnidarian-dinoflagellate symbiosis (Burriesci et al. 2012; Hillyer et al. 2017; Matthews et al. 2018). Further, the differential abundance of proteins involved in host metabolic processes at pH 7.68 suggest that this is probable – discussed further in **Section 2.4.3**. Finally, glutamates may be used by the symbionts to synthesise other amino acids and proteins which may be stored within the symbiont cell or transferred to the host (Wang and Douglas 1999; Pernice et al. 2012; Hillyer et al. 2017), although evidence of this was not seen here. In a metabolomic study of *ex hospite B. minutum* under acidification, Jiang and Lu (2019) observed decreased symbiont amino acid pools. Interestingly, a similar decrease was observed in *B. minutum*

under heat stress (*in hospite* in Aiptasia; Hillyer et al. 2016). The reason such a decrease was not observed in the present study is unclear, however may be due to physiological differences between *in hospite* and *ex hospite* algae, or the greater sensitivity of metabolomic methods over proteomics in detecting such changes (Sogin et al. 2016; Matthews et al. 2017). The differential upregulation of proteins involved in each of these pathways suggest enhanced metabolic processes in *B. minutum* in response to decreased pH, and that this is likely driven by increased photosynthetic activity.

Transmembrane transport

The upregulation of the translocase H^+-PPase indicates an increase in active cross-membrane transport by the dinoflagellate. This enzyme uses the energy from diphosphate hydrolysis to move H^+ membranes (Maeshima 2001) and proteomic analysis has identified H^+-PPase as being present on the cell wall of *B. minutum (*Tortorelli et al. 2021). H^+-PPases are involved in a wide range of metabolic processes such ion enrichment, and hormone and nutrient transfer (Schilling et al. 2017). The upregulated abundance of these proteins alongside indicative increases in photosynthetic activity and carbohydrate metabolism implies an increase in photosynthate transfer from symbiont to host (Brownlee 2009; McCulloch et al. 2012; Gibbin and Davy 2014). Such a shift in metabolite transfer has been suggested in corals at similar pH values based on reported upregulation of genes coding for carbohydrate metabolism and active transfer (Rivest et al. 2018; Scucchia et al. 2021; Lin et al. 2022).

H^+-PPases have been shown to acidify the plant vacuole (Maeshima 2001), and it is possible that the upregulation of H^+-PPase is due to *B. minutum* creating a H^+ gradient to increase intracellular CO_2 concentrations to fuel photosynthesis (Barrot et al. 2015). Lin et al. (2022) reported the over-abundance of H+-ATPase, a key H_2CO_3 transporter, in *Cladocopium* sp. at lower pH levels, which they suggested indicated an increased demand to cope with DIC-limitation. However, given that CO_2 can passively diffuse across cell membranes, the expenditure of ATP on active transporters for this purpose seems less likely. Significant downregulation of dissolved inorganic carbon (DIC) uptake-related genes in has been reported in Symbiodiniaceae under elevated pCO_2, suggesting that endosymbionts rely on passive diffusion of CO_2 across the symbiosome membrane as a more energy-efficient mode of carbon acquisition (Price et al. 2011; Ventura et al. 2016; Lin et al. 2018).

Oxidative stress

In *B. minutum*, DAPs active in ROS management under low pH included two HSPs (HSP 905 and HSP DnaJ), CAT and SOD. ROS occur as products of normal aerobic metabolic functioning, including respiration and photosynthesis (Kregel 2002; Kültz 2005). Accordingly, all organisms possess defence mechanisms against ROS, which may otherwise by harmful to cellular structures (Kregel 2002; Kültz 2005). At the protein level, defences include the antioxidant enzymes CAT, ascorbate peroxidase and SOD, which act to convert ROS back to O_2 and H_2O (Lesser 1996; 2006; Richier et al. 2005; Weis 2008). SOD acts to reduce superoxide ($O_2 \cdot^-$) to hydrogen peroxide (H_2O_2), which CAT then reduces to O_2 and H_2O (Lesser, 2006; Weis 2008; Roberty et al. 2015). HSP90s are a highly conserved class of molecular chaperone that are key regulators of proteostasis under both physiological and stress conditions (Schopf et al. 2017).

These protein abundances contrast with transcriptomic studies including symbiont responses to OA, which report no differential expression of oxidative stress-related genes (Gonzalez-Pech et al. 2017; Davies et al. 2018; Rivest et al. 2018; Urbarova et al. 2019; Lin et al. 2018; Succhia et al. 2021). Coupled with the minimal changes seen in the photophysiological data, and the roles of these DAPs in basal ROS defence mechanisms of *B. minutum*, this suggests that the proteomic response observed here is part of a normal homeostatic response to photosynthetic activity (Weis 2008; Warner and Suggett 2016). However, the differential regulation of two BIP5s indicate that these ROS management pathways may have been overwhelmed. Oxidative stress can lead to disruptions to protein folding and degradation at the endoplasmic reticulum (ER), resulting in the toxic accumulation of unfolded or misfolded proteins. This is known as ER stress and results in the unfolded protein response (UPR) (Haynes and Ron 2010; Rainbolt et al. 2014). This pathway provides a defence against oxidative stress by promoting the detoxification of ROS and mitochondrial protein homeostasis, through increased transcription of mitochondrial chaperones and proteases (Haynes and Ron 2010; Dimos et al. 2019). BIP5s are active during the UPR, so suggest some activation of this response in *B. minutum*. That these results seem counter to the wider photophysiological response to low pH observed here and warrant further investigation.

2.4.3 Response of the cnidarian host

Metabolism

Changes in metabolic rates are a common outcome of environmental fluctuations, and changes in associated gene expression have been observed in cnidarians exposed to elevated pCO_2 (Kaniewska et al. 2012; Vidal-Dupiol et al. 2013; Urbarova et al. 2019; Lin et al. 2018; 2022; Succhia et al. 2021). While protein abundance does not correlate perfectly with metabolic activity, differential abundance of a suite of proteins involved in metabolic processes suggests an overall upregulation of metabolism under low pH in this study. Protein abundance in symbiotic Aiptasia pointed towards an upregulation of cellular respiration at pH 7.68. Cellular respiration consists of three key stages: glycolysis and pyruvate oxidation, the TCA cycle and oxidative phosphorylation *via* the $_{m}$ETC (Jafri et al. 2001). No differences were observed in glycolytic enzymes. However, ACC, which is involved in pyruvate oxidation, was upregulated. Increased TCA cycle activity was signalled by the differential abundance of the enzymes ACL, MS and MDH. The $_{m}$ETC contains four respiratory chain multi-subunit complexes (CI-CIV), which coordinate to transfer electrons from NADH and succinate to O_2, creating a concentration gradient over the inner mitochondrial membrane which drives transmembrane transport and ATP synthesis (Jafri et al. 2001; Nicholls and Ferguson 2013). Proteins in two of these three complexes were also upregulated – CYTBC1 and CYTC6 in CIII and CIV, respectively. Also upregulated in this process were the proteins responsible for ATP synthesis from ADP (ATP5mg), and for the import of ADP into the mitochondrial matrix for ATP synthesis and export of ATP to fuel cellular processes (AAC). In aposymbiotic Aiptasia, indicative differences in cellular respiration were much more subtle, with differential abundance of only two proteins involved in respiratory pathways. These were MS, which is active in the TCA cycle, and NDUFS2 which is part of the $_{m}$ETC (at CI). However, no changes in glycolysis or pyruvate oxidation were observed, nor any other indicators of increased ATP synthesis. NDUFS2 also acts as an oxygen sensor and participates in oxidative stress responses – a role which may be more relevant in this instance and is discussed further below. Taken together, these results indicate an overall upregulation of cellular respiration that was much more abundant in symbiotic anemones than in aposymbiotic ones.

Several anabolism-annotated proteins were differentially abundant in both symbiotic and aposymbiotic Aiptasia at low pH, although the relative proportion was greater in the former (40.4%

vs. 26.3% of all DAPs). DAPs with similar functions across both symbiotic states related to transcription and translation (e.g., ribosomal proteins) and cytoskeletal processes, which were generally upregulated. These included multiple actin-like proteins active in cell adhesion, cell membrane structure and organisation, and tissue development. Based on pedal disc size (but not on protein content) symbiotic anemones grew more over the course of the experiment at pH 7.68 than at pH 7.95. The greater abundance of anabolic proteins at low pH aligns with this increased growth. In aposymbiotic anemones, it may be that this upregulation of cytoskeletal proteins is implicated as part of a wider adaptive response – discussed further below.

Despite these differential protein abundances suggesting growth in both symbiotic and aposymbiotic anemones under low pH, there were distinct differences in lipid metabolism between the two. At pH 7.68, symbiotic Aiptasia showed upregulation in the synthesis (ACC) and transport (SMCT1) of fatty acids (Watkins 1997; Sproles et al. 2018). Conversely, DAPs in aposymbiotic Aiptasia at low pH indicated an upregulation in lipid catabolism (TECR and two CP450 proteins) and the downregulation of lipid transport (APL) (Sungawa et al. 2009; Tumanov et al. 2015). The cytochrome P450 protein group is suggested to have a role in the catabolism of cholesterol into steroids (Miller and Auchus 2011; Oakley et al. 2014). Several transcriptomic studies have reported increased lipid metabolism in cnidarian responses to low pH, including upregulation of TECR-coding genes (Moya et al., 2012; Kaniewska et al. 2012; Vidal-Dupiol et al. 2013), which activates the first step of fatty-acid metabolism or β-oxidation (Watkins, 1997; Tumanov et al. 2015). These studies found that corals may use their fatty acid reserves under low pH (Moya et al. 2012; Kaniewska et al. 2012; Vidal-Dupiol et al. 2013), a response also seen under heat stress both in corals and anemones (Grottoli and Rodrigues, 2011; Imbs and Yakovleva, 2012; Hillyer et al. 2016). These contrasting results highlight two key features of the cnidarian-dinoflagellate symbiosis; firstly, the benefits provided to the host by the transfer of photosynthetically-derived products from its symbionts. Increased activity of the TCA cycle and ACC has been suggested as a compensatory response to a decline in mobile product translocation under thermal stress (Imbs and Yakovleva 2012; Hillyer et al. 2016). However, coupled with increases in abundance of photosynthetic proteins and no decline in photosynthetic performance observed in the symbiont here, the upregulation of these proteins may rather indicate enhanced lipid synthesis in response to increased availability of glucose *via* photosynthate transfer (McCulloch et al. 2012; Venn et al. 2013; Gibbin and Davy 2014; Oakley et al. 2014; Lin et al. 2022). The absence of

such a response in aposymbiotic Aiptasia supports this hypothesis. Secondly, the transcriptomic studies referenced above reported on calcifying cnidarians, which require greater energy for calcification under OA conditions (Krief et al. 2010; McCulloch et al. 2012; Venn et al. 2013). The results seen here suggest that soft-bodied cnidarians may instead be able to divert photosynthate to somatic growth and other energy-intensive processes such as cellular homeostasis (Hoadley et al. 2015; Urbarov et al. 2019).

Interestingly, indicators of increased heterotrophy were observed in both symbiotic and aposymbiotic anemones at low pH, although these were more pronounced in the aposymbiotic state. While symbiotic cnidarians derive ~95% of their energy requirements from the photosynthate provided by their endosymbionts, heterotrophic feeding provides additional essential nutrients such as N and P (Muscatine et al. 1984; Whitehead and Douglas 2003; Yellowlees et al. 2008; Horowitz et al. 2015). In aposymbiotic Aiptasia, DAPs included CTRC and precursor CTRB which are both involved in proteolysis, and AMCase, an enzyme responsible for the extracellular degradation of arthropod tissue such as that of the anemones' food, *Artemia* sp. nauplii. The enzyme CHB also plays this role and was upregulated in symbiotic anemones. The results agree with Oakley et al. (2014), where heterotrophic proteins were upregulated in aposymbiotic *vs.* symbiotic Aiptasia under ambient conditions. They observed greater abundance of enzymes matching chymotrypsin and others involved in protein metabolism including a V8-like Glu-specific endopeptidase, a transmembrane serine protease, amine oxidase and several aldehyde/alcohol dehydrogenases, as well as chitinase and chitin deacetylase (Oakley et al. 2014). Van-Praet (1982) also found an increase of both extracellular trypsin and chymotrypsin activity in non-symbiotic *Actinia equina* after seven days of starvation. All anemones in this study were fed at a frequency which is sufficient under ambient conditions. However, the lack of symbiont-derived nutritional supply in aposymbiotic Aiptasia may induce higher expression of heterotrophic processes to compensate with prey-derived nutrients (Oakley et al. 2014). Notwithstanding these symbiotic state-specific effects, inferred increased heterotrophic feeding under low pH aligns with several studies identifying this phenomenon in corals similarly exposed to low pH (Edmunds, 2011; Towle et al. 2015; Vidal-Dupiol et al. 2013; Kornder et al. 2018). While these published studies identified a link to the increased energetic costs of calcification under elevated pCO_2, the upregulation of other host cellular processes, as described below, may also incur increased energy demands.

Carbon concentrating mechanisms

As discussed in **Section 1.1.3**, *in hospite* Symbiodiniaceae are thought to be carbon limited at current ocean pH levels (Davy and Cook 2001; Tansik 2017) and rely on their host to supply CO_2 required for carbon fixation during photosynthesis (Allemand et al. 1998; Venn et al. 2008). As such, host CCMs play a vital role in the cnidarian-dinoflagellate symbiosis. At the diffusion boundary layer, host CCMs involve the secretion of H^+ by H^+-ATPase, which results in the protonation of HCO_3^- to H_2CO_3 (Furla et al. 2000). Uptake by Symbiodiniaceae is mediated by the H_2CO_3 transporter H^+-ATPase (Bertucci et al. 2013), while CAs derived from both partners catalyse the conversion of H_2CO_3 to membrane-diffusible CO_2 (Weis et al. 1989; Furla et al. 2000). Though no differential regulation of CCM-related proteins was observed in *B. minutum*, CAII was upregulated in the symbiotic host, implying an intensification of host CCMs (Furla et al. 2000; Bertucci et al. 2011; Zoccola et al. 2015), which was contrary to my original hypothesis. While the methods used in this study cannot determine the originating cellular compartments of the proteins identified, a study by Bertucci et al. (2011), using immunolocalisation and confocal microscopy, reported that CAII was mainly localised in endodermal and aboral tissues within the coral *Stylophora pistillata*. This suggests that this CA is co-located with the algal symbionts (rather than at the diffusion boundary layer) and likely has a role in DIC supply by the host, although these mechanisms are still poorly characterised (Bertucci et al. 2011; Hopkinson et al. 2015). If this is so, this may explain why there was no corresponding upregulation of H+-ATPase observed in the host data here.

No differential CA abundance was observed in aposymbiotic Aiptasia, which supports the hypothesis that the upregulation observed in symbiotic anemones was related to host CCMs, rather than an independent homeostatic response of the animal to regulate intracellular pH (pH_i) (Weis et al. 1989). CA activity measured in symbiotic cnidarians is significantly higher than that measured in non-symbiotic cnidarian species (Weis et al. 1989). Further, CA activity was reduced 2.5-fold in aposymbiotic *A. pulchella vs.* symbiotic anemones (Weis 1993). Here, CAII abundance in symbiotic Aiptasia was 3.27-fold and 3.73-fold greater than in aposymbiotic Aiptasia at pH 7.95 and pH 7.68, respectively. These results support the hypothesis that CA acts as a putative symbiosis marker (Bertucci et al. 2011; Lehnert et al., 2014).

CAs are sensitive to environmental changes, and it has been proposed that a shift in available carbon species towards CO_2 may reduce the need for host CCMs (Weis et al. 1989; Krief et al. 2010; Hoadley et al. 2015). Moreover, as these are energy-consuming processes, it has been suggested that if the host is challenged in any way, their CCMs may become less efficient with downstream impacts on photosynthetic rates (Leggat et al. 1999; Herrera et al. 2021). Downregulation of CA activity has been reported in both corals (Moya et al. 2012; Vidal-Dupiol et al. 2013; Zoccola et al. 2016) and soft bodied cnidarians (Graham et al. 2015; Ventura et al. 2016), under high pCO_2, at a variety of pH values. Of these studies, some reported changes in CAII or CAII-like proteins (Vidal-Dupiol et al. 2013; Zoccola et al. 2016) while others did not specify the CA isoform that was downregulated. Hoadley et al. (2015) reported no effect on gene expression of either extra- and intra-cellular CAs (respectively, CAI and CAII) in the corals *Pocillopora damicornis* and *Acropora millepora* after exposure to reduced pH over similar timescales to those used in the current study, while Lin et al. (2018) also reported no differential regulation of CA genes in the coral *Galaxea fascicularis* after 10 days. However, Vidal-Dupiol et al. (2013) found that genes coding for CAII-like proteins were upregulated at pH 7.8 and 7.4 but downregulated at the extreme level of pH 7.2 in *P. damicornis* during a three-week exposure. These variable results may be due to differing pH levels, experimental conditions, species-specific effects, or reporting on differing CA isoforms. Here, my results suggest an increase in metabolic activity and ATP synthesis in symbiotic Aiptasia, which would align to an upregulation of host CCMs.

Cellular homeostasis

As described in **Section 1.2.2**, the regulation of pH_i is critical for most aspects of cell metabolism, including membrane functioning, ion transport, enzyme regulation and intracellular signalling, as well as DNA, RNA and protein synthesis (Madshus 1988; Venn et al. 2009). These metabolic pathways are pH-sensitive and accordingly, pH_i regulation is tightly controlled (Boron 2004; Venn et al. 2009; Casey 2010; Tresguerres et al. 2017). In symbiotic Aiptasia, several proteins with active roles in pH homeostasis were differentially abundant under low pH, including PEPCK and CAII. By homology, CAII is proposed to be involved in pH_i regulation in cnidarians (Bertucci et al. 2011; Hopkinson et al. 2015), where its putative role is in preventing the back-diffusion of CO_2 and leakage of DIC across cell membranes (Furla et al. 2000; Bertucci et al. 2013). Other specific proteins that regulate pH_i likely include Na^+/H^+-exchangers, V-H^+-ATPases, Na^+/K^+-ATPases and HvCN families

(Laurent et al. 2014; Barrot et al. 2017; Capasso et al. 2021). Here, the differential abundance of multiple active transport proteins implies a homeostatic response in both symbiotic and aposymbiotic anemones. These included those annotated as Ca^{2+} and K^+ ion transporters and a Na^+ channel regulator (aposymbiotic anemones), and two Ca^{2+} HvCN proteins (symbiotic anemones). These proteins have roles in a wide range of biological processes but are not specifically annotated for pH homeostasis. As such, their upregulation may be due to the metabolic response described above rather than regulation of pH_i. pH_i was not measured in this study, however Gibbin et al. (2014) observed that in the pH_i of symbiotic host cells showed a full recovery to control levels within 105 min of CO_2-addition, whereas the pH_i of aposymbiotic host cells did not make the same recovery. In the cnidarian-dinoflagellate symbiosis, the ability of host cells to maintain pH_i under elevated pCO_2 is closely linked with the photosynthetic performance of its symbionts (Laurent et al. 2013; Gibbin et al. 2014). Algal photosynthesis results in alkalinisation of the host cell through uptake of excess CO_2 and H^+, which supports the host cell's buffering capacity to changes in extracellular pH (pH_e), such as those driven by OA (Venn et al. 2009; Gibbin et al. 2014). While multiple active transport-related proteins were upregulated in aposymbiotic Aiptasia, the absence of pH homeostasis-annotated DAPs in this group suggests that pH_i regulation was more active in symbiotic anemones.

Oxidative stress

ROS occur as inevitable products of aerobic metabolism, and like all organisms, cnidarians have evolved defensive ROS management pathways (Kültz 2005; Weis 2008). Over-production of ROS can overwhelm these mechanisms and has been implicated in the breakdown of the cnidarian-dinoflagellate symbiosis, particularly in response to thermal stress (Lesser 1996; 2006; Richier et al. 2005; Weis 2008). In non-photosynthetic organisms, the primary source of ROS are the central metabolic processes active *via* the $_m$ETC (Kültz 2005; Dunn et al. 2012). Here, as hypothesised, DAPs in both anemone groups included those involved in ROS responses. Further, these proteins exhibited some of the largest fold-changes among all DAPs. In symbiotic Aiptasia, these included the upregulation of CAT, ENO1 and HSP70, and downregulation of GST. Upregulation of CAT has been widely reported in response to thermal stress (e.g., Lesser, 2006; Weis 2008; Krueger et al. 2015) and under elevated pCO_2 (Moya et al. 2015; Jiang et al. 2019). Multiple transcriptomic studies have reported the upregulation of HSPs in cnidarians exposed to low pH, with HSP70 being one of the most frequently identified (e.g., Kaniewska et al. 2012; Moya et al., 2012; 2015; Kenkel et al. 2017;

Lin et al. 2018; Urbarova et al. 2019). HSPs are an indicator of cellular stress, and over-expression HSP70 has been reported in response to a range to environmental stressors (Kregel 1985; Kültz 2005). Oxidative damage to proteins occurs in multiple forms, and the glutathione (GSH) and thioredoxin (TXN) systems repair such damage (Kültz 2005). GSH is a ROS-scavenger, playing a critical role during oxidative stress in both partners by reducing ROS availability (Lesser 2006; Baird et al. 2009). GST catalyses the conjugation of GSH, so acting as a precursor (Dickinson and Forman 2002; Kültz 2005). Here, GST was differentially abundant in both symbiotic and aposymbiotic anemone tissues under low pH, but not in *B. minutum*. This accords with the reported expression of this antioxidant pathway in Aiptasia under heat stress by Hillyer et al. (2017), who also did not detect stress-induced GST in the symbiont. Collectively, these results point towards differing levels of oxidative stress within each partner at low pH.

In aposymbiotic Aiptasia, stress-related DAPs under low pH included two CYP450 proteins (CYP20A1 and CYP3A4), NDUFS2, PDI, GST and TXNDC12. TXNDC12 and CYP3A4 exhibited the greatest fold-changes in this sample group, being upregulated 3.25-fold and 2.82-fold, respectively. PDI and TXNDC12 are localised to the ER and belong to the TXN protein family (Galligan and Peterson 2012; Kitchen et al. 2019). Differential expression of TXN-like genes has been reported under thermal stress in corals, which strongly implicates their role in ROS management (Kültz 2005; Starcevic et al. 2010; Souter et al. 2011; Rosic et al. 2014). NDUFS proteins act as an oxygen sensor and, along with CYP450 proteins, provide resistance to oxidative stress by regenerating reduced antioxidants such as GSH (Zangar et al. 2004; Ricaurte et al. 2016; Oakley et al 2017; Bandara 2021). Overall, these results point to a strong oxidative stress response in aposymbiotic anemones under low pH. The upregulation of ROS-scavenging proteins in aposymbiotic *vs.* symbiotic Aiptasia has been reported under ambient conditions (Lehnert et al. 2014; Oakley et al. 2016), perhaps reflecting the comparative energy deficit of these animals relative to photosynthate-fuelled symbiotic anemones, thereby placing them at greater likelihood of physiological stress (Gibbin and Davy 2014; Oakley et al. 2016).

The changes in lipid metabolism and transport observed in aposymbiotic Aiptasia here may also be related to such a ROS response. High levels of cellular ROS can be damaging to the lipid bilayer of cell membranes (Tchernov et al. 2004). Increasing lipid saturation may therefore provide enhanced

stability and protection against ROS damage and has been observed in response to thermal stress (Hillyer et al. 2016). The strong upregulation of cytoskeletal-annotated DAPs observed in aposymbiotic anemones under low pH would support this hypothesis. Further, oxidative stress can lead to disruptions to protein folding and degradation at the ER, resulting in the UPR (as described in **Section 2.4.2**) (Haynes and Ron 2010; Rainbolt et al. 2014). Here, the differential regulation of UPR-annotated proteins in aposymbiotic Aiptasia under low pH showed a marked contrast between the symbiotic states. DAPs in this group included two Efl2s, PDI, and TXDNC12, which are mitochondrial chaperones that act to reduce both misfolded proteins and ROS (Galligan and Peterson 2012; Kitchen et al. 2019). No UPR-annotated DAPs were detected in symbiotic Aiptasia. Differential regulation of these pathways has been observed across multiple heat stress studies (e.g., Dunn et al. 2012; Oakley et al. 2017; Dimos et al. 2019) and under decreased pH (Kaniewska et al. 2012; Moya et al. 2015; Urbarova et al. 2019), providing strong evidence for their role in the cnidarian oxidative stress response.

The ultimate outcome of the UPR is apoptosis, a form of programmed cell death (PCD) (Dunn et al. 2007; 2012). Regulation of cell growth, proliferation and death occur under normal cellular functioning, however these processes become upregulated as part of the oxidative stress response (Kültz 2005; Dunn et al. 2007). This can temporarily increase stress tolerance through the removal of damaged cells *via* apoptosis (Kültz 2005; Dunn et al. 2007; 2009). In symbiotic Aiptasia, several proteins involved in the regulation of apoptotic processes were more highly abundant under low pH, including CAT, ENO1, PD6 and RPS7 (Dunn et al. 2007; 2009; Weis 2008; Alderdice et al. 2021). This hints at differential regulation of cell death in this group, however these proteins are annotated as mediating both the positive (PD6 and RPS7) and negative (CAT and ENO1) regulation of apoptotic pathways, providing a mixed picture. Apoptotic mechanisms are thought to operate to maintain dynamic equilibrium between host and symbiont cell growth and proliferation (Fitt 2000; Dunn 2009; Lehnert et al. 2014). Lehnert et al. (2014) found that PCD-related genes were differentially abundant (both up- and downregulated) in symbiotic relative to aposymbiotic Aiptasia under non-stressful conditions. However, as they noted, the direction of gene expression does not necessarily follow functionality, and the results here add to this complexity. Further, the differential regulation of these proteins may be more relevant to their roles in transcription and ROS management, as described above.

In aposymbiotic anemones, regulation of cell proliferation was much more evident, including differential regulation of ACTL6A, CTRB, NSFL1C, and a suite of proteins involved in the apoptotic signalling pathway (e.g., PD6, PDI, TXDNC12) and apoptotic cell clearance (RAB14). This supports the model of a heightened stress response in the aposymbiotic state under low pH. The shifts required to maintain cellular homeostasis under external stressors, such as ROS and UPR responses, incur increased energetic costs due to their demand for NADH/NADPH and ATP (Kültz 2005). This may contribute towards the metabolic changes observed in aposymbiotic Aiptasia, particularly in lipid catabolism, given that they lack energetic support from endosymbionts (Gibbin and Davy 2013; Lehnert et al. 2014; Hillyer et al. 2016). Interestingly, Kaniewska et al. (2012) and Urbarova et al. (2019) reported upregulation of apoptotic transcripts in corals under low pH. While non-bleached calcifying corals do benefit from symbiont-derived photosynthate, they also face increased costs of calcification under elevated pCO_2, so are also likely to suffer from an energetic deficit, which may trigger similar pathways to those observed here in aposymbiotic Aiptasia (McCulloch et al. 2012; Venn et al. 2013; Vidal-Dupiol et al. 2013; Scucchia et al. 2021).

Immune response

The host immune response has been characterised as a crucial element of the cnidarian-dinoflagellate symbiosis (Schwarz 2008; Neubauer et al. 2017; Weis 2019). This response mediates cell proliferation of the symbiont and is closely connected to the ROS management and PCD pathways described above. Here, immunity-annotated DAPs were observed in both symbiotic states. In symbiotic Aiptasia, these included the upregulation of two ALPs, COLA, GBP6, GAPR-1, IFI44, and TYR3. IFI44 exhibited the greatest fold-change (↑2.78-fold) of all DAPs among this sample group and is an interferon-induced protein. Urbarova et al. (2019) reported similar fold-increases in interferon regulatory factor (IRF) and IFI genes in *A. viridis* at low pH. Both genes are involved in innate immunity and pathogen recognition, and upregulation of IRF has also been reported under heat stress (van de Water et al. 2018). Differential regulation of a COL protein was also observed by Lin et al. (2022) under low pH. Taken alongside the indicative increase of *B. minutum* cell densities and upregulation of DAPs involved in photosynthetic activity over time, these results suggest an upregulated immune response to growing numbers of increasingly productive symbionts. Interestingly, MTf was also downregulated in symbiotic Aiptasia over time. This protein is involved in cellular iron homeostasis, and iron is a key nutrient required for photosynthesis (Sunda and

Huntsman 1995; Reich et al. 2021). This could imply that the anemones were restricting iron supply to their symbionts as a means of controlling population densities. However, we know little about the role of iron in the cnidarian-dinoflagellate symbiosis and more work is needed in this area (Reich et al. 2021).

In aposymbiotic Aiptasia, the reverse effect was observed, with immune response-annotated proteins largely being downregulated, including ADAMTS, IFI44, MMR, RAB14 and TNFAIP3. TNFAIP3 is part of the TNF family of proteins, increased expression of which has been reported in pH-stressed cnidarians (Kaniewska et al. 2015; Urbarova et al. 2019; Lin et al. 2022). Genes encoding TNF receptors and receptor-associated proteins were also upregulated in heat-stress studies (Barshis et al. 2013; Pinzón et al. 2015). TNFAIP3 has roles in multiple immune response pathways, including NF-kβ signalling, myD88-DAPendent toll-like receptor signalling and the ERK cascade. NF-kβ signalling is active in apoptosis and is here annotated to the proapoptotic gene p53 (Kültz 2005; Weis 2019). These results imply a strongly downregulated immune response in aposymbiotic Aiptasia, aligned to the pronounced oxidative stress response described above relative to symbiotic anemones under low pH. Transcriptomic studies have reported the downregulation of genes involved in the innate immune response in symbiotic *vs.* aposymbiotic cnidarians under ambient conditions, suggesting that downregulation of immunity plays a key role in the host's tolerance of Symbiodiniaceae (Lehnert et al. 2014; Wolfowicz et al. 2016; Neubauer et al. 2017; Mansfield and Gilmore 2019; Weis 2019). As such, the converse relationship seen here implies a stress response in aposymbiotic Aiptasia. A similar downregulation of innate immunity-related transcripts (Kaniewska et al. 2015; Urbarova et al. 2019) and proteins (Lin et al. 2022) has been reported in pH-stressed cnidarians. However, these results highlight that the precise role of immunity in cnidarian responses to external stressors is an area requiring much future research (Weis 2019).

2.4.4 Proteomic response to ocean acidification: a putative model

Taken together, the results outlined here suggest that the Aiptasia-*B. minutum* symbiosis will be relatively resilient to future OA scenarios, as summarised in **Figure 2.10**. The data indicate that photosynthetic performance of *in hospite B. minutum* is likely be maintained under decreased pH, and that the proteomic response of this symbiont is characterised by the relative over-abundance of multiple photosynthesis-related proteins. In turn, these seemed to drive an upregulation of central

metabolic and biosynthetic processes, which may confer benefits to the host anemone through increased photosynthate transfer (Burriesci et al. 2012; Gibbin and Davy 2014; Hillyer et al. 2017). While proteins active in algal ROS management were upregulated, this was likely a basal homeostatic response to increased photosynthetic activity rather than a sign of undue oxidative stress (Kültz 2005; Weis 2008; Warner and Suggett 2016). The magnitude of change observed in *B. minutum* was relatively minor in comparison to that seen in the anemone host. This suggests that the cnidarian host provides some protection against the potential adverse effects of OA (Gonzalez-Pech et al. 2017; Jiang and Lu 2109; Urbarova et al. 2019). Further, the host may support enhanced photosynthesis through intensification of CCMs at the symbiosome surface, which acts as the host-symbiont interface (Furla et al. 2000; Bertucci et al. 2011; Zoccola et al. 2015).

In Aiptasia, the comparative differences between symbiotic states in response to low pH highlight both the importance and functionality of the cnidarian-dinoflagellate symbiosis. While there appeared to be an upward trend in metabolic and homeostatic processes in both symbiotic and aposymbiotic anemones, the nature of these responses was quite different. In symbiotic anemones, the results imply an overall increase in cellular respiration and ATP synthesis at low pH, together with enhanced fatty acid synthesis (Watkins 1997; Sproles et al. 2018). In aposymbiotic animals, changes in cellular respiration were far more subtle. Concurrently, the apparent increase in lipid catabolism implies an increased energy demand with no such rise in ATP production (Sungawa et al. 2009; Tumanov et al. 2015). Interestingly, both groups appeared to augment their nutritional requirements with greater heterotrophy (Edmunds, 2011; Towle et al. 2015; Vidal-Dupiol et al. 2013; Kornder et al. 2018). In both symbiotic and aposymbiotic states, ROS responses were evident in response to reduced pH. In symbiotic Aiptasia, ROS management appeared to align with normal homeostatic functioning. Conversely, in aposymbiotic animals, the results point to a strong oxidative stress response, including triggering of the UPR and apoptotic pathways (Kültz 2005; Dunn et al. 2007: Weis 2008). These contrasting results seem to highlight the key compensatory role of enhanced nutritional benefit derived from endosymbionts under low pH. Over time, however, this may come at some cost, as indicated by an apparent triggering of the innate immune response in host animals – potentially driven by photosynthetically-derived ROS (Schwarz 2008; Neubauer et al. 2017; Weis 2019). Together, these data suggest that, while the cnidarian-dinoflagellate holobiont may not exhibit external signs of OA effects, underlying cellular processes are likely coordinating to provide an acclimatory response.

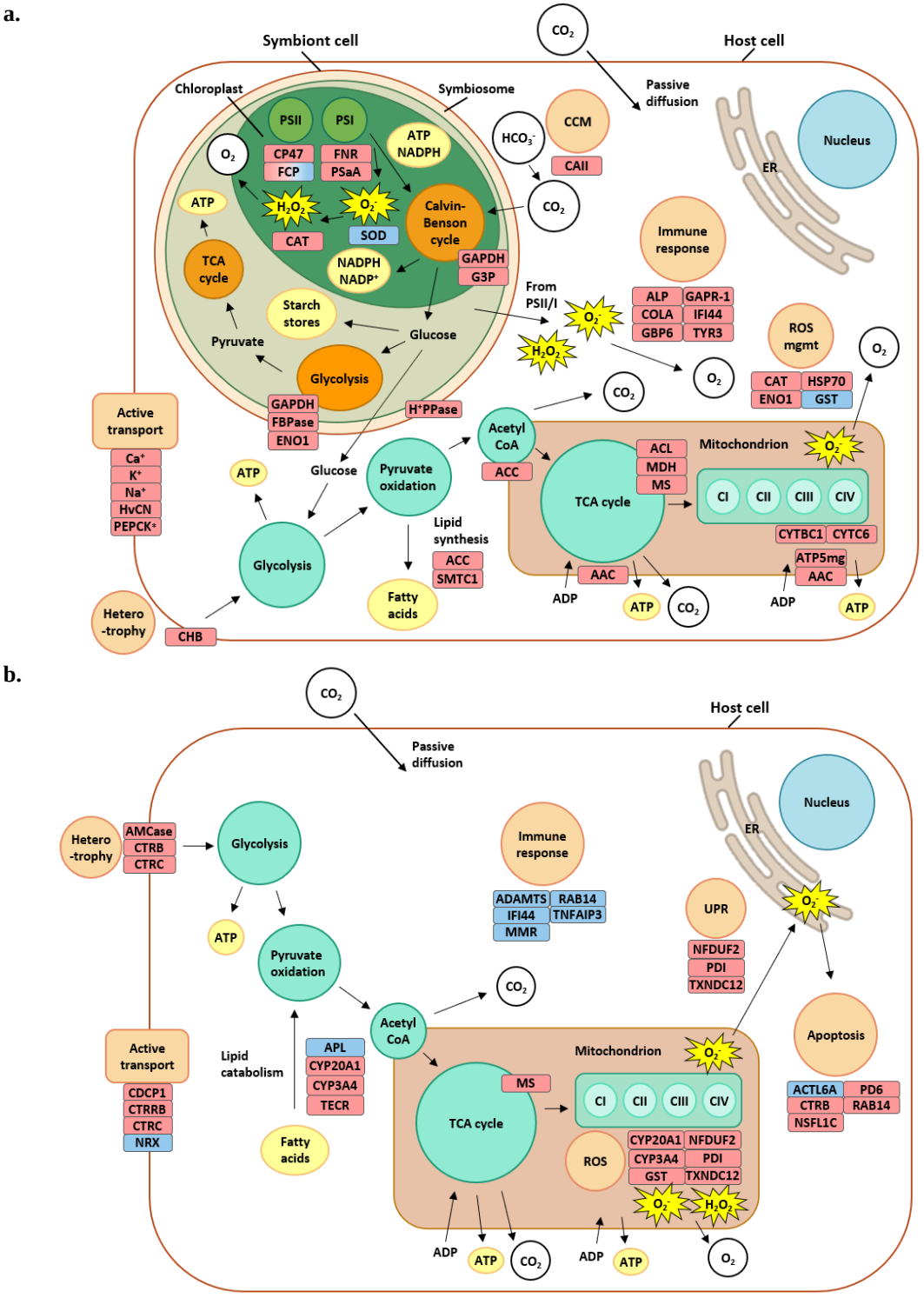

Figure 2.10: Putative model of cellular responses to decreased pH. a. the symbiotic Aiptasia-*Breviolum minutum* holobiont; **b.** aposymbiotic Aiptasia. This model is summarised in **Section 2.4.4**. ER = endoplasmic reticulum. ROS = oxidative stress response. UPR = unfolded protein response. Red and blue shading indicate proteins that were upregulated and downregulated respectively under pH 7.68 *vs.* pH 7.95. For protein abbreviations see **Table 2.4** for *B. minutum*, **Table 2.5** for aposymbiotic Aiptasia and **Table 2.6** for symbiotic Aiptasia.

2.4.5 Conclusions

This study is only the second to investigate the effects of low pH on the proteome of both partners in the cnidarian-dinoflagellate symbiosis and is the first to do so in the Aiptasia model system. The results outlined here add to the growing body of 'omics' work in this model system and provide useful proteomic resources for both host and symbiont. This is particularly valuable for the dinoflagellate *B. minutum*, as until recently, there has been a stronger emphasis on understanding host responses to low pH. The approach used here highlights the value in using multiple methods to investigate the response of both partners, given the strongly inter-related nature of their responses to future ocean scenarios (Scucchia et al. 2021). Taking my results alongside those of Lin et al. (2022), it appears that maintaining and enhancing metabolic homeostasis, nutrient cycling and host adaptive immune responses constitute key mechanisms in early-stage OA responses. While specific proteins differ between the two studies, trends in biological processes and overall organismal responses are comparable, suggesting that a characteristic response may exist across different cnidarian-dinoflagellate interactions, albeit with varying and potentially species-specific pathways. Overall, this study provides a valuable baseline from which to identify candidate protein complexes for further investigation, and longer-term effects of OA on the proteome of both partners in the cnidarian-dinoflagellate symbiosis.

Photo courtesy of Matthew Nitschke

Chapter 3: Effects of Ocean Acidification on the Establishment of the Cnidarian-Dinoflagellate Symbiosis

3.1 Introduction

Coral reefs form iconic ecosystems that are among the most biodiverse on the planet, supporting around a third of all marine species *via* provision of food and habitat (Harborne et al. 2017; Doney et al. 2020). These ecosystems depend upon the symbiotic relationship between stony corals and Symbiodiniaceae, a diverse family of photosynthetic dinoflagellates which live intracellularly within their host (Fitt and Trench 1983; LaJeunesse et al. 2018). In harbouring these symbionts, the host receives photosynthetic products – including glucose, lipids and fatty acids – that serve around 95% of their energy needs (Muscatine et al. 1984; Whitehead and Douglas 2003; Yellowlees et al. 2008; Burriesci et al. 2012). In return, the symbionts receive a stable, high light environment and nutritional waste products in the form of inorganic nitrogen, phosphorus, and carbon (Muller-Parker and D'Elia 1997; Venn et al. 2008; Yellowlees et al. 2008; Davy et al. 2012). This vitally important symbiosis requires optimal environmental conditions to function effectively and is under threat from climate change stressors, most notably ocean warming and ocean acidification (OA) (Ainsworth 2016; Hughes et al. 2017; Doney 2020).

Around 30% of anthropogenic CO_2 released since pre-industrial times has been absorbed by the oceans, which subsequently decreases pH and alters carbonate chemistry *via* the availability of dissolved inorganic carbon (DIC) species (Sabine et al. 2004; Doney et al. 2009; 2020; Gruber et al. 2019; IPCC 2019). How OA affects the establishment of the coral-algal symbiosis is not well understood. This early stage has fundamental importance for the successful development and functioning of this symbiosis (Albright 2011; Nitschke et al. 2016; Sun et al. 2020; Jiang et al. 2021). Disruption to early life-stages can have detrimental impacts on recruitment success, species abundance and distribution, and population maintenance, with serious ecological implications (Albright 2011; Hédouin and Gates 2013; Woods et al. 2016). For individual coral colonies, absence of symbionts signifies a nutritional deficit, which may be compounded by the additional energetic costs imposed under elevated pCO_2 levels (Yellowlees et al. 2008; Albright 2011; Yuan et al. 2018).

Corals acquire their symbionts in one of two ways: either *via* maternal transmission or horizontal transmission. Approximately 15% of coral species inherit their symbionts maternally, whereby Symbiodiniaceae are present in the egg or brooded planula larva prior to release from the maternal colony (Baird et al. 2009; Fabina et al. 2012). In this method, symbionts are passed on from one generation to the next (Baird et al. 2009; Fabina et al. 2012). Conversely, around 85% of coral species adopt horizontal transmission, which occurs when larvae are released without symbionts and take them up from the environment (Rodriguez-Lanetty et al. 2006; Baird et al. 2009; Harii et al. 2009). This process re-establishes symbiosis with each new generation and allows for greater variation in symbiont-host combinations, which may differ from those of the parent colonies (Fandallah 1983; Harrison 2011). However, homologous types (i.e., those found natively in the adult corals) appear to be favoured over heterologous types (i.e., non-native) (Rodriguez-Lanetty et al. 2006). Horizontal transmission may also occur following a bleaching event, which most often occurs due to elevated sea surface temperatures (Hughes et al. 2017; Kishimoto et al. 2020). Here, corals may be repopulated with the same type of symbiont that they originally harboured, or 'switch' to a more thermally tolerant type (Loram et al. 2007; Stat et al. 2009; Cunning et al. 2015; Cumbo et al. 2018). However, cnidarian-dinoflagellate symbioses often exhibit a high degree of inter-partner specificity, limiting the potential for 'switching' as an adaptive mechanism to external stressors (Stat et al. 2009; Cunning et al. 2015; Hoadley et al. 2016a; 2019; Gabay et al. 2018; 2019). Further, both larvae and adults appear to exhibit similar mechanisms for discriminating between compatible and incompatible symbionts (Hambleton et al. 2014). Given the relative proportion of cnidarian species adapted for horizontal transmission, understanding how it is affected by environmental change is of significant interest.

The establishment of cnidarian-dinoflagellate symbioses involves a complex array of inter-partner processes that are still being unravelled (Yuyama et al. 2018; Weis 2019; Mohamed et al. 2020). These processes fall into three stages: inter-partner signalling and recognition, colonisation by the symbiont of host cells, and intracellular selection of symbionts by the host (**Figure 1.2a**) (Davy et al. 2012; Yuyama et al. 2018). Symbionts are taken up orally from the environment into specific cells within the gastrodermal layer (Rodriguez-Lanetty et al. 2006; Bucher et al. 2016). The initial contact between host and symbiont triggers a series of molecular signalling cascades involving pattern recognition and cell adhesion molecules (Wolfowicz et al. 2016; Neubauer et al. 2016; 2017; Weis

2019). Microbial cell surfaces are covered with microbe-associated-molecular patterns (MAMPs) that can be detected by pattern recognition receptors (PRRs) on the host's cell surfaces (Wood-Charlson et al. 2006; Neubauer et al. 2016; Weis 2019). The most well researched of these are the interactions between cnidarian lectins and algal glycans, and there is some evidence that specific glycan-lectin binding is active in the recognition of compatible Symbiodiniaceae species (Wood-Charlson et al. 2006). Recognition then activates the host's innate immune pathways which either tolerate or defend against symbiont presence (Poole et al. 2016; Weis 2019). Here, symbiont cells are either marked for destruction *via* lysis, or taken into the host's cells *via* phagocytosis (Poole et al. 2016). Multiple studies have corroborated this role for the immune system in host-symbiont recognition, providing evidence that molecular pathways involved in innate immunity are differentially expressed during the onset of symbiosis. These include transcription factor NF-κB, TSR proteins and the TGFβ signalling pathway (Detournay et al. 2012; Wolfowicz et al. 2016; Berthelier et al. 2017; Neubauer et al. 2017). Transcription factor NF-κB plays a key role in immunity cascades and is decreased in cnidarians that have been newly inoculated with symbionts, which suggests that symbionts may modulate the host immune response by repressing NF-κB expression (Wolfowicz et al. 2016; Mansfield et al. 2017; Weis 2019).

If marked as compatible, symbionts are phagocytosed by host gastrodermal cells, where they are enveloped in a host-derived vacuole called the symbiosome (Hohman et al. 1982; Rodriguez-Lanetty et al. 2006; Bucher et al. 2016). While phagosomes typically mature by fusing with lysosomes to degrade invasive microbes, in symbiont recognition this process is arrested (Hohman et al. 1982; Mohamed et al. 2016). The phagosome membrane instead becomes the symbiosome membrane and serves to protect the algal cell from lysosomal degradation, as well as playing key roles in nutrient transport (Hohman et al. 1982; Fitt and Trench 1983; Davy et al. 2012). Rab and G-protein-coupled receptor (GPCR) family proteins on the symbiosome surface then enable the persistence of healthy algal cells and exclusion of dysfunctional algae, likely through modulation of host immune pathways (Chen et al. 2003; 2005; Peng et al. 2010; Mohamed et al. 2016; Matthews et al. 2017). The host distinguishes between compatible and incompatible symbiont types during this process, which may relate to host differentiation based on specific symbiont glycan profiles (Koike et al. 2004; Wolfowicz et al. 2016; Weis 2019). However, the precise mechanisms by which inter-partner specificity occurs are still the subject of investigation.

The influence of OA on these processes is poorly understood. While studies exist on the effects of low pH on the early life-stages of coral planulae and juveniles, these have focused on planula settlement, survival, and post-settlement growth. Findings here have included reduced settlement, metamorphosis, and growth rates, and at the cellular level, downregulation of nutrient transport and energy metabolism pathways (Albright et al. 2008; Suwa et al. 2010; Anlauf et al. 2011; Nakamura et al. 2011; Bergman et al. 2018; Yuan et al. 2018; Jiang et al. 2019). Others have reported no effect of low pH on settlement or survivorship rates (Kurihara 2008; Anlauf et al. 2011). To date, only three papers have examined the effects of OA on the establishment of cnidarian-dinoflagellate symbioses or on re-uptake of symbionts post-bleaching (Suwa et al. 2010; Sun et al. 2020; Jiang et al. 2021). Suwa et al. (2010) observed delayed symbiont uptake in the first few days post-inoculation, coupled with decreased growth rates in juvenile polyps of the coral *Acropora digitifera* under decreased pH compared to controls. Conversely, no observable effects of low pH were seen on colonisation rates of newly-settled corals *Acropora intermedia* or *Platygyra daedalea* (Sun et al. 2020; Jiang et al. 2021). As such, the effects of OA equivocal remain equivocal.

Research suggests that colonisation rates are affected by both heat and light stress, indicating that they are vulnerable to the impacts of wider environmental disturbances (Baird et al. 2010; Abrego et al. 2012; Schnitzler et al. 2012; Yorifuji et al. 2017; Cumbo et al. 2018; Sun et al. 2020). Further studies are therefore needed to assess whether OA influences this key life event in the cnidarian-dinoflagellate symbiosis. This study contributes to the currently limited body of knowledge by examining the impacts of OA on the establishment of symbiosis between the cnidarian model organism *Exaiptasia diaphana* (‘Aiptasia’) and its native symbiont *Breviolum minutum*. Similarly to many corals, Aiptasia acquires its symbionts *via* horizontal transmission and forms associations with some of the same Symbiodiniaceae species (Thornhill 2013; 2014), and especially *B. minutum* through much of its Indo-Pacific range (Weis et al. 2008; Xiang et al. 2013; Bucher et al. 2016). Aiptasia regularly reproduces and so does not present the same constraints as reef-building corals which typically spawn once annually (Harrison 2011). Additionally, Aiptasia can be rendered symbiont-free and maintained in an aposymbiotic state if sufficiently fed (Lehnert et al. 2014; Matthews et al. 2016). These factors make this sea anemone a valuable model system in which to study cnidarian-dinoflagellate symbiosis establishment (Bucher et al. 2016; Wolfowicz et al. 2016). My objective was to establish whether decreased pH impacts the capacity of Aiptasia to acquire and

establish a symbiosis with *B. minutum*. The findings outlined in **Chapter 2** suggest that OA could affect the innate immune response of host animals, including differential regulation of proteins active in the NF-kβ signalling pathway outlined above, as well as the regulation of pathways involved in metabolism and nutrient transfer between the two partners. These data suggest that establishment of successful symbiosis may be influenced by OA. Based on these findings and indications from the limited number of published studies to date, my hypotheses were that: 1) exposure to decreased pH would reduce symbiont uptake and colonisation rate; and 2) there would be greater impact of low pH in the first few days of symbiosis than at later time points.

3.2 Methods

3.2.1 Experimental organisms

This experiment used a clonal stock of the symbiotic sea Aiptasia, (culture ID: NZ1), as described in **Section 2.2.1** (*n* = 660, pedal disc size 2-4 mm). Anemones were rendered aposymbiotic *via* menthol bleaching and aposymbiotic status confirmed *via* fluorescence microscopy (within a 20% subsample), as previously described in **Section 2.2.1**. Three jars of menthol-treated anemones (*n* = 60) were kept alongside the experimental system under the same 12:12 h light:dark cycle for the duration of the experiment as controls, and were confirmed as aposymbiotic under fluorescence microscopy at the conclusion of the experiment (IX53, Olympus, Japan with X-Cite 120Q, Excelitas Technologies, USA; settings: FITC, magnification x10 and x20, ISO200). Sub-cultures of the homologous symbiont of Aiptasia, *Breviolum minutum*, were taken from a long-term laboratory stock (culture ID: FLAp2) and maintained in 250 mL culture flasks in f/2 medium: ASW 1:2000 (AlgaBoost, AusAqua, Australia), refreshed every 2-4 weeks. Experimental cultures were kept in incubators (Constant Climate Chamber HPP with LED light module: cold white 6,500 K, warm white 2,700 K, Memmert, Germany) at 25 °C under a standard light regime of ~40 µmol photons m^{-2} s^{-1} photosynthetically active radiation (PAR), 60% humidity, on a 12:12 h light:dark cycle for six months prior to the experiment start date.

3.2.2 Experimental set-up

The same custom built closed-loop CO_2 system was used in these experiments as that described in **Section 2.2.2,** with pH levels manipulated by CO_2 gas bubbling. Two pH treatments, pH 8.05 and pH 7.68, were selected based on IPCC (2019) scenarios for 2100, where pH 8.05 corresponds to SSP1-1.9 (sustainability; most comparable to present day) and pH 7.68 corresponds to SSP5-8.5 (fossil-fuelled development; worst-case predicted scenario). However, as *per* the limitations outlined in **Section 2.2.2,** the system was unable to operate at the target levels of pH 8.05 (ambient condition) and pH 7.68 (low condition) concurrently. Achieving a steady pH 7.68 in the "low" condition resulted in an "ambient" condition of pH 7.85. While this did not represent a true control condition aligned to present day seawater pH values (IPCC 2019), the difference between these two conditions was considered sufficient to be biologically interesting. Further, pH 7.85 aligns with IPCC (2019) SSP2-4.5 (intermediate emissions; "middle of the road" scenario).

In addition to the mitigations outlined in **Section 2.2.2**, for this experiment the number of "ambient" condition header tanks was increased, and the number of "low" condition header tanks reduced, each by one. This provided an acceptable number of experimental tanks in the two low conditions (n = 7/n = 8 – outlined below; **Figure 3.1**) while reducing the overall volume of CO_2 released into the system. Accordingly, for this experiment, the distribution of experimental tanks was: 1) for pH 7.85: n = 15 tanks, each containing 20 anemones; 2) for pH 7.68 with no pre-exposure of symbionts prior to inoculation: n = 8 tanks, each containing 20 anemones; and 3) for pH 7.68 with symbionts pre-exposed for 6 h prior to inoculation: n = 7 tanks, each containing 20 anemones (**Figure 3.1**). Experimental tanks were treated as the evaluation unit, with individual anemones within each tank classed as technical replicates to reduce variability (Hurlbert 1984; Cornwall and Hurd 2016).

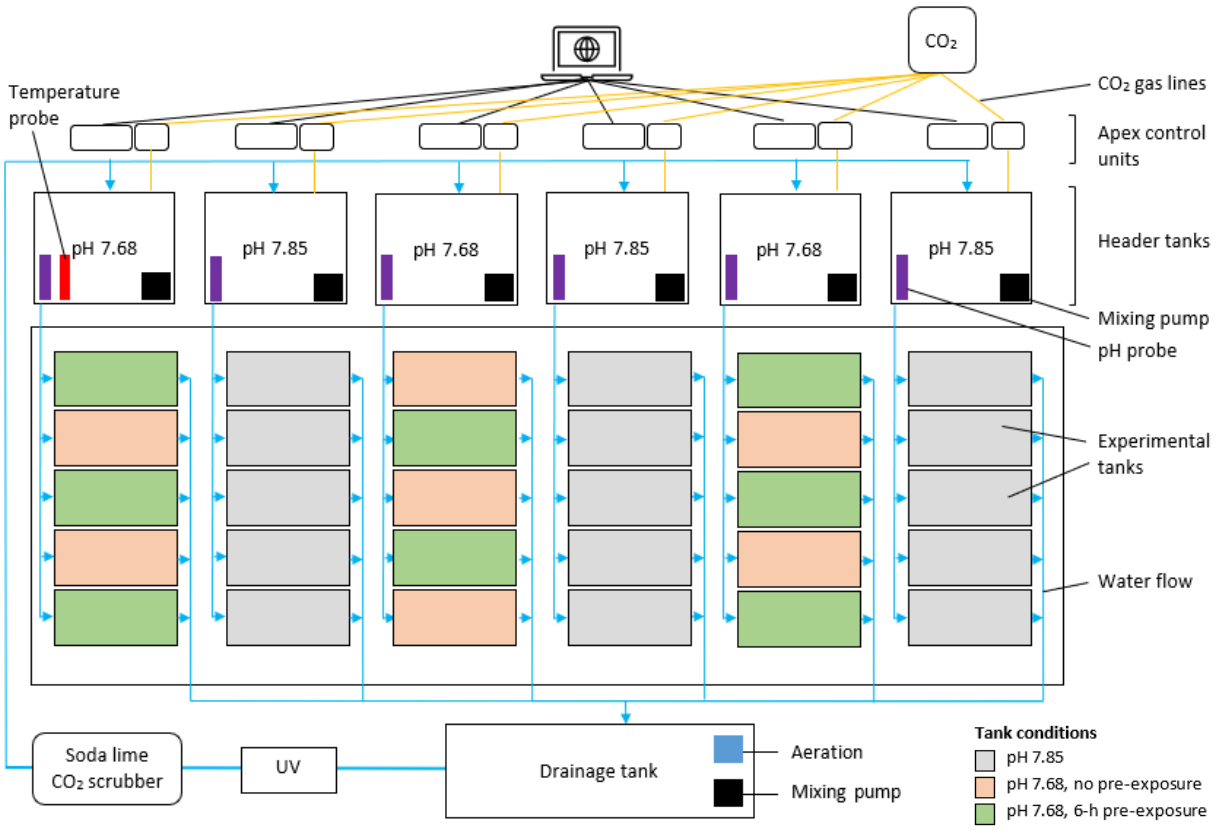

Figure 3.1: Experimental set-up schematic. This experimental set-up is based on best practice guidance for OA experiments (Riebesell et al. 2010; Cornwall and Hurd 2016). Yellow lines indicate gas flow; blue lines indicate water flow. For full schematic description see **Section 2.2.2**.

3.2.3 Sampling and preparation of experimental organisms

System measures

System measurements of pH and A_T were taken as described in **Section 2.2.3**, with some minor differences in the sampling regime. Water parameters were measured through manual sampling of header tanks and experimental tanks three times *per* week at different times over the diel cycle to capture any variability due to photosynthesis and respiration (Hurd et al. 2009; McGraw et al. 2010). A_T samples were collected weekly from two experimental tanks *per* pH condition, as well as the corresponding header tanks so that any header tank effects could be detected. System measurements during the experiment are outlined in **Table 3.1** and **Figure 3.2**. Mean pH was consistent across header and experimental tanks.

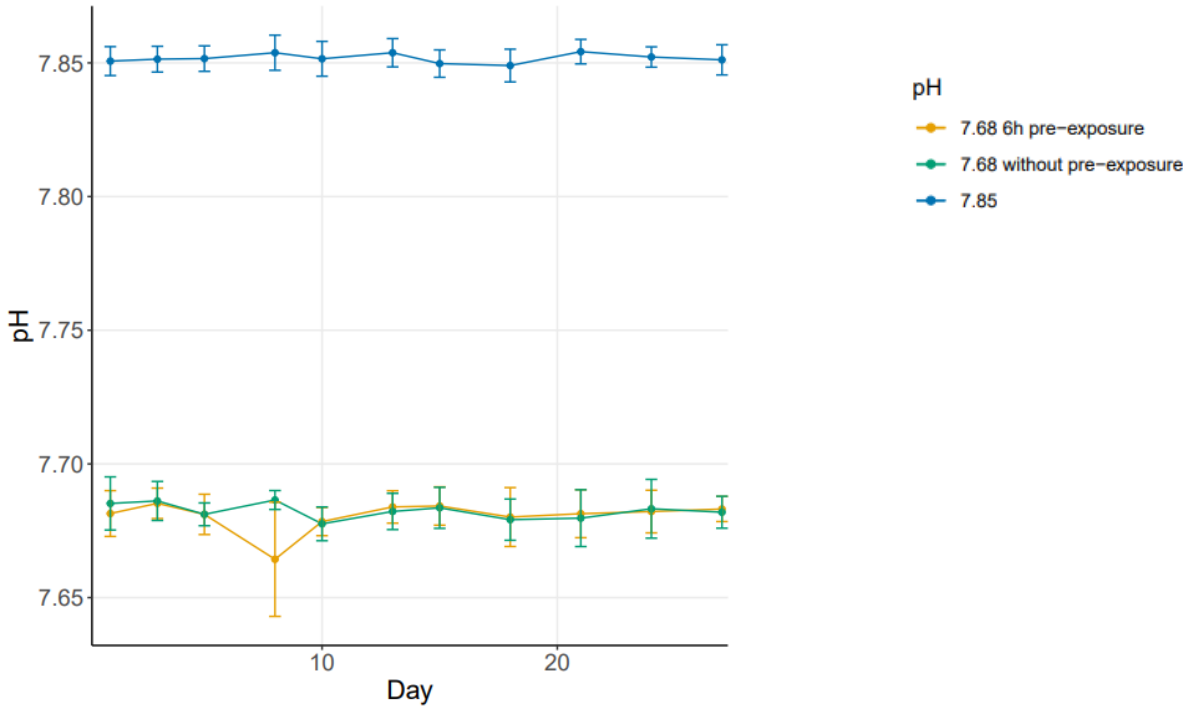

Figure 3.2: pH values for each treatment over the duration of the experiment. Values represent mean ± standard deviation. At each time point, n = 15 *per* treatment.

Table 3.1: Experimental system parameters. Mean values and standard deviations (where applicable) of system parameters during the two experiments. pH_T and A_T are measured values, DIC_T and pCO_2 are calculated values. A_T, DIC = µmol kg^{-1}, pCO_2 = µatm.

Condition	Temperature	Salinity	pH_T	A_T	DIC_T	pCO_2
pH 7.85	24 ± 0.05 °C	35 ppt	7.85 ± 0.03	2189 ± 19	2066	665
pH 7.68 no pre-exposure	24 ± 0.05 °C	35 ppt	7.68 ± 0.03	2192 ± 18	2122	1029
pH 7.68 6-h pre-exposure	24 ± 0.05 °C	35 ppt	7.68 ± 0.03	2192 ± 18	2122	1029

Acclimation of experimental organisms

Experimental organisms were pre-exposed to the target pH levels to mitigate any potential effects of pH shock (Kamenos et al. 2013; Munday et al. 2013; Munguia and Alenius 2013). Aposymbiotic anemones were haphazardly distributed among treatment conditions in the experimental system and allowed to settle for 48 h before the ramping period. The pH of tanks for the two pH 7.68 treatments (i.e., with either 6-h or no pre-exposure of symbionts) was reduced by 0.05 pH units *per* day to pH 7.68, followed by a two-week acclimation period. As described above, reducing the pH of the "low"

condition affected the entire experimental system, thereby ramping the "ambient" condition anemones to pH 7.85 at the same rate of 0.05 pH units *per* day by default.

A similar acclimation schedule was planned for the *B. minutum* cultures. CO_2 gas bubbling is considered disruptive to algal cultures (Rost et al. 2008; Hurd et al. 2009), therefore HCl and $NaHCO_3$ addition was deemed more appropriate to manipulate pH. Algal cultures are known to modify the pH of their environment through photosynthesis and respiration (Rost et al. 2008; Hurd et al. 2009), and this was confirmed through pre-experiment measurements of the *B. minutum* culture flasks. A commonly used method is to use tris(hydroxymethyl)amino methane (Tris) as a buffer to stabilise pH to the target levels. Although previous work has not addressed this issue with Symbiodiniaceae cultures, similar methods have been applied with the microalgae *Phaeodactylum tricornutum* (Fabregas et al. 2003), *Nannochloropsis gaditana* (Rocha et al. 2003; Ren et al. 2013) and *Chlorella* sp. (Nguyen et al. 2016).

As this approach was not well documented for Symbiodiniaceae cultures, an acclimation trial was conducted prior to the present experiment. HCl and $NaHCO_3$ were added by titration to stock f/2 medium to achieve "high" and "low" pH f/2 media, which were then added to culture flasks by titration to achieve the target pH when medium was refreshed. A concentration of 5 mM Tris was used to minimise non-treatment effects on the algal cultures (Fabregas et al. 1993; Rocha et al. 2003; Nguyen et al. 2016). To assess any such effects, four conditions from the same starting culture of *B. minutum* FLAp2 were established in 80 mL culture flasks, with a cell density of ~3.6 x 10^6/mL: 1) control – f/2 medium only; 2) f/2 medium + Tris; 3) pH 8.05 – f/2 medium + Tris + HCl/$NaHCO_3$ modified f/2; 4) pH 7.68 – f/2 medium + Tris + HCl/$NaHCO_3$ modified f/2 (all n = 3 flasks). All culture flasks were established at pH 8.05 and, for condition (4), reduced by 0.05 pH units *per* day to the reach the target pH level, followed by a one-week acclimation period. pH measurements were taken before and after medium changes. To maintain consistency between all four conditions, 25% of medium was refreshed daily, and where necessary for conditions (3) and (4), pH was brought to the target level by titration. *B. minutum* cultures modified pH by 0.03-0.15 units *per* day. Adverse effects were observed across all conditions except (1) control (as outlined in the supplementary material (**S2.1**). This indicates a detrimental effect of Tris- or HCl/$NaHCO_3$-modified f/2 medium, or both, on the *B. minutum* cultures. Time constraints did not allow for further trials to be conducted, so

this acclimation method was discarded. To mitigate against and identify any potential effects of pH shock, two conditions were introduced into the experimental design for *B. minutum* cultures: 1) no pre-exposure; and 2) a 6-h pre-exposure to pH 7.68, as described below.

3.2.4 Experimental inoculation

To assess the effects of decreased pH on symbiont uptake, Aiptasia were inoculated with *B. minutum* culture subjected to two conditions: 1) no pre-exposure; and 2) a 6-h pre-exposure at pH 7.68 prior to inoculation. Anemones were not fed for one week prior to inoculation with symbionts to encourage symbiont uptake (Tortorelli et al. 2020). Two days prior to inoculation, f/2 medium was refreshed to encourage cultures into log growth phase. While in the motile stage, Symbiodiniaceae can seek out potential hosts *via* chemoreception (Pasternak et al. 2006) thereby increasing the likelihood of successful colonisation. Motile Symbiodiniaceae cells were observed under brightfield microscopy (Zeiss, Germany; x10 magnification) on the day of inoculation. pH measurements were taken at frequent intervals throughout the inoculation process, and pH was within ± 0.02 pH units of target levels (see below) at each measurement interval. Culture flasks were mixed thoroughly, and a 300 mL sample taken. This sample was vortexed to achieve an even suspension of symbiont cells, from which a 1 mL aliquot was taken and fixed with 4 µL 37% formalin to avoid cell degradation. Cell density of the sample was determined from this 1 mL aliquot by haemocytometer (Neubauer Improved, Germany; 10 µL, dilution factor 1:4, n = 7 counts) as 4.09 x 10^6 cells/mL.

Culture flasks were mixed thoroughly and sufficient volume of culture for 3 x 10^6 cells *per* experimental tank (n = 30 x 0.732 mL) was pipetted from the 300 mL sample into 15 mL Falcon tubes and centrifuged for 3 min at 500 x g to obtain algal pellets. *B. minutum* cultures were then resuspended in ASW in three 250 mL bottles (Schott, Germany; one *per* condition), with ASW volume determined by the number of experimental tanks in each condition (i.e., 10 mL per tank), as follows: 1) Ambient pH: 45 x 10^6 cells in 150 mL ambient ASW; 2) Low pH, no pre: 21 x 10^6 cells in 70 mL ambient ASW; and 3) Low pH, 6-h pre-exposure: 24 x 10^6 cells in 80 mL pH 7.68 ASW. Each Schott bottle was placed into an incubator (Constant Climate Chamber HPP, Memmert, Germany; 25 °C; ~40 µmol photons m^{-2} s^{-1} PAR; 60% humidity) for 6 h. After 6 h, each bottle was mixed thoroughly, and 10 mL aliquots pipetted into 15 mL Falcon tubes and centrifuged for 3 min at

500 x g to obtain algal pellets of ~3 x 10^6 cells. Pellets were resuspended in 1 mL ASW containing freshly hatched *Artemia* sp. brine shrimp to induce feeding. One 1 mL aliquot was delivered into each ~300 mL experimental tank, each containing 20 aposymbiotic anemones, by pipetting the symbiont/brine shrimp mix directly onto the oral disc of each anemone. Water flow in the experimental system was switched off prior to feeding to avoid symbionts being lost. Tanks were left to incubate for 16 h, and then cleaned with a 50% water change and water flow restored.

During the experiment, organisms were maintained at 24 °C (± 0.5 °C) under a standard light regime of ~40 µmol photons m^{-2} s^{-1} PAR on a 12:12 h light:dark cycle (4 x 54W Master TLS HO bulbs, Philips, Holland). ASW (Sea Salt, Aquaforest, Poland) was used in the experimental system and was made up with ddH_2O to salinity 35 ppt and pH 8.28 at 24 °C. Anemones were fed once *per* week with freshly hatched *Artemia* sp. nauplii at around 17:00 h, with experimental tanks cleaned and a 50 L (i.e., 50%) ASW change the following morning.

3.2.5 Biological measurements

Symbiont cell counts, host protein quantification and estimation of symbiont cell density

Samples were collected prior to inoculation at Day 1 for protein quantification, and at Days 3, 7, 14 and 28 for protein quantification and cell counts *via* high throughput confocal microscopy (HTCM; n = 7 *per* treatment/time-point). Based on pre-experiment trials, two anemones from the same experimental tank were used *per* n to provide sufficient biomass for analysis. Samples were haphazardly selected and then carefully removed from experimental tanks, placed into 0.5 mL tubes on ice, and stored at -80 °C until processing. All samples were rinsed twice in 500 µL ASW prior to processing, to remove any Symbiodiniaceae cells external to the anemones. Samples were mechanically homogenised (Ultra-Turrax T10 basic, IKA, Germany) in 500 µL ASW and centrifuged for 4 min at 300 x g to separate the host (supernatant) and algal (pellet) fractions.

Cell counts were performed immediately, with algal pellets resuspended in 500 µL ASW, mixed thoroughly by pipette, and an aliquot taken and fixed with 37% formalin to a 4% final volume to avoid cell degradation. Due to low cell densities at the first three time-points (Days 3, 7 and 14), an undiluted 220 µL aliquot was used to achieve reliable measurements. By Day 28, cell densities were

greatly increased, so 20 µL aliquots were taken and diluted 1:20 in 380 µL ASW, and then processed and read by HTCM as described in **Section 2.2.3**. Images were analysed using IN Carta Image Analysis Software (GE Healthcare, USA; settings 90% sensitivity, 10 µm minimum diameter) using ImageJ (Abramoff et al. 2004; all images). In ImageJ, images were processed as batches, using a macro as described in **Section 2.2.3**. There was < 3% variation between IN Carta and ImageJ results, with any differences and a minimum 15% subsample *per* batch validated manually. Host samples were centrifuged for 2 min at 1000 x g to remove any particulates, with 10 µL aliquoted and diluted 10:90 with 90 µL ddH_2O. Qubit^{TM} protein assays (Invitrogen, USA) were run as previously described (**Section 2.2.3**) and cell counts were then normalised to host protein content to calculate symbiont density.

Visualisation of colonisation rates

Colonisation rates within each experimental condition were visualised using fluorescence microscopy (IX53, Olympus, Japan with X-Cite 120Q, Excelitas Technologies, USA; settings: FITC, magnification x10 and x4, ISO200). Images were taken immediately prior to sample collection i.e., at Days 1, 3, 7, 14 and 28. Anemones (n = 5 *per* treatment/time-point) were placed into 60 µL 50:50 $MgCl_2$:ASW relaxation solution ~30 min prior to imaging to minimise movement and so optimise image quality.

Photosynthetic health

During the experiment, PAM fluorometry was used to take weekly measurements of chlorophyll fluorescence of Symbiodiniaceae cells *in hospite* (n = 7 *per* treatment/time-point) as an indicator of photosynthetic health, with methods and settings as described in **Section 2.2.3**. Briefly, these included light- and dark-adapted measures of minimum and maximum fluorescence, which were then used to calculate the effective quantum yield of PSII ($\Phi_{PSII} = F_m' - F_t/F_m'$; Genty et al. 1989) and maximum quantum yield of PSII ($F_v/F_m = F_m - F_0/F_m$; Kitajima and Butler 1975). Light adaptation measurements were taken at 14:30 h after 9 h light exposure. Dark-adapted measurements were then taken at 15:30 h after ~30 min dark adaptation.

3.2.6 Statistical analysis

Statistical analysis was conducted as outlined in **Section 2.2.4**, with some minor amendments. Linear mixed effects models were constructed to test the effects of the explanatory variables of pH (factorial variable) and time (numeric variable), and their interaction terms. Models were constructed for each response variable: estimated symbiont cell density; dark- and light-adapted chlorophyll fluorescence; and anemone protein content. 'Header tank' was included as a random effect. Given the non-normal distribution of data over time, Q-Q plots were validated using the non-parametric Kruskal-Wallis rank sum test. Details of linear models and statistical tests are available in the supplementary material (**S2.2**).

3.3 Results

All results presented below are based on general linear models unless otherwise specified, with full model details provided in the supplementary material (**S2.2**).

Symbiont cell densities and host growth rates

Overall, pH had minimal effect on colonisation rate as measured by estimated cell densities of *B. minutum per* µg of host protein (R^2 = 0.01, $F_{2, 80}$ = 0.34, p = 0.71) (**Figure 3.3a** and visualised in **Figure 3.4**). Over time, there were no observable differences seen between pH conditions at Days 3, 7 or 28. However, at Day 14, cell densities in anemones at pH 7.68 that were inoculated with symbionts pre-exposed to low pH were 42% and 44% lower than in the two conditions without pre-exposure (pH 7.68 and pH 7.95, respectively; both p = 0.03). Cell densities in all conditions increased over time, with a marked increase from Day 14 onwards (R^2 = 0.82, $F_{3,79}$ = 123.2, p < 0.001). Host growth rate, as measured by protein content, did not vary with pH (R^2 = 0.01, $F_{2, 81}$ = 0.23, p = 0.79) (**Figure 3.3b**). Anemones grew significantly by Day 28 relative to the earlier time-points (β = 26.8 µg additional protein content; R^2 = 0.42, $F_{3,80}$ = 19.06, p < 0.001).

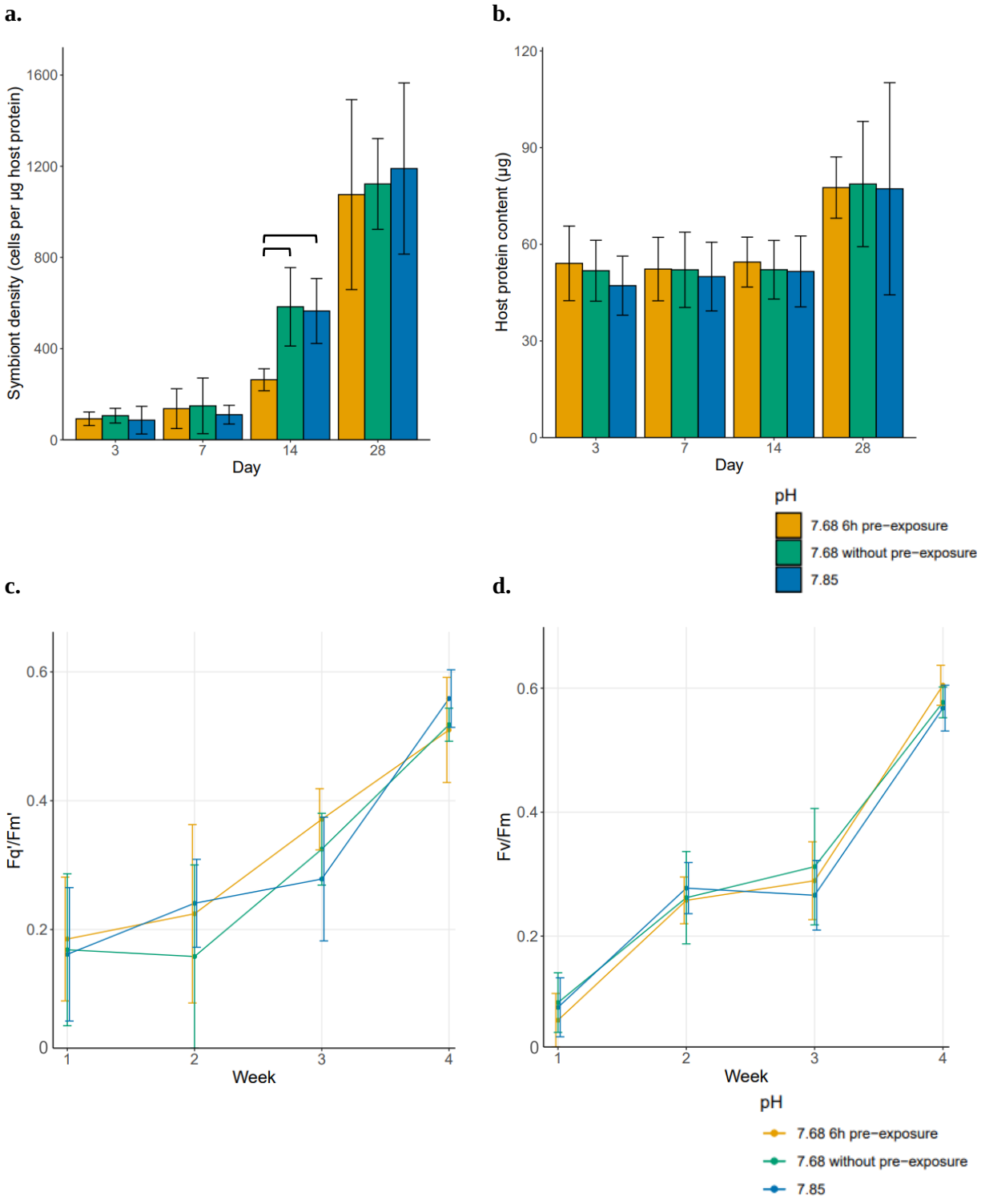

Figure 3.3: Physiological measures of colonisation success. a) Estimated cell densities of freshly isolated *Breviolum minutum per* µg of host protein; **b)** Protein content of Aiptasia; and measures of photosynthetic health of *in hospite Breviolum minutum*; **c**) Light-adapted chlorophyll fluorescence measurements (ΦPSII); **d)** Dark-adapted chlorophyll fluorescence measurements (F_v/F_m). Values represent mean ± standard deviation; $n = 7$ for all measurements. Brackets indicate values which are statistically different between treatments ($p < 0.05$, for statistical tests see supplementary material (**S2.2**)).

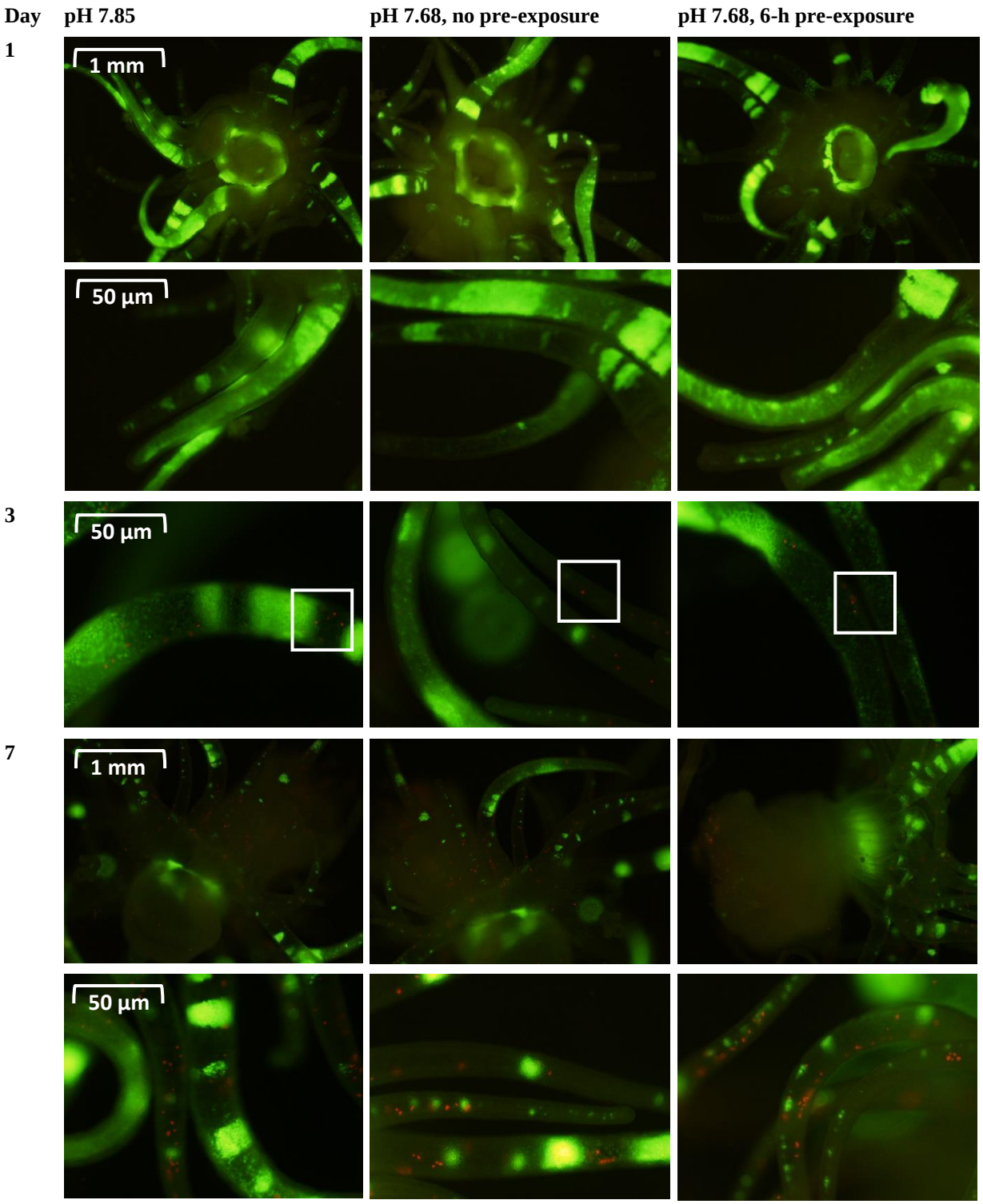

Figure 3.4: Colonisation of Aiptasia by *Breviolum minutum* visualised by fluorescence microscopy. Images at Day 1 were taken prior to the inoculation of anemones with symbiont culture. Absence of symbiont cells is evident by a lack of red chlorophyll autofluorescence, and the images are dominated by Aiptasia green fluorescent proteins (GFPs; Parkinson et al. 2018). At Day 3, single symbiont cells are visible in the host epidermis, marked by white boxes. By Day 14, colonisation rates are increasing, and the difference in symbiont densities between the pre-exposed pH 7.68 condition and the two conditions without pre-exposure is apparent. By Day 28, anemones are well colonised, and symbiont densities are again comparable. Images taken at x4 (whole anemone) and x10 (tentacle) magnification. x4 magnification images not available for Day 3.

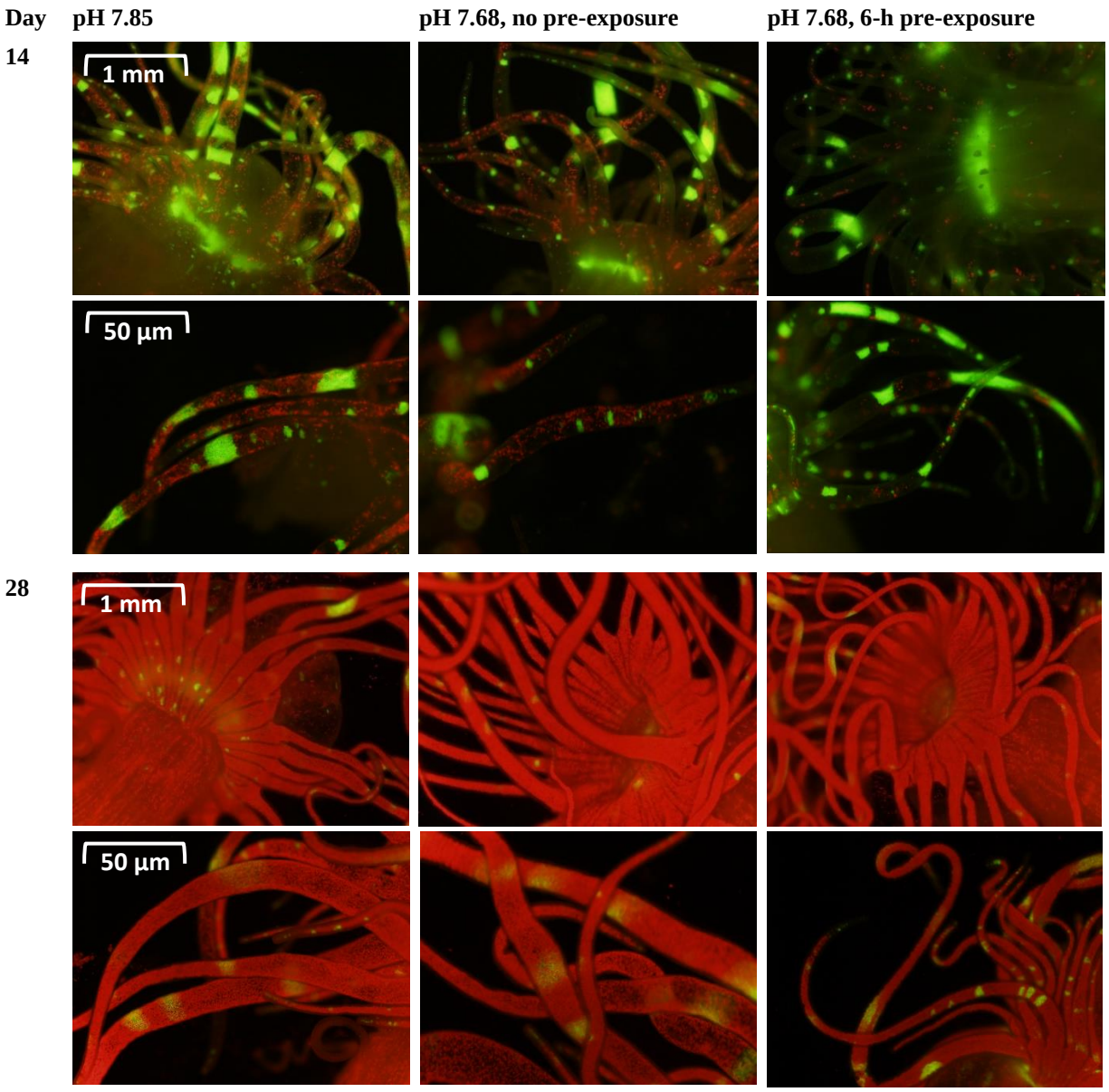

Figure 3.4 continued: Colonisation of Aiptasia by *B. minutum*. For figure legend see previous page.

Photosynthetic health

Low pH had no observable effect on the photosynthetic performance of *in hospite B. minutum.* Light-adapted chlorophyll fluorescence measurements (Φ_{PSII}) showed no significant difference with pH (R^2 = 0.01, $F_{2,83}$ = 0.26, p = 0.77) (**Figure 3.3c**). There was also no difference in dark-adapted chlorophyll fluorescence (F_v/F_m) between pH treatments (R^2 < 0.01, $F_{2,84}$ = 0.01, p = 0.99) (**Figure 3.3d**). In line

with the increases in cell density, both chlorophyll fluorescence parameters increased over time (Φ_{PSII}: $R^2 = 0.71$, $F_{3,82} = 66.58$, $p < 0.001$; F_v/F_m: $R^2 = 0.70$, $F_{3,83} = 337.9$, $p < 0.001$). Increases in Φ_{PSII} were evident from Week 2 ($p < 0.001$), with the greatest difference (2.5-fold) seen from Week 3 to Week 4. Similarly, F_v/F_m values increased 2-fold from Week 1 to Week 2, and 3-fold from Week 3 to Week 4 (both $p < 0.001$).

3.4 Discussion

Contrary to my hypotheses, low pH did not reduce symbiont uptake, colonisation rate and final symbiont density during symbiosis establishment in the Aiptasia-*B. minutum* symbiosis, except for when the symbiont was pre-exposed to reduced pH. This implies that the host may provide some buffering to its symbionts from the effects of reduced pH – likely due to a more regulated internal environment and the transfer of nutrients to support algal physiological health (as described in **Chapter 2**; Muller-Parker and D'Elia 1997; Venn et al. 2008; Davy et al. 2012).

3.4.1 Symbiont colonisation success

Symbiont population densities during this experiment were noticeably lower than the ranges of those reported elsewhere for Aiptasia when re-colonised with *B. minutum* under ambient conditions and over comparable timescales (Starzak et al. 2014; Matthews 2016; Gabay et al. 2018; 2019). These previous studies reported average cell densities of 2-4 x 10^6 algal cells *per* mg of host protein at 2-4 weeks in ambient conditions. In comparison, cell densities in the current study reached ~1 x 10^6 algal cells *per* mg of host protein after four weeks. The reasons for these differences are unknown, though they could relate to multiple causal factors including different experimental conditions, physiological health of the organisms, symbiont culture growth stage and/or inoculation protocol. However, these previous studies observed similar profiles of colonisation over time to those seen here, suggesting that colonisation was nevertheless proceeding in a positive manner, even under reduced pH.

3.4.2 Impact of OA on colonisation success

There have been only three previous studies of the impacts of OA on the establishment of the cnidarian-dinoflagellate symbiosis, though both elevated temperature and light stress are known to impact symbiont infectivity in corals (Cumbo et al. 2018; Kishimoto et al. 2020). Suwa et al. (2010) observed delayed symbiont uptake coupled with decreased growth rates in juvenile polyps of the coral *A. digitifera* under decreased pH compared to controls. In their study, colonisation rates of juvenile *A. digitifera* at pH 7.3 and pH 7.6 lagged behind those at pH 8.0 at Days 2 and 3 post-inoculation, however, by Day 4 these differences had dissipated and colonisation rates were comparable across all three pH levels. These findings are similar to those in the current study where symbionts had been pre-exposed to low pH, with an initial and short-term decrease in colonisation rates, followed by recovery. The ecological significance of such a delay in the onset of symbiosis is unknown – but may imply fitness costs in the crucial early developmental stages of juveniles (Graham et al. 2008; Albright 2011). Conversely, in two of these OA studies, results were similar to those in the current study when symbionts were not pre-exposed to reduced pH. No observable effects of low pH were seen on colonisation rates of newly-settled corals *A. intermedia* over 33 days (Sun et al. 2020) or *P. daedalea* over 28 days (Jiang et al. 2021), when maintained at reduced pH levels of 7.86 and 7.69, respectively. These findings suggest that the response to OA may be species-specific. However, both latter studies used visual inspection of polyps by microscopy to characterise their degree of pigmentation, thereby indicating symbiont presence, and used this as a proxy for symbiont establishment (Abrego et al. 2012; Nitschke et al. 2016). As both groups of authors noted, while this method can indicate whether symbiosis has been established, it does not provide an accurate assessment of the extent of colonisation and may not identify the presence of symbionts at very low densities during the early stages of colonisation (Sun et al. 2020; Jiang et al. 2021). It is therefore possible that any variation in symbiont cell densities during the first few days post-inoculation would not have been identified.

Notably, in none of these published studies were the symbionts pre-exposed to low pH prior to inoculation. Sudden declines in pH can cause physiological stress in many organisms resulting from a failure to acclimate to reduced pH (Kamenos et al. 2013; Munday et al. 2013; Munguia and Alenius 2013). It might therefore be expected that low pH would induce a more marked response than was

observed here, or in the majority of the previous studies with corals. Symbiont behaviour and physiology during symbiosis establishment have not previously been investigated under low pH, however no significant differences were seen in the current study with respect to light- (Φ_{PSII}) or dark-adapted (F_v/F_m) measures of chlorophyll fluorescence, indicating that low pH had little effect on photosynthetic performance *in hospite*. Indeed, both Φ_{PSII} and F_v/F_m increased in line with cell density, signifying a close coupling of symbiont biomass and photosynthetic activity, and signalling a healthy symbiont population (Ralph et al. 2015; Warner and Suggett 2016). Likewise, growth of Aiptasia was not affected by reduced pH in the current study, further reflecting the maintenance of photosynthetic performance. This contrasts with the study of Suwa et al. (2010), who reported that *A. digitifera* polyps were significantly smaller at low pH than in ambient conditions, consistent with the aforementioned impacts on symbiont colonisation in their study. It is therefore notable that, in the present study, the only impact of OA on symbiosis establishment was seen when the symbionts were pre-exposed to reduced pH. This finding suggests that, in the *in hospite* state, the host buffers its symbiont population from the potentially negative influence of reduced pH.

As with symbiosis establishment, there are few studies of the impacts of OA on isolated Symbiodiniaceae, and existing research suggests that responses are species-specific. Brading et al. (2011) found that the response of cultured Symbiodiniaceae to low pH differed between *B. minutum* and three *Symbiodinium* species (previously ITS2 types A1, A2 and A13; Pochon and Gates 2010; LaJeunesse et al. 2018), with either no effect or an enhancement of photosynthetic performance at pH 7.7. Conversely, Hill et al. (2019) observed structural damage to the chloroplasts of *Symbiodinium* sp. (previously ITS2 type A4; Pochon and Gates 2010; LaJeunesse et al. 2018) at pH 7.5, resulting in a significantly reduced photosynthetic yield (F_v/F_m). These differing results may be due to pH level, exposure duration, or physiological factors such as variations in carbon concentrating mechanisms between species, though as yet these are not well characterised (Hill et al. 2019; Raven et al. 2020). More widely, studies of marine dinoflagellates point to reduced growth rates under acute exposure to low pH (< 2 days) (Dason and Colman 2004; Li et al. 2021), while recovery was observed after prolonged exposure (> 8 days) (Li et al. 2021). The observation here, that acute pre-exposure to reduced pH compromises symbiont colonisation, aligns with Jiang and Lu (2019), who observed a decrease in the cell density of *B. minutum* in culture when exposed to low pH (7.69), coupled with indicators of metabolic depression. This contrasts with the upregulation of proteins involved in the

metabolic pathways of *in hospite B. minutum* under low pH reported in **Chapter 2**, which once again highlights the potential physiological buffering provided by the symbiosis. Notably, however, Brading et al. (2011) observed a lack of sensitivity of cultured *B. minutum* to low pH (7.7) based on growth and respiratory rates. As such, any impact of OA on the physiology and ability of free-living Symbiodiniaceae to form effective symbioses remains equivocal and an important avenue for further research.

Furthermore, how the host buffers the symbiont population, both physically and physiologically, remains unclear. It is known that the host actively regulates intracellular pH (pH_i – as described in **Chapter 1**), and controls the pH of the symbiosome, which is believed to promote photosynthesis (Barott et al. 2015; Capasso et al. 2021). Accordingly, the symbiosome is typically acidic, being as low as pH 4, so it is somewhat surprising that isolated symbionts were susceptible to low external pH/elevated pCO_2 (Venn et al. 2008; Barott et al. 2015). Further, the pH_i of *B. minutum* freshly isolated from Aiptasia was measured as 7.25 in the light and 7.10 in the dark (Gibbin and Davy 2013), suggesting that the dinoflagellate itself naturally regulates its internal pH to a level that is lower than that used in the current study. It may therefore be more likely that the initial lag in colonisation rate observed here is related to carbon chemistry parameters other than pH. For example, changes in the availability of dissolved inorganic carbon (DIC) may impact photosynthetic efficiency and growth rates in dinoflagellates (Buxton et al. 2009; Hill et al. 2019; Raven et al. 2020). However, more work is needed to identify any such limiting effects and their underlying physiological causes (Raven et al. 2020). Additionally, other aspects of symbiosis, such as host-derived nutrition, may provide support to the symbiont and may be required for effective environmental acclimation, once again providing a degree of buffering from the external environment. For instance, nutrient supply is thought to mediate the thermal sensitivity of dinoflagellates, with optimal nutrient balances playing a key role in the stability of cnidarian-dinoflagellate symbioses (Dubinsky et al. 1994; Parkhill et al. 2001; Wooldridge 2009; Wiedenmann et al. 2013; Morris et al. 2019). These potential influences have implications for the health and availability of free-living Symbiodiniaceae populations to form symbioses – discussed further in **Chapter 4**.

3.4.3 Ecological implications and future work

The results of this study indicate that the model cnidarian Aiptasia remains able to establish a functional symbiosis with *B. minutum* under predicted future OA scenarios. However, colonisation rates may be reduced from those seen in ambient conditions and may be affected by the capacity of Symbiodiniaceae to maintain their physiological health if exposed to low pH when *ex hospite*. This latter finding is novel and particularly significant when considering that the majority of symbiotic cnidarians (including many reef-building corals) acquire their symbionts *de novo* from the surrounding environment with each new generation (Rodriguez-Lanetty et al. 2006; Baird et al. 2009; Harii et al. 2009). Indeed, of particular relevance, Noonan et al. (2013) found significant under-representation of horizontally-transmitting coral species in CO_2 seep communities, suggesting that sensitivity of free-living Symbiodiniaceae to elevated pCO_2 may inhibit symbiosis establishment in this environment. These combined observations raise the worrying possibility that the infectivity of free-living Symbiodiniaceae may be compromised by future OA conditions, ultimately impacting the survival of coral reefs. More reassuringly, the data presented here and in Suwa et al. (2010) suggest that any such effects are temporary. While apparently transient, however, the energetic consequences of any such delayed colonisation success for holobiont performance and survival require investigation. Further, much more work is needed to assess the wider applicability of the findings in this study. For example, conducting similar experiments over longer timeframes and under a wider range of future scenarios, including combined OA and ocean warming conditions, would provide a more realistic context. Also, there is a need to assess the generality of these observations across a much wider diversity of coral and Symbiodiniaceae species, particularly given the wide physiological diversity within each genus (Baker 2003; Stat et al. 2006; Baird 2009; LaJeunesse et al. 2018). The lack of existing data on these topics presents many potential research opportunities, and considerations for future research directions will be discussed further in **Chapter 4**.

Photo courtesy of Matthew Nitschke

Chapter 4: General Discussion

4.1 Summary

Ocean acidification poses a threat to coral reefs globally, however the nature of the impact of this environmental stressor on the keystone species underpinning these ecosystems – corals and their endosymbiotic algae – is not well understood. This thesis therefore aimed to provide further insights into the impacts of OA on the establishment and maintenance of the cnidarian-dinoflagellate symbiosis. My research utilised the well-established model system for this symbiosis: the sea anemone *Exaiptasia diaphana* ('Aiptasia') and its native symbiont *Breviolum minutum*.

To achieve my research aim, I formed two specific objectives. The first was to determine the impact of decreased pH on the ongoing health and maintenance of the cnidarian-dinoflagellate symbiosis and was addressed in **Chapter 2**. I coupled proteomics, the large-scale study of the structure and function of proteins, with a range of physiological measures to examine the responses of both Aiptasia and *B. minutum*. By using a broad-scale approach, I was able to identify a wide range of proteins that were differentially expressed between the control condition (pH 7.95) and under decreased pH (pH 7.68) following a 26-day exposure. Physiological data, including symbiont density and photosynthetic health, indicated no adverse effects of reduced pH. Meanwhile, proteomic data indicated a response characterised by increased photosynthetic and metabolic activity, most likely due to increased availability of CO_2, but upregulation of homeostatic pathways and the host's innate immune response. Collectively, these results suggest that, while this model cnidarian-dinoflagellate symbiosis may not exhibit external impacts of OA exposure (at the levels used here) and may even benefit from the elevated supply of CO_2, underlying cellular processes are likely coordinating to facilitate acclimation and limit cellular stress.

My second objective was to establish whether decreased pH impacts the capacity of Aiptasia to establish a symbiosis with *B. minutum* and was addressed in **Chapter 3**. I measured symbiont colonisation success under two predicted future OA scenarios, both with and without pre-exposure of cultured *B. minutum* to reduced pH. I found that reduced pH only impacted symbiont colonisation when symbionts had been pre-exposed to the lower pH of 7.68, though the effect was temporary.

There were no other impacts on symbiosis establishment, photosynthetic health or host biomass. These data suggest that the host may provide some buffering to its symbionts from the effects of reduced pH, and that Aiptasia remains able to acquire and establish a functional symbiosis with *B. minutum* under predicted future OA scenarios. These findings provide a baseline to inform future studies of such effects in the Aiptasia model system and ultimately in reef corals. In the remainder of this chapter, I will discuss the implications of my findings for our understanding of how the cnidarian-dinoflagellate might respond to future OA scenarios and the implications for coral reefs, as well as highlight potential avenues for future research.

4.2 The future of coral reefs under ocean acidification

The future of coral reefs is of fundamental importance both ecologically and economically. These incredibly diverse ecosystems provide the foundation for a dizzying array of marine life and are an essential source of food, income and security for millions of people worldwide (Hoegh-Guldberg et al. 2007; Pratchett et al. 2014; Robinson et al. 2019). The research in this thesis using the Aiptasia model system indicates that soft-bodied cnidarians will be relatively resilient to future OA scenarios. While changes were seen at the proteomic level in response to reduced pH, physiological indicators indicated that these changes are most appropriately characterised as acclimation, rather than stress or decline. Most intriguingly, delayed acquisition of free-living symbionts that had been pre-exposed to low pH suggests that symbiosis establishment during early life-stages or recovery from bleaching episodes could be compromised under future OA scenarios. However, and more reassuringly, this effect appeared to be temporary. Nevertheless, inhibition at these early stages or during post-bleaching uptake could have detrimental implications for growth and development of corals and other symbiotic cnidarians, as well as their recovery from bleaching, given the nutritional benefits provided by the symbiosis (Hoegh-Guldberg 2007; 2017; Baker et al. 2008; Harii et al. 2009; Edmunds et al. 2013; Suzuki et al. 2013; Glynn and Manzello 2015). The metamorphosis of corals from larvae to newly-settled juveniles involves changes to behaviour, structure and physiology, including the onset of calcification and protein synthesis, with associated metabolic costs (Allemand et al. 2011). For example, Edmunds et al. (2013) found that respiration rates of new coral recruits increased by 70% within the first four days post-settlement, indicating a strong increase in energy demand during this early period. Their study examined brooded coral larvae with maternally-inherited symbionts, and

even here found that OA induced metabolic depression and reduced protein biomass, without affecting polyp size. Further, in horizontally-transmitting *Acropora* sp. under ambient conditions, a four-day delay in the uptake of symbionts both reduced post-settlement survival rates and significantly influenced the composition of symbiont species in surviving recruits at least one month after settlement (Suzuki et al. 2013). More widely and irrespective of symbiotic state, OA has been reported to reduce both settlement and metamorphosis rates, and the skeletal development of new recruits due to increased calcification costs (Nakamura et al. 2011; Yuan et al. 2018). Taken together, these studies suggest that, for horizontally-transmitting species facing acidified conditions, delays in symbiosis establishment and the receipt of associated energetic input may be particularly detrimental. If this is the case, then cnidarian species that acquire their symbionts maternally may be at an advantage over those acquiring them *via* horizontal transmission from the environment. This may be particularly so where parent colonies have been exposed to similarly elevated pCO_2, as there is some evidence that parental conditioning to OA can influence the performance of offspring, including settlement, survival and growth rates (Putnam et al. 2020).

Coral colonies undergoing bleaching are prone to marked nutritional deficit due to the reduction or absence of photosynthate transfer from their symbionts (Baker et al. 2008; Hughes et al. 2010; Hoegh-Guldberg et al. 2017). Corals can survive bleaching events by reacquiring symbionts; however, in part this is dependent on a population of viable Symbiodiniaceae being readily available in the surrounding environment (Lewis and Coffroth 2004; Coffroth et al. 2006; Littman et al. 2008; Linares et al. 2011; Nitschke et al. 2016; Newkirk 2020). As such, a pool of healthy free-living Symbiodiniaceae is a key contributor to the reestablishment of symbiosis. While corals can supplement their energy needs in the short-term *via* increased heterotrophy and catabolism of lipid reserves, this is unsustainable over longer periods (Yamashiro et al. 2005; Grottoli et al. 2006; Anthony et al. 2009; Hughes and Grottoli 2013). Prolonged loss of photosynthetically-derived energy can lead to starvation, disease, reproductive failure, and reduced competitive ability (Glynn 1991; Brown 1997; Hoegh-Guldberg 2007; 2017; Baker et al. 2008; Glynn and Manzello 2015). Given this nutritional deficit, even short delays to the reacquisition of Symbiodiniaceae may therefore put corals at greater risk of suffering mortality from bleaching events. Further, some studies have suggested that corals can acquire resilience to bleaching through the uptake of thermally-tolerant symbiont genotypes, although this is debated due to partner specificity (Baker 2003; Stat et al. 2006; Kemp et

al. 2014; Cunning et al. 2015; Hoadley et al. 2015; 2016; Silverstein et al. 2012; 2015: Gabay et al. 2019). Work is needed to establish which free-living symbiont types may be affected by OA, as this will further inform our understanding of the potential for 'partner switching' as an adaptive strategy to future ocean conditions.

Impacts of OA on symbiosis establishment and functioning may influence competitiveness, with implications for species diversity. When compared to studies of calcifying cnidarians, the results seen here imply that soft-bodied cnidarians may fare better than reef-building corals in the more acidified oceans of the future. These findings are consistent with previous studies of sea anemones, including those associated with shallow water CO_2 seeps. Several studies have reported increased rates of photosynthesis, growth and abundance of the symbiotic sea anemone *Anemonia viridis* along a natural CO_2 gradient at Vulcano, Italy (pH 8.17 – 7.66), with acclimatory responses including differential regulation of carbonic anhydrases, so suggesting adaptation to altered DIC availability (Suggett et al. 2012; Ventura et al. 2016; Urbarova et al. 2019). Similarly positive outcomes have been reported in laboratory studies of OA effects in *A. viridis* (Jarrold et al. 2013; Ventura et al. 2016), the North American sea anemone *Anthopleura elegantissima* (Towanda and Thuesen 2012) and Aiptasia (Gibbin and Davy 2013; Hoadley et al. 2015), all reporting enhanced photosynthetic performance and, in the case of Aiptasia, enhanced recovery from cellular acidosis (Gibbin et al. 2014). These reports all infer a high degree of resilience of phototrophic, symbiotic sea anemones to elevated pCO_2.

Sponges are similarly robust under OA, indicating that they may also feature more strongly in future reef communities at the expense of reef-building corals (Duckworth et al. 2012; Goodwin et al. 2013; Bell et al. 2013; 2018; Bennett et al. 2017; 2018). Such a shift in reef community composition would have implications for the multitude of marine species which derive habitat from the complex structures provided by coral reefs. Indeed, while reefs dominated by soft-bodied cnidarians and sponges would provide greater structural variety than the algal-dominated reefs predicted under worst-case scenarios (Connell et al. 2013; Ainsworth and Mumby 2015; Colombara et al. 2017; Roth et al. 2018), this would still represent a much simpler reef topography than is provided by the morphologically-complex coral species that dominate present-day reefs (Hoegh-Guldberg et al. 2007; Sunday et al. 2017; Roth et al. 2018; Bell et al. 2021). Such reductions in complex habitat may have cascading effects on reefal communities. For example, reduced availability of refuges would leave

prey species more vulnerable to predation, reducing their chances of survival (Fabricius et al. 2011; 2014; Rogers et al. 2014; Sunday et al. 2017). Over the longer-term, this would likely affect population densities and species composition as the more vulnerable species are depleted (Rogers et al. 2014; Ainsworth and Mumby 2015; Cruz et al. 2015; Robinson et al. 2019).

However, there are currently limited data available on shifts towards reefs dominated by non-coral animals. More recent studies have tended to focus on changes in coral community composition or shifts towards algal-dominated reefs (Norström et al. 2009; Bell et al. 2021; Reverter et al. 2021). While anemones seem relatively unaffected by pH values as low as 7.6 (Suggett et al. 2012; Ventura et al. 2016; Urbarova et al. 2019) and shifts towards anemone-dominated reefs have been reported in relation to other environmental stressors (Chen and Dai 2004; Tkachenko et al. 2007; Tkachenko and Britayev 2016), such observations are currently limited to the few sites detailed in these studies (Vulcano Islands, Sicily, Italy: Suggett et al. 2012; Ventura et al. 2016; Urbarova et al. 2019; Kenting National Park, southern Taiwan: Chen and Dai 2004; Tkachenko et al. 2007; Hon Cau Island, central Vietnam: Tkachenko and Britayev 2016). The picture for soft corals is more mixed, with studies at CO_2 seeps indicating greater abundance relative to stony corals at moderately decreased pH (~7.8), but with an absence of both hard and soft corals at more extreme pH levels (< 7.7) (Fabricius et al. 2011; Inoue et al. 2013). Corals are highly sensitive to environmental change, as indicated by a wide body of research on responses to changes in temperature, light and acidification levels, as well as to local stressors such as sedimentation, pollution or physical damage (e.g., severe weather events) (e.g., De'ath et al. 2012; Anthony et al. 2015; Bessell-Browne et al. 2017; Cheal et al. 2017; DeCarlo et al. 2017; Hughes et al. 2017; Camp et al. 2018; Comeau et al. 2018; Fisher et al. 2019). Such variables may have a confounding influence in field studies, such as those conducted near to natural CO_2 seeps. Data from a wider range of sites are therefore needed to elucidate the direct impacts of elevated CO_2 *vs.* other environmental factors. Reviews by Norström et al. (2009) and updated by Bell et al. (2021) indicate that sponges and soft corals may be the primary successors to stony corals on future reefs – however both reviews point to the paucity of field data available from which to draw strong conclusions. Accordingly, future research, and particularly reef monitoring programmes, should include non-coral species in their surveying efforts to facilitate a better understanding of the nature of such community shifts and their ecological implications.

4.3 Limitations

The Aiptasia model system provides many benefits in the study of the cnidarian-dinoflagellate symbiosis due to its tractability, rapid growth and reproductive rates, non-calcifying status and ability to live in an aposymbiotic state (Weis et al. 2008; Baumgarten et al. 2015). However, some of these characteristics also pose limitations when translating research findings in Aiptasia to the complex world of coral reefs. Corals are slow growing and have long evolutionary horizons, so may be more limited in their ability to rapidly acclimatise to external stressors than fast-growing anemones (Baker 2008; Weis 2010; Hoegh-Guldberg et al. 2017). Significantly for studies of OA, Aiptasia enables the discrete investigation of non-calcification physiological processes under low pH. However, coral physiological processes are complicated by the contrasting processes of photosynthesis and calcification (i.e., their requirements for vastly different internal pH levels), and their associated energetic costs (Krief et al. 2010; Allemand et al. 2011; McCulloch et al. 2012; 2017; Venn et al. 2009; 2013). Such physiological influences may have ramifications across other cellular pathways that are not discernible in the absence of calcification. Additionally, the use of algal cultures is typical in the study of *ex hospite* Symbiodiniaceae, however, they may not be strictly comparable to free-living Symbiodiniaceae. Cultured algae are maintained in nutrient-rich medium at benign light and temperature levels, in contrast to the more variable conditions and oligotrophic waters surrounding coral reefs (Maruyama and Weis 2020). Accordingly, outcomes may differ between these two *ex hospite* states – with the worrying possibility that effects of OA in free-living Symbiodiniaceae may be more severe than those seen here in cultured algae, due to the compounding influence of nutrient scarcity. Nonetheless, the Aiptasia model system remains invaluable in providing insights into the cellular-level workings of cnidarians, which can then be tested in corals (Pernice et al. 2011; Shinzato et al. 2011; Hawkins et al. 2014).

While proteomic methodologies such as those applied here provide valuable and wide-ranging data that can inform insights into a broad range of biological questions, they do have some limitations. Within any organism, protein abundances range over many orders of magnitude. This leads to challenges in detecting minor proteins amongst highly abundant ones, known as the ‘dynamic range problem’ (Zubarev 2013). As such, proteins with low abundances but important functional roles may not be detected in broad-scale proteomic analyses. Accordingly, the results presented here are most

appropriately interpreted as the most abundant proteins within whole-organism homogenates (Zubarev 2013; Oakley et al. 2014). Targeted studies are required for more precise location of proteins within a cell, which can help further elucidate their functional roles (e.g., Peng et al. 2010; Tortorelli et al. 2021). Further, proteins are commonly annotated by homology and with multiple GO terms, indicating both their potential involvement in multiple functional processes, and the degree of further work required in this field (Weis 2019). The use of functional studies to help identify both proteins and their relevant cellular pathways will only enhance the power of proteomics as a tool to uncover the inner workings of the cnidarian-dinoflagellate symbiosis.

4.4 Future directions

To further elucidate the mechanisms influencing cnidarian-dinoflagellate responses under more acidified conditions, we need to go beneath physiological responses and look at what is happening at the cellular level. Here, processes unfold which are the ultimate drivers of the organismal response – which then plays out at the ecosystem scale. This was the first study to investigate the proteomic response of both partners in this model system not only to OA, but to any environmental variable. Further, it was only the second to examine proteomic responses to OA in the cnidarian-dinoflagellate symbiosis. As such, I applied a 'shotgun' proteomics approach which examines all differentially expressed proteins within the target organism. Working from this established baseline, future studies should use more targeted proteomics approaches, for example by isolating specific cellular compartments to assist with protein localisation, and so provide more specific clues as to the functional processes that these proteins regulate. Several existing studies provide a baseline for comparison, for example characterisation of the symbiosome membrane (Peng et al. 2010), skeletal proteome (Ramos-Silva et al. 2013) and symbiont cell wall (Tortorelli et al. 2021). Future studies using other 'omics' methodologies, such as metabolomics, would be useful to enhance localisation and provide a more precise understanding of the pathways involved in the OA responses seen here. Additionally, future research over longer time periods would help to elucidate the suggested trends in these data – for example the impact on symbiont cell densities, cellular respiration and the host's innate immune response. These should include additional measures of photosynthetic activity (e.g., maximum values of non-photochemical quenching) and respiration, given that these appear to be among the more differentially regulated pathways under OA conditions.

My study of the establishment of the cnidarian-dinoflagellate symbiosis under acidified conditions indicates that the establishment of functional symbiosis is not unduly affected by pH levels aligned to two of the predicted IPCC (2019) scenarios for 2100 (SSP2/pH 7.85 and SSP3/pH 7.68). Future research would benefit from adding the originally intended control condition (SSP7/pH 8.05), particularly in light of the potential difference in cell densities observed here in comparison to other studies of symbiosis establishment in the Aiptasia model system (Starzak et al. 2014; Matthews 2016; Gabay et al. 2018; 2019). Further, adding a pre-industrial pH level (8.2) would avoid 'shifting baselines' and provide an accurate comparative measure of the degree of change experienced by coral reefs in the last 100-150 years (Knowlton and Jackson 2008; Hoegh-Guldberg et al. 2014). Repeating this study over longer timescales may help confirm if the differences observed here are material, and if so whether they are sustained over time. Such experiments should run until at least the point at which symbiont population densities stabilise, to examine any residual effects on the development of stable symbiosis (typically by around 12 weeks post-inoculation) (Starzak et al. 2014). Additionally, future studies should include a variety of pre-exposure periods for both host and symbiont prior to inoculation, to identify the impacts of pre-contact exposure to low pH on colonisation success. Here, controlling both pH and nutrient levels over the long term, particularly in algal cultures, may present a more realistic comparison to reef conditions (Putnam et al. 2015; Marayuma and Weis 2020). The additional use of 'omics' methodologies would further help to unravel the impacts of OA on the respective partners and the inter-partner processes occurring during the establishment phase of symbiosis. Such techniques have been used effectively in the study of heat stress to elucidate cellular responses (Hillyer et al. 2016; Cziesielski et al. 2018; Rosset et al. 2019), and could be used similarly for OA. The data presented in **Chapter 2** provide a useful starting point to identify proteins and pathways which may have significant roles during this critical life event in the cnidarian-dinoflagellate symbiosis, for example those involved in innate immunity and inter-partner signalling (Poole et al. 2016; Neubauer et al. 2016; 2017; Wolfowicz et al. 2016).

In the face of increasing threats posed by climate change, existing reef management and conservation approaches are likely to be insufficient for preserving coral reefs into the future (Anthony et al. 2017; Weis 2019). As such, the development of tools to assist corals to adapt to climate change stressors is more urgent than ever. Potential solutions to mitigate OA effects in vertically-transmitting species include the pre-conditioning of parent colonies to low pH during brooding periods, which has been

shown to confer resilience to offspring (Putnam et al. 2015; 2020). However, it remains to be seen whether any such advantages can be conferred to horizontally-transmitting species through gradual pre-exposure (Cornwall et al. 2018). Selective breeding or modification of coral genotypes (i.e., gene editing) may be a more promising avenue to enhance resilience to climate stressors (van Oppen et al. 2015; Clevesa et al. 2018; Novak et al. 2020; Parkinson et al. 2020). Such approaches rely on detailed knowledge of cellular pathways to inform targets for genetic engineering (van Oppen et al. 2015; Weis 2019). The data outlined here provide candidate pathways and proteins around which to focus such technologies to build OA resilience, particularly those involved in host immune responses. Interferon pathways and collagen alpha chain proteins look to be promising targets for manipulation given their upregulation under low pH observed here (see also Urbarova et al. 2019; Lin et al. 2022). The downregulation of iron homeostasis is also worthy of further exploration, as a potential limiting factor on symbiont population densities.

Without action to reduce the impact of climate change stressors, the future for coral reefs as we know them today is uncertain, with calcifying species at risk and unknown ecological consequences of reef shifts towards non-calcifying species. Molecular tools provide a 'ray of hope' in developing corals adapted to the effects of OA. To keep pace with the rapid pace of climate change, more work is urgently needed to understand the cellular level processes most influential in driving cnidarian-dinoflagellate OA responses.

References

Abramoff, M. D., Magalhaes, P. J., & Ram, S. J. (2004). Image Processing with ImageJ. *Biophotonics International*, *11*(7), 36-42.

Abrego, D., Willis, B. L., & van Oppen, M. J. H. (2012). Impact of Light and Temperature on the Uptake of Algal Symbionts by Coral Juveniles. *Plos One*, *7*(11), Article e50311.

Aebersold, R., & Mann, M. (2003). Mass spectrometry-based proteomics. *Nature*, *422*(6928), 198-207.

Ainsworth, C. H., & Mumby, P. J. (2015). Coral-algal phase shifts alter fish communities and reduce fisheries production. *Global Change Biology*, *21*(1), 165-172.

Ainsworth, T. D., Heron, S. F., Ortiz, J. C., Mumby, P. J., Grech, A., Ogawa, D., ... & Leggat, W. (2016). Climate change disables coral bleaching protection on the Great Barrier Reef. *Science (New York, N.Y.)*, *352*(6283), 338-342.

Albright, R. (2011). Reviewing the effects of ocean acidification on sexual reproduction and early life history stages of reef-building corals. *Journal of Marine Biology*, *14*.

Albright, R., Takeshita, Y., Koweek, D. A., Ninokawa, A., Wolfe, K., Rivlin, T., ... & Caldeira, K. (2018). Carbon dioxide addition to coral reef waters suppresses net community calcification. *Nature*, *555*(7697), 516-519.

Alderdice, R., Suggett, D. J., Cardenas, A., Hughes, D. J., Kuhl, M., Pernice, M., & Voolstra, C. R. (2021). Divergent expression of hypoxia response systems under deoxygenation in reef-forming corals aligns with bleaching susceptibility. *Global Change Biology*, *27*(2), 312-326.

Allemand, D., Furla, P., & Benazet-Tambutte, S. (1998). Mechanisms of carbon acquisition for endosymbiont photosynthesis in Anthozoa. *Canadian Journal of Botany-Revue Canadienne De Botanique*, *76*(6), 925-941.

Allemand, D., Tambutté, É., Zoccola, D., & Tambutté, S. (2011). *Coral Calcification, Cells to Reefs*. Springer Netherlands.

Anderson, K. D., Cantin, N. E., Casey, J. M., & Pratchett, M. S. (2019). Independent effects of ocean warming versus acidification on the growth, survivorship and physiology of two *Acropora* corals. *Coral Reefs*, *38*(6), 1225-1240.

Anlauf, H., D'Croz, L., & O'Dea, A. (2011). A corrosive concoction: The combined effects of ocean warming and acidification on the early growth of a stony coral are multiplicative. *Journal of Experimental Marine Biology and Ecology*, *397*(1), 13-20.

Anthony, K., Bay, L. K., Costanza, R., Firn, J., Gunn, J., Harrison, P., ... & Walshe, T. (2017). New interventions are needed to save coral reefs. *Nature Ecology & Evolution*, *1*(10), 1420-1422.

Anthony, K. R. N., Hoogenboom, M. O., Maynard, J. A., Grottoli, A. G., & Middlebrook, R. (2009). Energetics approach to predicting mortality risk from environmental stress: a case study of coral bleaching. *Functional Ecology*, *23*(3), 539-550.

Anthony, K. R. N., Kline, D. I., Diaz-Pulido, G., Dove, S., & Hoegh-Guldberg, O. (2008). Ocean acidification causes bleaching and productivity loss in coral reef builders. *Proceedings of the National Academy of Sciences of the United States of America*, *105*(45), 17442-17446.

Anthony, K. R. N., Marshall, P. A., Abdulla, A., Beeden, R., Bergh, C., Black, R., ... & Wear, S. (2015). Operationalizing resilience for adaptive coral reef management under global environmental change. *Global Change Biology*, *21*(1), 48-61.

Apprill, A. (2020). The role of symbioses in the adaptation and stress responses of marine organisms. *Annual Review of Marine Science, Vol 12*, *12*, 291-314.

Aranda, D. A., & Manzano, N. B. (2017). Effects of near-future-predicted ocean temperatures on early development and calcification of the queen conch *Strombus gigas*. *Aquaculture International*, *25*(5), 1869-1881.

Aranda, M., Li, Y., Liew, Y. J., Baumgarten, S., Simakov, O., Wilson, M. C., ... & Voolstra, C. R. (2016). Genomes of coral dinoflagellate symbionts highlight evolutionary adaptations conducive to a symbiotic lifestyle. *Scientific Reports*, *6*, Article 39734.

Austin, P. A., Ross, I. S., & Mills, J. D. (1992). Light dark regulation of photosynthetic enzymes within intact-cells of the cyanobacterium nostoc sp mac. *Biochimica Et Biophysica Acta*, *1099*(3), 226-232.

Baghdasarian, G., & Muscatine, L. (2000). Preferential expulsion of dividing algal cells as a mechanism for regulating algal-cnidarian symbiosis. *Biological Bulletin*, *199*(3), 278-286.

Baghdasarian, G., Osberg, A., Mihora, D., Putnam, H., Gates, R. D., & Edmunds, P. J. (2017). effects of temperature and pCO_2 on population regulation of *Symbiodinium* spp. in a tropical reef coral. *Biological Bulletin*, *232*(2), 123-139.

Baird, A. H., Guest, J. R., & Willis, B. L. (2009). Systematic and biogeographical patterns in the reproductive biology of scleractinian corals. *Annual Review of Ecology Evolution and Systematics*, *40*, 551-571.

Baker, A. C. (2003). Flexibility and specificity in coral-algal symbiosis: Diversity, ecology, and biogeography of Symbiodinium. *Annual Review of Ecology Evolution and Systematics*, *34*, 661-689.

Baker, A. C., Glynn, P. W., & Riegl, B. (2008). Climate change and coral reef bleaching: An ecological assessment of long-term impacts, recovery trends and future outlook. *Estuarine Coastal and Shelf Science*, *80*(4), 435-471.

Baker, D. M., Freeman, C. J., Wong, J. C. Y., Fogel, M. L., & Knowlton, N. (2018). Climate change promotes parasitism in a coral symbiosis. *Isme Journal*, *12*(3), 921-930.

Bandara, A. B., Drake, J. C., James, C. C., Smyth, J. W., & Brown, D. A. (2021). Complex I protein NDUFS2 is vital for growth, ROS generation, membrane integrity, apoptosis, and mitochondrial energetics. *Mitochondrion*, *58*, 160-168.

Bardou, P., Mariette, J., Escudié, F., Djemiel, C., & Klopp, C. (2014). jvenn: an interactive Venn diagram viewer. *BMC bioinformatics*, *15*(1), 1-7.

Barott, K. L., Barron, M. E., & Tresguerres, M. (2017). Identification of a molecular pH sensor in coral. *Proceedings of the Royal Society B-Biological Sciences*, *284*(1866), Article

Barott, K. L., Venn, A. A., Perez, S. O., Tambutte, S., & Tresguerres, M. (2015). Coral host cells acidify symbiotic algal microenvironment to promote photosynthesis. *Proceedings of the National Academy of Sciences of the United States of America*, *112*(2), 607-612.

Barshis, D. J., Ladner, J. T., Oliver, T. A., Seneca, F. O., Traylor-Knowles, N., & Palumbi, S. R. (2013). Genomic basis for coral resilience to climate change. *Proceedings of the National Academy of Sciences of the United States of America*, *110*(4), 1387-1392.

Bassham, J. A. (1971). Photosynthetic carbon metabolism. *Proceedings of the National Academy of Sciences of the United States of America*, *68*(11), 2877-2882.

Baumgarten, S., Simakov, O., Esherick, L. Y., Liew, Y. J., Lehnert, E. M., Michell, C. T., ... & Voolstra, C. R. (2015). The genome of Aiptasia, a sea anemone model for coral symbiosis. *Proceedings of the National Academy of Sciences of the United States of America*, *112*(38), 11893-11898.

Bayer, T., Aranda, M., Sunagawa, S., Yum, L. K., DeSalvo, M. K., Lindquist, E., ... & Medina, M. (2012). Symbiodinium transcriptomes: genome insights into the dinoflagellate symbionts of reef-building corals. *Plos One*, *7*(4), Article e35269.

Bayram, S., Furst, S., Forbes, M., & Kempa, S. (2020). Analysing central metabolism in ultra-high resolution: At the crossroads of carbon and nitrogen. *Molecular Metabolism*, *33*, 38-47.

Bell, J. J., Davy, S. K., Jones, T., Taylor, M. W., & Webster, N. S. (2013). Could some coral reefs become sponge reefs as our climate changes? *Global Change Biology*, *19*(9), 2613-2624.

Bell, J. J., Micaroni, V., & Strano, F. (2022). Regime shifts on tropical coral reef ecosystems: future trajectories to animal-dominated states in response to anthropogenic stressors. *Emerging Topics in Life Sciences*, *6*(1), 95-106.

Bell, J. J., Rovellini, A., Davy, S. K., Taylor, M. W., Fulton, E. A., Dunn, M. R., ... & Webster, N. S. (2018). Climate change alterations to ecosystem dominance: how might sponge-dominated reefs function? *Ecology*, *99*(9), 1920-1931.

Bennett, G. M., & Moran, N. A. (2015). Heritable symbiosis: The advantages and perils of an evolutionary rabbit hole. *Proceedings of the National Academy of Sciences of the United States of America*, *112*(33), 10169-10176.

Bennett, H., Bell, J. J., Davy, S. K., Webster, N. S., & Francis, D. S. (2018). Elucidating the sponge stress response; lipids and fatty acids can facilitate survival under future climate scenarios. *Global Change Biology*, *24*(7), 3130-3144.

Bennett, H. M., Altenrath, C., Woods, L., Davy, S. K., Webster, N. S., & Bell, J. J. (2017). Interactive effects of temperature and pCO_2 on sponges: from the cradle to the grave. *Global Change Biology*, *23*(5), 2031-2046.

Bergman, J. L., Harii, S., Kurihara, H., & Edmunds, P. J. (2018). Behaviour of brooded coral larvae in response to elevated pCO_2. *Frontiers in Marine Science*, *5*, Article 51.

Berthelier, J., Schnitzler, C. E., Wood-Charlson, E. M., Poole, A. Z., Weis, V. M., & Detournay, O. (2017). Implication of the host TGF beta pathway in the onset of symbiosis between larvae of the coral *Fungia scutaria* and the dinoflagellate *Symbiodinium* sp. (clade C1f). *Coral Reefs*, *36*(4), 1263-1268.

Bertucci, A., Moya, A., Tambutte, S., Allemand, D., Supuran, C. T., & Zoccola, D. (2013). Carbonic anhydrases in anthozoan corals – A review. *Bioorganic & Medicinal Chemistry*, *21*(6), 1437-1450.

Bertucci, A., Tambutte, S., Supuran, C. T., Allemand, D., & Zoccola, D. (2011). A new coral carbonic anhydrase in *Stylophora pistillata*. *Marine Biotechnology*, *13*(5), 992-1002.

Bessell-Browne, P., Negri, A. P., Fisher, R., Clode, P. L., Duckworth, A., & Jones, R. (2017). Impacts of turbidity on corals: The relative importance of light limitation and suspended sediments. *Marine Pollution Bulletin*, *117*(1-2), 161-170.

Bieri, T., Onishi, M., Xiang, T., Grossman, A. R., & Pringle, J. R. (2016). Relative contributions of various cellular mechanisms to loss of algae during cnidarian bleaching. *PLoS ONE*, *11*(4).

Bindoff, N.L., Cheung, W.W.L., Kairo, J.G., Arístegui, J., Guinder, V.A., Hallberg, R., … & Williamson, P. (2019). Changing Ocean, Marine Ecosystems, and Dependent Communities. In: Pörtner, H.-O., Roberts, D.C., Masson-Delmotte, V., Zhai, P., Tignor, M., Poloczanska, E., … & Weyer N.M. (Eds.), *IPCC Special Report on the Ocean and Cryosphere in a Changing Climate* (pp.447-587). Cambridge University Press.

Biscere, T., Zampighi, M., Lorrain, A., Jurriaans, S., Foggo, A., Houlbreque, F., & Rodolfo-Metalpa, R. (2019). High pCO_2 promotes coral primary production. *Biology Letters*, *15*(7), Article 20180777.

Blackstone, N. W., & Golladay, J. M. (2018). Why do corals bleach? Conflict and conflict mediation in a host/symbiont community. *Bioessays*, *40*(8), Article 1800021.

Blank, R. J., & Trench, R. K. (1985). Speciation and symbiotic dinoflagellates. *Science*, *229*(4714), 656-658.

Boron, W. F. (2004). Regulation of intracellular pH. *Advances in Physiology Education*, *28*(4), 160-179.

Boulotte, N. M., Dalton, S. J., Carroll, A. G., Harrison, P. L., Putnam, H. M., Peplow, L. M., & van Oppen, M. J. H. (2016). Exploring the Symbiodinium rare biosphere provides evidence for symbiont switching in reef-building corals. *Isme Journal*, *10*(11), 2693-2701.

Boyd, P. W., Cornwall, C. E., Davison, A., Doney, S. C., Fourquez, M., Hurd, C. L., ... & McMinn, A. (2016). Biological responses to environmental heterogeneity under future ocean conditions. *Global Change Biology*, *22*(8), 2633-2650.

Brading, P., Warner, M. E., Davey, P., Smith, D. J., Achterberg, E. P., & Suggett, D. J. (2011). Differential effects of ocean acidification on growth and photosynthesis among phylotypes of Symbiodinium (Dinophyceae). *Limnology and Oceanography*, *56*(3), 927-938.

Brading, P., Warner, M. E., Smith, D. J., & Suggett, D. J. (2013). Contrasting modes of inorganic carbon acquisition amongst Symbiodinium (Dinophyceae) phylotypes. *New Phytologist*, *200*(2), 432-442.

Browman, H. I. (2016). Applying organized scepticism to ocean acidification research Introduction. *Ices Journal of Marine Science*, *73*(3), 529-536.

Brown, B. (1997). Coral bleaching: causes and consequences. *Coral Reefs*, *16*, S129-S138.

Brownlee, C. (2009). pH regulation in symbiotic anemones and corals: A delicate balancing act. *Proceedings of the National Academy of Sciences of the United States of America*, *106*(39), 16541-16542.

Bucher, M., Wolfowicz, I., Voss, P. A., Hambleton, E. A., & Guse, A. (2016). Development and symbiosis establishment in the cnidarian endosymbiosis model aiptasia sp. *Scientific Reports*, *6*, Article 19867.

Buck, J., Sinclair, M. L., Schapal, L., Cann, M. J., & Levin, L. R. (1999). Cytosolic adenylyl cyclase defines a unique signalling molecule in mammals. *Proceedings of the National Academy of Sciences of the United States of America*, *96*(1), 79-84.

Burriesci, M. S., Raab, T. K., & Pringle, J. R. (2012). Evidence that glucose is the major transferred metabolite in dinoflagellate-cnidarian symbiosis. *Journal of Experimental Biology*, *215*(19), 3467-3477.

Buxton, L., Badger, M., & Ralph, P. (2009). Effects of moderate heat stress and dissolved inorganic carbon concentration on photosynthesis and respiration of *Symbiodinium* sp. (Dinophyceae) in culture and in symbiosis. *Journal of Phycology*, *45*(2), 357-365.

Büchel, C. (2020). Light harvesting complexes in chlorophyll *c*-containing algae. *Biochimica Et Biophysica Acta-Bioenergetics*, *1861*(4), Article 148027.

Camp, E. F., Schoepf, V., Mumby, P. J., Hardtke, L. A., Rodolfo-Metalpa, R., Smith, D. J., & Suggett, D. J. (2018). The future of coral reefs subject to rapid climate change: lessons from natural extreme environments. *Frontiers in Marine Science*, *5*, Article Unsp 4.

Canadell, J.G., Monteiro, P.M.S., Costa, M.H., Cotrim da Cunha, L., Cox, P.M., Eliseev, A.V., … & Zickfeld, K. (2021). Global Carbon and other Biogeochemical Cycles and Feedbacks. In: Masson-Delmotte, V., Zhai, P., Pirani, A., Connors, S.L., Péan, C., Berger, S., … & Zhou B. (Eds.), *Climate Change 2021: The Physical Science Basis*. *Contribution of Working Group I to the Sixth Assessment Report of the Intergovernmental Panel on Climate Change* (pp.673–816). Cambridge University Press.

Capasso, L., Ganot, P., Planas-Bielsa, V., Tambutte, S., & Zoccola, D. (2021). Intracellular pH regulation: characterization and functional investigation of H^+ transporters in *Stylophora pistillata*. *Bmc Molecular and Cell Biology*, *22*(1), Article 18.

Carroll, S. L., & Coyne, V. E. (2021). A proteomic analysis of the effect of ocean acidification on the haemocyte proteome of the South African abalone *Haliotis midae*. *Fish & Shellfish Immunology*, *117*, 274-290.

Casey, J. R., Grinstein, S., & Orlowski, J. (2010). Sensors and regulators of intracellular pH. *Nature Reviews Molecular Cell Biology*, *11*(1), 50-61.

Castillo, K. D., Ries, J. B., Bruno, J. F., & Westfield, I. T. (2014). The reef-building coral Siderastrea siderea exhibits parabolic responses to ocean acidification and warming. *Proceedings of the Royal Society B-Biological Sciences*, *281*(1797), Article 20141856.

Chan, K. Y. K., Grunbaum, D., Arnberg, M., & Dupont, S. (2016). Impacts of ocean acidification on survival, growth, and swimming behaviours differ between larval urchins and brittlestars. *Ices Journal of Marine Science*, *73*(3), 951-961.

Chang, X. J., Zheng, C. Q., Wang, Y. W., Meng, C., Xie, X. L., & Liu, H. P. (2016). Differential protein expression using proteomics from a crustacean brine shrimp (*Artemia sinica*) under CO_2-driven seawater acidification. *Fish & Shellfish Immunology*, *58*, 669-677.

Chaston, J., & Douglas, A. E. (2012). Making the most of "omics" for symbiosis research. *Biological Bulletin, 223*(1), 21-29.

Cheal, A. J., Macneil, M. A., Emslie, M. J., & Sweatman, H. (2017). The threat to coral reefs from more intense cyclones under climate change. *Global Change Biology*, *23*(4), 1511-1524.

Chen, C. A. (2004). Local phase shift from *Acropora*-dominant to *Condylactis*-dominant community in the Tiao-Shi Reef, Kenting National Park, southern Taiwan. *Coral Reefs*, *23*(4), 508-508.

Chen, M., Hong, M., Huang, Y., Liu, M., Cheng, Y., & Fang, L. (2005). ApRab11, a cnidarian homologue of the recycling regulatory protein Rab11, is involved in the establishment and maintenance of the Aiptasia-Symbiodinium endosymbiosis. *Biochemical and Biophysical Research Communications*, *338*(3), 1607-1616.

Chen, M. C., Cheng, Y. M., Sung, P. J., Kuo, C. E., & Fang, L. S. (2003). Molecular identification of Rab7 (ApRab7) in *Aiptasia pulchella* and its exclusion from phagosomes harboring zooxanthellae. *Biochemical and Biophysical Research Communications*, *308*(3), 586-595.

Chen, Y. Q., Cann, M. J., Litvin, T. N., Iourgenko, V., Sinclair, M. L., Levin, L. R., & Buck, J. (2000). Soluble adenylyl cyclase as an evolutionarily conserved bicarbonate sensor. *Science*, *289*(5479), 625-628.

Clevesa, P. A., Strader, M. E., Bay, L. K., Pringle, J. R., & Matz, M. V. (2018). CRISPR/Cas9-mediated genome editing in a reef-building coral. *Proceedings of the National Academy of Sciences of the United States of America*, *115*(20), 5235-5240.

Coffroth, M. A., Lewis, C. F., Santos, S. R., & Weaver, J. L. (2006). Environmental populations of symbiotic dinoflagellates in the genus *Symbiodinium* can initiate symbioses with reef cnidarians. *Current Biology*, *16*(23), R985-R987.

Cohen, A. L., & Holcomb, M. (2009). Why corals care about ocean acidification: uncovering the mechanism. *Oceanography*, *22*(4), 118-127.

Colombara, A. M., Quinn, D., & Chadwick, N. E. (2017). Habitat segregation and population structure of Caribbean sea anemones and associated crustaceans on coral reefs at Akumal Bay, Mexico. *Bulletin of Marine Science*, *93*(4), 1025-1047.

Comeau, S., Carpenter, R. C., & Edmunds, P. J. (2017). Effects of pCO_2 on photosynthesis and respiration of tropical scleractinian corals and calcified algae. *Ices Journal of Marine Science*, *74*(4), 1092-1102.

Comeau, S., Cornwall, C. E., DeCarlo, T. M., Krieger, E., & McCulloch, M. T. (2018). Similar controls on calcification under ocean acidification across unrelated coral reef taxa. *Global Change Biology*, *24*(10), 4857-4868.

Connell, S. D., Kroeker, K. J., Fabricius, K. E., Kline, D. I., & Russell, B. D. (2013). The other ocean acidification problem: CO_2 as a resource among competitors for ecosystem dominance. *Philosophical Transactions of the Royal Society B-Biological Sciences*, *368*(1627), Article 20120442.

Cooper, G. M. (2019). Genomics, Proteomics and Systems Biology In: Cooper, G. M. *The cell: A molecular approach*. (pp. 157-184). Oxford University Press.

Cornwall, C. E., Comeau, S., DeCarlo, T. M., Larcombe, E., Moore, B., Giltrow, K., ... & McCulloch, M. T. (2020). A coralline alga gains tolerance to ocean acidification over multiple generations of exposure. *Nature Climate Change*.

Cornwall, C. E., Comeau, S., DeCarlo, T. M., Moore, B., D'Alexis, Q., & McCulloch, M. T. (2018). Resistance of corals and coralline algae to ocean acidification: physiological control of calcification under natural pH variability. *Proceedings of the Royal Society B-Biological Sciences*, *285*(1884), Article 20181168.

Cornwall, C. E., Comeau, S., Kornder, N. A., Perry, C. T., Hooidonk, R. V., DeCarlo, T. M., . . . Lowe, R. J. (2021). Global declines in coral reef calcium carbonate production under ocean acidification and warming. *Proceedings of the National Academy of Sciences of the United States of America*, *118*(21), Article e2015265118. https://doi.org/10.1073/pnas.2015265118

Cornwall, C. E., Diaz-Pulido, G., & Comeau, S. (2019). Impacts of ocean warming on coralline algal calcification: meta-analysis, knowledge gaps, and key recommendations for future research. *Frontiers in Marine Science*, *6*, Article Unsp 186.

Cornwall, C. E., Hepburn, C. D., McGraw, C. M., Currie, K. I., Pilditch, C. A., Hunter, K. A., ... & Hurd, C. L. (2013). Diurnal fluctuations in seawater pH influence the response of a calcifying macroalga to ocean acidification. *Proceedings of the Royal Society B-Biological Sciences*, *280*(1772), Article 20132201.

Cornwall, C. E., & Hurd, C. L. (2016). Experimental design in ocean acidification research: problems and solutions. *Ices Journal of Marine Science*, *73*(3), 572-581.

Cox, J., Hein, M. Y., Luber, C. A., Paron, I., Nagaraj, N., & Mann, M. (2014). Accurate proteome-wide label-free quantification by delayed normalization and maximal peptide ratio extraction, termed MaxLFQ. *Molecular & Cellular Proteomics*, *13*(9), 2513-2526.

Crawley, A., Kline, D. I., Dunn, S., Anthony, K., & Dove, S. (2010). The effect of ocean acidification on symbiont photorespiration and productivity in *Acropora formosa*. *Global Change Biology*, *16*(2), 851-863.

Cumbo, V. R., van Oppen, M. J. H., & Baird, A. H. (2018). Temperature and Symbiodinium physiology affect the establishment and development of symbiosis in corals. *Marine Ecology Progress Series*, *587*, 117-127.

Cunning, R., Silverstein, R. N., & Baker, A. C. (2015). Investigating the causes and consequences of symbiont shuffling in a multi-partner reef coral symbiosis under environmental change. *Proceedings of the Royal Society B-Biological Sciences*, *282*(1809), Article 20141725.

Cziesielski, M. J., Liew, Y. J., Cui, G. X., Schmidt-Roach, S., Campana, S., Marondedze, C., & Aranda, M. (2018). Multi-omics analysis of thermal stress response in a zooxanthellate cnidarian reveals the importance of associating with thermotolerant symbionts. *Proceedings of the Royal Society B-Biological Sciences*, *285*(1877), Article 20172654.

Dagenais-Bellefeuille, S., & Morse, D. (2013). Putting the N in dinoflagellates. *Frontiers in Microbiology*, *4*, Article 1.

Dani, V., Priouzeau, F., Pagnotta, S., Carette, D., Laugier, J. P., & Sabourault, C. (2016). Thermal and menthol stress induce different cellular events during sea anemone bleaching. *Symbiosis*, *69*(3), 175-192.

Dason, J. S., & Colman, B. (2004). Inhibition of growth in two dinoflagellates by rapid changes in external pH. *Canadian Journal of Botany-Revue Canadienne De Botanique*, *82*(4), 515-520.

David, R., & Peter, W. (2007). Signal integration in the endoplasmic reticulum unfolded protein response. *Nature Reviews Molecular Cell Biology*, *8*(7), 519. https://doi.org/10.1038/nrm2199

Davies, S., Marchetti, A., Ries, J., & Castillo, K. (2016). Thermal and pCO_2 stress elicit divergent transcriptomic responses in a resilient coral. *Frontiers In Marine Science*, *3*.

Davy, S. K., Allemand, D., & Weis, V. M. (2012). Cell biology of cnidarian-dinoflagellate symbiosis. *Microbiology and Molecular Biology Reviews*, *76*(2), 229-261.

Davy, S. K., & Cook, C. B. (2001). The relationship between nutritional status and carbon flux in the zooxanthellate sea anemone Aiptasia pallida. *Marine Biology*, *139*(5), 999-1005.

DeCarlo, T. M., Cohen, A. L., Wong, G. T. F., Davis, K. A., Lohmann, P., & Soong, K. (2017). Mass coral mortality under local amplification of 2 degrees C ocean warming. *Scientific Reports*, *7*, Article 44586.

DeCarlo, T. M., Comeau, S., Cornwall, C. E., & McCulloch, M. T. (2018). Coral resistance to ocean acidification linked to increased calcium at the site of calcification. *Proceedings of the Royal Society B-Biological Sciences*, *285*(1878), Article 20180564.

Detournay, O., Schnitzler, C. E., Poole, A., & Weis, V. M. (2012). Regulation of cnidarian-dinoflagellate mutualisms: Evidence that activation of a host TGF beta innate immune pathway promotes tolerance of the symbiont. *Developmental and Comparative Immunology*, *38*(4), 525-537.

De'Ath, G., Fabricius, K. E., Sweatman, H., & Puotinen, M. (2012). The 27–year decline of coral cover on the Great Barrier Reef and its causes. *Proceedings of the National Academy of Sciences*, *109*(44), 17995-17999.

Diaz-Pulido, G., Anthony, K. R. N., Kline, D. I., Dove, S., & Hoegh-Guldberg, O. (2012). Interactions between ocean acidification and warming on the mortality and dissolution of coralline algae. *Journal of Phycology*, *48*(1), 32-39.

Dickinson, D. A., & Forman, H. J. (2002). Glutathione in defence and signalling - Lessons from a small thiol. *Cell Signalling, Transcription, and Translation as Therapeutic Targets*, *973*, 488-504.

Dickson, A. G., Sabine, C. L., & Christian, J. R. (2007). *Guide to best practices for ocean CO_2 measurements*. North Pacific Marine Science Organization.

Dimos, B. A., Mahmud, S. A., Fuess, L. E., Mydlarz, L. D., & Pellegrino, M. W. (2019). Uncovering a mitochondrial unfolded protein response in corals and its role in adapting to a changing world. *Proceedings of the Royal Society B-Biological Sciences*, *286*(1905), Article 20190470.

Dineshram, R., Quan, Q., Sharma, R., Chandramouli, K., Yalamanchili, H. K., Chu, I., & Thiyagarajan, V. (2015). Comparative and quantitative proteomics reveal the adaptive strategies of oyster larvae to ocean acidification. *Proteomics*, *15*(23-24), 4120-4134.

Doney, S. C., Busch, D. S., Cooley, S. R., & Kroeker, K. J. (2020). The impacts of ocean acidification on marine ecosystems and reliant human communities. *Annual Review of Environment and Resources, Vol 45*, *45*, 83-112.

Doney, S. C., Fabry, V. J., Feely, R. A., & Kleypas, J. A. (2009). Ocean acidification: the other CO_2 problem. *Annual Review of Marine Science*, *1*, 169-192.

Douglas, A. E. (2008). Conflict, cheats and the persistence of symbioses. *New Phytologist*, *177*(4), 849-858.

Downs, C. A., Kramarsky-Winter, E., Martinez, J., Kushmaro, A., Woodley, C. M., Loya, Y., & Ostrander, G. K. (2009). Symbiophagy as a cellular mechanism for coral bleaching. *Autophagy*, *5*(2), 211-216.

Dubinsky, Z., & Jokiel, P. L. (1994). Ratio of energy and nutrient fluxes regulates symbiosis between zooxanthellae and corals. *Pacific Science*, *48*, 313-324.

Dubinsky, Z., & Berman-Frank, I. (2001). Uncoupling primary production from population growth in photosynthesizing organisms in aquatic ecosystems. *Aquatic Sciences*, *63*(1), 4-17.

Duckworth, A. R., West, L., Vansach, T., Stubler, A., & Hardt, M. (2012). Effects of water temperature and pH on growth and metabolite biosynthesis of coral reef sponges. *Marine Ecology Progress Series*, *462*, 67-77.

Dunn, S. R., Pernice, M., Green, K., Hoegh-Guldberg, O., & Dove, S. G. (2012). Thermal stress promotes host mitochondrial degradation in symbiotic cnidarians: are the batteries of the reef going to run out? *Plos One*, *7*(7), Article e39024.

Dunn, S. R., Schnitzler, C. E., & Weis, V. M. (2007). Apoptosis and autophagy as mechanisms of dinoflagellate symbiont release during cnidarian bleaching: every which way you lose. *Proceedings of the Royal Society B-Biological Sciences*, *274*(1629), 3079-3085.

Dunn, S. R., Thomason, J. C., Tissier, M. D. A. L., & Bythell, J. C. (2004). Heat stress induces different forms of cell death in sea anemones and their endosymbiotic algae depending on temperature and duration. *Cell Death and Differentiation*, *11*(11), 1213.

Edmunds, P. (2011). Zooplanktivory ameliorates the effects of ocean acidification on the reef coral Porites spp. *Limnology and Oceanography*, *56*(6), 2402-2410.

Fabina, N. S., Putnam, H. M., Franklin, E. C., Stat, M., & Gates, R. D. (2012). Transmission mode predicts specificity and interaction patterns in coral-symbiodinium networks. *Plos One*, *7*(9), Article e44970.

Fabregas, J., Vazquez, V., Cabezas, B., & Otero, A. (1993). Tris not only controls the pH in microalgal cultures, but also feeds bacteria. *Journal of Applied Phycology*, *5*(5), 543-545.

Fabricius, K. E., De'ath, G., Noonan, S., & Uthicke, S. (2014). Ecological effects of ocean acidification and habitat complexity on reef-associated macroinvertebrate communities. *Proceedings of the Royal Society B-Biological Sciences*, *281*(1775), Article 20132479.

Fabricius, K. E., Langdon, C., Uthicke, S., Humphrey, C., Noonan, S., De'ath, G., ... & Lough, J. M. (2011). Losers and winners in coral reefs acclimatized to elevated carbon dioxide concentrations. *Nature Climate Change*, *1*(3), 165-169.

Fabricius, K. E., Noonan, S. H. C., Abrego, D., Harrington, L., & De'ath, G. (2017). Low recruitment due to altered settlement substrata as primary constraint for coral communities under ocean acidification. *Proceedings of the Royal Society B-Biological Sciences, 284*(1862), Article 20171536.

Fabry, V. J., Seibel, B. A., Feely, R. A., & Orr, J. C. (2008). Impacts of ocean acidification on marine fauna and ecosystem processes. *Ices Journal of Marine Science, 65*(3), 414-432.

Fadlallah, Y. H. (1983). Sexual reproduction, development and larval biology in scleractinian corals. *Coral reefs, 2*(3), 129-150.

Fagoonee, I., Wilson, H. B., Hassell, M. P., & Turner, J. R. (1999). The dynamics of zooxanthellae populations: A long-term study in the field. *Science, 283*(5403), 843-845.

Fangue, N. A., O'Donnell, M. J., Sewell, M. A., Matson, P. G., MacPherson, A. C., & Hofmann, G. E. (2010). A laboratory-based, experimental system for the study of ocean acidification effects on marine invertebrate larvae. *Limnology and Oceanography-Methods, 8*, 441-452.

Feely, R. A., Sabine, C. L., Lee, K., Berelson, W., Kleypas, J., Fabry, V. J., & Millero, F. J. (2004). Impact of anthropogenic CO_2 on the $CaCO_3$ system in the oceans. *Science (New York, N.Y.), 305*(5682), 362-366.

Fernie, A. R., Carrari, F., & Sweetlove, L. J. (2004). Respiratory metabolism: glycolysis, the TCA cycle and mitochondrial electron transport. *Current Opinion in Plant Biology, 7*(3), 254-261.

Ferrier-Pages, C., Godinot, C., D'Angelo, C., Wiedenmann, J., & Grover, R. (2016). Phosphorus metabolism of reef organisms with algal symbionts. *Ecological Monographs, 86*(3), 262-277.

Feussner, I., & Polle, A. (2015). What the transcriptome does not tell – proteomics and metabolomics are closer to the plants' patho-phenotype. *Current Opinion in Plant Biology, 26*, 26-31.

Fisher, R., Bessell-Browne, P., & Jones, R. (2019). Synergistic and antagonistic impacts of suspended sediments and thermal stress on corals. *Nature Communications, 10*, Article 2346.

Fitt, W. K. (2000). Cellular growth of host and symbiont in a cnidarian-zooxanthellar symbiosis. *Biological Bulletin, 198*(1), 110-120.

Fitt, W. K., & Trench, R. K. (1983). Endocytosis of the symbiotic dinoflagellate *Symbiodinium-Microadriaticum* Freudenthal by endodermal cells of the scyphistomae of *Cassiopeia-Xamachana* and resistance of the algae to host digestion. *Journal of Cell Science, 64*(Nov), 195-212.

Fransolet, D., Roberty, S., & Plumier, J. C. (2012). Establishment of endosymbiosis: The case of cnidarians and Symbiodinium. *Journal of Experimental Marine Biology and Ecology, 420*, 1-7.

Freudenthal, H. D. (1962). *Symbiodinium* gen nov and *Symbiodinium microadriaticum* sp. nov, a zooxanthella – taxonomy, life cycle, and morphology. *Journal of Protozoology, 9*(1), 45-52.

Furla, P., Galgani, I., Durand, I., & Allemand, D. (2000). Sources and mechanisms of inorganic carbon transport for coral calcification and photosynthesis. *Journal of Experimental Biology, 203*(22), 3445.

Gabay, Y., Parkinson, J. E., Wilkinson, S. P., Weis, V. M., & Davy, S. K. (2019). Inter-partner specificity limits the acquisition of thermotolerant symbionts in a model cnidarian-dinoflagellate symbiosis. *Isme Journal, 13*(10), 2489-2499.

Gabay, Y., Weis, V. M., & Davy, S. K. (2018). Symbiont identity influences patterns of symbiosis establishment, host growth, and asexual reproduction in a model cnidarian-dinoflagellate symbiosis. *Biological Bulletin, 234*(1), 1-10.

Galligan, J. J., & Petersen, D. R. (2012). The human protein disulfide isomerase gene family. *Human Genomics, 6*, Article 6.

Gardner, S. G., Raina, J. B., Ralph, P. J., & Petrou, K. (2017). Reactive oxygen species (ROS) and dimethylated sulphur compounds in coral explants under acute thermal stress. *Journal of Experimental Biology, 220*(10), 1787-1791.

Gates, R. D. (1990). Seawater temperature and sublethal coral bleaching in jamaica. *Coral Reefs, 8*(4), 193-197.

Gates, R. D., Baghdasarian, G., & Muscatine, L. (1992). Temperature stress causes host-cell detachment in symbiotic cnidarians - implications for coral bleaching. *Biological Bulletin, 182*(3), 324-332.

Gattuso, J.P., Lee, K., Rost, B., & Schulz, K. (2010). Approaches and tools to manipulate the carbonate chemistry In: Riebesell, U., Fabry, V.J., Hansson, L. & Gattuso, J.P., (Eds.) *Guide to Best Practices for Ocean Acidification Research and Data Reporting* (pp.41-52). Publications Office of the European Union.

Ge, R. Q., Liang, J. Y., Yu, K. F., Chen, B., Yu, X. P., Deng, C. Q., ... & Qin, L. Y. (2021). Regulation of the coral-associated bacteria and Symbiodiniaceae in A*cropora valida* under ocean acidification. *Frontiers in Microbiology, 12*, Article 767174.

Genty, B., Briantais, J. M., & Baker, N. R. (1989). The relationship between the quantum yield of photosynthetic electron-transport and quenching of chlorophyll fluorescence. *Biochimica Et Biophysica Acta, 990*(1), 87-92.

Gerencser, G. A., Levin, R., & Zhang, J. L. (2002). Sodium-phosphate symport by *Aplysia californica* gut. *Zoological Science, 19*(2), 163-166.

Gheitanchi Mashini, A. (2022). The Impact of Symbiont Diversity on Cellular Integration and Function in the Cnidarian-Dinoflagellate Symbiosis. Victoria University of Wellington - Te Herenga Waka.

Gibbin, E. M., & Davy, S. K. (2013). Intracellular pH of symbiotic dinoflagellates. *Coral Reefs, 32*(3), 859-863.

Gibbin, E. M., & Davy, S. K. (2014). The photo-physiological response of a model cnidarian-dinoflagellate symbiosis to CO_2-induced acidification at the cellular level. *Journal of Experimental Marine Biology and Ecology, 457*, 1-7.

Gibbin, E. M., Putnam, H. M., Davy, S. K., & Gates, R. D. (2014). Intracellular pH and its response to CO_2-driven seawater acidification in symbiotic versus non-symbiotic coral cells. *Journal of Experimental Biology*, *217*(11), 1963-1969.

Gibbin, E. M., Putnam, H. M., Gates, R. D., Nitschke, M. R., & Davy, S. K. (2015). Species-specific differences in thermal tolerance may define susceptibility to intracellular acidosis in reef corals. *Marine Biology*, *162*(3), 717-723.

Glazier, A., Herrera, S., Weinnig, A., Kurman, M., Gomez, C. E., & Cordes, E. (2020). Regulation of ion transport and energy metabolism enables certain coral genotypes to maintain calcification under experimental ocean acidification. *Molecular Ecology*, *29*(9), 1657-1673.

Glynn, P. W. (1983). Extensive bleaching and death of reef corals on the pacific coast of Panama. *Environmental Conservation*, *10*(2), 149-154.

Glynn, P. W. (1991). Coral-reef bleaching in the 1980s and possible connections with global warming. *Trends in Ecology & Evolution*, *6*(6), 175-179. https://doi.org/10.1016/0169-5347(91)90208-f

Glynn, P. W., & Manzello, D. P. (2015). Bioerosion and coral reef growth: a dynamic balance. In: *Coral reefs in the Anthropocene* (pp.67-97). Springer.

Godinot, C., Grover, R., Allemand, D., & Ferrier-Pages, C. (2011). High phosphate uptake requirements of the scleractinian coral *Stylophora pistillata*. *Journal of Experimental Biology*, *214*(16), 2749-2754.

Goff, L. J. (1982). Symbiosis and parasitism – another viewpoint. *Bioscience*, *32*(4), 255-256.

Gonzalez-Pech, R. A., Bhattacharya, D., Ragan, M. A., & Chan, C. X. (2019). Genome evolution of coral reef symbionts as intracellular residents. *Trends in Ecology & Evolution*, *34*(9), 799-806.

Gonzalez-Pech, R. A., Vargas, S., Francis, W. R., & Worheide, G. (2017). Transcriptomic resilience of the *Montipora digitata* holobiont to low pH. *Frontiers in Marine Science*, *4*, Article Unsp 403.

Goodwin, C., Rodolfo-Metalpa, R., Picton, B., & Hall-Spencer, J. M. (2014). Effects of ocean acidification on sponge communities. *Marine Ecology-an Evolutionary Perspective*, *35*, 41-49.

Graham, E. R., Parekh, A., Devassy, R. K., & Sanders, R. W. (2015). Carbonic anhydrase activity changes in response to increased temperature and pCO_2 in Symbiodinium-zoanthid associations. *Journal of Experimental Marine Biology and Ecology*, *473*, 218-226.

Gran, G. (1952). Determination of the equivalence point in potentiometric titrations. Part II. *Analyst*, *77*(920), 661-671.

Grottoli, A. G., & Rodrigues, L. J. (2011). Bleached *Porites compressa* and *Montipora capitata* corals catabolize delta C-13-enriched lipids. *Coral Reefs*, *30*(3), 687-692.

Grottoli, A. G., Rodrigues, L. J., & Juarez, C. (2004). Lipids and stable carbon isotopes in two species of Hawaiian corals, *Porites compressa* and *Montipora verrucosa*, following a bleaching event. *Marine Biology*, *145*(3), 621-631.

Grottoli, A. G., Rodrigues, L. J., & Palardy, J. E. (2006). Heterotrophic plasticity and resilience in bleached corals. *Nature*, *440*(7088), 1186-1189.

Gruber, N., Clement, D., Carter, B. R., Feely, R. A., van Heuven, S., Hoppema, M., ... & Wanninkhof, R. (2019). The oceanic sink for anthropogenic CO_2 from 1994 to 2007. *Science (New York, N.Y.)*, *363*(6432), 1193.

Hambleton, E. A., Guse, A., & Pringle, J. R. (2014). Similar specificities of symbiont uptake by adults and larvae in an anemone model system for coral biology. *Journal of Experimental Biology*, *217*(9), 1613-1619.

Hanes, S. D., & Kempf, S. C. (2013). Host autophagic degradation and associated symbiont loss in response to heat stress in the symbiotic anemone, *Aiptasia pallida*. *Invertebrate Biology*, *132*(2), 95-107.

Harborne, A. R., Rogers, A., Bozec, Y. M., Mumby, P. J., & Annual, R. (2017). Multiple stressors and the functioning of coral reefs. *Annual Review of Marine Science, Vol 9*, *9*, 445-468.

Harii, S., Yasuda, N., Rodriguez-Lanetty, M., Irie, T., & Hidaka, M. (2009). Onset of symbiosis and distribution patterns of symbiotic dinoflagellates in the larvae of scleractinian corals. *Marine Biology*, *156*(6), 1203-1212.

Harrison, P. L. (2011). Sexual reproduction of scleractinian corals. *Coral Reefs: An Ecosystem in Transition*, 59-85.

Hawkins, T. D., Bradley, B. J., & Davy, S. K. (2013). Nitric oxide mediates coral bleaching through an apoptotic-like cell death pathway: evidence from a model sea anemone-dinoflagellate symbiosis. *Faseb Journal*, *27*(12), 4790-4798.

Hawkins, T. D., & Davy, S. K. (2012). Nitric oxide production and tolerance differ among Symbiodinium types exposed to heat stress. *Plant and Cell Physiology*, *53*(11), 1889-1898.

Hawkins, T. D., Krueger, T., Becker, S., Fisher, P. L., & Davy, S. K. (2014). Differential nitric oxide synthesis and host apoptotic events correlate with bleaching susceptibility in reef corals. *Coral Reefs*, *33*(1), 141-153.

Haynes, C. M., & Ron, D. (2010). The mitochondrial UPR – protecting organelle protein homeostasis. *Journal of Cell Science*, *123*(22), 3849-3855.

Hedouin, L., & Gates, R. D. (2013). Assessing fertilization success of the coral *Montipora capitata* under copper exposure: Does the night of spawning matter? *Marine Pollution Bulletin*, *66*(1-2), 221-224.

Heron, S. F., Maynard, J. A., van Hooidonk, R., & Eakin, C. M. (2016). Warming trends and bleaching stress of the world's coral reefs 1985-2012. *Scientific Reports*, *6*, Article 38402.

Herre, E. A., Knowlton, N., Mueller, U. G., & Rehner, S. A. (1999). The evolution of mutualisms: exploring the paths between conflict and cooperation. *Trends in Ecology & Evolution*, *14*(2), 49-53.

Herrera, M., Liew, Y. J., Venn, A., Tambutte, E., Zoccola, D., Tambutte, S., ... & Aranda, M. (2021). New insights from transcriptomic data reveal differential effects of CO_2 acidification stress on photosynthesis of an endosymbiotic dinoflagellate *in hospite*. *Frontiers in Microbiology*, *12*, Article 666510.

Hetz, C. (2012). The unfolded protein response: controlling cell fate decisions under ER stress and beyond. *Nature Reviews Molecular Cell Biology, 13*(2), 89-102.

Hill, L. J., Parades, W. C., Willemes, M. J., Pereira, M. G., Salomon, P. S., Mariath, R., . . . Salgado, L. T. (2019). Acidification-induced cellular changes in Symbiodinium isolated from *Mussismilia braziliensis*. *Plos One, 14*(8), Article e0220130.

Hill, R., Brown, C. M., Dezeeuw, K., Campbell, D. A., & Ralph, P. J. (2011). Increased rate of D1 repair in coral symbionts during bleaching is insufficient to counter accelerated photo-inactivation. *Limnology and Oceanography*, *56*(1), 139-146.

Hillyer, K. E., Dias, D. A., Lutz, A., Roessner, U., & Davy, S. K. (2017). Mapping carbon fate during bleaching in a model cnidarian symbiosis: the application of C-13 metabolomics. *New Phytologist*, *214*(4), 1551-1562.

Hillyer, K. E., Tumanov, S., Villas-Boas, S., & Davy, S. K. (2016). Metabolite profiling of symbiont and host during thermal stress and bleaching in a model cnidarian-dinoflagellate symbiosis. *Journal of Experimental Biology*, *219*(4), 516-527.

Hoadley, K. D., Lewis, A. M., Wham, D. C., Pettay, D. T., Grasso, C., Smith, R., ... & Warner, M. E. (2019). Host-symbiont combinations dictate the photo-physiological response of reef-building corals to thermal stress. *Scientific Reports*, *9*, Article 9985.

Hoadley, K. D., Pettay, D. T., Dodge, D., & Warner, M. E. (2016). Contrasting physiological plasticity in response to environmental stress within different cnidarians and their respective symbionts. *Coral Reefs*, *35*(2), 529-542.

Hoadley, K. D., Rollison, D., Pettay, D. T., & Warner, M. E. (2015). Differential carbon utilization and asexual reproduction under elevated pCO_2 conditions in the model anemone, *Exaiptasia pallida*, hosting different symbionts. *Limnology and Oceanography*, *60*(6), 2108-2120.

Hoegh-Guldberg, O., Mumby, P. J., Hooten, A. J., Steneck, R. S., Greenfield, P., Gomez, E., ... & Hatziolos, M. E. (2007). Coral reefs under rapid climate change and ocean acidification. *Science*, *318*(5857), 1737-1742.

Hoegh-Guldberg, O., Poloczanska, E. S., Skirving, W., & Dove, S. (2017). Coral reef ecosystems under climate change and ocean acidification. *Frontiers in Marine Science, 4*, Article Unsp 158.

Hofmann, G. E., Barry, J. P., Edmunds, P. J., Gates, R. D., Hutchins, D. A., Klinger, T., & Sewell, M. A. (2010). The effect of ocean acidification on calcifying organisms in marine ecosystems: an organism-to-ecosystem perspective. In: Futuyma, D. J., Shafer, H. B., & Simberloff, D. (Eds.), *Annual Review of Ecology, Evolution, and Systematics, 41*, 127-147.

Hohman, T. C., McNeil, P. L., & Muscatine, L. (1982). Phagosome-lysosome fusion inhibited by algal symbionts of *Hydra viridis*. *Journal of Cell Biology*, *94*(1), 56-63.

Hopkinson, B. M., Tansik, A. L., & Fitt, W. K. (2015). Internal carbonic anhydrase activity in the tissue of scleractinian corals is sufficient to support proposed roles in photosynthesis and calcification. *Journal of Experimental Biology*, *218*(13), 2039-2048.

Horwitz, R., Borell, E. M., Yam, R., Shemesh, A., & Fine, M. (2015). Natural high pCO_2 increases autotrophy in *Anemonia viridis* (Anthozoa) as revealed from stable isotope (C, N) analysis. *Scientific Reports, 5*(1), 1-9.

Hughes, A. D., & Grottoli, A. G. (2013). Heterotrophic compensation: a possible mechanism for resilience of coral reefs to global warming or a sign of prolonged stress? *Plos One*, *8*(11), Article e81172.

Hughes, A. D., Grottoli, A. G., Pease, T. K., & Matsui, Y. (2010). Acquisition and assimilation of carbon in non-bleached and bleached corals. *Marine Ecology Progress Series*, *420*, 91-101.

Hughes, T. P., Barnes, M. L., Bellwood, D. R., Cinner, J. E., Cumming, G. S., Jackson, J. B. C., ... & Scheffer, M. (2017). Coral reefs in the Anthropocene. *Nature*, *546*(7656), 82-90.

Huntley, R. P., Sawford, T., Mutowo-Meullenet, P., Shypitsyna, A., Bonilla, C., Martin, M. J., & O'Donovan, C. (2015). The GOA database: Gene Ontology annotation updates for 2015. *Nucleic Acids Research*, *43*(D1), D1057-D1063.

Hurd, C. L., Hepburn, C. D., Currie, K. I., Raven, J. A., & Hunter, K. A. (2009). Testing the effects of ocean acidification on algal metabolism: considerations for experimental designs. *Journal of Phycology*, *45*(6), 1236-1251.

Hurlbert, S. H. (1984). Pseudoreplication and the design of ecological field experiments. *Ecological monographs*, *54*(2), 187-211.

Iguchi, A., Ozaki, S., Nakamura, T., Inoue, M., Tanaka, Y., Suzuki, A., ... & Sakai, K. (2012). Effects of acidified seawater on coral calcification and symbiotic algae on the massive coral *Porites australiensis*. *Marine Environmental Research*, *73*, 32-36.

Imbs, A. B., & Yakovleva, I. M. (2012). Dynamics of lipid and fatty acid composition of shallow-water corals under thermal stress: an experimental approach. *Coral Reefs*, *31*(1), 41-53.

Innis, T., Allen-Waller, L., Brown, K. T., Sparagon, W., Carlson, C., Kruse, E., ... & Barott, K. L. (2021). Marine heatwaves depress metabolic activity and impair cellular acid-base homeostasis in reef-building corals regardless of bleaching susceptibility. *Global Change Biology*, *27*(12), 2728-2743.

Inoue, S., Kayanne, H., Yamamoto, S., & Kurihara, H. (2013). Spatial community shift from hard to soft corals in acidified water. *Nature Climate Change*, *3*(7), 683-687.

IPCC (2019). Summary for Policymakers. In Pörtner, H.-O., Roberts, D.C., Masson-Delmotte, V., Zhai, P., Tignor, M., Poloczanska, E., … & Weyer N.M. (Eds.), *IPCC Special Report on the Ocean and Cryosphere in a Changing Climate* (pp. 3-35). Cambridge University Press.

IPCC, 2021: Summary for Policymakers. In Masson-Delmotte, V., Zhai, P., Pirani, A., Connors, S.L., Péan, C., Berger, S., … & Zhou B. (Eds.), *Climate Change 2021: The Physical Science Basis*. *Contribution of Working Group I to the Sixth Assessment Report of the Intergovernmental Panel on Climate Change.* (pp. 3–82). Cambridge University Press.

Jafri, M. S., Dudycha, S. J., & O'Rourke, B. (2001). Cardiac energy metabolism: models of cellular respiration. *Annual review of biomedical engineering*, *3*(1), 57-81.

Jarrold, M. D., Calosi, P., Verberk, W., Rastrick, S. P. S., Atfield, A., & Spicer, J. I. (2013). Physiological plasticity preserves the metabolic relationship of the intertidal non-calcifying anthozoan-Symbiodinium symbiosis under ocean acidification. *Journal of Experimental Marine Biology and Ecology*, *449*, 200-206.

Jeong, H. J., Jang, S. H., Moestrup, O., Kang, N. S., Lee, S. Y., Potvin, E., & Noh, J. H. (2014). *Ansanella granifera* gen. et sp nov (Dinophyceae), a new dinoflagellate from the coastal waters of Korea. *Algae*, *29*(2), 75-99.

Jiang, J., Zhang, H., Orf, G. S., Lu, Y., Xu, W. X., Harrington, L. B., ... & Blankenship, R. E. (2014). Evidence of functional trimeric chlorophyll *a/c*2-peridinin proteins in the dinoflagellate Symbiodinium. *Biochimica Et Biophysica Acta-Bioenergetics*, *1837*(11), 1904-1912. https://doi.org/10.1016/j.bbabio.2014.07.023

Jiang, J. Y., & Lu, Y. D. (2019). Metabolite profiling of *Breviolum minutum* in response to acidification. *Aquatic Toxicology*, *213*, Article 105215.

Jiang, L., Quo, Y. J., Zhang, F., Zhang, Y. Y., McCook, L. J., Yuan, X. C., ... & Huang, H. (2019). Diurnally fluctuating pCO_2 modifies the physiological responses of coral recruits under ocean acidification. *Frontiers in Physiology*, *9*, Article 1952.

Jiang, L., Zhou, G. W., Zhang, Y. Y., Lei, X. M., Yuan, T., Guo, M. L., ... & Huang, H. (2021). Plasticity of symbiont acquisition in new recruits of the massive coral *Platygyra daedalea* under ocean warming and acidification. *Coral Reefs*, *40*(5), 1563-1576.

Jokiel, P. L. (2011). Ocean acidification and control of reef coral calcification by boundary layer limitation of proton flux. *Bulletin of Marine Science*, *87*(3), 639-657.

Kamenos, N. A., Burdett, H. L., Aloisio, E., Findlay, H. S., Martin, S., Longbone, C., ... & Calosi, P. (2013). Coralline algal structure is more sensitive to rate, rather than the magnitude, of ocean acidification. *Global Change Biology*, *19*(12), 3621-3628.

Kaniewska, P., Campbell, P. R., Kline, D. I., Rodriguez-Lanetty, M., Miller, D. J., Dove, S., & Hoegh-Guldberg, O. (2012). Major cellular and physiological impacts of ocean acidification on a reef building coral. *Plos One*, *7*(4), Article e34659.

Kaniewska, P., Chan, C.-K., Kline, D., Ling, E., Rosic, N., Edwards, D., ... & Dove, S. (2015). Transcriptomic changes in coral holobionts provide insights into physiological challenges of future climate and ocean change: e0139223. *PLoS ONE*, *10*(10).

Kelly, M. W., Padilla-Gamino, J. L., & Hofmann, G. E. (2016). High pCO_2 affects body size, but not gene expression in larvae of the California mussel (*Mytilus californianus*). *Ices Journal of Marine Science*, *73*(3), 962-969.

Kemp, D. W., Hernandez-Pech, X., Iglesias-Prieto, R., Fitt, W. K., & Schmidt, G. W. (2014). Community dynamics and physiology of *Symbiodinium* spp. before, during, and after a coral bleaching event. *Limnology and Oceanography*, *59*(3), 788-797.

Kemp, D. W., Thornhill, D. J., Rotjan, R. D., Iglesias-Prieto, R., Fitt, W. K., & Schmidt, G. W. (2015). Spatially distinct and regionally endemic Symbiodinium assemblages in the threatened Caribbean reef-building coral *Orbicella faveolata*. *Coral Reefs*, *34*(2), 535-547.

Kenkel, C. D., Moya, A., Strahl, J., Humphrey, C., & Bay, L. K. (2018). Functional genomic analysis of corals from natural CO_2-seeps reveals core molecular responses involved in acclimatization to ocean acidification. *Global Change Biology*, *24*(1), 158-171.

Kishimoto, M., Baird, A. H., Maruyama, S., Minagawa, J., & Takahashi, S. (2020). Loss of symbiont infectivity following thermal stress can be a factor limiting recovery from bleaching in cnidarians. *Isme Journal*, *14*(12), 3149-3152.

Kitajima, M., & Butler, W. L. (1975). Quenching of chlorophyll fluorescence and primary photochemistry in chloroplasts by dibromothymoquinone. *Biochimica Et Biophysica Acta*, *376*(1), 105-115.

Kitchen, S. A., Ratan, A., Bedoya-Reina, O. C., Burhans, R., Fogarty, N. D., Miller, W., & Baums, I. B. (2019). Genomic variants among threatened *Acropora* corals. *G3-Genes Genomes Genetics*, *9*(5), 1633-1646.

Klein, S. G., Pitt, K. A., Nitschke, M. R., Goyen, S., Welsh, D. T., Suggett, D. J., & Carroll, A. R. (2017). Symbiodinium mitigate the combined effects of hypoxia and acidification on a noncalcifying cnidarian. *Global Change Biology*, *23*(9), 3690-3703.

Kleypas, J. A., McManus, J. W., & Menez, L. A. B. (1999). Environmental limits to coral reef development: Where do we draw the line? *American Zoologist*, *39*(1), 146-159.

Knowlton, N., & Jackson, J. B. C. (2008). Shifting baselines, local impacts, and global change on coral reefs. *Plos Biology*, *6*(2), 215-220.

Koike, K., Jimbo, M., Sakai, R., Kaeriyama, M., Muramoto, K., Ogata, T., . . . Kamiya, H. (2004). Octocoral chemical signalling selects and controls dinoflagellate symbionts. *Biological Bulletin*, *207*(2), 80-86.

Kornder, N. A., Riegl, B. M., & Figueiredo, J. (2018). Thresholds and drivers of coral calcification responses to climate change. *Global Change Biology*, *24*(11), 5084-5095.

Koskinen, P., Toronen, P., Nokso-Koivisto, J., & Holm, L. (2015). PANNZER: high-throughput functional annotation of uncharacterized proteins in an error-prone environment. *Bioinformatics*, *31*(10), 1544-1552.

Kostic, A. D., Howitt, M. R., & Garrett, W. S. (2013). Exploring host-microbiota interactions in animal models and humans. *Genes & Development*, *27*(7), 701-718.

Kregel, K. C. (2002). Heat shock proteins: modifying factors in physiological stress responses and acquired thermotolerance. *Journal of Applied Physiology*, *92*(5), 2177-2186.

Krief, S., Hendy, E. J., Fine, M., Yam, R., Meibom, A., Foster, G. L., & Shemesh, A. (2010). Physiological and isotopic responses of scleractinian corals to ocean acidification. *Geochimica Et Cosmochimica Acta*, *74*(17), 4988-5001.

Kroeker, K. J., Kordas, R. L., Crim, R., Hendriks, I. E., Ramajo, L., Singh, G. S., . . . Gattuso, J. P. (2013). Impacts of ocean acidification on marine organisms: quantifying sensitivities and interaction with warming. *Global Change Biology*, *19*(6), 1884-1896.

Krueger, T., Hawkins, T. D., Becker, S., Pontasch, S., Dove, S., Hoegh-Guldberg, O., ... & Davy, S. K. (2015). Differential coral bleaching – contrasting the activity and response of enzymatic antioxidants in symbiotic partners under thermal stress. *Comparative Biochemistry and Physiology, Part A*, *190*, 15-25.

Krueger, T., Horwitz, N., Bodin, J., Giovani, M. E., Escrig, S., Fine, M., & Meibom, A. (2020). Intracellular competition for nitrogen controls dinoflagellate population density in corals. *Proceedings of the Royal Society B-Biological Sciences*, *287*(1922), Article 20200049.

Kurihara, H. (2008). Effects of CO_2-driven ocean acidification on the early developmental stages of invertebrates. *Marine Ecology Progress Series*, *373*, 275-284.

Kültz, D. (2005). Molecular and evolutionary basis of the cellular stress response. *Annual Review of Physiology*, *67*, 225-257.

Kvitt, H., Rosenfeld, H., & Tchernov, D. (2016). The regulation of thermal stress induced apoptosis in corals reveals high similarities in gene expression and function to higher animals. *Scientific Reports*, *6*, Article 30359.

Kvitt, H., Rosenfeld, H., Zandbank, K., & Tchernov, D. (2011). Regulation of apoptotic pathways by *Stylophora pistillata* (Anthozoa, Pocilloporidae) to survive thermal stress and bleaching. *Plos One*, *6*(12), Article e28665.

LaJeunesse, T. C., Parkinson, J. E., Gabrielson, P. W., Jeong, H. J., Reimer, J. D., Voolstra, C. R., & Santos, S. R. (2018). Systematic revision of Symbiodiniaceae highlights the antiquity and diversity of coral endosymbionts. *Current Biology*, *28*(16), 2570-2580.

LaJeunesse, T. C., Smith, R. T., Finney, J., & Oxenford, H. (2009). Outbreak and persistence of opportunistic symbiotic dinoflagellates during the 2005 Caribbean mass coral 'bleaching' event. *Proceedings of the Royal Society B-Biological Sciences*, *276*(1676), 4139-4148.

Laurent, J., Tambutte, S., Tambutte, E., Allemand, D., & Venn, A. (2013). The influence of photosynthesis on host intracellular pH in scleractinian corals. *Journal of Experimental Biology*, *216*(8), 1398-1404.

Laurent, J., Venn, A., Tambutte, E., Ganot, P., Allemand, D., & Tambutte, S. (2014). Regulation of intracellular pH in cnidarians: response to acidosis in *Anemonia viridis*. *Febs Journal*, *281*(3), 683-695.

Lauvset, S. K., Gruber, N., Landschutzer, P., Olsen, A., & Tjiputra, J. (2015). Trends and drivers in global surface ocean pH over the past 3 decades. *Biogeosciences*, *12*(5), 1285-1298.

Lee, S. Y., Jeong, H. J., & Lajeunesse, T. C. (2020). *Cladocopium infistulum* sp. nov. (Dinophyceae), a thermally tolerant dinoflagellate symbiotic with giant clams from the western Pacific Ocean. *Phycologia*, *59*(6), 515-526.

Leggat, W., Badger, M. R., & Yellowlees, D. (1999). Evidence for an inorganic carbon-concentrating mechanism in the symbiotic dinoflagellate Symbiodinium sp. *Plant Physiology*, *121*(4), 1247-1255.

Lehnert, E. M., Burriesci, M. S., & Pringle, J. R. (2012). Developing the anemone Aiptasia as a tractable model for cnidarian-dinoflagellate symbiosis: the transcriptome of aposymbiotic *A. pallida*. *Bmc Genomics*, *13*, Article 271.

Lehnert, E. M., Mouchka, M. E., Burriesci, M. S., Gallo, N. D., Schwarz, J. A., & Pringle, J. R. (2014). Extensive differences in gene expression between symbiotic and aposymbiotic cnidarians. *G3-Genes Genomes Genetics*, *4*(2), 277-295.

Lesser, M. P. (1996). Elevated temperatures and ultraviolet radiation cause oxidative stress and inhibit photosynthesis in symbiotic dinoflagellates. *Limnology And Oceanography*, *41*(2), 271-283.

Lesser, M. P. (1997). Oxidative stress causes coral bleaching during exposure to elevated temperatures. *Coral Reefs*, *16*(3), 187-192.

Lesser, M. P. (2006). Oxidative stress in marine environments: Biochemistry and physiological ecology. *Annual Review of Physiology*, *68*, 253-278.

Lesser, M. P. (2011). *Coral bleaching: Causes and mechanisms*. Springer.

Lesser, M. P., Stat, M., & Gates, R. D. (2013). The endosymbiotic dinoflagellates (*Symbiodinium* sp.) of corals are parasites and mutualists. *Coral Reefs*, *32*(3), 603-611.

Lewis, A. M., Chan, A. N., & LaJeunesse, T. C. (2019). New species of closely related endosymbiotic dinoflagellates in the greater Caribbean have niches corresponding to host coral phylogeny. *Journal of Eukaryotic Microbiology*, *66*(3), 469-482.

Lewis, C. L., & Coffroth, M. A. (2004). The acquisition of exogenous algal symbionts by an octocoral after bleaching. *Science*, *304*(5676), 1490-1492.

Li, Y., Liew, Y. J., Cui, G., Cziesielski, M. J., Zahran, N., Michell, C. T., ... & Aranda, M. (2018). DNA methylation regulates transcriptional homeostasis of algal endosymbiosis in the coral model Aiptasia. *Science Advances*, *4*(8), Article eaat2142.

Li, Y. Y., Zhou, Z. L., Li, Y. J., Wang, Y. Q., Xu, M. X., Zhou, B., ... & Wang, Y. (2021). The bloom-forming dinoflagellate *Karenia mikimotoi* adopts different growth modes when exposed to short or long period of seawater acidification. *Toxins*, *13*(9), Article 629.

Lilley, R. M., Ralph, P. J., & Larkum, A. W. D. (2010). The determination of activity of the enzyme Rubisco in cell extracts of the dinoflagellate alga *Symbiodinium* sp. by manganese chemiluminescence and its response to short-term thermal stress of the alga. *Plant, Cell & Environment*, *33*(6), 995-1004.

Lin, S. J., Cheng, S. F., Song, B., Zhong, X., Lin, X., Li, W. J., ... & Morse, D. (2015). The *Symbiodinium kawagutii* genome illuminates dinoflagellate gene expression and coral symbiosis. *Science*, *350*(6261), 691-694.

Lin, Z. Y., Wang, L. Y., Chen, M. L., & Chen, J. M. (2018). The acute transcriptomic response of coral-algae interactions to pH fluctuation. *Marine Genomics, 42*, 32-40.

Lin, Z. Y., Wang, L. Y., Chen, M. L., Zheng, X. Q., & Chen, J. M. (2022). Proteome and microbiota analyses characterizing dynamic coral-algae-microbe tripartite interactions under simulated rapid ocean acidification. *Science of the Total Environment, 810,* Article 152266.

Linares, C., Pratchett, M. S., & Coker, D. J. (2011). Recolonisation of *Acropora hyacinthus* following climate-induced coral bleaching on the Great Barrier Reef. *Marine Ecology Progress Series*, *438*, 97-104.

Littman, R. A., van Oppen, M. J. H., & Willis, B. L. (2008). Methods for sampling free-living Symbiodinium (zooxanthellae) and their distribution and abundance at Lizard Island (Great Barrier Reef). *Journal of Experimental Marine Biology and Ecology*, *364*(1), 48-53.

Loram, J. E., Trapido-Rosenthal, H. G., & Douglas, A. E. (2007). Functional significance of genetically different symbiotic algae Symbiodinium in a coral reef symbiosis. *Molecular Ecology*, *16*(22), 4849-4857.

Luz, D., Zebral, Y., Klein, R., Marques, J., Marangoni, L., Pereira, C., ... & Bianchini, A. (2018). Oxidative stress in the hydrocoral *Millepora alcicornis* exposed to CO_2-driven seawater acidification. *Coral Reefs*, *37*(2), 571-579.

Madshus, I. H. (1988). Regulation of intracellular pH in eukaryotic cells. *Biochemical Journal*, *250*(1), 1-8.

Maeshima, M. (2000). Vacuolar H^+-pyrophosphatase. *Biochimica Et Biophysica Acta-Biomembranes*, *1465*(1-2), 37-51.

Man, S. M., & Kanneganti, T. D. (2016). Converging roles of caspases in inflammasome activation, cell death and innate immunity. *Nature Reviews Immunology*, *16*(1), 7-21.

Mansfield, K. M., & Gilmore, T. D. (2019). Innate immunity and cnidarian-Symbiodiniaceae mutualism. *Developmental and Comparative Immunology*, *90*, 199-209.

Manzello, D. P., Enochs, I. C., Carlton, R., Bruckner, A., Kolodziej, G., Dempsey, A., & Renaud, P. (2021). Pacific-wide pH snapshots reveal that high coral cover correlates with low, but variable pH. *Bulletin of Marine Science*, *97*(1), 239-256.

Maruyama, S., & Weis, V. M. (2021). Limitations of using cultured algae to study cnidarian-algal symbioses and suggestions for future studies. *Journal of Phycology*, *57*(1), 30-38.

Mason, R. A. B. (2018). Decline in symbiont densities of tropical and subtropical scleractinian corals under ocean acidification. *Coral Reefs*, *37*(3), 945-953.

Matthews, J. L., Crowder, C. M., Oakley, C. A., Lutz, A., Roessner, U., Meyer, E., ... & Davy, S. K. (2017). Optimal nutrient exchange and immune responses operate in partner specificity in the cnidarian-dinoflagellate symbiosis. *Proceedings of the National Academy of Sciences of the United States of America*, *114*(50), 13194-13199.

Matthews, J. L., Oakley, C. A., Lutz, A., Hillyer, K. E., Roessner, U., Grossman, A. R., ... & Davy, S. K. (2018). Partner switching and metabolic flux in a model cnidarian - dinoflagellate symbiosis. *Proceedings of the Royal Society B-Biological Sciences*, *285*(1892), Article 20182336.

Matthews, J. L., Sproles, A. E., Oakley, C. A., Grossman, A. R., Weis, V. M., & Davy, S. K. (2016). Menthol-induced bleaching rapidly and effectively provides experimental aposymbiotic sea anemones (*Aiptasia* sp.) for symbiosis investigations. *Journal of Experimental Biology*, *219*(3), 306-310.

Mazmanian, S. K., Liu, C. H., Tzianabos, A. O., & Kasper, D. L. (2005). An immunomodulatory molecule of symbiotic bacteria directs maturation of the host immune system. *Cell*, *122*(1), 107-118.

McCulloch, M., Falter, J., Trotter, J., & Montagna, P. (2012). Coral resilience to ocean acidification and global warming through pH up-regulation. *Nature Climate Change*, *2*(8), 623-633.

McGraw, C. M., Cornwall, C. E., Reid, M. R., Currie, K. I., Hepburn, C. D., Boyd, P., ... & Hunter, K. A. (2010). An automated pH-controlled culture system for laboratory-based ocean acidification experiments. *Limnology and Oceanography-Methods*, *8*, 686-694.

McLachlan, R. H., Price, J. T., Solomon, S. L., & Grottoli, A. G. (2020). Thirty years of coral heat-stress experiments: a review of methods. *Coral Reefs*.

Metsalu, T., & Vilo, J. (2015). ClustVis: a web tool for visualizing clustering of multivariate data using Principal Component Analysis and heatmap. *Nucleic acids research*, *43*(W1), W566-W570.

Meyer, E., & Weis, V. M. (2012). Study of cnidarian-algal symbiosis in the "omics" age. *Biological Bulletin*, *223*(1), 44-65.

Michelet, L., Zaffagnini, M., Morisse, S., Sparla, F., Perez-Perez, M. E., Francia, F., ... & Lemaire, S. D. (2013). Redox regulation of the Calvin-Benson cycle: something old, something new. *Frontiers in Plant Science*, *4*, Article 470.

Migliaccio, O., Pinsino, A., Maffioli, E., Smith, A. M., Agnisola, C., Matranga, V., ... & Palumbo, A. (2019). Living in future ocean acidification, physiological adaptive responses of the immune system of sea urchins resident at a CO_2 vent system. *Science of the Total Environment*, *672*, 938-950.

Miller, D. J., & Yellowlees, D. (1989). Inorganic nitrogen uptake by symbiotic marine cnidarians – a critical-review. *Proceedings of the Royal Society Series B-Biological Sciences*, *237*(1286), 109-125.

Miller, W. L., & Auchus, R. J. (2011). The Molecular Biology, Biochemistry, and Physiology of Human Steroidogenesis and Its Disorders. *Endocrine Reviews*, *32*(1), 81-151.

Miyagawa, Y., Tamoi, M., & Shigeoka, S. (2001). Overexpression of a cyanobacterial fructose-1,6-/sedoheptulose-1,7-bisphosphatase in tobacco enhances photosynthesis and growth. *Nature Biotechnology*, *19*(10), 965-969.

Mohamed, A. R., Andrade, N., Moya, A., Chan, C. X., Negri, A. P., Bourne, D. G., ... & Miller, D. J. (2020). Dual RNA-sequencing analyses of a coral and its native symbiont during the establishment of symbiosis. *Molecular Ecology*, *29*(20), 3921-3937.

Mohamed, A. R., Cumbo, V., Harii, S., Shinzato, C., Chan, C. X., Ragan, M. A., . . . Miller, D. J. (2016). The transcriptomic response of the coral *Acropora digitifera* to a competent Symbiodinium strain: the symbiosome as an arrested early phagosome. *Molecular Ecology*, *25*(13), 3127-3141.

Morris, L. A., Voolstra, C. R., Quigley, K. M., Bourne, D. G., & Bay, L. K. (2019). Nutrient availability and metabolism affect the stability of coral-Symbiodiniaceae symbioses. *Trends in Microbiology*, *27*(8), 678-689.

Morse, D., Tse, S. P. K., & Lo, S. C. L. (2018). Exploring dinoflagellate biology with high-throughput proteomics. *Harmful Algae*, *75*, 16-26.

Moya, A., Huisman, L., Ball, E. E., Hayward, D. C., Grasso, L. C., Chua, C. M., . . . Miller, D. J. (2012). Whole transcriptome analysis of the coral *Acropora millepora* reveals complex responses to CO_2-driven acidification during the initiation of calcification. *Molecular Ecology*, *21*(10), 2440-2454.

Moya, A., Huisman, L., Foret, S., Gattuso, J. P., Hayward, D. C., Ball, E. E., & Miller, D. J. (2015). Rapid acclimation of juvenile corals to CO_2-mediated acidification by upregulation of heat shock protein and Bcl-2 genes. *Molecular Ecology*, *24*(2), 438-452.

Muller-Parker, G., & D'Elia, C. F. (1997). Interaction between corals and their symbiotic algae. In: Birkeland, C. (Ed.), *Life and Death of Coral Reefs*, (pp. 96-113). Chapman Hall.

Munday, P. L., Warner, R. R., Monro, K., Pandolfi, J. M., & Marshall, D. J. (2013). Predicting evolutionary responses to climate change in the sea. *Ecology Letters*, *16*(12), 1488-1500.

Munguia, P., & Alenius, B. (2013). The role of preconditioning in ocean acidification experiments: a test with the intertidal isopod *Paradella dianae*. *Marine and Freshwater Behaviour and Physiology*, *46*(1), 33-44.

Muscatine, L., Falkowski, P. G., Porter, J. W., & Dubinsky, Z. (1984). Fate of photosynthetic fixed carbon in light-adapted and shade-adapted colonies of the symbiotic coral *Stylophora pistillata*. *Proceedings of the Royal Society Series B-Biological Sciences*, *222*(1227), 181-202.

Muscatine, L., McCloskey, L. R., & Marian, R. E. (1981). Estimating the daily contribution of carbon from zooxanthellae to coral animal respiration. *Limnology and Oceanography*, *26*(4), 601-611.

Nakamura, M., Ohki, S., Suzuki, A., & Sakai, K. (2011). Coral larvae under ocean acidification: survival, metabolism, and metamorphosis (larvae under acidification). *PLoS ONE*, *6*(1), e14521.

Neubauer, E. F., Poole, A. Z., Neubauer, P., Detournay, O., Tan, K., Davy, S. K., & Weis, V. M. (2017). A diverse host thrombospondin-type-1 repeat protein repertoire promotes symbiont colonization during establishment of cnidarian-dinoflagellate symbiosis. *Elife*, *6*, Article e24494.

Neubauer, E. F., Poole, A. Z., Weis, V. M., & Davy, S. K. (2016). The scavenger receptor repertoire in six cnidarian species and its putative role in cnidarian-dinoflagellate symbiosis. *Peerj*, *4*, Article e2692.

Newkirk, C. R., Frazer, T. K., Martindale, M. Q., & Schnitzler, C. E. (2020). adaptation to bleaching: are thermotolerant Symbiodiniaceae strains more successful than other strains under elevated temperatures in a model symbiotic cnidarian? *Frontiers in Microbiology*, *11*, Article 822.

Nguyen, P. L., & van Baalen, M. (2020). On the difficult evolutionary transition from the free-living lifestyle to obligate symbiosis. *Plos One*, *15*(7), Article e0235811.

Nguyen, T. T., Bui, X. T., Pham, M. D., Guo, W. S., & Ngo, H. H. (2016). Effect of Tris-(hydroxymethyl)-amino methane on microalgae biomass growth in a photobioreactor. *Bioresource Technology*, *208*, 1-6.

Nicholls, D. G., & Ferguson, S. J. (2013). Respiratory chains. *Bioenergetics 4*, 91-157.

Nitschke, M. R., Craveiro, S. C., Brandao, C., Fidalgo, C., Serodio, J., Calado, A. J., & Frommlet, J. C. (2020). Description of *Freudenthalidium* gen. nov. and *Halluxium* gen. nov. to formally recognize clades fr3 and h as genera in the family Symbiodiniaceae (Dinophyceae). *Journal of Phycology*, *56*(4), 923-940.

Nitschke, M. R., Davy, S. K., & Ward, S. (2016). Horizontal transmission of Symbiodinium cells between adult and juvenile corals is aided by benthic sediment. *Coral Reefs*, *35*(1), 335-344.

Noonan, S. H. C., Fabricius, K. E., & Humphrey, C. (2013). Symbiodinium community composition in scleractinian corals is not affected by life-long exposure to elevated carbon dioxide. *Plos One*, *8*(5), Article e63985.

Norstrom, A. V., Nystrom, M., Lokrantz, J., & Folke, C. (2009). Alternative states on coral reefs: beyond coral-macroalgal phase shifts. *Marine Ecology Progress Series*, *376*, 295-306.

Novak, B. J., Fraser, D., & Maloney, T. H. (2020). Transforming ocean conservation: applying the genetic rescue toolkit. *Genes*, *11*(2), Article 209.

Oakley, C. A., Ameismeier, M. F., Peng, L. F., Weis, V. M., Grossman, A. R., & Davy, S. K. (2016). Symbiosis induces widespread changes in the proteome of the model cnidarian Aiptasia. *Cellular Microbiology*, *18*(7), 1009-1023.

Oakley, C. A., & Davy, S. K. (2018). Cell Biology of Coral Bleaching. In: *Coral Bleaching: Patterns, Processes, Causes and Consequences, 2nd Edition*, *233*, 189-211.

Oakley, C. A., Durand, E., Wilkinson, S. P., Peng, L. F., Weis, V. M., Grossman, A. R., & Davy, S. K. (2017). Thermal shock induces host proteostasis disruption and endoplasmic reticulum stress in the model symbiotic cnidarian Aiptasia. *Journal of Proteome Research*, *16*(6), 2121-2134.

Oakley, C. A., Schmidt, G. W., & Hopkinson, B. M. (2014). Thermal responses of Symbiodinium photosynthetic carbon assimilation. *Coral Reefs*, *33*(2), 501-512.

Ohad, I. (1994). Light-induced degradation of the photosystem II reaction centre D1 protein in vivo: an integrative approach. *Photoinhibition of Photosynthesais: from Molecular Mechanisms to the Field*, 161-178.

Pajot, A., Lavaud, J., Carrier, G., Garnier, M., Saint-Jean, B., Rabilloud, N., ... & Nicolau, E. (2022). The fucoxanthin chlorophyll *a/c*-binding protein in *Tisochrysis lutea*: influence of nitrogen and light on fucoxanthin and chlorophyll *a/c*-binding protein gene expression and fucoxanthin synthesis. *Frontiers in Plant Science*, *13*, Article 830069.

Parkhill, J. P., Maillet, G., & Cullen, J. J. (2001). Fluorescence-based maximal quantum yield for PSII as a diagnostic of nutrient stress. *Journal of Phycology*, *37*(4), 517-529.

Parkinson, J. E., Baker, A. C., Baums, I. B., Davies, S. W., Grottoli, A. G., Kitchen, S. A., ... & Kenkel, C. D. (2020). Molecular tools for coral reef restoration: Beyond biomarker discovery. *Conservation Letters*, *13*(1), Article e12687.

Parkinson, J. E., Baumgarten, S., Michell, C. T., Baums, I. B., LaJeunesse, T. C., & Voolstra, C. R. (2016). Gene expression variation resolves species and individual strains among coral-associated dinoflagellates within the genus Symbiodinium. *Genome Biology and Evolution*, *8*(3), 665-680.

Pasternak, Z., Blasius, B., Abelson, A., & Achituv, Y. (2006). Host-finding behaviour and navigation capabilities of symbiotic zooxanthellae. *Coral Reefs*, *25*(2), 201-207.

Paxton, C. W., Davy, S. K., & Weis, V. M. (2013). Stress and death of cnidarian host cells play a role in cnidarian bleaching. *Journal of Experimental Biology*, *216*(15), 2813-2820.

Peng, S. E., Wang, Y. B., Wang, L. H., Chen, W. N. U., Lu, C. Y., Fang, L. S., & Chen, C. S. (2010). Proteomic analysis of symbiosome membranes in Cnidaria-dinoflagellate endosymbiosis. *Proteomics*, *10*(5), 1002-1016.

Perez, S., & Weis, V. (2006). Nitric oxide and cnidarian bleaching: an eviction notice mediates breakdown of a symbiosis. *Journal of Experimental Biology*, *209*(14), 2804-2810.

Pernice, M., Dunn, S. R., Miard, T., Dufour, S., Dove, S., & Hoegh-Guldberg, O. (2011). Regulation of apoptotic mediators reveals dynamic responses to thermal stress in the reef building coral *Acropora millepora*. *Plos One*, *6*(1), Article e16095.

Pernice, M., Meibom, A., Van Den Heuvel, A., Kopp, C., Domart-Coulon, I., Hoegh-Guldberg, O., & Dove, S. (2012). A single-cell view of ammonium assimilation in coral-dinoflagellate symbiosis. *Isme Journal*, *6*(7), 1314-1324.

Pinzon, J. H., Kamel, B., Burge, C. A., Harvell, C. D., Medina, M., Weil, E., & Mydlarz, L. D. (2015). Whole transcriptome analysis reveals changes in expression of immune-related genes during and after bleaching in a reef-building coral. *Royal Society Open Science*, *2*(4), Article 140214.

Pochon, X., & Gates, R. D. (2010). A new Symbiodinium clade (Dinophyceae) from *Soritid foraminifera* in Hawai'i. *Molecular Phylogenetics and Evolution*, *56*(1), 492-497.

Pochon, X., & LaJeunesse, T. C. (2021). *Miliolidium* n. gen, a new Symbiodiniacean genus whose members associate with *Soritid foraminifera* or are free-living. *Journal of Eukaryotic Microbiology*, *68*(4), Article e12856.

Poole, A. Z., Kitchen, S. A., & Weis, V. M. (2016). The role of complement in cnidarian-dinoflagellate symbiosis and immune challenge in the sea anemone *Aiptasia pallida*. *Frontiers in Microbiology*, *7*, Article 519.

Pratchett, M. S., Hoey, A. S., & Wilson, S. K. (2014). Reef degradation and the loss of critical ecosystem goods and services provided by coral reef fishes. *Current Opinion in Environmental Sustainability*, *7*, 37-43.

Price, N. N., Hamilton, S. L., Tootell, J. S., & Smith, J. E. (2011). Species-specific consequences of ocean acidification for the calcareous tropical green algae Halimeda. *Marine Ecology Progress Series*, *440*, 67-78.

Pupier, C. A., Grover, R., Fine, M., Rottier, C., van de Water, J., & Ferrier-Pages, C. (2021). Dissolved nitrogen acquisition in the symbioses of soft and hard corals with Symbiodiniaceae: a key to understanding their different nutritional strategies? *Frontiers in Microbiology*, *12*, Article 657759.

Putnam, H. M., & Gates, R. D. (2015). Preconditioning in the reef-building coral *Pocillopora damicornis* and the potential for trans-generational acclimatization in coral larvae under future climate change conditions. *Journal of Experimental Biology*, *218*(15), 2365-2372.

Putnam, H. M., Ritson-Williams, R., Cruz, J. A., Davidson, J. M., & Gates, R. D. (2020). Environmentally-induced parental or developmental conditioning influences coral offspring ecological performance. *Scientific Reports*, *10*(1), Article 13664.

R Core Team (2021). *R: A language and environment for statistical computing*. R Foundation for Statistical Computing.

Radecker, N., Pogoreutz, C., Voolstra, C. R., Wiedenmann, J., & Wild, C. (2015). Nitrogen cycling in corals: the key to understanding holobiont functioning? *Trends in Microbiology*, *23*(8), 490-497.

Rainbolt, T. K., Saunders, J. M., & Wiseman, R. L. (2014). Stress-responsive regulation of mitochondria through the ER unfolded protein response. *Trends in Endocrinology & Metabolism*, *25*(10), 528-537.

Ralph, P. J., Hill, R., Doblin, M. A., & Davy, S. K. (2015). Theory and application of pulse amplitude modulated chlorophyll fluorometry in coral health assessment. 506-523.

Ramos-Silva, P., Kaandorp, J., Huisman, L., Marie, B., Zanella-Cleon, I., Guichard, N., . . . Marin, F. (2013). The skeletal proteome of the coral *Acropora millepora*: the evolution of calcification by co-option and domain shuffling. *Molecular Biology and Evolution*, *30*(9), 2099-2112.

Rands, M. L., Loughman, B. C., & Douglas, A. E. (1993). The symbiotic interface in an alga invertebrate symbiosis. *Proceedings of the Royal Society B-Biological Sciences*, *253*(1337), 161-165.

Raven, J., Caldeira, K., Elderfield, H., Hoegh-Guldberg, O., Liss, P., Riebesell, U., ... & Watson, A. (2005). *Ocean acidification due to increasing atmospheric carbon dioxide*. The Royal Society.

Raven, J. A., Suggett, D. J., & Giordano, M. (2020). Inorganic carbon concentrating mechanisms in free-living and symbiotic dinoflagellates and chromerids. *Journal of Phycology*, *56*(6), 1377-1397.

Rehman, A. U., Szabo, M., Deak, Z., Sass, L., Larkum, A., Ralph, P., & Vass, I. (2016). *Symbiodinium* sp. cells produce light-induced intra- and extracellular singlet oxygen, which mediates photodamage of the photosynthetic apparatus and has the potential to interact with the animal host in coral symbiosis. *New Phytologist*, *212*(2), 472-484.

Reich, H. G., Tu, W. C., Rodriguez, I. B., Chou, Y. L., Keister, E. F., Kemp, D. W., ... & Ho, T. Y. (2021). Iron availability modulates the response of endosymbiotic dinoflagellates to heat stress. *Journal of Phycology*, *57*(1), 3-13.

Reid, P. C. (2016). Ocean warming: setting the scene. In: Laffoley, D., & Baxter, J.M. (Eds.), 2016. Explaining ocean warming: Causes, scale, effects and consequences. Full report. (pp.17-44). IUCN.

Ren, M., Ogden, K., & Lian, B. (2013). Effect of culture conditions on the growth rate and lipid production of microalgae *Nannochloropsis gaditana*. *Journal of Renewable and Sustainable Energy*, *5*(6), Article 063138.

Reverter, M., Helber, S. B., Rohde, S., de Goeij, J. M., & Schupp, P. J. (2022). Coral reef benthic community changes in the Anthropocene: Biogeographic heterogeneity, overlooked configurations, and methodology. *Global Change Biology*, *28*(6), 1956-1971.

Reynaud, S., Leclercq, N., Romaine-Lioud, S., Ferrier-Pages, C., Jaubert, J., & Gattuso, J. P. (2003). Interacting effects of CO_2 partial pressure and temperature on photosynthesis and calcification in a scleractinian coral. *Global Change Biology*, *9*(11), 1660-1668.

Ricaurte, M., Schizas, N. V., Ciborowski, P., & Boukli, N. M. (2016). Proteomic analysis of bleached and unbleached *Acropora palmata*, a threatened coral species of the Caribbean. *Marine Pollution Bulletin*, *107*(1), 224-232.

Richier, S., Furla, P., Plantivaux, A., Merle, P. L., & Allemand, D. (2005). Symbiosis-induced adaptation to oxidative stress. *Journal of Experimental Biology*, *208*(2), 277-285.

Richmond, R. H., Tisthammer, K. H., & Spies, N. P. (2018). The effects of anthropogenic stressors on reproduction and recruitment of corals and reef organisms. *Frontiers in Marine Science*, *5*, Article Unsp 226.

Riebesell, U., Fabry, V. J., Hansson, L., & Gattuso, J.-P. (2010). Guide to best practices for ocean acidification research and data reporting. In *Guide to best practices for ocean acidification research and data reporting*: Publications Office of the European Union.

Ritchie, R. J. (2006). Consistent sets of spectrophotometric chlorophyll equations for acetone, methanol and ethanol solvents. *Photosynthesis Research*, *89*(1), 27-41.

Rivest, E. B., Comeau, S., & Cornwall, C. E. (2017). The role of natural variability in shaping the response of coral reef organisms to climate change. *Current Climate Change Reports*, *3*(4), 271-281.

Roberts, J. M., Fixter, L. M., & Davies, P. S. (2001). Ammonium metabolism in the symbiotic sea anemone *Anemonia viridis*. *Hydrobiologia*, *461*, 25-35.

Roberty, S., & Plumier, J. C. (2022). Bleaching physiology: who's the 'weakest link' - host vs. symbiont? *Emerging Topics in Life Sciences*, *6*(1), 17-32.

Robinson, J. P. W., Wilson, S. K., Robinson, J., Gerry, C., Lucas, J., Assan, C., ... & Graham, N. A. J. (2019). Productive instability of coral reef fisheries after climate-driven regime shifts. *Nature Ecology & Evolution*, *3*(2), 183-190.

Rocha, J. M. S., Garcia, J. E. C., & Henriques, M. H. F. (2003). Growth aspects of the marine microalga *Nannochloropsis gaditana*. *Biomolecular Engineering*, *20*(4-6), 237-242.

Rocker, M. M., Noonan, S., Humphrey, C., Moya, A., Willis, B. L., & Bay, L. K. (2015). Expression of calcification and metabolism-related genes in response to elevated pCO_2 and temperature in the reef-building coral *Acropora millepora*. *Marine Genomics*, *24*, 313-318.

Rodriguez-Lanetty, M., Wood-Charlson, E. M., Hollingsworth, L. L., Krupp, D. A., & Weis, V. M. (2006). Temporal and spatial infection dynamics indicate recognition events in the early hours of a dinoflagellate/coral symbiosis. *Marine Biology*, *149*(4), 713-719.

Rogers, A., Blanchard, J. L., & Mumby, P. J. (2014). Vulnerability of coral reef fisheries to a loss of structural complexity. *Current Biology*, *24*(9), 1000-1005.

Rosic, N., Kaniewska, P., Chan, C. K. K., Ling, E. Y. S., Edwards, D., Dove, S., & Hoegh-Guldberg, O. (2014). Early transcriptional changes in the reef-building coral *Acropora aspera* in response to thermal and nutrient stress. *Bmc Genomics*, *15*, Article 1052.

Rosset, S., Wiedenmann, J., Reed, A. J., & D'Angelo, C. (2017). Phosphate deficiency promotes coral bleaching and is reflected by the ultrastructure of symbiotic dinoflagellates. *Marine Pollution Bulletin*, *118*(1-2), 180-187.

Rosset, S. L., Oakley, C. A., Ferrier-Pages, C., Suggett, D. J., Weis, V. M., & Davy, S. K. (2021). The molecular language of the cnidarian-dinoflagellate symbiosis. *Trends in Microbiology*, *29*(4), 320-333.

Rost, B., Zondervan, I., & Wolf-Gladrow, D. (2008). Sensitivity of phytoplankton to future changes in ocean carbonate chemistry: current knowledge, contradictions and research directions. *Marine Ecology Progress Series*, *373*, 227-237.

Roth, F., Saalmann, F., Thomson, T., Coker, D. J., Villalobos, R., Jones, B. H., ... & Carvalho, S. (2018). Coral reef degradation affects the potential for reef recovery after disturbance. *Marine Environmental Research*, *142*, 48-58.

Roth, M. S. (2014). The engine of the reef: photobiology of the coral-algal symbiosis. *Frontiers in Microbiology*, *5*, Article 422.

Rowan, R. (2004). Coral bleaching – thermal adaptation in reef coral symbionts. *Nature*, *430*(7001), 742-742.

Rowan, R., & Knowlton, N. (1995). Intraspecific diversity and ecological zonation in coral algal symbiosis. *Proceedings of the National Academy of Sciences of the United States of America*, *92*(7), 2850-2853.

Sabine, C. L., Feely, R. A., Gruber, N., Key, R. M., Lee, K., Bullister, J. L., ... & Rios, A. F. (2004). The oceanic sink for anthropogenic CO_2. *Science (New York, N.Y.)*, *305*(5682), 367-371.

Sampayo, E. M., Ridgway, T., Bongaerts, P., & Hoegh-Guldberg, O. (2008). Bleaching susceptibility and mortality of corals are determined by fine-scale differences in symbiont type. *Proceedings of the National Academy of Sciences of the United States of America*, *105*(30), 10444-10449.

Schilling, R. K., Tester, M., Marschner, P., Plett, D. C., & Roy, S. J. (2017). AVP1: one protein, many roles. *Trends in Plant Science*, *22*(2), 154-162.

Schneider, K., & Erez, J. (2006). The effect of carbonate chemistry on calcification and photosynthesis in the hermatypic coral *Acropora eurystoma*. *Limnology and Oceanography*, *51*(3), 1284-1293.

Schnitzler, C. E., Hollingsworth, L. L., Krupp, D. A., & Weis, V. M. (2012). Elevated temperature impairs onset of symbiosis and reduces survivorship in larvae of the Hawaiian coral, *Fungia scutaria*. *Marine Biology*, *159*(3), 633-642.

Schopf, F. H., Biebl, M. M., & Buchner, J. (2017). The HSP90 chaperone machinery. *Nature Reviews Molecular Cell Biology*, *18*(6), 345-360.

Schwammle, V., Hagensen, C. E., Rogowska-Wrzesinska, A., & Jensen, O. N. (2020). PolySTest: robust statistical testing of proteomics data with missing values improves detection of biologically relevant features. *Molecular & Cellular Proteomics*, *19*(8), 1396-1408.

Schwarz, J. A. (2008). Understanding the intracellular niche in cnidarian-symbiodinium symbioses: parasites lead the way. *Vie Et Milieu-Life and Environment*, *58*(2), 141-151.

Scucchia, F., Malik, A., Zaslansky, P., Putnam, H. M., & Mass, T. (2021). Combined responses of primary coral polyps and their algal endosymbionts to decreasing seawater pH. *Proceedings of the Royal Society B-Biological Sciences*, *288*(1953), Article 20210328.

Shinzato, C., Shoguchi, E., Kawashima, T., Hamada, M., Hisata, K., Tanaka, M., . . . Satoh, N. (2011). Using the *Acropora digitifera* genome to understand coral responses to environmental change. *Nature*, *476*(7360), 320-U382.

Shoguchi, E., Shinzato, C., Kawashima, T., Gyoja, F., Mungpakdee, S., Koyanagi, R., ... & Satoh, N. (2013). Draft assembly of the *Symbiodinium minutum* nuclear genome reveals dinoflagellate gene structure. *Current Biology*, *23*(15), 1399-1408.

Silverstein, R. N., Correa, A. M. S., & Baker, A. C. (2012). Specificity is rarely absolute in coral-algal symbiosis: implications for coral response to climate change. *Proceedings of the Royal Society B-Biological Sciences*, *279*(1738), 2609-2618.

Silverstein, R. N., Cunning, R., & Baker, A. C. (2015). Change in algal symbiont communities after bleaching, not prior heat exposure, increases heat tolerance of reef corals. *Global Change Biology*, *21*(1), 236-249.

Sogin, E. M., Putnam, H. M., Anderson, P. E., & Gates, R. D. (2016). Metabolomic signatures of increases in temperature and ocean acidification from the reef-building coral, *Pocillopora damicornis*. *Metabolomics*, *12*(4), Article Unsp 71.

Souter, P., Bay, L. K., Andreakis, N., Csaszar, N., Seneca, F. O., & van Oppen, M. J. H. (2011). A multilocus, temperature stress-related gene expression profile assay in *Acropora millepora*, a dominant reef-building coral. *Molecular Ecology Resources*, *11*(2), 328-334.

Sproles, A. E., Oakley, C. A., Matthews, J. L., Peng, L. F., Owen, J. G., Grossman, A. R., ... & Davy, S. K. (2019). Proteomics quantifies protein expression changes in a model cnidarian colonised by a thermally tolerant but suboptimal symbiont. *Isme Journal*, *13*(9), 2334-2345.

Starcevic, A., Dunlap, W. C., Cullum, J., Shick, J. M., Hranueli, D., & Long, P. F. (2010). Gene expression in the scleractinian *Acropora microphthalma* exposed to high solar irradiance reveals elements of photoprotection and coral bleaching. *Plos One*, *5*(11), Article e13975.

Starzak, D. E., Quinnell, R. G., Cook, C. B., & Davy, S. K. (2020). Influence of symbiont species on the glycerol and glucose pools in a model cnidarian-dinoflagellate symbiosis. *Biological Bulletin*, *239*(2), 143-151.

Starzak, D. E., Quinnell, R. G., Nitschke, M. R., & Davy, S. K. (2014). The influence of symbiont type on photosynthetic carbon flux in a model cnidarian-dinoflagellate symbiosis. *Marine Biology*, *161*(3), 711-724.

Stat, M., Carter, D., & Hoegh-Guldberg, O. (2006). The evolutionary history of Symbiodinium and scleractinian hosts – symbiosis, diversity, and the effect of climate change. *Perspectives in Plant Ecology Evolution and Systematics*, *8*(1), 23-43.

Sten, O., Boris, Z., & Pierluigi, N. (2003). Calcium: regulation of cell death: the calcium-apoptosis link. *Nature Reviews Molecular Cell Biology*, *4*(7), 552.

Strahl, J., Francis, D. S., Doyle, J., Humphrey, C., & Fabricius, K. E. (2016). Biochemical responses to ocean acidification contrast between tropical corals with high and low abundances at volcanic carbon dioxide seeps. *Ices Journal of Marine Science*, *73*(3), 897-909.

Streamer, M., McNeil, Y. R., & Yellowlees, D. (1993). Photosynthetic carbon-dioxide fixation in zooxanthellae. *Marine Biology*, *115*(2), 195-198.

Suggett, D. J., Hall-Spencer, J. M., Rodolfo-Metalpa, R., Boatman, T. G., Payton, R., Pettay, D. T., ... & Lawson, T. (2012). Sea anemones may thrive in a high CO_2 world. *Global Change Biology*, *18*(10), 3015-3025.

Suggett, D. J., Warner, M. E., & Leggat, W. (2017). Symbiotic dinoflagellate functional diversity mediates coral survival under ecological crisis. *Trends in Ecology & Evolution*, *32*(10), 735-745.

Sun, Y. F., Jiang, L., Gong, S. Q., Guo, M. L., Yuan, X. C., Zhou, G. W., ... & Huang, H. (2020). Impact of ocean warming and acidification on symbiosis establishment and gene expression profiles in recruits of reef coral *Acropora intermedia*. *Frontiers in Microbiology*, *11*, Article 532447.

Sunagawa, S., Wilson, E. C., Thaler, M., Smith, M. L., Caruso, C., Pringle, J. R., ... & Schwarz, J. A. (2009). Generation and analysis of transcriptomic resources for a model system on the rise: the sea anemone *Aiptasia pallida* and its dinoflagellate endosymbiont. *Bmc Genomics*, *10*, Article 258.

Sunda, W. G., & Huntsman, S. A. (1995). Iron uptake and growth limitation in oceanic and coastal phytoplankton. *Marine Chemistry*, *50*(1-4), 189-206.

Sunday, J. M., Fabricius, K. E., Kroeker, K. J., Anderson, K. M., Brown, N. E., Barry, J. P., ... & Harley, C. D. G. (2017). Ocean acidification can mediate biodiversity shifts by changing biogenic habitat. *Nature Climate Change*, *7*(1), 81-85.

Supasri, K. M., Kumar, M., Mathew, M. J., Signal, B., Padula, M. P., Suggett, D. J., & Ralph, P. J. (2021). Evaluation of filter, paramagnetic, and STAGETips aided workflows for proteome profiling of Symbiodiniaceae dinoflagellate. *Processes*, *9*(6), Article 983.

Sutton, A. J., Feely, R. A., Maenner-Jones, S., Musielwicz, S., Osborne, J., Dietrich, C., ... & Weller, R. A. (2019). Autonomous seawater pCO_2 and pH time series from 40 surface buoys and the emergence of anthropogenic trends. *Earth System Science Data*, *11*(1), 421-439.

Suwa, R., Nakamura, M., Morita, M., Shimada, K., Iguchi, A., Sakai, K., & Suzuki, A. (2010). Effects of acidified seawater on early life stages of scleractinian corals (Genus Acropora). *Fisheries Science*, *76*(1), 93-99.

Suzuki, G., Yamashita, H., Kai, S., Hayashibara, T., Suzuki, K., Iehisa, Y., . . . Komori, T. (2013). Early uptake of specific symbionts enhances the post-settlement survival of *Acropora* corals. *Marine Ecology Progress Series*, *494*, 149-158.

Takahashi, A., & Kurihara, H. (2013). Ocean acidification does not affect the physiology of the tropical coral *Acropora digitifera* during a 5-week experiment. *Coral Reefs*, *32*(1), 305-314.

Takahashi, S., Whitney, S. M., & Badger, M. R. (2009). Different thermal sensitivity of the repair of photodamaged photosynthetic machinery in cultured Symbiodinium species. *Proceedings of the National Academy of Sciences of the United States of America*, *106*(9), 3237-3242.

Tansik, A. L., Fitt, W. K., & Hopkinson, B. M. (2017). Inorganic carbon is scarce for symbionts in scleractinian corals. *Limnology and Oceanography*, *62*(5), 2045-2055.

Taylor, D.L. (1974). Symbiotic marine algae; taxonomy and biological fitness. In: Vernberg, W.B. (Ed.), *Symbiosis in the Sea* (pp.245-262). University of South Carolina Press.

Tchernov, D., Gorbunov, M. Y., de Vargas, C., Yadav, S. N., Milligan, A. J., Haggblom, M., & Falkowski, P. G. (2004). Membrane lipids of symbiotic algae are diagnostic of sensitivity to thermal bleaching in corals. *Proceedings of the National Academy of Sciences of the United States of America*, *101*(37), 13531-13535.

Thompson, E. L., Parker, L., Amaral, V., Bishop, M. J., O'Connor, W. A., & Raftos, D. A. (2016). Wild populations of Sydney rock oysters differ in their proteomic responses to elevated carbon dioxide. *Marine and Freshwater Research*, *67*(12), 1964-1972.

Thornhill, D. J., Howells, E. J., Wham, D. C., Steury, T. D., & Santos, S. R. (2017). Population genetics of reef coral endosymbionts (Symbiodinium, Dinophyceae). *Molecular Ecology*, *26*(10), 2640-2659.

Thornhill, D. J., Lewis, A. M., Wham, D. C., & LaJeunesse, T. C. (2014). Host-specialist lineages dominate the adaptive radiation of reef coral endosymbionts. *Evolution*, *68*(2), 352-367.

Thornhill, D. J., Xiang, Y., Pettay, D. T., Zhong, M., & Santos, S. R. (2013). Population genetic data of a model symbiotic cnidarian system reveal remarkable symbiotic specificity and vectored introductions across ocean basins. *Molecular Ecology*, *22*(17), 4499-4515.

Timmins-Schiffman, E., Coffey, W. D., Hua, W., Nunn, B. L., Dickinson, G. H., & Roberts, S. B. (2014). Shotgun proteomics reveals physiological response to ocean acidification in *Crassostrea gigas*. *Bmc Genomics*, *15*, Article 951.

Tivey, T. R., Parkinson, J. E., & Weis, V. M. (2020). Host and symbiont cell cycle coordination is mediated by symbiotic state, nutrition, and partner identity in a model cnidarian-dinoflagellate symbiosis. *Mbio*, *11*(2), Article e02626-19.

Tkachenko, K. S., & Britayev, T. A. (2016). Unusually high abundance of the actiniarian *Anemonia manjano* Carlgren, 1900 outcompeting Scleractinians in central Vietnam. *Marine Biodiversity*, *46*(3), 545-546.

Tkachenko, K. S., Wu, B. J., Fang, L. S., & Fan, T. Y. (2007). Dynamics of a coral reef community after mass mortality of branching *Acropora* corals and an outbreak of anemones. *Marine Biology*, *151*(1), 185-194.

Tolleter, D., Seneca, F. O., DeNofrio, J. C., Krediet, C. J., Palumbi, S. R., Pringle, J. R., & Grossman, A. R. (2013). Coral bleaching independent of photosynthetic activity. *Current Biology*, *23*(18), 1782-1786.

Tomanek, L., Zuzow, M. J., Ivanina, A. V., Beniash, E., & Sokolova, I. M. (2011). Proteomic response to elevated pCO_2 level in eastern oysters, *Crassostrea virginica*: evidence for oxidative stress. *Journal of Experimental Biology*, *214*(11), 1836-1844. https://doi.org/10.1242/jeb.055475

Toronen, P., & Holm, L. (2022). PANNZER-A practical tool for protein function prediction. *Protein Science*, *31*(1), 118-128.

Torres, O., Kwiatkowski, L., Sutton, A. J., Dorey, N., & Orr, J. C. (2021). Characterizing mean and extreme diurnal variability of ocean CO_2 system variables across marine environments. *Geophysical Research Letters*, *48*(5), Article e2020GL090228.

Tortorelli, G., Belderok, R., Davy, S. K., McFadden, G. I., & van Oppen, M. J. H. (2020). Host genotypic effect on algal symbiosis establishment in the coral model, the anemone *Exaiptasia diaphana*, from the Great Barrier Reef. *Frontiers in Marine Science*, *6*, Article 833.

Tortorelli, G., Oakley, C. A., Davy, S. K., Van Oppen, M. J. H., & McFadden, G. I. (2021). Cell wall proteomic analysis of the cnidarian photosymbionts *Breviolum minutum* and *Cladocopium goreaui*. *Journal of Eukaryotic Microbiology*, Article e12870.

Towanda, T., & Thuesen, E. (2012). Prolonged exposure to elevated CO_2 promotes growth of the algal symbiont *Symbiodinium muscatinei* in the intertidal sea anemone *Anthopleura elegantissima*. *Biology Open*, *1*(7), 615-621.

Towle, E. K., Enochs, I. C., & Langdon, C. (2015). Threatened Caribbean coral is able to mitigate the adverse effects of ocean acidification on calcification by increasing feeding rate. *Plos One*, *10*(4), Article e0123394.

Tremblay, P., Fine, M., Maguer, J. F., Grover, R., & Ferrier-Pages, C. (2013). Photosynthate translocation increases in response to low seawater pH in a coral-dinoflagellate symbiosis. *Biogeosciences*, *10*(6), 3997-4007.

Tresguerres M., Barott K.L., Barron M.E., Deheyn D.D., Kline D.I., & L.B., L. (2017). Cell biology of reef-building corals: ion transport, acid/base regulation, and energy metabolism. In: Weihrauch D., O'Donnell M. (Eds.), *Acid-Base Balance and Nitrogen Excretion in Invertebrates*, (pp.193-218). Springer.

Tumanov, S., Bulusu, V., & Kamphorst, J. J. (2015). Analysis of fatty acid metabolism using stable isotope tracers and mass spectrometry. *Metabolic Analysis Using Stable Isotopes*, *561*, 197-217.

Urbarova, I., Foret, S., Dahl, M., Emblem, A., Milazzo, M., Hall-Spencer, J. M., & Johansen, S. D. (2019). Ocean acidification at a coastal CO_2 vent induces expression of stress-related transcripts and transposable elements in the sea anemone Anemonia viridis. *Plos One*, *14*(5), Article e0210358.

van de Water, J., De Mares, M. C., Dixon, G. B., Raina, J. B., Willis, B. L., Bourne, D. G., & van Oppen, M. J. H. (2018). Antimicrobial and stress responses to increased temperature and bacterial pathogen challenge in the holobiont of a reef-building coral. *Molecular Ecology*, *27*(4), 1065-1080.

van der Heijden, M. G. A., Klironomos, J. N., Ursic, M., Moutoglis, P., Streitwolf-Engel, R., Boller, T., ... & Sanders, I. R. (1998). Mycorrhizal fungal diversity determines plant biodiversity, ecosystem variability and productivity. *Nature*, *396*(6706), 69-72.

van Oppen, M. J. H., Oliver, J. K., Putnam, H. M., & Gates, R. D. (2015). Building coral reef resilience through assisted evolution. *Proceedings of the National Academy of Sciences of the United States of America*, *112*(8), 2307-2313.

Van Praët, M. (1982). Amylase and trypsin-and chymotrypsin-like proteases from *Actinia equina* L.; Their role in the nutrition of this sea anemone. *Comparative Biochemistry and Physiology Part A: Physiology*, *72*(3), 523-528.

Vargas, S., Zimmer, T., Conci, N., Lehmann, M., & Worheide, G. (2021). Transcriptional response of the calcification and stress response toolkits in an octocoral under heat and pH stress. *Molecular Ecology*.

Vaudel, M., Sickmann, A., & Martens, L. (2014). Introduction to opportunities and pitfalls in functional mass spectrometry-based proteomics. *Biochimica Et Biophysica Acta-Proteins and Proteomics*, *1844*(1), 12-20.

Venn, A., Tambutte, E., Holcomb, M., Allemand, D., & Tambutte, S. (2011). Live tissue imaging shows reef corals elevate pH under their calcifying tissue relative to seawater. *Plos One*, *6*(5), Article e20013.

Venn, A. A., Loram, J. E., & Douglas, A. E. (2008). Photosynthetic symbioses in animals. *Journal of Experimental Botany*, *59*(5), 1069-1080.

Venn, A. A., Tambutte, E., Holcomb, M., Laurent, J., Allemand, D., & Tambutte, S. (2013). Impact of seawater acidification on pH at the tissue-skeleton interface and calcification in reef corals. *Proceedings of the National Academy of Sciences of the United States of America*, *110*(5), 1634-1639.

Venn, A. A., Tambutte, E., Lotto, S., Zoccola, D., Allemand, D., & Tambutte, S. (2009). Imaging intracellular pH in a reef coral and symbiotic anemone. *Proceedings of the National Academy of Sciences of the United States of America*, *106*(39), 16574-16579.

Ventura, P., Jarrold, M. D., Merle, P. L., Barnay-Verdier, S., Zamoum, T., Rodolfo-Metalpa, R., ... & Furla, P. (2016). Resilience to ocean acidification: decreased carbonic anhydrase activity in sea anemones under high pCO_2 conditions. *Marine Ecology Progress Series*,

Vidal-Dupiol, J., Zoccola, D., Tambutté, E., Grunau, C., Cosseau, C., Smith, K. M., ... & Dupont, S. (2013). Genes related to ion-transport and energy production are upregulated in response to CO_2-driven pH decrease in corals: new insights from transcriptome analysis. *PLoS ONE*, *8*(3).

Voolstra, C. R. (2013). A journey into the wild of the cnidarian model system Aiptasia and its symbionts. *Molecular Ecology*, *22*(17), 4366-4368.

Wakefield, T. S., & Kempf, S. C. (2001). Development of host- and symbiont-specific monoclonal antibodies and confirmation of the origin of the symbiosome membrane in a cnidarian-dinoflagellate symbiosis. *Biological Bulletin*, *200*(2), 127-143.

Wall, C., Fan, T. Y., & Edmunds, P. (2014). Ocean acidification has no effect on thermal bleaching in the coral *Seriatopora caliendrum*. *Coral Reefs*, *33*(1), 119-130.

Wall, C. B., Mason, R. A. B., Ellis, W. R., Cunning, R., & Gates, R. D. (2017). Elevated pCO_2 affects tissue biomass composition, but not calcification, in a reef coral under two light regimes. *Royal Society Open Science*, *4*(11), Article 170683.

Wang, J. T., & Douglas, A. E. (1999). Essential amino acid synthesis and nitrogen recycling in an alga-invertebrate symbiosis. *Marine Biology*, *135*(2), 219-222.

Wardle, D. A., Bardgett, R. D., Klironomos, J. N., Setala, H., van der Putten, W. H., & Wall, D. H. (2004). Ecological linkages between aboveground and belowground biota. *Science*, *304*(5677), 1629-1633.

Warner, M. E., Fitt, W. K., & Schmidt, G. W. (1999). Damage to photosystem II in symbiotic dinoflagellates: A determinant of coral bleaching. *Proceedings of the National Academy of Sciences of the United States of America*, *96*(14), 8007-8012.

Warner, M. E., & Suggett, D. J. (2016). The photobiology of *Symbiodinium* spp.: linking physiological diversity to the implications of stress and resilience. In *The Cnidaria, past, present and future* (pp. 489-509). Springer.

Watkins, P. A. (1997). Fatty acid activation. *Progress in Lipid Research*, *36*(1), 55-83.

Webster, N. S., Uthicke, S., Botte, E. S., Flores, F., & Negri, A. P. (2013). Ocean acidification reduces induction of coral settlement by crustose coralline algae. *Global Change Biology*, *19*(1), 303-315.

Weis, V. M. (1993). Effect of dissolved inorganic carbon concentration on the photosynthesis of the symbiotic sea-anemone *Aiptasia pulchella* Carlgren – role of carbonic anhydrase. *Journal of Experimental Marine Biology and Ecology*, *174*(2), 209-225.

Weis, V. M. (2008). Cellular mechanisms of Cnidarian bleaching: stress causes the collapse of symbiosis. *Journal of Experimental Biology*, *211*(19), 3059-3066.

Weis, V. M. (2010). The susceptibility and resilience of corals to thermal stress: adaptation, acclimatization or both? *Molecular Ecology*, *19*(8), 1515-1517.

Weis, V. M. (2019). Cell biology of coral symbiosis: foundational study can inform solutions to the coral reef crisis. *Integrative and Comparative Biology*, *59*(4), 845-855.

Weis, V. M., Davy, S. K., Hoegh-Guldberg, O., Rodriguez-Lanetty, M., & Pringe, J. R. (2008). Cell biology in model systems as the key to understanding corals. *Trends in Ecology & Evolution*, *23*(7), 369-376.

Weis, V. M., Reynolds, W. S., deBoer, M. D., & Krupp, D. A. (2001). Host-symbiont specificity during onset of symbiosis between the dinoflagellates *Symbodinium* spp and planula larvae of the scleractinian coral *Fungia scutaria*. *Coral Reefs*, *20*(3), 301-308.

Weis, V. M., Smith, G. J., & Muscatine, L. (1989). A CO_2 supply mechanism in zooxanthellate cnidarians – role of carbonic anhydrase. *Marine Biology*, *100*(2), 195-202.

Whitehead, L. F., & Douglas, A. E. (2003). Metabolite comparisons and the identity of nutrients translocated from symbiotic algae to an animal host. *Journal of Experimental Biology*, *206*(18), 3149-3157.

Whitney, S. M., Shaw, D. C., & Yellowlees, D. (1995). Evidence that some dinoflagellates contain a ribulose-1,5-bisphosphate carboxylase oxygenase related to that of the alpha-proteobacteria. *Proceedings of the Royal Society B-Biological Sciences*, *259*(1356), 271-275.

Wiedenmann, J., D'Angelo, C., Smith, E. G., Hunt, A. N., Legiret, F. E., Postle, A. D., & Achterberg, E. P. (2013). Nutrient enrichment can increase the susceptibility of reef corals to bleaching. *Nature Climate Change*, *3*(2), 160-164.

Wilkins, M. R., Sanchez, J. C., Gooley, A. A., Appel, R. D., Humphery Smith, I., Hochstrasser, D. F., & Williams, K. L. (1996). Progress with proteome projects: Why all proteins expressed by a genome should be identified and how to do it. *Biotechnology and Genetic Engineering Reviews, Vol 13*, *13*, 19-50.

Wiśniewski, J. R., Zougman, A., Nagaraj, N., & Mann, M. (2009). Universal sample preparation method for proteome analysis. *Nature Methods*, *6*(5), 359.

Wolfowicz, I., Baumgarten, S., Voss, P. A., Hambleton, E. A., Voolstra, C. R., Hatta, M., & Guse, A. (2016). *Aiptasia* sp. larvae as a model to reveal mechanisms of symbiont selection in cnidarians. *Scientific Reports*, *6*, Article 32366.

Wood-Charlson, E. M., Hollingsworth, L. L., Krupp, D. A., & Weis, V. M. (2006). Lectin/glycan interactions play a role in recognition in a coral/dinoflagellate symbiosis. *Cellular Microbiology*, *8*(12), 1985-1993.

Woods, R. M., Baird, A. H., Mizerek, T. L., & Madin, J. S. (2016). Environmental factors limiting fertilisation and larval success in corals. *Coral Reefs*, *35*(4), 1433-1440.

Wooldridge, S. A. (2009). A new conceptual model for the warm-water breakdown of the coral-algae endosymbiosis. *Marine and Freshwater Research*, *60*(6), 483-496.

Wooldridge, S. A. (2010). Is the coral-algae symbiosis really 'mutually beneficial' for the partners? *Bioessays*, *32*(7), 615-625.

Xiang, T. T., Hambleton, E. A., DeNofrio, J. C., Pringle, J. R., & Grossman, A. R. (2013). Isolation of clonal axenic strains of the symbiotic dinoflagellate Symbiodinium and their growth and host specificity. *Journal of Phycology*, *49*(3), 447-458.

Xiang, T. T., Lehnert, E., Jinkerson, R. E., Clowez, S., Kim, R. G., DeNofrio, J. C., ... & Grossman, A. R. (2020). Symbiont population control by host-symbiont metabolic interaction in Symbiodiniaceae-cnidarian associations. *Nature Communications*, *11*(1), Article 108.

Yamashiro, H., Oku, H., & Onaga, K. (2005). Effect of bleaching on lipid content and composition of Okinawan corals. *Fisheries Science*, *71*(2), 448-453.

Yellowlees, D., Rees, T. A. V., & Leggat, W. (2008). Metabolic interactions between algal symbionts and invertebrate hosts. *Plant Cell and Environment*, *31*(5), 679-694.

Yorifuji, M., Harii, S., Nakamura, R., & Fudo, M. (2017). Shift of symbiont communities in *Acropora tenuis* juveniles under heat stress. *Peerj*, *5*, Article e4055.

Yuan, X. C., Yuan, T., Huang, H., Jiang, L., Zhou, W. H., & Liu, S. (2018). Elevated CO_2 delays the early development of scleractinian coral *Acropora gemmifera*. *Scientific Reports*, *8*, Article 2787.

Yuyama, I., Ishikawa, M., Nozawa, M., Yoshida, M., & Ikeo, K. (2018). Transcriptomic changes with increasing algal symbiont reveal the detailed process underlying establishment of coral-algal symbiosis. *Scientific Reports*, *8*, Article 16802.

Zangar, R. C., Davydov, D. R., & Verma, S. (2004). Mechanisms that regulate production of reactive oxygen species by cytochrome P450. *Toxicology and Applied Pharmacology*, *199*(3), 316-331.

Zhang, M., Zhen, Y., Mi, T. Z., & Lin, S. J. (2021). Integrated transcriptome sequencing (RNAseq) and proteomic studies reveal resource reallocation towards energy metabolism and defence in *Skeletonema marinoi* in response to CO_2 increase. *Applied and Environmental Microbiology*, *87*(5), Article e02614-20.

Zhou, G. W., Yuan, T., Cai, L., Zhang, W. P., Tian, R. M., Tong, H. Y., ... & Huang, H. (2016). Changes in microbial communities, photosynthesis and calcification of the coral *Acropora gemmifera* in response to ocean acidification. *Scientific Reports*, *6*, Article 35971.

Zoccola, D., Ganot, P., Bertucci, A., Caminiti-Segonds, N., Techer, N., Voolstra, C. R., ... & Tambutte, S. (2015). Bicarbonate transporters in corals point towards a key step in the evolution of cnidarian calcification. *Scientific Reports*, *5*, Article 09983.

Zoccola, D., Innocenti, A., Bertucci, A., Tambutte, E., Supuran, C. T., & Tambutte, S. (2016). Coral carbonic anhydrases: regulation by ocean acidification. *Marine Drugs*, *14*(6), Article 109.

Zubarev, R. A. (2013). The challenge of the proteome dynamic range and its implications for in-depth proteomics. *Proteomics*, *13*(5), 723-726.

Supplementary material

Due to the large volume of statistical and proteomic data generated in this thesis, all supplementary data have been uploaded to a publicly available repository (GitHub), as follows:

Supplementary for Chapter 2

S1.1. Linear models and statistical tests for Chapter 2

https://github.com/JacquieBown/S1.1-Linear-models-and-statistical-tests

S1.2 Differentially abundant proteins and GO term annotations – *Breviolum minutum*
S1.3. Differentially abundant proteins and GO term annotations – aposymbiotic Aiptasia
S1.4. Differentially abundant proteins and GO term annotations – symbiotic Aiptasia

https://github.com/JacquieBown/S1.2-S1.4-Differentially-abundant-proteins

S1.5. Full list of identified proteins – *B. minutum*
S1.6. Full list of identified proteins – Aiptasia

https://github.com/JacquieBown/S1.5-S1.6-Full-lists-of-identified-proteins

S1.7. Detected "hypothetical" proteins in *Breviolum minutum*
S1.8. Detected "hypothetical" proteins in Aiptasia

https://github.com/JacquieBown/S1.7-S1.8-Hypothetical-proteins

S1.9. Differentially abundant proteins in Aiptasia by symbiotic state

https://github.com/JacquieBown/S1.9-DAPs-Aiptasia-by-symbiotic-state

S1.10. Gene ontology terms by functional category for *Breviolum minutum*
S1.11. Gene ontology terms by functional category for aposymbiotic Aiptasia
S1.12. Gene ontology terms by functional category for symbiotic Aiptasia

https://github.com/JacquieBown/S1.10-S1.12-GO-terms-by-functional-category

Supplementary for Chapter 3

S2.1. *Breviolum minutum* pre-exposure trial

https://github.com/JacquieBown/S2.1-Culture-pre-exposure-trial

S2.2. Linear models and statistical tests for Chapter 3

https://github.com/JacquieBown/S2.2-Linear-models-and-statistical-tests